https://ntrs.nasa.gov/search.jsp?R=19780018035 2020-03-22T02:54:31+00:00Z

General Disclaimer

One or more of the Following Statements may affect this Document

- This document has been reproduced from the best copy furnished by the organizational source. It is being released in the interest of making available as much information as possible.

- This document may contain data, which exceeds the sheet parameters. It was furnished in this condition by the organizational source and is the best copy available.

- This document may contain tone-on-tone or color graphs, charts and/or pictures, which have been reproduced in black and white.

- This document is paginated as submitted by the original source.

- Portions of this document are not fully legible due to the historical nature of some of the material. However, it is the best reproduction available from the original submission.

Produced by the NASA Center for Aerospace Information (CASI)

5/78

R-O 6-78

JPL BIBLIOGRAPHY 39-19

(NASA-CR-157186) PUBLICATIONS OF THE JET PROPULSION LABORATORY, 1977 (Jet Propulsion Lab.) 172 p HC A08/MF A01 CSCL 05B

N78-25978

Unclas

G3/82 22972

Publications of the Jet Propulsion Laboratory 1977

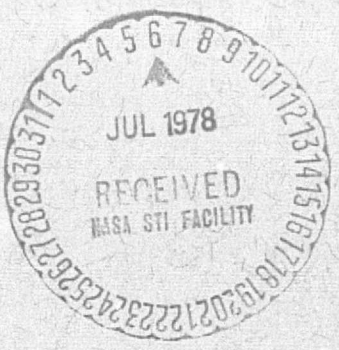

National Aeronautics and Space Administration

Jet Propulsion Laboratory
California Institute of Technology
Pasadena, California

JPL BIBLIOGRAPHY 39-19

Publications of the Jet Propulsion Laboratory 1977

May 1, 1978

National Aeronautics and
Space Administration

Jet Propulsion Laboratory
California Institute of Technology
Pasadena, California

Foreword

JPL Bibliography 39-19 describes and indexes the externally distributed technical reporting, released during calendar year 1977, that resulted from scientific and engineering work performed, or managed, by the Jet Propulsion Laboratory. Six classes of publications are included:

(1) Technical Reports (32-series), in which the information is complete for a specific accomplishment and is intended for a wide audience.

(2) Technical Memorandums (33-series), in which the information is complete for a specific accomplishment but is intended for a limited audience to satisfy unique requirements.

(3) Articles from the bimonthly *Deep Space Network (DSN) Progress Report* (42-series). Each collection of articles in this new class of publication beginning with 42-20 presents a periodical survey of current accomplishments by the Deep Space Network. Formerly, each collection of articles was published as a separate volume of Technical Report 32-1526.

(4) Special Publications (43-series), in which the information is complete for a specific accomplishment and is presented in a special format to emphasize its unique character and direction.

(5) JPL Publications (77-series for 1977), in which the information is complete for a specific accomplishment and can be tailored to wide or limited audiences and be presented in an established standard format or special format to meet unique requirements.

(6) Articles published in the open literature.

Effective January 1977, the JPL Publication replaced the Technical Report, Technical Memorandum, and Special Publication. However, the discontinued classes may still appear in future issues of the Bibliography if succeeding volumes or revisions are published in their former series.

The publications are indexed by: (1) author, (2) subject, and (3) publication type and number. A descriptive entry appears under the name of each author of each publication; an abstract is included with the entry for the primary (first-listed) author.

JPL personnel can obtain loan copies of formal documents cited from the JPL Library. Personnel of outside organizations can obtain copies of documents cited by addressing a written request to the Technical Information and Documentation Division, Jet Propulsion Laboratory, 4800 Oak Grove Drive, Pasadena, California 91103.

Contents

PAGE BLANK NOT FILMED

Author Index With Abstracts

ABRAMS, M. J.

A001 **Detection of Alteration Associated With a Porphyry Copper Deposit in Southern Arizona**

M. J. Abrams and B. S. Siegal

Technical Memorandum 33-810, February 1, 1977

The author has identified the following significant results. Alteration associated with a known porphyry copper deposit, Red Mountain near Patagonia, Arizona, has been delineated using spectral reflectance data, acquired by Landsat, a field spectrometer, and by NASA's Bendix 24-channel Multispectral Scanner.

A002 **Mapping of Hydrothermal Alteration in the Cuprite Mining District, Nevada, Using Aircraft Scanner Images for the Spectral Region 0.46 to 2.36 μm**

M. J. Abrams, R. P. Ashley (U. S. Geological Survey), L. C. Rowan (U. S. Geological Survey), A. F. H. Goetz, and A. B. Kahle

Geology, Vol. 5, No. 12, pp. 713–718, December 1977

Color composites of Landsat Multispectral Scanner ratio images that display variations in the intensity of ferric-iron absorption bands are highly effective for mapping limonitic altered rocks but are ineffective for mapping nonlimonitic altered rocks. Analysis of 0.45- to 2.5-μm field and laboratory spectra shows that iron-deficient opalized rocks in the Cuprite mining district, Nevada, have an intense OH-absorption band near 2.2 μm, owing to their content of clay minerals and alunite, and that this spectral feature is absent or weak in adjacent unaltered tuff and basalt. Altered rocks in the district can be discriminated from unaltered rocks with few ambiguities by use of color-ratio composite images derived from multispectral (0.46 to 2.36 μm) aircraft data. In addition, some effects of mineralogical zoning can be discriminated within the altered area. Only variations in amounts of limonite can be discerned in shorter wavelength aircraft data, Landsat Multispectral Scanner bands, and color aerial photographs.

ACKERKNECHT, W. E.

A003 **Effects of an Ion-Thruster Exhaust Plume on S-Band Carrier Transmission**

W. E. Ackerknecht and P. H. Stanton

J. Spacecraft Rockets, Vol. 14, No. 7, pp. 445–446, July 1977

The use of electric thrusters for spacecraft propulsion introduces a plasma medium that can affect the spacecraft-Earth communication link. The study reported here was undertaken 1) to develop models of the effects of an ion-thruster exhaust plume on S-band signals, and 2) to measure the effects. Theoretical models of the plume were obtained to give estimates of the plume effects of the rf signal. Based on knowledge of the plume characteristics and the anticipated experimental configuration, the plasma was modeled as a lossless, isotropic, linear, adiabatic, electron plasma. Using these assumptions, the models predicted that the rf wave would experience 1) a transmission loss due to spreading of the wave by the plume, and 2) a phase shift due to the nonunity refractive index within the plume. The absorption and reflection losses were predicted to be negligible. Details of the interaction models are described elsewhere.

Measurements were performed on a 30-cm diam mercury ion thruster at the Jet Propulsion Laboratory. S-band antennas were mounted inside the ion-thruster test chamber, a cw S-band signal was transmitted through the plume, and the amplitude and phase of the received signal were recorded under various test conditions.

ADAMS, M.

A004 **Spalling and Cracking in Alumina by Compression**

M. Adams and G. Sines

J. Amer. Ceram. Soc., Vol. 60, Nos. 5-6, pp. 221–226, May–June 1977

Crack damage produced by compressive loads in a dense alumina ceramic was studied with a replication technique that recorded damage done to the specimen's surface. The characteristics of the spalling produced in an externally pressurized, tubular specimen were evaluated at twelve stress levels up to failure. The study revealed that crack extension begins at a compressive stress approximately one quarter of that required to cause failure and that the amount of crack damage increases greatly as the failure stress is approached. The nature of the spalled particles and the mechanisms of spalling are discussed. Mechanisms of compressive failure are suggested.

ADAMSKI, T. P.

A005 Pioneer Mission Support

T. P. Adamski

The Deep Space Network Progress Report 42-37: November and December 1976, pp. 35–38, February 15, 1977

This article reports on some recent activities within the Deep Space Network in support of the Pioneer Project's in-flight spacecraft. The amount of tracking coverage provided by the Network and the current status of operational testing of the Mark III Data Subsystems are presented.

A006 Helios Mission Support

P. S. Goodwin, E. S. Burke, and T. P. Adamski

The Deep Space Network Progress Report 42-37: November and December 1976, pp. 39–42, February 15, 1977

For abstract, see Goodwin, P. S.

A007 Pioneer Mission Support

T. P. Adamski

The Deep Space Network Progress Report 42-39: March and April 1977, pp. 9–16, June 15, 1977

This article reports on activities within the Deep Space Network in support of the Pioneer Project's in-flight spacecraft during the period December 1976 through March 1977. The amount of tracking coverage provided by the Network and a summary of operational testing of the Mark III Data Subsystems are presented.

A008 Pioneer Mission Support

T. P. Adamski

The Deep Space Network Progress Report 42-41: July and August 1977, pp. 33–38, October 15, 1977

This article reports on activities within the Deep Space Network in support of the Pioneer Project's in-flight spacecraft during the period April through July 1977. The amount of tracking coverage provided by the Network and a summary of operational testing of the Mark III Data Subsystems at DSS 14 are presented.

ADEYEMI, O. H.

A009 A Markov Model for X-Band Atmospheric Antenna-Noise Temperature

O. H. Adeyemi

The Deep Space Network Progress Report 42-38: January and February 1977, pp. 99–102, April 15, 1977

A five-state Markov model is suggested for the X-band antenna-noise temperatures based on data collected at Goldstone. The states of the model are determined by changes in the "cloud and rain" condition of the atmosphere so as to take advantage of the correlation observed between the antenna temperatures and changes in rain rates. Then an indication is given of how to obtain the estimates of the parameters of the model from the data.

AJELLO, J. M.

A010 A Photoionization Study of the Charge Transfer Reactions: $Xe^+ + O_2 \rightarrow O_2^+ + Xe$ and $O_2^+ + Xe \rightarrow Xe^+ + O_2$

J. M. Ajello and J. B. Laudenslager

Chem. Phys. Lett., Vol. 44, No. 2, pp. 344–347, December 1, 1976

Photoionization mass spectrometer techniques have been employed to study the charge transfer reactions: $Xe^+ + O_2 \rightarrow O_2^+ + Xe$ and $O_2^+ + Xe \rightarrow Xe^+ + O_2$. The results show the reaction of $Xe^+(^2P_{3/2})$ ions with O_2 molecules is much more efficient than the reaction of $Xe^+(^2P_{1/2})$ ions with O_2 molecules. The charge transfer reaction of O_2^+ ions with Xe atoms was detected for O_2^+ ions in the a $^4\Pi_u$ state.

A011 Complex Refractive Index of Martian Dust: Wavelength Dependence and Composition

K. Pang and J. M. Ajello

Icarus, Vol. 30, pp. 63–74, 1977

For abstract, see Pang, K.

A012 High-Resolution Threshold Photoelectron Spectroscopy by Electron Attachment

J. M. Ajello and A. Chutjian

J. Chem. Phys., Vol. 65, No. 12, pp. 5524–5525, December 15, 1976

A new technique is discussed for measuring high-resolution threshold photoelectron spectra of atoms, molecules, and radicals. The measurement technique involves (1) photoionization of a gaseous species A, (2) attachment of the threshold, or nearly zero-energy electron to some "trapping" molecule (here, SF_6 or $CFCl_3$), and (3) mass detection of the attachment product (SF_6^- or Cl^-, respectively). This new technique is referred to as threshold photoelectron spectroscopy by electron attachment (TPSA).

A013 **A Photoionization Study of the Formation of NO_2^+ by Reaction of Excited O_2^+ Ions With NO**

J. M. Ajello and P. Rayermann

J. Chem. Phys., Vol. 66, No. 3, pp. 1372–1374, February 1, 1977

We report the first observation of the ion-molecule reaction, $O_2^+ + NO \rightarrow NO_2^+ + O$, obtained with a photoionization mass spectrometer.

A014 **Studies of Ar and N_2 Using Threshold Photoelectron Spectroscopy by Electron Attachment (TPSA)**

A. Chutjian and J. M. Ajello

J. Chem. Phys., Vol. 66, No. 10, pp. 4544–4550, May 15, 1977

For abstract, see Chutjian, A.

ALBERDA, M. E.

A015 **Implementation of a Maximum Likelihood Convolutional Decoder in the DSN**

M. E. Alberda

The Deep Space Network Progress Report 42-37: November and December 1976, pp. 176–183, February 15, 1977

The DSN is implementing a high data rate convolutional decoder capability for mission support starting in 1977. This article describes the development status of this decoder and the factors which were considered in defining the specific functional requirements. The design is discussed to the block diagram level. A description of the detailed design is provided, along with a description of the test software developed and a brief summary of the performance evaluation testing completed so far.

ANANDA, M.

A016 **Lunar Farside Gravity: An Assessment of Satellite to Satellite Tracking Techniques and Gravity Gradiometry**

M. Ananda, J. Lorell, and W. Flury (European Space Operations Center)

Proc. Seventh Lunar Sci. Conf., pp. 2623–2638, 1976

The estimation of local gravity anomalies represented by point masses using gravity gradiometer and satellite to satellite tracking data is discussed. A simulation analysis has been performed to study the recovery of local gravity anomalies from both rotating single axis gravity gradiometer and satellite to satellite tracking measurements. A Lunar Polar Orbiter mission concept is adopted for the orbits and data links. The sensitivity of the gravity determination to data noise, mass point spatial distribution (model errors), unmodelled gravity (gravity anomalies outside the area of interest), and orbit errors is studied. Figure of merit for the comparison is the R.M.S. error of radial acceleration.

ANANDA, M. P.

A017 **Lunar Gravity: A Mass Point Model**

M. P. Ananda

J. Geophys. Res., Vol. 82, No. 20, pp. 3049–3064, July 10, 1977

A point mass representation of a quasi-global gravity field of the moon is developed by processing Apollo 15 and 16 subsatellite and Lunar Orbiter 5 Doppler tracking data. The model is generated by reducing the long periodic variations in the mean orbit element rates. The gravity model consists of 117 point masses distributed over the region of $\pm 30^\circ$ in latitude about the lunar equator. This model resolves all the previously known 'mascons' in the nearside as broad positive gravity regions. The nearside acceleration map evaluated at 100 km above the lunar surface shows good agreement with the line of sight acceleration results. The lunar farside gravity map shows strong broad positive gravity regions for the highland areas. However, all the major ringed basins are resolved as localized negative anomalies in contrast with the nearside basins. This model does not indicate any evidence for the existence of any mascon type feature in the lunar farside. When radial acceleration values are compared with the topographic values obtained from laser altimeter data, there exists a relatively good agreement between the topography and gravity profiles, indicating that the gravity highs and lows correspond to topographic highs and lows for the lunar farside. Also, the 117 masses have been mapped to a twentieth-degree and twentieth-order harmonic coefficient field, and the low-order coefficients show reasonable agreement with other known fields.

A018 **Lunar Gravity: A Long-Term Keplerian Rate Method**

A. J. Ferrari and M. P. Ananda

J. Geophys. Res., Vol. 82, No. 20, pp. 3085–3097, July 10, 1977

For abstract, see Ferrari, A. J.

ANDERSON, J. D.

A019 **The Electron Density profile of the Outer Corona and the Interplanetary Medium From Mariner-6 and Mariner-7 Time-Delay Measurements**

D. O. Muhleman (California Institute of Technology), P. B. Esposito, and J. D. Anderson

Astrophys. J., Vol. 211, No. 3, Pt. 1, pp. 943–957, February 1, 1977

For abstract, see Muhleman, D. O.

A020 **Gravitational Fields and Interior Structure of the Giant Planets**

J. D. Anderson and W. B. Hubbard (University of Arizona)

Progr. Astronaut. Aeronaut., Vol. 50, pp. 71–83, 1977

A review of the analysis and interpretation of gravity data from the Pioneer 10 flyby of Jupiter in December 1973 is presented. The relationship between the external gravitational field of a giant planet and the distribution of matter in its interior is discussed in terms of a new theory of gravity sounding. The objective of this review is to provide an elementary understanding of the information contained in gravitational data for purposes of planning future planetary missions and for purposes of anticipating what will be learned from future flybys with Pioneer 11 and the Mariner Jupiter/Saturn spacecraft.

ANICICH, V. G.

A021 **Ion Cyclotron Resonance Studies of Some Reactions of N^+ Ions**

V. G. Anicich, W. T. Huntress, Jr., and J. H. Futrell (University of Utah)

Chem. Phys. Lett., Vol. 47, No. 3, pp. 488–489, May 1, 1977

Product distributions and rate constants for the reactions of ground state N^+ ions with CO, NO, CO_2, and CH_4 were measured. Rate constants were obtained using ion cyclotron resonance (ICR) trapped ion methods at JPL, and product distributions were obtained using a tandem (Dempster–ICR) mass spectrometer at the University of Utah. Rapid nitrogen isotope exchange was also observed in N^+–N_2 collisions.

A022 **Product Distributions for Some Thermal Energy Charge Transfer Reactions of Rare Gas Ions**

V. G. Anicich, J. B. Laudenslager, W. T. Huntress, Jr., and J. H. Futrell (University of Utah)

J. Chem. Phys., Vol. 67, No. 10, pp. 4340–4350, November 15, 1977

Ion cyclotron methods were used to measure the product distributions for thermal energy charge transfer reactions of He^+, Ne^+, and Ar^+ ions with N_2, O_2, CO, NO, CO_2, and N_2O. Except for the He^+–N_2 reaction, no molecular ions were formed by thermal energy charge transfer from He^+ and Ne^+ with these target molecules. The propensity for dissociative ionization channels in these highly exothermic charge transfer reactions at thermal energies contrasts with the propensity for formation of parent molecular ions observed in photoionization experiments and in high energy charge transfer processes. This difference is explained in terms of more stringent requirements for energy resonance and favorable Franck–Condon factors at thermal ion velocities.

A023 **Product Distribution and Rate Constants for the Reactions of CH_3^+, CH_4^+, $C_2H_2^+$, $C_2H_3^+$, $C_2H_4^+$, $C_2H_5^+$, and $C_2H_6^+$ Ions with CH_4, C_2H_2, C_2H_4, and C_2H_6**

J. K. Kim, V. G. Anicich, and W. T. Huntress, Jr.

J. Phys. Chem., Vol. 81, No. 19, pp. 1798–1805, 1977

For abstract, see Kim, J. K.

A024 **Calibration of a Marginal Oscillator Sensitivity for Use in ICR Spectrometry**

V. G. Anicich and W. T. Huntress, Jr.

Rev. Sci. Instrum., Vol. 48, No. 5, pp. 542–544, May 1977

A new design of a Q-spoiler, a constant reference load, is introduced and evaluated. The device is useful in the calibration of a marginal oscillator's relative sensitivity variations with frequency. In a capacitive divider design, the loading of the marginal oscillator with respect to frequency is largely dependent on the choice of components. The new design uses a large resistance and compensates for the resistor's capacitance by switching between the resistor and another leg of the circuit that has a matched capacitance.

ANSELMO, V. J.

A025 **Feasibility Study on the Design of a Probe for Rectal Cancer Detection**

V. J. Anselmo, R. E. Frazer, D. H. LeCroissette, J. A. Roseboro, and M. I. Smokler

JPL Publication 77-31, April 15, 1977

Rectal cancer mortality can be reduced if the examination technique can be improved in terms of detection capability, patient acceptance, and cost reduction. A review of existing clinical techniques and of relevant aerospace technology has included evaluation of the applicability of visual, thermal, ultrasound, and radioisotope modalities of examination. Of these, only the visual modality appears, for the present, to offer a basis for the

desired improvements. The improvements would be achieved by redesigning the proctosigmoidoscope to have reduced size, additional visibility, and the capability of readily providing a color photograph of the entire rectosigmoid mucosa in a single composite view.

A026 **Multispectral Photographic Analysis: A New Quantitative Tool to Assist in the Early Diagnosis of Thermal Burn Depth**

V. J. Anselmo and B. E. Zawacki (Los Angeles County/USC Medical Center)

Ann. Biomed. Eng., Vol. 5, pp. 179–193, 1977

Intercomparisons are made between three spectrally filtered photographs of experimental burns on guinea pigs and accidental burns on humans. The original photographs are taken on Kodak 35 mm Plus X and High Speed Infrared films. The transparencies are digitized and processed by a computer to form three additional photographs, each of which has an optical density proportional to the ratio of the target spectral reflectances. These images are color processed to form a pseudo color photograph which indicates the relative magnitude of the spectral reflectance ratio of the injured tissue. It is shown that these ratios, displayed by color patterns, have potential diagnostic value for the determination of burn depth in man.

A027 **Effect of Evaporative Surface Cooling on Thermographic Assessment of Burn Depth**

V. J. Anselmo and B. E. Zawacki (University of Southern California)

Radiology, Vol. 123, No. 2, pp. 331–332, May 1977

Differences in surface temperature between evaporating and nonevaporating partial- and full-thickness burn injuries were studied in 20 male, white guinea pigs. Evaporative cooling can disguise the temperature differential of the partial-thickness injury and lead to a false full-thickness diagnosis. A full-thickness burn with blister intact may retain enough heat to result in a false partial-thickness diagnosis. By the fourth postburn day, formation of a dry eschar may allow a surface temperature measurement without the complication of differential evaporation. For earlier use of thermographic information, evaporation effects must be accounted for or eliminated.

ANSPAUGH, B. E.

A028 **Electrical Characteristics of 2-Ω-cm 0.046-cm-Thick Silicon Solar Cells as a Function of Intensity and Temperature**

P. A. Berman, T. F. Miyahara, and B. E. Anspaugh

JPL Publication 77-27, July 1, 1977

For abstract, see Berman, P. A.

A029 **Electrical Characteristics of 2-Ω-cm 0.046-cm-Thick Silicon Solar Cells as a Function of Intensity and Temperature**

P. A. Berman, T. F. Miyahara, and B. E. Anspaugh

JPL Publication 77-27, Rev. 1, August 15, 1977

For abstract, see Berman, P. A.

ARENZ, R. J.

A030 **On the Form of the Strain Energy Function for a Family of SBR Materials**

R. J. Arenz

J. Appl. Polym. Sci., Vol. 21, pp. 2453–2463, 1977

A strain energy function of the Valanis-Landel type, $W = w(\lambda_1) + w(\lambda_2) + w(\lambda_3)$, is shown to be applicable to styrene–butadiene rubber (SBR) materials having varying crosslink densities ν_c. A previously obtained functional form of the strain energy derivative $w'(\lambda)$, normalized by dividing by ν_c, is confirmed by one of the validity check plots in which a single curve represents the whole body of large-deformation test results for all degrees of biaxiality and crosslink density.

ARP, H.

A031 **Image Processing of Galaxy Photographs**

H. Arp (Hale Observatories) and J. Lorre

Astrophys. J., Vol. 210, No. 1, Pt. 1, pp. 58–64, November 15, 1976

Photographic plates of particularly interesting galaxies and groups of galaxies have been obtained with the 5-m Hale and 4-m Kitt Peak National Observatory telescopes. They were scanned with a PDS scanning microphotometer and processed by a wide range of digital algorithms at the Image Processing Laboratory at the Jet Propulsion Laboratory. This paper demonstrates some of the available techniques for transforming pictorial data in order to enhance the contrast and clarity of nebulous features, detect previously invisible features, and moderately improve resolution (partial seeing compensation). It is also demonstrated that plates of the same object may be added to obtain maximum information and detectivity, and that plates taken in different spectral regions may be subtracted or ratioed to exhibit color differences, both

qualitatively and semiquantitatively, across any area and group of objects photographed.

Stephan's Quintet, NGC 7331, and the sky area between these objects have been analyzed. In a result which opens up important possibilities for extragalactic photography, real nebulous filaments are shown to exist throughout this area. Such extremely faint features may or may not generally be associated with galaxies. But specific features that are almost certainly associated with these galaxies are: (1) an extremely long, narrow, sinuous filament that emerges southward from NGC 7331; (2) a broad, strong, luminous tail that appears to emerge from the low-redshift galaxy NGC 7320 in Stephan's Quintet and connnects to a high-redshift member of the group; and (3) filaments that appear to proceed from the high-redshift members of Stephan's Quintet to the center of the nebulous network between NGC 7331 and the Quintet.

In Seyfert's Sextet it is shown that there is a short nebulous filament extending from the high-redshift spiral toward the nebulous tail of the adjacent low-redshift lenticular galaxy. Enhanced resolution of this same spiral shows large knots in a well-defined and peculiar three-armed spiral system.

Increased spatial resolution in the jet in M87 is presented which shows six rather evenly spaced, compact luminous objects all in a straight line emerging from the nucleus.

ASHLEY, R. P.

A032 Mapping of Hydrothermal Alteration in the Cuprite Mining District, Nevada, Using Aircraft Scanner Images for the Spectral Region 0.46 to 2.36 μm

M. J. Abrams, R. P. Ashley (U. S. Geological Survey), L. C. Rowan (U. S. Geological Survey), A. F. H. Goetz, and A. B. Kahle

Geology, Vol. 5, No. 12, pp. 713–718, December 1977

For abstract, see Abrams, M. J.

ATWOOD, D. L.

A033 Viking Lander Camera Radiometry Calibration Report

M. R. Wolf, D. L. Atwood, and M. E. Morrill

JPL Publication 77-62, Vols. I and II, November 1, 1977

For abstract, see Wolf, M. R.

AUMANN, H. H.

A034 The Abundance of Acetylene in the Atmosphere of Jupiter

G. S. Orton and H. H. Aumann

Icarus, Vol. 32, pp. 431–436, 1977

For abstract, see Orton, G. S.

A035 Remote Sounding of Cloudy Atmospheres. III. Experimental Verifications

M. T. Chahine, H. H. Aumann, and F. W. Taylor

J. Atmos. Sci., Vol. 34, No. 5, pp. 758–765, May 1977

For abstract, see Chahine, M. T.

BACK, L. D.

B001 Analysis of Pulsatile, Viscous Blood Flow Through Diseased Coronary Arteries of Man

L. D. Back, J. R. Radbill, and D. W. Crawford (University of Southern California)

J. Biomech., Vol. 10, pp. 339–353, 1977

The rheologic effects of multiple "non-obstructive" plagues in main coronary arteries of man were examined by numerically solving the fluid dynamic equations of motion for pulsatile viscous flow of blood through an arterial section using the actual variation of flow rate during the cardiac cycle. Flow regions identified by the calculations include spatial flow acceleration, deceleration, separation, reattachment and redevelopment. Shear stresses exerted by flowing blood on the endothelial surface varied greatly during the cardiac cycle, and there were large variations in shear stress along plaques. Wall shear stresses were relatively large even in regions of mild constriction. The computer program can be utilized in conjunction with coronary angiography to study the flow field for plaques of various sizes and shapes and with variable longitudinal spacing to obtain the level of wall shear stress to determine the existence and extent of separated flow regions.

BACK, L. H.

B002 Flow and Heat Transfer Measurements in a Pseudo-Shock Region With Surface Cooling

R. F. Cuffel and L. H. Back

AIAA J., Vol. 14, No. 12, pp. 1716–1722, December 1976

For abstract, see Cuffel, R. F.

B003 Blast Wave Analysis for Detonation Propulsion

K. Kim, G. Varsi, and L. H. Back

AIAA J., Vol. 15, No. 10, pp. 1500–1502, October 1977

For abstract, see Kim, K.

BAERWALD, R. K.

B004 Monopropellant Thruster Exhaust Plume Contamination Measurements

R. K. Baerwald and R. S. Passamaneck

JPL Publication 77-61, September 15, 1977

The potential spacecraft contaminants in the exhaust plume of a 0.89N (0.2 lbf) monopropellant hydrazine thruster were measured in an ultrahigh vacuum molecular sink facility. The engine plume was directed toward five quartz crystal microbalances (QCMs) located at angles of approximately 0, ±15, and ±30 deg with respect to the nozzle centerline. The crystal temperatures were controlled such that the mass adhering to the crystal surface at temperatures of from 106 to 256 K could be measured. Thruster duty cycles of 25 ms on/5 seconds off, 100 ms on/10 seconds off, and 200 ms on/20 seconds off were investigated. The change in contaminant production with thruster life was assessed by subjecting the thruster to a 100,000 pulse aging sequence and comparing the before and after contaminant deposition rates.

BAMFORD, R.

B005 Evaluation of a Cost-Effective Loads Approach

J. A. Garba, B. K. Wada, R. Bamford, and M. R. Trubert

J. Spacecraft Rockets, Vol. 13, No. 11, pp. 675–683, November 1976

For abstract, see Garba, J. A.

BATELAAN, P. D.

B006 Calibration of Block 4 Translator Path Delays at DSS 14 and CTA 21

T. Y. Otoshi, P. D. Batelaan, K. B. Wallace, and F. Ibanez

The Deep Space Network Progress Report 42-37: November and December 1976, pp. 188–197, February 15, 1977

For abstract, see Otoshi, T. Y.

B007 DSN Water Vapor Radiometer Development—A Summary of Recent Work, 1976–1977

S. D. Slobin and P. D. Batelaan

The Deep Space Network Progress Report 42-40: May and June 1977, pp. 71–75, August 15, 1977

For abstract, see Slobin, S. D.

BATHKER, D. A.

B008 Microwave Performance Characterization of Large Space Antennas

D. A. Bathker

JPL Publication 77-21, May 15, 1977

The purpose of this report is to place in perspective various broad classes of microwave antenna types and to discuss key functional and qualitative limitations. The goal is to assist the user and program manager groups in matching applications with anticipated performance capabilities of large microwave space antenna configurations with apertures generally from 100 wavelengths upwards. The microwave spectrum of interest is taken from 500 MHz to perhaps 1000 GHz. The types of antennas discussed are phased arrays, lenses, reflectors, and hybrid combinations of phased arrays with reflectors or lenses. The performance characteristics of these broad classes of antennas are examined and compared.

Given that large antennas in space are required in the above 50-dB-gain category (perhaps as much as 80 to 90 dB), the passive reflector type antenna remains the only demonstrated approach, albeit the available demonstrations are using ground-based reflectors. When high-gain systems are considered in the context of low-noise-level reception, the reflector antenna class is found virtually lossless and therefore desirable; further, the reflector bandwith is limited only by the feed used and the structural surface tolerance. For systems requiring high gain and modest scan capability, say, ±15 beamwidths, hybrid combinations of a reflector fed by a small phased array are an attractive approach. For systems requiring wide scan capability, there appears to be no substitute for a full phased array; however, no demonstrations in the above 50-dB-gain category have been reported. Within the more modest gain antenna category, say, 30–50 dB, specific requirements must be very carefully assessed to arrive at the best configuration

B009 S-/X-Band Microwave Optics Design and Analysis for DSN 34-Meter-Diameter Antenna

D. L. Nixon and D. A. Bathker

The Deep Space Network Progress Report 42-41: July and August 1977, pp. 146–165, October 15, 1977

For abstract, see Nixon, D. L.

B010 The High-Power *X*-Band Planetary Radar at Goldstone: Design, Development, and Early Results

R. Hartop and D. A. Bathker

IEEE Trans. Microwave Theor. Tech., Vol. MTT-24, No. 12, pp. 958–963, December 1976

For abstract, see Hartop, R.

BAUMERT, L. D.

B011 Minimum-Weight Codewords in the (128,64) BCH Code

L. D. Baumert and L. R. Welch (University of Southern California)

The Deep Space Network Progress Report 42-42: September and October 1977, pp. 92–94, December 15, 1977

In this article we determine the number of weight 22 codewords in the (128,64) BCH code which is being studied for use on future deep-space missions.

BEATTY, R. W.

B012 Development and Evaluation of a Set of Group Delay Standards

T. Y. Otoshi and R. W. Beatty (National Bureau of Standards)

IEEE Trans. Instrum. Meas., Vol. IM-25 No. 4, pp. 335–342, December 1976

For abstract, see Otoshi, T. Y.

BEJCZY, A. K.

B013 Effect of Hand-Based Sensors on Manipulator Control Performance

A. K. Bejczy

Mech. Mach. Theor., Vol. 12, pp. 547–567, 1977

Manipulator task categories and motion phases require various hand-based information systems to meet the control performance requirements. The effect of proximity, tactile and force/torque sensors on the performance of remote manipulator control is discussed. An overview is presented on various experimental hand-based information systems which provide the manipulator controller some non-visual "awareness" of the task environment. The rest of the paper describes and evaluates various control experiments performed at JPL using hand-mounted proximity sensors to guide and control hand motion near solid objects.

B014 Pattern Recognition and Control in Manipulation

A. K. Bejczy and R. Tomovic (University of California, Los Angeles)

Proc. IEEE Conf. Decision and Control, Clearwater Beach, Fla., Dec. 1–3, 1976, pp. 374–381

A new approach to the use of sensors in manipulator or robot control is discussed. The concept addresses the problem of contact or near-contact type of recognition of three-dimensional forms of objects by proprioceptive and/or exteroceptive sensors integrated with the terminal device. This recognition of object shapes both enhances and simplifies the automation of object handling. Several examples have been worked out for the "Belgrade hand" and for a parallel jaw terminal device, both equipped with proprioceptive (position) and exteroceptive (proximity) sensors. The control applications are discussed in the framework of a multilevel man-machine system control. The control applications create interesting new issues which, in turn, invite novel theoretical considerations. An important issue is the problem of stability in control when the control is referenced to patterns.

BENDER, D. F.

B015 Radar Detectability of Asteroids: A Survey of Opportunities for 1977 through 1987

R. F. Jurgens and D. F. Bender

Icarus, Vol. 31, pp. 483–497, 1977

For abstract, see Jurgens, R. F.

BENJAUTHRIT, B.

B016 Review of Finite Fields: Applications to Discrete Fourier Transforms and Reed-Solomon Coding

J. S. L. Wong, T. K. Truong, B. Benjauthrit, B. D. L. Mulhall, and I. S. Reed

JPL Publication 77-23, July 15, 1977

For abstract, see Wong, J. S. L.

B017 Encoding and Decoding a Telecommunication Standard Command Code

B. Benjauthrit and T. K. Truong

The Deep Space Network Progress Report 42-38: January and February 1977, pp. 115–119, April 15, 1977

This paper describes a simple encoder/decoder implementation scheme for the (63,56) BCH code which can be used to correct single errors and to detect any even-number of errors. The scheme is feasible for onboard-spacecraft implementation.

B018 X-Band Antenna Gain and System Noise Temperature of 64-Meter Deep Space Stations

B. Benjauthrit and B. D. L. Mulhall

The Deep Space Network Progress Report 42-39: March and April 1977, pp. 76–99, June 15, 1977

This report presents a new set of measured data on the X-band performance of the three 64-meter Deep Space Stations. These data will be useful for future mission telecommunication design and predictions. The test configuration and measurement procedure are described. A method of modelling attenuation due to the atmosphere is given. A short review of radio source brightness temperature and flux density is also included.

B019 On the Fundamental Structure of Galois Switching Functions

B. Benjauthrit and I. S. Reed (University of Southern California)

The Deep Space Network Progress Report 42-40: May and June 1977, pp. 117–13, August 15, 1977

It is shown that the fundamental structure of Galois switching functions follows naturally from that of Boolean switching functions. An expanded formula for deriving multinomial Galois switching functions is provided with illustrations of its application.

B020 DSN Telemetry System Performance Using a Maximum Likelihood Convolutional Decoder

B. Benjauthrit and R. Kemp

The Deep Space Network Progress Report 42-42: September and October 1977, pp. 149–161, December 15, 1977

This report describes results of telemetry system performance testing conducted at Goddard Merritt Island Space Flight Station using DSN equipment and a Maximum Likelihood Convolutional Decoder (MCD) for code rates 1/2 and 1/3, constraint length 7 and special test software. The test results confirm the superiority of the rate 1/3 over that of the rate 1/2. The overall system performance losses determined at the output of the Symbol Synchronizer Assembly are less than 0.5 dB for both code rates. Comparison of the performance is also made with existing mathematical models. Error statistics of the decoded data are examined. The MCD operational threshold is found to be about 1.96 dB.

BERDAHL, C. M.

B021 Precision Insolation Measurement Under Field Conditions

M. S. Reid, R. A. Gardner, and C. M. Berdahl

The Deep Space Network Progress Report 42-37: November and December 1976, pp. 169–175, February 15, 1977

For abstract, see Reid, M. S.

B022 Precision Insolation Measurement Under Field Conditions

M. S. Reid, C. M. Berdahl, and R. A. Gardner

Proc. SPIE, Vol. 85, pp. 90–92, 1976

For abstract, see Reid, M. S.

BERGSTRALH, J. T.

B023 Sodium D-Line Emission From Io: A Second Year of Synoptic Observation From Table Mountain Observatory

J. T. Bergstralh, J. W. Young, D. L. Matson, and T. V. Johnson

Astrophys. J., Vol. 211, No. 1, Pt. 2, pp. L51–L55, January 1, 1977

We report new measurements of the sodium D-line emission from Io (JI) made during a synoptic patrol of the 1975 apparition; we also report previously unpublished measurements from our patrol of the 1974 apparition. Our extended data set permits us to draw several conclusions about the nature of Io's sodium cloud: (1) The highest quality data selected from our extended 1974 patrol fall somewhat closer to the theoretical excitation function for resonant scattering than we previously reported, and consequently our earlier conclusion that resonant scattering is the *dominant* emission mechanism is strengthened. (2) There is no significant difference in the emission rates at similar phase angles between our 1974 and 1975 measurements, which suggests that the production mechanism which maintains the sodium cloud near Io underwent no major variation in the interval between the two apparitions. (3) The asymmetry between the peak emission rates at 90° and 270° orbital phase is present in our selected data, but is somewhat less pronounced than we reported previously. (4) The D_2/D_1 intensity ratios we measured are consistent with a constant value of 1.6 ± 0.3, which corresponds to a

moderate value, $\tau_0 \cong 1$, of the maximum optical depth possible in the center of the D_1 line.

B024 Interpretation of Spatial and Temporal Variations of Hydrogen Quadrupole Absorptions in the Jovian Atmosphere Observed During the 1972 Apparition

G. E. Hunt (Meteorological Office, Bracknell, Berkshire, England) and J. T. Bergstralh

Icarus, Vol. 30, pp. 511–530, 1977

For abstract, see Hunt, G. E.

BERGSTROM, S. L.

B025 Microbiological Profiles of the Viking Spacecraft

J. R. Puleo, N. D. Fields, S. L. Bergstrom, G. S. Oxborrow, P. D. Stabekis, and R. C. Koukol

Appl. Environ. Microbiol., Vol. 33, No. 2, pp. 379–384, February 1977

For abstract, see Puleo, J. R.

BERMAN, A. L.

B026 A Comprehensive Two-Way Doppler Noise Model for Near-Real-Time Validation of Doppler Data

A. L. Berman

The Deep Space Network Progress Report 42-37: November and December 1976, pp. 224–238, February 15, 1977

Recent articles have described the functional dependence of plasma-induced doppler noise ("media" noise) upon geometric parameters which approximate integrated signal path electron density (the "ISED" model). In this article, doppler noise generated within the tracking system ("system" noise) is modeled as a function of the dominant variable—doppler sample interval. Additionally, the relationship between media noise and doppler sample interval is empirically determined, and the ratio of media noise for S- and X-band downlinks is solved for. These functional relationships are incorporated into the previous media noise modeling to obtain a comprehensive two-way doppler noise model—ISEDC.

B027 Viking S-Band Doppler RMS Phase Fluctuations Used to Calibrate the Mean 1976 Equatorial Corona

A. L. Berman and J. A. Wackley

The Deep Space Network Progress Report 42-38: January and February 1977, pp. 152–166, April 15, 1977

Viking S-band doppler rms phase fluctuations (noise) and comparisons of Viking doppler noise to Viking differenced S-X range measurements are used to construct a mean equatorial electron density model for 1976: $N_e(r) = (2.39 \times 10^8/r^6) + (1.67 \times 10^6/r^{2.30})$, where N_e is in electrons/cm^3 and r is heliocentric distance in solar radii. At 1 AU, the model yields: $N_e(214) = 7.3$ electrons/cm^3. Using Pioneer doppler noise results (at high heliographic latitudes, also from 1976), an equivalent nonequatorial electron density model is approximated as: $N_e(r, f_s) = [(2.39 \times 10^8/r^6) + (1.67 \times 10^6/r^{2.30})]\ 10^{-0.9(|\phi_s|/90)}$, where f_s is the heliographic latitude in degrees.

B028 Viking Doppler Noise Used to Determine the Radial Dependence of Electron Density in the Extended Corona

A. L. Berman, J. A. Wackley, S. T. Rockwell, and M. Kwan

The Deep Space Network Progress Report 42-38: January and February 1977, pp. 167–171, April 15, 1977

The common form for radial dependence of electron density in the extended corona is: $N_e(r) \sim B/r^{2+\xi}$. By assuming proportionality between doppler noise and integrated signal path electron density, Viking doppler noise can be used to solve for a numerical value of ξ. This process yields: $\xi = 0.30$.

B029 Proportionality Between Doppler Noise and Integrated Signal Path Electron Density Validated by Differenced S-X Range

A. L. Berman

The Deep Space Network Progress Report 42-38: January and February 1977, pp. 172–183, April 15, 1977

Other articles on this subject have hypothesized that doppler rms phase jitter (noise) is proportional to integrated signal path electron density. In this article, observations of Viking differenced S-band/X-band (S-X) range are shown to correlate strongly with Viking doppler noise. A ratio of proportionality between downlink S-band plasma-induced range error and two-way doppler noise is calculated as: (Downlink S-band plasma range error/2-way S-band doppler noise) $\simeq$ 7 m/mHz. A new parameter (similar to the parameter ϵ which defines the ratio of "local" electron density fluctuations to mean electron density) is defined as a function of observed data sample interval (τ): $\epsilon'(\tau) = 7.9 \times 10^{-4}(\tau/60)^{0.7}$, where the time-scale of the observations is 15τ. This parameter is interpreted to yield the ratio of "net" observed phase (or electron density) fluctuations to integrated electron density (in rms meters/meter). Using this parameter and the "thin phase-changing screen" approximation, a value for the scale size L is calculated: $L = a[7.9 \times 10^{-4}/\epsilon]^2[\tau/60]^{1.4}$. To be consistent with doppler noise observations, it is seen necessary for L to be proportional to

closest approach distance a, and a strong function of the observed data sample interval, and hence the time-scale of the observations.

B030 Modification of the DSN Radio Frequency Angular Tropospheric Refraction Model

A. L. Berman

The Deep Space Network Progress Report 42-38: January and February 1977, pp. 184–186, April 15, 1977

The previously derived DSN Radio Frequency Angular Tropospheric Refraction Model contained an assumption which was subsequently seen to be at a variance with the theoretical basis of angular refraction. The modification necessary to correct the model is minor in that the value of a constant is changed. The accuracy of the modified model is now considered to be: maximum error of 0.003 deg for elevation angle range 90 deg $\geq$ el $\geq$ 5 deg and 0.010 deg for 5 deg $\geq$ el $\geq$ +3 deg.

B031 Phase Fluctuation Spectra: New Radio Science Information to Become Available in the DSN Tracking System Mark III-77

A. L. Berman

The Deep Space Network Progress Report 42-40: May and June 1977, pp. 134–140, August 15, 1977

The DSN Tracking System Mark III-77 currently being implemented at the Deep Space Stations will automatically provide doppler noise (rms phase jitter) computed concurrently over three evenly spaced decades of data sample interval and associated time-scale: data sample intervals of 0.1, 1, 10, and 100 seconds with time-scales of 1.8, 18, 180, and 1800 seconds, respectively. It is here suggested that these data translate directly into "average" phase fluctuation spectra, and hence represent a new and convenient source of radio science information. Temporal phase fluctuation spectra derived from Viking and Helios doppler noise data yield a power law relationship with frequency as follows:

$$P_\phi(f) \sim f^{2.42}$$

for the following approximate range of frequencies: 3.3×10^{-3} Hz $> f >$ 5.6×10^{-4} Hz.

B032 DSN Radio Science System Mark III-78 Real-Time Display Capability

A. L. Berman

The Deep Space Network Progress Report 42-40: May and June 1977, pp. 141–145, August 15, 1977

This article describes the current plan to provide radio science real-time display capability in response to multimission radio science requirements. The implementation occurs in two phase: (I) Provides display of doppler frequency and high-resolution graphical display of all closed-loop radio metric parameters, and (II) Provides spectrum display of open-loop receiver output.

B033 The CTA 21 Radio Science Subsystem—Non-Real-Time Bandwidth Reduction of Wideband Radio Science Data

A. L. Berman and J. I. Molinder

The Deep Space Network Progress Report 42-41: July and August 1977, pp. 127–134, October 15, 1977

The concept of a centralized facility at JPL to reduce the bandwidth of wideband digital recordings originated with the Pioneer Venus Differential Long Baseline Interferometry (DLBI) Experiment. This article presents a functional description of the resulting facility, the CTA 21 Radio Science Subsystem (CRS), located within JPL at the Compatibility Test Area (CTA 21). Particularly emphasized is a mathematical derivation and description of the digital filter process which comprises the core of the CRS.

B034 Electron Density in the Extended Corona—Two Views

A. L. Berman

The Deep Space Network Progress Report 42-41: July and August 1977, pp. 135–145, October 15, 1977

Recent analyses of Viking and Mariner solar conjunction radio metric data have led to two significantly different views of the average radial dependence of electron density in the extended corona ($5r_\odot \lesssim r \lesssim 1$ AU):

$$N_e(r) \propto r^{-2}$$

and

$$N_e(r) \propto r^{-2.3}$$

This article compares the two models and concludes that the "steeper" model ($r^{-2.3}$): (1) is in excellent agreement with other experimental observations of coronal electron density, (2) is consistent with the predicted and observed radial dependence of the solar wind velocity, and (3) augments the case of a turbulence scale that expands linearly with radial distance, when considered in combination with recent observations of the radial dependence of RMS phase fluctuations.

B035 Planetary Atmosphere Modeling and Predictions

A. L. Berman

The Deep Space Network Progress Report 42-42: September and October 1977, pp. 125–129, December 15, 1977

The capability to generate spacecraft frequency predictions which include the refractive bending effects induced during signal passage through a planetary atmosphere is a pivotal element of the DSN Radio Science System. This article describes the current implementation effort to develop planetary atmosphere modeling and prediction capability.

B036 An Empirical Model for the Solar Wind Velocity

A. L. Berman

The Deep Space Network Progress Report 42-42: September and October 1977, pp. 130–134, December 15, 1977

An analytic expression for the average radial component of the Solar Wind velocity between 1 solar radius and 1 AU is developed as follows: $v_r(r) = [440/(r^{-0.3} + 3.35 \times 10^{-7}\, r^{4.0})]$ km/s, where r is the radial distance in AU. The model is constructed by (1) assuming the conservation of particle flow in the Solar Wind and (2) application of a twelve-year average measured value of the Solar Wind radial velocity at 1 AU.

B037 RMS Electron Density Fluctuation at 1 AU

A. L. Berman

The Deep Space Network Progress Report 42-42: September and October 1977, pp. 135–140, December 15, 1977

Analytic expressions at 1 AU for the average RMS Electron Density Fluctuation and the ratio of RMS Electron Density Fluctuation to Electron Density, both as functions of the observational time scale, are constructed from average spacecraft in situ density measurements at approximately 1 AU and columnar phase fluctuation measurements over a wide variety of signal closest approach points. Additionally, the (one-dimensional) Electron Density Fluctuation spectrum and the Doppler phase fluctuation "scale" are derived, and various extrapolations to the region interior to 1 AU are made.

BERMAN, P. A.

B038 Electrical Characteristics of 2-Ω-cm 0.046-cm-Thick Silicon Solar Cells as a Function of Intensity and Temperature

P. A. Berman, T. F. Miyahara, and B. E. Anspaugh

JPL Publication 77-27, July 1, 1977

Electrical characteristics of Mariner '71 type of silicon solar cells are presented in graphical and tabular format as a function of intensity and temperature.

B039 Electrical Characteristics of 2-Ω-cm 0.046-cm-Thick Silicon Solar Cells as a Function of Intensity and Temperature

P. A. Berman, T. F. Miyahara, and B. E. Anspaugh

JPL Publication 77-27, Rev. 1, August 15, 1977

Electrical characteristics of Mariner '71 type of silicon solar cells are presented in graphical and tabular format as a function of intensity and temperature.

BIERMAN, G. J.

B040 A Parameter Estimation Subroutine Package

G. J. Bierman and M. W. Nead

JPL Publication 77-26, July 1, 1977

Linear least squares estimation and regression analyses continue to play a major role in orbit determination and related areas. In this report we document a library of FORTRAN subroutines that have been developed to facilitate analyses of a variety of parameter estimation problems. Our purpose is to present an easy to use multipurpose set of algorithms that are reasonably efficient and which use a minimal amount of computer storage. Subroutine inputs, outputs, usage and listings are given, along with examples of how these routines can be used. The following outline indicates the scope of this report: Section I, introduction with reference to background material; Section II, examples and applications; Section III, a subroutine directory summary; Section IV, the subroutine directory user description with input, output and usage explained; and Section V, subroutine FORTRAN listings. The routines are compact and efficient and are far superior to the normal equation data processing algorithms that are often used for least squares analyses.

B041 Givens Transformation Techniques for Kalman Filtering

C. L. Thornton and G. J. Bierman

Acta Astronautica, Vol. 4, pp. 847–863, 1977

For abstract, see Thornton, C. L.

B042 Additional Comments on "Multistage Least-Squares Parameter Estimation"

G. J. Bierman

IEEE Trans. Automat. Contr., Vol. AC-21, pp. 883–885, December 1976

The purpose of this correspondence is to call attention to other solutions to the problem addressed in the paper by J. M. Mendel (*IEEE Trans. Automat. Contr.*, Vol. AC-20, pp. 775–782, Dec. 1975) that of adding or deleting parameters or measurements from a given linear model. The solution algorithms proposed in the article are numerically ill-conditioned and are less efficient, in terms of both computational and storage requirements, than the methods described here. Several numerically stable, compact, flexible, and efficient algorithms for analyzing the parameter estimation problem are described and others are referenced.

B043 Gram-Schmidt Algorithms for Covariance Propagation

C. L. Thornton and G. J. Bierman

Int. J. Control, Vol. 25, No. 2, pp. 243–260, 1977

For abstract, see Thornton, C. L.

B044 Numerical Comparison of Discrete Kalman Filter Algorithms: Orbit Determination Case Study

G. J. Bierman and C. L. Thornton

Proc. IEEE Conf. Decision and Control, Clearwater, Fla., Dec. 1–3, 1976, pp. 859–872

Numerical characteristics of various Kalman filter algorithms are illustrated with a realistic orbit determination study. The case study of this paper highlights the numerical deficiencies of the conventional and stabilized Kalman algorithms. Computational errors associated with these algorithms are found to be so large as to obscure important mismodeling effects and thus cause misleading estimates of filter accuracy. The positive result of this study is that the U-D covariance factorization algorithm has excellent numerical properties and is computationally efficient, having CPU costs that differ negligibly from the conventional Kalman costs. Accuracies of the U-D filter using single precision arithmetic consistently match the double precision reference results. Numerical stability of the U-D filter is further demonstrated by its insensitivity to variations in the a priori statistics.

BILLS, B. G.

B045 A Lunar Density Model Consistent With Topographic, Gravitational, Librational, and Seismic Data

B. G. Bills and A. J. Ferrari

J. Geophys. Res., Vol. 82, No. 8, pp. 1306–1314, March 10, 1977

A series of models of the lunar interior are derived from topographic, gravitational, librational, and seismic data. The librational parameters and low-degree gravity harmonics result primarily from surface height variations and only secondarily from lateral density variations. The moon departs from isostasy, even for the low-degree harmonics, with a maximum superisostatic stress of 200 bars under the major mascon basins. The mean crustal thicknesses under different physiographic regions are: mascons, 30–35 km; irregular maria, 50–60 km; and highlands, 90–110 km. A possible composition consistent with our model is an anorthositic crust, underlain by a predominantly forsterite upper mantle which grades into a refractory rich lower mantle surrounding a pyrrhotite core.

BORDEN, C. S.

B046 Costs and Energy Efficiency of a Dual-Mode System

R. C. Heft and C. S. Borden

JPL Publication 77-34, April 30, 1977

For abstract, see Heft, R. C.

BORN, G. H.

B047 Mission Design for SEASAT-A, An Oceanographic Satellite

E. Cutting, G. H. Born, J. C. Frautnick, W. I. McLaughlin, R. A. Neilson, and J. A. Thielen (Lockheed Missiles & Space Co.)

Preprint 77-31, AIAA Fifteenth Aerosp. Sci. Meet., Los Angeles, Calif., Jan. 24–26, 1977

For abstract, see Cutting, E.

BOWYER, J. M.

B048 Rocket Motor Exhaust Products Generated by the Space Shuttle Vehicle During Its Launch Phase (1976 Design Data)

J. M. Bowyer

JPL Publication 77-9, March 1, 1977

This memorandum presents the principal chemical species emitted and/or entrained by the rocket motors of the Space Shuttle Vehicle during the launch phase of its trajectory. Results are presented for two extreme trajectories, both of which were calculated in 1976. Thus, the results presented in this memorandum supersede those presented in JPL Technical Memorandum 33-712, which utilized 1973 design data.

BRADY, W. F.

B049 **Maneuver Sequence Design for the Post-Jupiter Leg of the Pioneer Saturn Mission**

R. B. Frauenholz and W. F. Brady

J. Spacecraft Rockets, Vol. 14, No. 7, pp. 395–400, July 1977

For abstract, see Frauenholz, R. B.

BRANDT, M. A.

B050 **Quantum Mechanical and Crossed Beam Study of Vibrational Excitation of N_2 by Electron Impact at 30–75 eV**

D. G. Truhlar (University of Minnesota), M. A. Brandt (University of Minnesota), S. K. Srivastava, S. Trajmar, and A. Chutjian

J. Chem. Phys., Vol. 66, No. 2, pp. 655–663, January 15, 1977

For abstract, see Truhlar, D. G.

BRATENAHL, A.

B051 **Acceleration of Energetic Particles of the Outer Regions of Planetary Magnetospheres: Inferences From Laboratory and Space Experiments**

B. T. Tsurutani, B. E. Goldstein, and A. Bratenahl

Planet. Space Sci., Vol. 24, No. 10, pp. 995–999, 1976

For abstract, see Tsurutani, B. T.

BRECKENRIDGE, W. G.

B052 **Calibration of Viking Imaging System Pointing, Image Extraction, and Optical Navigation Measure**

W. G. Breckenridge, J. W. Fowler, and E. M. Morgan (General Electric Co.)

JPL Publication 77-28, September 15, 1977

The pointing of Viking Orbiter science instruments is controlled by the scan platform. The pointing control and knowledge accuracy required for science and optical navigation data acquisition and evaluation requires calibration of the scan platform and the imaging system. The mathematical models used and the calibration procedure and results obtained for the two Viking spacecraft are described. Included are both ground and in-flight scan platform calibrations, and the additional calibrations unique to optical navigation.

B053 **In-Flight Gyro Drift Rate Calibration on the Viking Orbiters**

W. G. Breckenridge and A. J. Treder

AAS/AIAA Astrodyn. Conf., Jackson Hole, Wyoming, September 8, 1977, 33 pp.

The drift rates of the attitude control gyros on the Viking Orbiters were calibrated several times in flight. The process by which these rates were estimated as functions of time is novel for a space flight project though relatively standard estimation techniques were used. The process is described fully, and the results obtained from the twelve Viking single-axis gyros are analyzed. Although the possibility was explored, no significantly repeatable function of drift rate versus time or temperature was discovered; the overall mean was found to predict drift rate with acceptable accuracy.

BROWN, L. R.

B054 **Line Positions and Strengths of Methane in the 2862 to 3000 cm^{-1} Region**

R. A. Toth, L. R. Brown (Florida State University), and R. H. Hunt (Florida State University)

J. Mol. Spectros., Vol. 67, Nos. 1–3, pp. 1–33, September 15, 1977

For abstract, see Toth, R. A.

BROWN, W. E., JR.

B055 **Models of Radar Imaging of the Ocean Surface Waves**

C. Elachi and W. E. Brown, Jr.

IEEE Trans. Anten. Prop., Vol. AP-25, No. 1, pp. 84–95, January 1977

For abstract, see Elachi, C.

BRYAN, A. I.

B056 **Summary Report and Status of the Deep Space Network—Mariner Jupiter/Saturn 1977 Flight Project Telecommunications Compatibility**

A. I. Bryan, R. P. Kemp, and B. D. Madsen

The Deep Space Network Progress Report 42-38: January and February 1977, pp. 16–37, April 15, 1977

The DSN–Mariner Jupiter/Saturn 1977 telecommunications compatibility tests, conducted during the time periods 15–20 November 1976, 7–16 December 1976 and 5 January 1977, are an ongoing series of engineering level

tests to determine the flight-ground interface compatibility and performance characteristics between these two systems. This report describes these tests in summary form and provides a status of the interface.

B057 Summary Report and Status of the Deep Space Network-Voyager Flight Project Telecommunications Compatibility

A. I. Bryan, R. P. Kemp, and B. D. Madsen

The Deep Space Network Progress Report 42-40: May and June 1977, pp. 21–40, August 15, 1977

The DSN-Voyager telecommunications compatibility tests are an ongoing series of Engineering level tests to determine the flight-ground interface compatibility and performance characteristics between these two systems. This report provides a summary and status of tests conducted between CTA 21-Voyager Flight 1 spacecraft, CTA 21-Voyager Flight 2 spacecraft, and MIL 71-Voyager Flight 1 spacecraft.

B058 Voyage Flight Project—DSN Telecommunications Compatibility Test Program

A. I. Bryan, R. P. Kemp, and B. D. Madsen

The Deep Space Network Progress Report 42-42: September and October 1977, pp. 13–27, December 15, 1977

The Voyager Flight Project—DSN Telecommunications Compatibility Test Program consisted of three phases: Subsystem Design, System Design and System Verification Tests, which were performed at JPL and at the U.S. Air Force Eastern Test Range and Kennedy Space Center Complexes. Subsystem Design Tests were performed during mid 1976. System Design Tests were performed during late 1976 and early 1977. System Verification Tests were performed during the spring and summer of 1977. This article describes the System Design Tests and test results that provided the basis for establishment of telecommunications design between the DSN and the Voyager Flight Project.

BRYANT, N. A.

B059 IBIS: A Geographic Information System Based on Digital Image Processing and Image Raster Data Type

N. A. Bryant and A. L. Zobrist

IEEE Trans. Geosci. Electron., Vol. GE-15, No. 3, pp. 152–159, July 1977

There is a pressing need for geographic information systems which can manage spatially referenced data, which perform certain types of spatially oriented processing, and which are current and comprehensive. Polygon-overlay and grid-cell information systems access data for selected areas, but their data files are time consuming to generate and frequently costly to process. Updating land use changes for such systems may become prohibitively expensive. In response to the present dilemma, a system is presented that makes use of digital image processing techniques to interface existing geocoded data sets and information management systems with thematic maps and remotely sensed imagery. The basic premise is that geocoded data sets can be referenced to a raster scan that is equivalent to a grid-cell data set.

Several technical problems have been overcome to achieve a workable system. First, digital image file handling, image manipulation, and image processing capabilities must be provided. Second, image data must be registered or indexed to spatially referenced tabular data so that processing steps which involve both types can operate. Third, a data interface must be provided between the different data types so that the results of processing can be represented. Finally, image processing analogs must be developed for existing geo-base file computational steps (e.g., overlay, aggregation, cross tabulation, etc.). The system is now in use on a test basis.

BUCKLES, B. J.

B060 Tracking System Performance Tests in the MDS Era

B. J. Buckles

The Deep Space Network Progress Report 42-40: May and June 1977, pp. 194 – 199, August 15, 1977

This article describes tracking system performance tests as developed to support DSN Mark III Data Subsystem implementation project and prepass readiness tests. Tracking SPT software and test configurations are described. Future test software requirements and areas of current development are noted.

BUEHLER, M. F.

B061 Creative Revision: From Rough Draft to Published Paper

M. F. Buehler

IEEE Trans. Prof. Commun., Vol. PC-19, No. 2, pp. 26–32, December 1976

The process of revising a technical or scientific paper can be performed more efficiently by the people involved (author, co-author, supervisor, editor) when the revision is controlled by breaking it into a series of steps. The revision process recommended here is based on the levels-of-edit concept that resulted from a study of the

technical editorial function at the Jet Propulsion Laboratory of the California Institute of Technology. Types of revision discussed are Substantive, Policy, Language, Mechanical Style, Format, Integrity, and Copy Clarification.

B062 Controlled Flexibility in Technical Editing: The Levels-of-Edit Concept at JPL

M. F. Buehler

J. Soc. Tech. Commun., Vol. 24, No. 1, pp. 1–4, 1977

Five levels of edit are categorized, tailored to the type of publication. The amount of effort is proportioned to the cost and time available.

BULKLEY, E. O.

B063 Lunar Crater Arcs

L. D. Jaffe and E. O. Bulkley

The Moon, Vol. 16, pp. 71–114, 1976

For abstract, see Jaffe, L. D.

BULLARD, E.

B064 An Analysis of the Technical Status of High Level Radioactive Waste and Spent Fuel Management Systems

T. English, C. Miller, E. Bullard, R. Campbell, A. Chockie, E. Divita, C. Douthitt (California Institute of Technology), E. Edelson, and L. Lees (California Institute of Technology)

JPL Publication 77-69, December 1, 1977

For abstract, see English, T.

BUNCE, R.

B065 DSN System Performance Test Doppler Noise Models; Noncoherent Configuration

R. Bunce

The Deep Space Network Progress Report 42-37: November and December 1976, pp. 239–250, February 15, 1977

Recent DSN System Performance Test requirements (for pending missions) contain implied long-term measurements for which existing noncoherent test models are inadequate. The new models needed are those of the first two moments, mean and variance, of doppler noise under long-term conditions, and in noncoherent test mode. In this paper, the newer model for variance, the Allan technique, now adopted for testing, is analyzed in the subject mode. A model is generated (including considerable contribution from the station secondary frequency standard), and rationalized with existing data.

A mean-frequency model is subsequently proposed, based on data available, but this model is not considered rigorous. It is an introductory idea, to be evaluated and incorporated if proved valid. It uses a fractional-calculus integral to obtain a quasi-stable result, as observed, with integrable spectrum poles.

The variance model is definitely sound; the Allan technique mates theory and measure. The mean-frequency model is an estimate; this problem is yet to be rigorously resolved. The unaltered defining expressions are nonconvergent, and the observed mean is quite erratic.

BURGESS, J. W.

B066 Comparative Studies of Ion-Implant Josephson-Effect Structures

R. K. Kirschman, J. A. Hutchby (Langley Research Center), J. W. Burgess (Langley Research Center), R. P. McNamara (California Institute of Technology), and H. A. Notarys (California Institute of Technology)

IEEE Trans. Magnet., Vol. MAG-13, No. 1, pp. 731–734, January 1977

For abstract, see Kirschman, R. K.

BURKE, E. S.

B067 Helios Mission Support

P. S. Goodwin, E. S. Burke, and T. P. Adamski

The Deep Space Network Progress Report 42-37: November and December 1976, pp. 39–42, February 15, 1977

For abstract, see Goodwin, P. S.

B068 Helios Mission Support

P. S. Goodwin, E. S. Burke, and G. M. Rockwell

The Deep Space Network Progress Report 42-38: January and February 1977, pp. 50–54, April 15, 1977

For abstract, see Goodwin, P. S.

B069 Helios Mission Support

P. S. Goodwin, E. S. Burke, and G. M. Rockwell

The Deep Space Network Progress Report 42-39: March and April 1977, pp. 17–22, June 15, 1977

For abstract, see Goodwin, P. S.

B070 Helios Mission Support

P. S. Goodwin, E. S. Burke, and G. M. Rockwell

The Deep Space Network Progress Report 42-40: May and June 1977, pp. 52–56, August 15, 1977

For abstract, see Goodwin, P. S.

BURKE, J. D.

B071 Lunar Polar Orbiter: A global Survey of the Moon

J. D. Burke

Acta Astronautica, Vol. 4, pp. 907–920, 1977

Lunar data from previous automated and manned exploratory missions have now been analyzed to the point where it is possible to define objectives for new missions to the Moon. The most logical next step is a polar orbiter designed to measure the Moon's gravity field, figure, heat flow, magnetism and surface composition. NASA has commissioned a study of this mission at JPL with participation by lunar scientists from JSC, and also has tentatively selected a group of investigators who constitute a Science Working Team. This paper describes the mission objectives and reports progress in the mission-definition study. As presently visualized, the orbiter will be launched by a Delta vehicle in 1980. After insertion into an eccentric, polar lunar orbit it will deploy a small, spinning subsatellite whose purpose is to relay precise radio Doppler measurements from the orbiter on the Moon's far side. After subsatellite delivery, the orbiter will maneuver into a low, circular polar orbit whence the instrument fields of view will be continuously pointed to the nadir for a nominal mission time of one year. Tracking and data acquisition will be via 26-m ground antennas and the JPL Mission Control and Computing Center, with distributed computing elements used in both flight and ground systems to simplify the data interfaces. Significant design advances are intended to include: (1) all systems designed to cost, (2) advanced scientific sensors aboard the spacecraft, (3) ground operations systems designed for largely automated, routine operation, and (4) design and operations concepts applicable to a variety of low-cost orbital missions in the Solar System.

BURT, R. W.

B072 A Maintenance and Operations Cost Model for the DSN

R. W. Burt and H. L. Kirkbride

The Deep Space Network Progress Report 42-38: January and February 1977, pp. 109–114, April 15, 1977

A cost model for the DSN is developed which is useful in analyzing the 10-year Life Cycle Cost of the Bent Pipe Project. The philosophy behind the development and the use made of a computer data base are detailed; the applicability of this model to other projects is discussed.

B073 Maintenance and Operations Cost Model for DSN Subsystems

R. W. Burt and J. R. Lesh

The Deep Space Network Progress Report 42-40: May and June 1977, pp. 91 – 96, August 15, 1977

A procedure is described which partitions the recurring costs of the Deep Space Network (DSN) over the individual DSN subsystems. The procedure results in a table showing the maintenance, operations, sustaining engineering and supportive costs for each subsystem.

BURUM, D. P.

B074 ADRF Experiments Using Near $n\pi$ Pulse Strings

W. K. Rhim, D. P. Burum, and D. D. Elleman

Phys. Lett., Vol. 62A, No. 7, pp. 507–508, October 3, 1977

For abstract, see Rhim, W. K.

B075 Multiple-Pulse Spin Locking in Dipolar Solids

W. K. Rhim, D. P. Burum, and D. D. Elleman

Phys. Rev. Lett., Vol. 37, No. 26, pp. 1764–1766, December 27, 1976

For abstract, see Rhim, W. K.

BUTMAN, S. A.

B076 The Effects of Bandpass Limiters on n-Phase Tracking Systems

S. A. Butman and J. R. Lesh

IEEE Trans. Commun., Vol. COM-25, No. 6, pp. 569–576, June 1977

The combination of a bandpass limiter and nth power tracking loop is considered. It is shown that the performance of the combination does not depend on the form of the nonlinear function used to create the nth harmonic signal as long as some energy in that zone is produced. Furthermore, the order in which the limiter and nth power nonlinearity occur is unimportant so that the

results apply equally well to the n-phase Costas type of implementations of the nth power loops. Closed form expressions for the signal suppression factors are obtained, and it is shown that the coherent and noncoherent SNR's out of the nth power-limiter combination can be expressed in terms of two of these suppression factors. This latter point enables one to estimate the loop SNR of an nth power-limited phase locked loop by simply calculating the suppression factors for nth and $(2n)$th power loops. Finally, nth power phase locked loops without limiters are compared with similar loops with limiters where it is shown that the presence of the limiter can actually enhance the output SNR at moderate to large values of input SNR.

CALLAHAN, P. S.

C001 A Preliminary Analysis of Viking S-X Doppler Data and Comparison to Results of Mariner 6, 7, and 9 DRVID Measurements of the Solar Wind Turbulence

P. S. Callahan

The Deep Space Network Progress Report 42-39: March and April 1977, pp. 23–29, June 15, 1977

More than 135 passes of Viking S-X doppler data have been used to investigate the solar wind turbulence from 3 August to 15 December 1976. The results of this analysis are compared to previous investigations using Mariner DRVID data to attempt to find the changes in the turbulence over the sunspot cycle. It is found that: (1) electron density fluctuations decline with heliocentric distance as $r^{1.8\pm0.2}$; (2) the level of the turbulence may be a factor 2 lower near sunspot minimum than at maximum; and (3) the spectrum of the fluctuations may be steeper($\sim\div3.0$ vs $\sim\div2.6$) near sunspot minimum. The expected range error for various time scales and geometries is derived from the results.

C002 A First-Principles Derivation of Doppler Noise Expected From Solar Wind Density Fluctuations

P. S. Callahan

The Deep Space Network Progress Report 42-42: September and October 1977, pp. 42–53, December 15, 1977

The level of Doppler noise (DN) expected from solar wind (SW) density fluctuations (DF) is derived beginning with the expression for refractive index variations. The calculation takes account of up- and downlink paths and of the method actually used to produce the DN values. The usual assumptions that the DF are frozen in, that the large-scale radial variation can be separated from the DF, that the DF power spectrum is a power law with "outer scale" k_o, and that the DF are homogeneous on scales less than $2c\Delta t$, Δt = sample time, are made. The result agrees quite well with the observations of DN by Berman (1977). Corrections for the finite number of points used in the actual algorithm are discussed.

CAMPBELL, R.

C003 An Analysis of the Technical Status of High Level Radioactive Waste and Spent Fuel Management Systems

T. English, C. Miller, E. Bullard, R. Campbell, A. Chockie, E. Divita, C. Douthitt (California Institute of Technology), E. Edelson, and L. Lees (California Institute of Technology)

JPL Publication 77-69, December 1, 1977

For abstract, see English, T.

CAMY-PEYRET, C.

C004 Spectrum of $H_2{}^{18}O$ and $H_2{}^{17}O$ in the 5030 to 5640 cm^{-1} Region

R. A. Toth, J. M. Flaud (Campus d'Orsay, France), and C. Camy-Peyret (Campus d'Orsay, France)

J. Mol. Spectros., Vol. 67, Nos. 1–3, pp. 185–205, September 15, 1977

For abstract, see Toth, R. A.

C005 Spectrum of $H_2{}^{18}O$ and $H_2{}^{17}O$ in the 6974 to 7387 cm^{-1} Region

R. A. Toth, J. M. Flaud (Laboratoire de Physique Moleculaire et d' Optique, Orsay), and C. Camy-Peyret (Laboratoire de Physique Moleculaire et d' Optique, Orsay)

J. Mol. Spectros., Vol. 67, Nos. 1–3, pp. 206–218, September 15, 1977

For abstract, see Toth, R. A.

C006 Strengths of H_2O Lines in the 5000–5750 cm^{-1} Region

R. A. Toth, C. Camy-Peyret (Laboratoire de Physique Moleculaire et d'Optique, Orsay), and J. M. Flaud (Laboratoire de Physique Moleculaire et d'Optique, Orsay)

J. Quant. Spectros. Radiat. Transfer, Vol. 18, pp. 515–523, 1977

For abstract, see Toth, R. A.

CANNON, R.

C007 Computation of Spacecraft Signal Raypath Trajectories Relative to the Sun

R. Cannon and C. Stelzried

The Deep Space Network Progress Report 42-38: January and February 1977, pp. 77–82, April 15, 1977

A computer program (CTS 41B) used to determine the trajectory of a spacecraft signal raypath has been updated to increase its usefulness during solar conjunctions (CTS 41C). The closest point of approach of the raypath to the sun is projected onto the surface and the solar latitude and longitude calculated. A sample computation and plots are given for the 1976 Viking solar conjunction. Eventually it may be possible to predict the communication link performance degradation in the near sun region due to solar activity.

CAPONE, L. A.

C008 The Photochemistry of Ammonia in the Jovian Atmosphere

S. S. Prasad and L. A. Capone (Ames Research Center)

J. Geophys. Res., Space Phys., Vol. 81, No. 31, pp. 5596–5600, November 1, 1976

For abstract, see Prasad, S. S.

CAPUTO, R.

C009 An Initial Comparative Assessment of Orbital and Terrestrial Central Power Systems: Final Report

R. Caputo

JPL Publication 77-44, March 15, 1977

This initial study compares a silicon photovoltaic orbital power system, which is constructed from an earth source of materials, to likely terrestrial (fossil, nuclear, and solar) approaches to central power generation around the year 2000. A total social cost framework is used that considers not only the projection of commercial economics (direct or internal costs), but also considers external costs such as RD&D investment, health impacts, resource requirements, environmental impacts, and other social costs.

CARLSON, F. R., JR.

C010 Detection of Combined Occurrences

A. L. Zobrist and F. R. Carlson, Jr. (University of Southern California)

Commun. ACM, Vol. 20, No. 1, pp. 31–35, January 1977

For abstract, see Zobrist, A. L.

CARTER, J. R., JR.

C011 Solar Cell Radiation Handbook

H. Y. Tada (TRW Systems Group) and J. R. Carter, Jr.

JPL Publication 77-56, November 1, 1977

For abstract, see Tada, H. Y.

CARTWRIGHT, D. C.

C012 Electron Impact Excitation of the Rydberg States in O_2 in the 7–10 eV Energy-Loss Region

S. Trajmar, D. C. Cartwright (Los Alamos Scientific Laboratory), and R. I. Hall (Universite Pierre et Marie Curie, Paris, France)

J. Chem. Phys., Vol. 65, No. 12, pp. 5275–5279, December 15, 1976

For abstract, see Trajmar, S.

CHAHINE, M. T.

C013 Remote Sounding of Cloudy Atmospheres. II. Multiple Cloud Formations

M. T. Chahine

J. Atmos. Sci., Vol. 34, No. 5, pp. 744–757, May 1977

The dual frequency-range principle developed in Part I (Chahine, 1974) for infrared remote sounding of atmospheric temperature profiles in the presence of a single cloud layer is extended here to the case of multiple cloud formations. The approach requires no *a priori* knowledge of the spectral properties of the clouds or the number of cloud layers in the fields of view. The method of solution requires measurements over adjacent fields of view and leads to the determination of the clear-column atmospheric temperature profiles with the same degree of accuracy and vertical resolution permitted under cloudless conditions. Numerical verifications are carried out to illustrate the stability and accuracy of the method using simulated radiance data, from the 4.3 and 15 μm CO_2 bands in the terrestrial atmosphere, in the presence of up to three cloud layers in the fields of view.

C014 Remote Sounding of Cloudy Atmospheres. III. Experimental Verifications

M. T. Chahine, H. H. Aumann, and F. W. Taylor

J. Atmos. Sci., Vol. 34, No. 5, pp. 758–765, May 1977

The cloud-filtering technique developed in Parts I and II of this study is experimentally verified in this paper. The verification is based on radiance data measured in the 4.3 and 15 μm CO_2 bands using a multidetector sounder mounted on an aircraft. The results presented here show that, from the aircraft height of 7.6 km and in the presence of multiple cloud formations, it is possible to recover simultaneously:

1) The clear-column atmospheric temperature profile with an rms error of 1 K with respect to radiosondes.

2) The land and sea surface temperature at all sun zenith angles. The accuracy of the recovered sea-surface temperature is 0.5–1 K with respect to measured bucket temperatures.

3) The humidity profile (water vapor mixing ratio) with a precision of 10%.

4) The fractional covers and heights of up to three cloud formations.

5) The types of clouds, i.e., whether convective or nonconvective.

CHAI, V. W.

C015 A Thermodynamic Analysis of a Solar-Powered Jet Refrigeration System

F. L. Lansing and V. W. Chai

The Deep Space Network Progress Report 42-41: July and August 1977, pp. 209–217, October 15, 1977

For abstract, see Lansing, F. L.

CHANEY, W. D.

C016 DSN Tracking System—Mark III-77

W. D. Chaney

The Deep Space Network Progress Report 42-40: May and June 1977, pp. 4–13, August 15, 1977

This article provides a description of the DSN Tracking System—Mark III-77 currently in use for multimission support. Tracking functions performed by the Deep Space Stations, Ground Communications Facility, and Network Operations Control Center are given. Changes that were made to the subsystems of the DSN Tracking System—Mark III-75 to implement the DSN Tracking System—Mark III-77 are briefly described.

CHAO, C. C.

C017 Improvements in Navigation Resulting from the Use of Dual Spacecraft Radiometric Data

C. C. Chao, H. L. Siegel, and V. J. Ondrasik

The Deep Space Network Progress Report 42-38: January and February 1977, pp. 55–65, April 15, 1977

When two interplanetary spacecraft lie along similar geocentric lines-of-sight, navigational advantages may be achieved by navigating one spacecraft with respect to the other. Opportunities to employ this technique will become more common as more multiprobe missions are launched. The two Viking spacecraft and the two Mariner Jupiter/Saturn '77 spacecraft will be within two and three degrees of each other, respectively, for a large portion of their missions. Results of simulated analysis as well as the processing of real tracking data from the two Viking spacecraft reveal the following advantages of the dual spacecraft navigation technique: (1) cancellation of platform parameter and transmission media modeling errors in short arc solutions, (2) accurate encounter guidance for the trailing spacecraft, (3) reduction of total tracking requirements, and (4) rapid determination of the orbit following a maneuver on either spacecraft.

CHAPMAN, P. C.

C018 Comparison of Model Test Results: Multipoint Sine Versus Single-Point Random

E. L. Leppert, S. H. Lee, F. D. Day, P. C. Chapman, and B. K. Wada

Preprint 760879, SAE Aerosp. Eng. Manuf. Meeting, San Diego, CA, Nov. 29–Dec. 2, 1976

For abstract, see Leppert, E. L.

CHASE, S. C., JR.

C019 Martian North Pole Summer Temperatures: Dirty Water Ice

H. H. Kieffer (University of California, Los Angeles), S. C. Chase, Jr. (Santa Barbara Research Center), T. Z. Martin (University of California, Los Angeles), E. D. Miner, and F. D. Palluconi

Science, Vol. 194, pp. 1341–1344, December 17, 1976

For abstract, see Kieffer, H. H.

CHEN, J. C.

C020 Matrix Perturbation for Structural Dynamic Analysis

J. C. Chen and B. K. Wada

AIAA J., Vol. 15, No. 8, pp. 1095–1100, August 1977

The objective of the effort was to investigate methodologies to reduce the cost of evaluating changes in dynamic loads when small modifications are made in the structure. A matrix perturbation technique has been developed to calculate the dynamic responses of a structural system that has been modified from the original design. The calculation is based on the results of the original design and the assumption that the structural modification is small. The advantage of the method is an update of the dynamic response caused by design changes without performing an entire analysis. This procedure can be used in a design load analysis cycle in which the structural design is subject to frequent changes. A sample problem is given to demonstrate the validity of the technique.

CHENG, D.

C021 X-Band Atmospheric Noise Temperature Statistics at Goldstone DSS 13, 1975–1976

S. Slobin, M. Reid, R. Gardner, and D. Cheng

The Deep Space Network Progress Report 42-38: January and February 1977, pp. 70–76, April 15, 1977

For abstract, see Slobin, S.

CHIRIVELLA, J. E.

C022 Small Monopropellant Thruster Contamination Measurement in a High-Vacuum Low-Temperature Facility

R. S. Passamaneck and J. E. Chirivella

J. Spacecraft Rockets, Vol. 14, No. 7, pp. 419–426, July 1977

For abstract, see Passamaneck, R. S.

CHOCKIE, A.

C023 An Analysis of the Technical Status of High Level Radioactive Waste and Spent Fuel Management Systems

T. English, C. Miller, E. Bullard, R. Campbell, A. Chockie, E. Divita, C. Douthitt (California Institute of Technology), E. Edelson, and L. Lees (California Institute of Technology)

JPL Publication 77-69, December 1, 1977

For abstract, see English, T.

CHRISTENSEN, P. R.

C024 Temperatures of the Martian Surface and Atmosphere: Viking Observation of Diurnal and Geometric Variations

H. H. Kieffer (University of California, Los Angeles), P. R. Christensen (University of California, Los Angeles), T. Z. Martin (University of California, Los Angeles), E. D. Miner, and F. D. Palluconi

Science, Vol. 194, pp. 1346–1351, December 17, 1976

For abstract, see Kieffer, H. H.

CHUTJIAN, A.

C025 High-Resolution Threshold Photoelectron Spectroscopy by Electron Attachment

J. M. Ajello and A. Chutjian

J. Chem. Phys., Vol. 65, No. 12, pp. 5524–5525, December 15, 1976

For abstract, see Ajello, J. M.

C026 Quantum Mechanical and Crossed Beam Study of Vibrational Excitation of N_2 by Electron Impact at 30–75 eV

D. G. Truhlar (University of Minnesota), M. A. Brandt (University of Minnesota), S. K. Srivastava, S. Trajmar, and A. Chutjian

J. Chem. Phys., Vol. 66, No. 2, pp. 655–663, January 15, 1977

For abstract, see Truhlar, D. G.

C027 Studies of Ar and N_2 Using Threshold Photoelectron Spectroscopy by Electron Attachment (TPSA)

A. Chutjian and J. M. Ajello

J. Chem. Phys., Vol. 66, No. 10, pp. 4544–4550, May 15, 1977

Threshold photoelectron spectra of Ar and N_2 are studied by the technique of attachment of the threshold electron to SF_6 followed by detection of the SF_6^-. Studies on Ar provide a measure of the rejection ratio for nonthreshold electrons of this technique. This ratio is compared to that for two other types of electron detectors. Collisional ionization of high Rydberg-state electrons by SF_6 is also observed and discussed. In N_2 direct ionization to vibrational levels of the $X^2\Sigma_g^+$, $A^2\Pi_u$, and $B^2\Sigma_u^+$ states of N_2^+ are clearly resolved. Moreover, resonant autoionizations are found to greatly enhance the population of the vibrational levels of the X state and

the $v' = 2$ level of the A state over that expected from direct photoionization alone. Extra peaks lying between the vibrational levels are detected which correspond to autoionization into high levels of the N_2^+ ion. From intensity considerations a rotational propensity rule is given which states that an autoionizing N_2 state prefers to decay to N_2^+ states with a minimum change in rotational angular momentum. Normalization of the threshold spectra to the absolute cross section scale is also discussed.

C028 Electron Impact Excitation of SF_6

S. Trajmar and A. Chutjian

J. Phys. B: At. Mol. Phys., Vol. 10, No. 14, pp. 2943–2949, 1977

For abstract, see Trajmar, S.

CITRON, O. R.

C029 Institutional and Environmental Aspects of Geothermal Energy Development

O. R. Citron

Nucl. Technol., Vol. 34, pp. 38–42, June 1977

The increasing interest in exploiting the variety of geothermal resources has prompted an examination of the institutional barriers to their introduction for commercial use. A significant effort was undertaken by the Jet Propulsion Laboratory as a part of a national study to identify existing constraints to geothermal development and possible remedial actions. These aspects included legislative and legal parameters plus environmental, social, and economic considerations.

CLAUSS, R.

C030 Simple Waveguide Reflection Maser With Broad Tunability

L. D. Flesner (University of California, San Diego), S. Schultz (University of California, San Diego), and R. Clauss

Rev. Sci. Instrum., Vol. 48, No. 8, pp. 1104–1105, August 1977

For abstract, see Flesner, L. D.

CLAUSS, R. C.

C031 X- and K-Band Maser Development: Effects of Interfering Signals

R. C. Clauss

The Deep Space Network Progress Report 42-42: September and October 1977, pp. 85–87, December 15, 1977

Signals at levels exceeding −90 dBmW at the input connection of a traveling-wave maser can affect maser performance in a variety of ways. Both S-band and X-band masers are considered where interfering signals are: (1) within the maser bandpass, (2) near the maser bandpass, and (3) far from the maser bandpass, where mixing with the maser pump can occur.

CLYNE, M. A. A.

C032 Kinetic Studies of Diatomic Free Radicals Using Mass Spectrometry: Part 4. The Br + OClO and BrO + ClO Reactions

M. A. A. Clyne (Queen Mary College, London) and R. T. Watson

J. Chem. Soc., Faraday Trans. I, Vol. 73, pp. 1169–1187, 1977

In a kinetic study of the reaction of ground state Br $^2P_{3/2}$ bromine atoms with chlorine dioxide, it has proved possible to determine not only the rate constant for the primary reaction, but also the rate constants for the various reactions of ClO with BrO radicals via different channels. The reaction kinetics were studied in a flow system using collision-free sampling of free radicals and stable molecules to a mass spectrometer. The thermochemistry and reaction kinetics of the XO + XO reactions (X = Cl, Br) are discussed. The ClO + ClO, BrO + BrO and BrO + ClO reactions are all thought to occur via related free radical channels XO + XO $\rightleftharpoons$ X + XOO. In addition, the ClO + ClO and BrO + ClO reactions occur through a similar and parallel channel, XO + XO $\rightleftharpoons$ X + OXO.

COCKRUM, R. H.

C033 The Effect of Oxidation-Expanded Defects Upon MOS Parameters

S. Prussin, S. P. Li, and R. H. Cockrum

J. Appl. Phys., Vol. 48, No. 11, pp. 4613–4617, November 1977

For abstract, see Prussin, S.

COLBURN, D. S.

C034 August 1972 Solar-Terrestrial Events: Observations of Interplanetary Shocks at 2.2 AU

E. J. Smith, L. Davis, Jr. (California Institute of Technology), P. J. Coleman, Jr. (University of California, Los Angeles), D. S. Colburn (Ames Research Center), P. Dyal (Ames Research Center), and D. E. Jones (Brigham Young University)

J. Geophys. Res., Space Phys., Vol. 82, No. 7, pp. 1077–1086, March 1, 1977

For abstract, see Smith, E. J.

COLEMAN, P. J., JR.

C035 August 1972 Solar-Terrestrial Events: Observations of Interplanetary Shocks at 2.2 AU

E. J. Smith, L. Davis, Jr. (California Institute of Technology), P. J. Coleman, Jr. (University of California, Los Angeles), D. S. Colburn (Ames Research Center), P. Dyal (Ames Research Center), and D. E. Jones (Brigham Young University)

J. Geophys. Res., Space Phys., Vol. 82, No. 7, pp. 1077–1086, March 1, 1977

For abstract, see Smith, E. J.

COLLINS, D.

C036 Experiments on the Properties of Superfluid Helium in Zero Gravity

P. Mason, D. Collins, D. Petrac, L. Yang, F. Edeskuty, and K. Williamson

Proc. Sixth Int. Cryog. Eng. Conf., Grenoble, France, May 11–14,1976, pp. 272–277

For abstract, see Mason, P.

CONLEY, J.

C037 Imaging Air Pollutants in the Near Ultraviolet

D. Norris, J. Conley, and S. Seng

Proc. SPIE, Vol. 91, pp. 116–122, 1976

For abstract, see Norris, D.

COOPER, M. A.

C038 Fluorine-19 NMR Studies of Fluoroaromatic Systems with Complete Proton Decoupling: The Signs and Magnitudes of Certain F...F and ^{13}C...F Spin–Spin Couplings

S. L. Manatt and M. A. Cooper (ICI, Ltd., Grangemouth, Scotland)

J. Amer. Chem. Soc., Vol. 99, No. 14, pp. 4561–4567, July 6, 1977

For abstract, see Manatt, S. L.

COSTOGUE, E. N.

C039 Performance Data for a Terrestrial Solar Photovoltaic/Water Electrolysis Experiment

E. N. Costogue and R. K. Yasui

Solar Energy, Vol. 19, pp. 205–210, 1977

This paper presents the performance data of a solar photovoltaic water electrolysis experiment conducted at JPL. The data indicated a feasible operation whereby a hydrogen electrolysis cell can be connected directly to a solar array source. The experiment goals were to examine the dynamic interaction of the solar array source and the hydrogen electrolysis cell with little consideration of optimization. An approach to optimization is discussed, which entails the use of electrolysis cells connected in series to match the voltage and current available at the maximum power point of the solar array. Connecting electrolysis cells directly to the solar array makes unnecessary the use of power-conditioning equipment. To assure solar array maximum power utilization, a maximum power point tracker may be required to continually match the power requirements of the electrolysis cells to the available power from the solar array source. A brief study of the technical problems facing a large-scale hydrogen production via electrolysis pointed out that there are operational voltage and current limitations, as well as power control and power management problems.

CRAWFORD, D. W.

C040 Analysis of Pulsatile, Viscous Blood Flow Through Diseased Coronary Arteries of Man

L. D. Back, J. R. Radbill, and D. W. Crawford (University of Southern California)

J. Biomech., Vol. 10, pp. 339–353, 1977

For abstract, see Back, L. D.

CROW, R. B.

C041 DSN Automation

R. B. Crow

The Deep Space Network Progress Report 42-37: November and December 1976, pp. 88–104, February 15, 1977

Automation of the DSN has been under consideration for the past several years and has been justified on anticipated reduction in life cycle cost, resulting from in-

creased productivity and reduced operations cost. This article summarizes an overall hierarchical automation philosophy along with the results of the RF automation effort undertaken 2 years ago. A brief description of each subassembly controller's salient features, the software development process, and the common software used by these controllers will be presented. Comments will be made with respect to the relative advantages of PL/M high-level language and assembly language, the operational effectiveness of operator "Macro commands," and the program development, and a list of suggested future effort will be given. This article provides for technology transfer and offers new ideas for consideration in future automation efforts.

CRUICKSHANK, M. J.

C042 Computer Image Processing in Marine Resource Exploration

P. R. Paluzzi, W. R. Normark (U. S. Geological Survey), G. R. Hess (U. S. Geological Survey), H. D. Hess (U. S. Geological Survey), and M. J. Cruickshank (U. S. Geological Survey)

Proc. MTS-IEEE Oceans '76 Conf., Washington, D. C., Sept. 13–15, 1976, pp. 4D-1–4D-10

For abstract, see Paluzzi, P. R.

CUFFEL, R. F.

C043 Flow and Heat Transfer Measurements in a Pseudo-Shock Region With Surface Cooling

R. F. Cuffel and L. H. Back

AIAA J., Vol. 14, No. 12, pp. 1716–1722, December 1976

An experimental investigation was conducted to acquire information on the flow structure, mean flowfield, and temperature distributions in a pseudo-shock region in a supersonic diffuser with surface cooling. The Mach number upstream was 2.9, and the wall to stagnation temperature ratio was 0.44. A Mach-disk-like shock wave emanated from the thin separated flow region near the beginning of the compression region, and reattachment occurred one diameter downstream so that the flow was not separated over most of the pseudo-shock region. The flow compression was a shock-free, predominantly viscous process. Along the pseudo-shock region the measured heat-transfer coefficient increased approximately as the 0.8 power of the measured wall static pressure. The estimated wall shear stress increased downstream of flow attachment, but was considerably less than the upstream value.

CULICK, F. E. C.

C044 Role of Condensed Phase Details in the Oscillatory Combustion of Composite Propellants

K. N. Ramohalli and F. E. C. Culick (California Institute of Technology)

Combust. Sci. Technol., Vol. 15, pp. 179–199, 1977

For abstract, see Ramohalli, K. N.

CUTTING, E.

C045 Mission Design for SEASAT-A, An Oceanographic Satellite

E. Cutting, G. H. Born, J. C. Frautnick, W. I. McLaughlin, R. A. Neilson, and J. A. Thielen (Lockheed Missiles & Space Co.)

Preprint 77-31, AIAA Fifteenth Aerosp. Sci. Meet., Los Angeles, Calif., Jan. 24–26, 1977

SEASAT-A is a NASA Earth satellite for measuring global ocean dynamics from space. Launch is planned for May 1978. The instruments on the spacecraft will provide data on wave height and direction, surface wind speed and direction, ice fields, ocean surface topography and weather. This paper is concerned with the mission design for SEASAT-A. A primary topic here is the selection of the orbit which best satisfies the measurement objectives of the various instruments. The maintenance of this orbit under drag and other perturbations is discussed. The design of the mission profile is outlined. Finally precision orbit determination for SEASAT-A is discussed since it is required to maximize ocean topography accuracy.

CUTTS, J. A.

C046 Galilean Satellites: Anomalous Temperatures Disputed

D. Morrison (University of Arizona), L. A. Lebofsky, J. A. Cutts (Planetary Science Institute), G. J. Veeder, and S. H. Gross (Polytechnic Institute of New York)

Science, Vol. 195, pp. 90–93, January 7, 1977

For abstract, see Morrison, D.

DACHEL, P. R.

D001 Hydrogen Maser Frequency Standards for the Deep Space Network

P. R. Dachel, S. M. Petty, R. F. Meyer, and R. L. Sydnor

ORIGINAL PAGE IS OF POOR QUALITY

The Deep Space Network Progress Report 42-40: May and June 1977, pp. 76–83, August 15, 1977

JPL has been operating two experimental hydrogen maser frequency standards at the Deep Space Network (DSN) stations at Goldstone, California, since 1970. Based on operating experience gained with these units and with a test bed maser system at JPL, a field-operable maser has been developed for use in the DSN. The first maser of this new design was installed at the DSN 64-meter station near Canberra, Australia, in December 1975. Second and third units are presently under construction for the remaining DSN 64-meter stations at Madrid, Spain, and Goldstone, California. While these DSN masers remain similar in basic configuration to the earlier experimental units, many design changes have been incorporated in both physics and electronics systems to effect improvements in the following areas: (1) short- and long-term frequency stability, (2) RF isolation of maser output lines, (3) lifetime of active physics components, (4) automatic fault detection and location, and (5) performance and reliability of the receiver-synthesizer system. Frequency stability measurements of the DSS 43 maser, using an updated experimental maser as a reference, resulted in a fractional frequency stability of 3.8×10^{-15} long term ($\tau = 90$ seconds) and 1.1×10^{-13} short term ($\tau = 1$ second).

DATTA, T.

D002 Electrical, Magnetic, and Optical Properties of the Tetrathiafulvalene (TTF) Pseudohalides, $(TTF)_{12}(SCN)_7$ and $(TTF)_{12}(SeCN)_7$

R. B. Somoano, A. Gupta, V. Hadek, M. Novotny (Stanford University), M. Jones (Tulane University), T. Datta (Tulane University), R. Deck (Tulane University), and A. M. Hermann (Tulane University)

Phys. Rev., Pt. B: Solid State, Vol. 15, No. 2, pp. 595–601, January 15, 1977

For abstract, see Somoano, R. B.

DAVIDSON, J.

D003 Word Processing Today

J. Davidson

J. Soc. Res. Admin., Vol. 8, No. 2, pp. 31–43, 1976

The goals of Multifunctional Word Processing are discussed: cost-effective acceptance of all input, establishing of a compatible media link for intermachine editing, the satisfying of all communication needs, and the compatible storage and retrieval of all forms.

DAVIES, D. W.

D004 Infrared Observations of Jupiter Cloud Zones

D. W. Davies

Icarus, Vol. 30, pp. 286–294, 1977

Images of Jupiter have been obtained at three wavelengths intervals in the infrared: 0.7–2.5, 1.2–1.3, and 1.5–1.7 μm. The images show evidence for two distinct zones of high-altitude clouds, one at 10° north latitude, the other at 22° south. The cloud zones also appear to be at different heights in the atmosphere and to have particles with different scattering properties.

D005 Behavior of Volatiles in Mars' Polar Areas: A Model Incorporating New Experimental Data

D. W. Davies, C. B. Farmer, and D. D. LaPorte (Santa Barbara Research Center)

J. Geophys. Res., Vol. 82, No. 26, pp. 3815–3822, September 10, 1977

A model has been developed to explain the north polar water vapor results obtained by the Viking orbiter Mars atmospheric water detector; it has also been used to compute the thickness of seasonally deposited CO_2 frost, the variation of the total atmospheric pressure, and wind velocities due to mass motions associated with CO_2 condensation. A north polar water ice thickness in excess of 1 m and an ice albedo a of $0.34^{+0.06}_{-0.03}$ are inferred from a comparison of the model and experimental data. The model results confirm an earlier conclusion that the atmosphere over the ice is saturated. It is suggested that concentration of the atmospheric inert gases in the polar region, combined with local topography and arctic circulation patterns, could be responsible for the south remnant cap not being at the south pole.

D006 Mars: Northern Summer Ice Cap—Water Vapor Observations from Viking 2

C. B. Farmer, D. W. Davies, and D. D. LaPorte (Santa Barbara Research Center)

Science, Vol. 194, pp. 1339–1341, December 17, 1976

For abstract, see Farmer, C. B.

DAVIS, E. K.

D007 Tracking and Data System Support for the Mariner Venus/Mercury 1973 Project

E. K. Davis and M. R. Traxler

Technical Memorandum 33-797, May 1, 1977

The Tracking and Data System provided outstanding support to the Mariner Venus/Mercury 1973 Project

during the period from January 1970 through March 1975. In this report, we have chronologically described the Tracking and Data System organizations, plans, processes, and technical configurations, which were developed and employed to facilitate achievement of mission objectives. In the Deep Space Network position of the Tracking and Data System, a number of special actions were taken to greatly increase the scientific data return and to assist the Project in coping with in-flight problems. The benefits of such actions were high; however, there was also a significant increase in risk as a function of the experimental equipment and procedures required. The excellent tracking and data acquisition support provided under these conditions is attributable to the dedication and professionalism of our engineering and operations people.

DAVIS, E. S.

D008 Options for Demonstrating the Use of Solar Energy in California Buildings

E. S. Davis and G. Yanow

JPL Publication 77-33, September 1976

Three programmatic options for demonstrating the most economically attractive applications of solar energy to buildings located in California are formulated. These options are presented to the State of California Energy Resources Conservation and Development Commission to provide 1) a framework for soliciting and selecting projects, 2) a basis for influencing the implementation of federal demonstration programs in California, and 3) factors for budget estimating and assumptions for planning purposes. These options are presented in tabular form corresponding to three budgetary limits: a $500,000 Program, a $1,000,000 Program, and a $3,000,000 Program.

The unique characteristics of solar energy demonstration programs and the involvement of key decision makers are discussed in detail. The demonstration programs are related to specific purposes. The priority structure used to select the generic projects making up each program is discussed in relationship to the purposes of the program. In addition, some implications of the nature of the demonstration program for management are outlined. Related information concerning the ERDA/HUD Solar Energy Demonstration Program in California, statistical data, and a general description of solar energy systems are appended to this report.

DAVIS, L., JR.

D009 August 1972 Solar-Terrestrial Events: Observations of Interplanetary Shocks at 2.2 AU

E. J. Smith, L. Davis, Jr. (California Institute of Technology), P. J. Coleman, Jr. (University of California, Los Angeles), D. S. Colburn (Ames Research Center), P. Dyal (Ames Research Center), and D. E. Jones (Brigham Young University)

J. Geophys. Res., Space Phys., Vol. 82, No. 7, pp. 1077–1086, March 1, 1977

For abstract, see Smith, E. J.

DAY, F. D.

D010 Comparison of Model Test Results: Multipoint Sine Versus Single-Point Random

E. L. Leppert, S. H. Lee, F. D. Day, P. C. Chapman, and B. K. Wada

Preprint 760879, SAE Aerosp. Eng. Manuf. Meeting, San Diego, CA, Nov. 29–Dec. 2, 1976

For abstract, see Leppert, E. L.

DE GROOT, N. F.

D011 CCIR Papers on Telecommunications for Deep Space Research

N. F. de Groot

The Deep Space Network Progress Report 42-42: September and October 1977, pp. 162–183, December 15, 1977

Three JPL papers on telecommunications for deep space research were recently adopted by Study Group 2 of the International Radio Consultative Committee (CCIR). In this article, we present a brief description of United States participation in the process of developing the technical basis for international allocation and regulation of the radio frequency spectrum. The first of the three papers is then presented in its CCIR format and style. The paper considers the telecommunication requirements for deep space research. Topics include functional requirements, methods and techniques, and equipment characteristics.

DECK, R.

D012 Electrical, Magnetic, and Optical Properties of the Tetrathiafulvalene (TTF) Pseudohalides, $(TTF)_{12}(SCN)_7$ and $(TTF)_{12}(SeCN)_7$

R. B. Somoano, A. Gupta, V. Hadek, M. Novotny (Stanford University), M. Jones (Tulane University), T. Datta (Tulane University), R. Deck (Tulane University), and A. M. Hermann (Tulane University)

Phys. Rev., Pt. B: Solid State, Vol. 15, No. 2, pp. 595–601, January 15, 1977

For abstract, see Somoano, R. B.

DeFOREST, S. E.

D013 Active Control of Spacecraft Potentials at Geosynchronous Orbit

R. Goldstein and S. E. DeForest (University of Alabama)

Progr. Astronaut. Aeronaut., Vol. 47, pp. 169–181, 1976

For abstract, see Goldstein, R.

DeMORE, W. B.

D014 Rate Constant for the Reaction of Atomic Bromine With Ozone

M. T. Leu and W. B. DeMore

Chem. Phys. Lett., Vol. 48, No. 2, pp. 317–320, June 1, 1977

For abstract, see Leu, M. T.

D015 Rate Constant for Formation of Chlorine Nitrate by the Reaction ClO + NO_2 + M

M. T. Leu, C. L. Lin, and W. B. DeMore

J. Phys. Chem., Vol. 81, No. 3, pp. 190–195, 1977

For abstract, see Leu, M. T.

DIVINE, N.

D016 Evaluation of Jupiter Longitudes in System III(1965)

P. K. Seidelmann (U. S. Naval Observatory) and N. Divine

Geophys. Res. Lett., Vol. 4, No. 2, pp. 65–68, February 1977

For abstract, see Seidelmann, P. K.

DIVITA, E.

D017 An Analysis of the Technical Status of High Level Radioactive Waste and Spent Fuel Management Systems

T. English, C. Miller, E. Bullard, R. Campbell, A. Chockie, E. Divita, C. Douthitt (California Institute of Technology), E. Edelson, and L. Lees (California Institute of Technology)

JPL Publication 77-69, December 1, 1977

For abstract, see English, T.

DOBROTIN, B. M.

D018 An Application of Microprocessors to a Mars Roving Vehicle

B. M. Dobrotin and D. A. Rennels

Proc. 1977 Joint Automat. Contr. Conf., San Francisco, Calif., June 22–24, 1977, pp. 185–196

This paper presents an approach to a microprocessor based computing system for a Mars Roving Vehicle. This represents a practical example in that it combines a breadboard robot (the Rover) with a distributed microprocessor computing system, both of which are under development at JPL and are being considered for a 1984 Mars Rover Mission. A summary of the Rover functions is presented, along with an approach of applying distributed computers. The Rover is then partitioned into its main subsystems (executive, locomotive, manipulation, and vision) and subsystem and system interfaces established. Computing requirements are discussed and a system diagram developed.

DONNER, M. D.

D019 Digital High Density (80 Mb/s) Tape

M. D. Donner

The Deep Space Network Progress Report 42-42: September and October 1977, pp. 110–118, December 15, 1977

This article describes work with a state-of-the-art high density digital PCM tape recorder–reproducer system recently purchased by JPL. The tape recorder is designed for 80 Mb/s operation at an overall bit error rate of 10^{-5} and for 40 Mb/s operation at 10^{-6}. The article describes the process of measuring the error rate. Also detailed is a data rate buffer designed for use in recent radar experiments and generalizable to most potential uses of the recorder system.

DOUTHITT, C.

D020 An Analysis of the Technical Status of High Level Radioactive Waste and Spent Fuel Management Systems

T. English, C. Miller, E. Bullard, R. Campbell, A. Chockie, E. Divita, C. Douthitt (California Institute of Technology), E. Edelson, and L. Lees (California Institute of Technology)

JPL Publication 77-69, December 1, 1977

For abstract, see English, T.

DOWDY, M. W.

D021 **Development and Qualification of the Propellant Management System for Viking 75 Orbiter**

M. W. Dowdy, R. E. Hise (Martin Marietta Corporation), and R. G. Peterson (Martin Marietta Corporation)

J. Spacecraft Rockets, Vol. 14, No. 3, pp. 133–140, March 1977

The Viking 75 Orbiter propulsion subsystem uses Earth storable propellants, monomethylhydrazine and nitrogen tetroxide, to provide midcourse corrections, Mars orbit insertion, and Mars orbit changes for the Viking spacecraft. A surface-tension propellant management system provides propellant center-of-mass control, supplies gas-free propellant to the engine, and insures liquid-free gas venting if required. The surface tension system consists of a passive sheet metal baffle assembly, a communication channel, and a pressurization/vent tube. This paper describes the development and qualification of the surface tension system and includes results of low-g drop tower tests of scale models, 1-g simulation tests of low-g large ullage settling and liquid withdrawal, structural qualification tests, and propellant surface-tension/contact-angle studies. Subscale testing and analyses were used to evaluate the ability of the system to maintain or recover the desired propellant orientation following possible disturbances during the Viking mission. This effort included drop tower tests to demonstrate that valid wick paths exist for moving any displaced propellant back over the tank outlet. Variations in surface tension resulting from aging, temperature, and lubricant contamination were studied and the effects of surface finish, referee fluid exposure, aging, and lubricant contamination on contact angle were assessed. Results of movies of typical subscale drop tower tests and full scale slosh tests are discussed.

DVORAK, J.

D022 **The Nature of the Gravity Anomalies Associated With Large Young Lunar Craters**

J. Dvorak (California Institute of Technology) and R. J. Phillips

Geophys. Res. Lett., Vol. 4, No. 9, pp. 380–382, September 1977

The negative Bouguer anomalies (i.e., mass deficiencies) associated with four young lunar craters are analyzed. Model calculations based on generalizations made from studies of terrestrial impact structures suggest that the major contribution to the Bouguer anomaly for these lunar craters is due to a lens of brecciated material confined within the present crater rim crest and extending vertically to at least a depth of one-third the crater rim diameter. Calculations also reveal a systematic variation in the magnitude of the mass deficiencies with the cube of the crater diameter.

DYAL, P.

D023 **August 1972 Solar-Terrestrial Events: Observations of Interplanetary Shocks at 2.2 AU**

E. J. Smith, L. Davis, Jr. (California Institute of Technology), P. J. Coleman, Jr. (University of California, Los Angeles), D. S. Colburn (Ames Research Center), P. Dyal (Ames Research Center), and D. E. Jones (Brigham Young University)

J. Geophys. Res., Space Phys., Vol. 82, No. 7, pp. 1077–1086, March 1, 1977

For abstract, see Smith, E. J.

DZURISIN, D.

D024 **Landform Degradation on Mercury, the Moon, and Mars: Evidence From Crater Depth/Diameter Relationships**

M. C. Malin and D. Dzurisin (California Institute of Technology)

J. Geophys. Res., Vol. 82, No. 2, pp. 376–388, January 10, 1977

For abstract, see Malin, M. C.

EDELSON, E.

E001 **An Analysis of the Technical Status of High Level Radioactive Waste and Spent Fuel Management Systems**

T. English, C. Miller, E. Bullard, R. Campbell, A. Chockie, E. Divita, C. Douthitt (California Institute of Technology), E. Edelson, and L. Lees (California Institute of Technology)

JPL Publication 77-69, December 1, 1977

For abstract, see English, T.

EDESKUTY, F.

E002 **Experiments on the Properties of Superfluid Helium in Zero Gravity**

P. Mason, D. Collins, D. Petrac, L. Yang, F. Edeskuty, and K. Williamson

Proc. Sixth Int. Cryog. Eng. Conf., Grenoble, France, May 11–14,1976, pp. 272–277

For abstract, see Mason, P.

EISENBERGER, I.

E003 Life-Cycle Costing: Practical Considerations

I. Eisenberger and G. Lorden

The Deep Space Network Progress Report 42-40: May and June 1977, pp. 102–109, August 15, 1977

The history and methodology of life-cycle costing are presented and analyzed, contrasting the potential benefits of the technique with the difficulties of its application. Examples and a short survey of the literature are given.

E004 Dynamic Spares Provisioning for the DSN

I. Eisenberger and G. Lorden

The Deep Space Network Progress Report 42-42: September and October 1977, pp. 119–124, December 15, 1977

A method is proposed to maintain cost-effective spares stockpiles for an entire DSN station or complex as new modules or subsystems are continuously added. Levels of spares are calculated individually for each new module type so as to conform to an established standard for the entire spares pool. Finding the spares levels is computationally simplified and in many cases is reduced to consulting a Down-Time Ratio Chart. A simple modification permits taking into account a criticality factor.

EL GABALAWI, N.

E005 Projection of Distributed-Collector Solar-Thermal Electric Power Plant Economics to Years 1990–2000

T. Fujita, N. El Gabalawi, G. Herrera, and R. H. Turner

JPL Publication 77-79, December 1977

For abstract, see Fujita, T.

ELACHI, C.

E006 Models of Radar Imaging of the Ocean Surface Waves

C. Elachi and W. E. Brown, Jr.

IEEE Trans. Anten. Prop., Vol. AP-25, No. 1, pp. 84–95, January 1977

A number of models which would explain ocean wave imagery taken with a synthetic aperture imaging radar are analyzed analytically and numerically. Actual radar imagery is used to support some conclusions. The models considered correspond to three sources of radar backscatter cross section modulation: tilt modulation, roughness variation, and the wave orbital velocity. The effect of the temporal changes of the surface structure, parametric interactions, and the resulting distortions are discussed.

E007 Effects of Random Phase Changes on the Formation of Synthetic Aperture Radar Imagery

C. Elachi and D. D. Evans

IEEE Trans. Anten. Prop., Vol. AP-25, No. 1, pp. 149–153, January 1977

The effects of Gaussian random and linear phase change on the response of the matched azimuth processor of a synthetic aperture imaging radar is analyzed numerically.

E008 Higher-Order Bragg Coupling in Periodic Media With Gain or Loss

D. L. Jaggard and C. Elachi

J. Appl. Phys., Vol. 48, No. 4, pp. 1461–1466, April 1977

For abstract, see Jaggard, D. L.

E009 Waves in Active and Passive Periodic Structures: A Review

C. Elachi

Proc. IEEE, Vol. 64, No. 12, pp. 1666–1698, December 1976

The theory and recent applications of waves in periodic structures are reviewed. Both the Floquet and coupled waves approach are analyzed in some detail. The theoretical part of the paper includes wave propagation in unbounded and bounded active or passive periodic media, wave scattering from periodic boundaries, source radiation (dipole, Cerenkov, transition, and Smith–Purcell) in periodic media, and pulse transmission through a periodic slab. The applications part covers the recent development in a variety of fields: distributed feedback oscillators, filters, mode converters, couplers, second-harmonic generators, deflectors, modulators, and transducers in the fields of integrated optics and integrated surface acoustics. We also review the work on insect compound eyes, mechanical structures, ocean waves, pulse compressions, temperature waves, and cholesteric liquid crystals. Particles interaction with crystals is briefly reviewed, especially in the case of zeolite crystals and superlattices. Recent advances in fabrication tech-

niques for very fine gratings are also covered. Finally, speculations about future problems and development in the field of waves in periodic structures are given.

E010 **Ocean Wave Patterns Under Hurricane Gloria: Observation with an Airborne Synthetic-Aperture Radar**

C. Elachi, T. W. Thompson, and D. King

Science, Vol. 198, pp. 609–610, November 11, 1977

Surface imagery of ocean waves under Hurricane Gloria (September 1976) has been obtained with an airborne synthetic-aperture imaging radar. Observations were obtained over most of the area within a radius of 150 kilometers around the center of the eye. These direct observations made it possible to derive the wave patterns in the region around a hurricane eye.

ELLEMAN, D. D.

E011 **ADRF Experiments Using Near $n\pi$ Pulse Strings**

W. K. Rhim, D. P. Burum, and D. D. Elleman

Phys. Lett., Vol. 62A, No. 7, pp. 507–508, October 3, 1977

For abstract, see Rhim, W. K.

E012 **Multiple-Pulse Spin Locking in Dipolar Solids**

W. K. Rhim, D. P. Burum, and D. D. Elleman

Phys. Rev. Lett., Vol. 37, No. 26, pp. 1764–1766, December 27, 1976

For abstract, see Rhim, W. K.

ELLIOTT, D. A.

E013 **Transformations From an Oblate Spheroid to a Plane and Vice Versa—The Equations Used in the Cartographic Projection Program MAP2**

D. A. Elliott and A. A. Schwartz

JPL Publication 77-7, February 15, 1977

This paper discusses the relationships between the coordinates of a point on the surface of an oblate spheroid and the coordinates of the projection of that point in several common map projections. Since several of the projections are conformal, some background material is presented which summarizes the theory of conformally mapping an oblate spheroid to the plane. Then, for each projection considered, the equations which map the spheroid to the plane and their inverses are given.

E014 **Digital Processing of the Mariner 10 Images of Venus and Mercury**

J. M. Soha, D. J. Lynn, J. A. Mosher, and D. A. Elliott

J. Appl. Photogr. Eng., Vol. 3, No. 2, pp. 82–92, 1977

For abstract, see Soha, J. M.

ELLIOTT, D. G.

E015 **Comparison of Experimental and Theoretical Reaction Rail Currents, Rail Voltages, and Airgap Fields for the Linear Induction Motor Research Vehicle**

D. G. Elliott

JPL Publication 77-36, July 1977

Measurements of reaction rail currents, reaction rail voltages, and airgap magnetic fields in tests of the Linear Induction Motor Research Vehicle (LIMRV) were compared with theoretical calculations from the mesh/matrix theory. It was found that the rail currents and magnetic fields predicted by the theory are within 20 percent of the measured currents and fields at most motor locations in most of the runs, but differ by as much as a factor of two in some cases. The most consistent difference is a higher experimental than theoretical magnetic field near the entrance of the motor and a lower experimental than theoretical magnetic field near the exit. The observed differences between the theoretical and experimental magnetic fields and currents do not account for the differences of as much as 26 percent between the theoretical and experimental thrusts.

EMERSON, R. F.

E016 **Antenna Pointing Subsystem Drive Tape Generator—Another New Interface**

R. F. Emerson

The Deep Space Network Progress Report 42-41: July and August 1977, pp. 101–102, October 15, 1977

The Antenna Pointing Subsystem (APS) program was changed to meet new needs. To continue service to radio science targets, a new interface between the ephemerides of these targets and the APS program was required. This report describes briefly the program, called APSTAPE, written for this purpose. An important feature of the program is that it performs a read-after-punch operation, which ensures that the drive tapes generated will be error free. The program described has been successfully used in the field.

ENGLISH, T.

E017 An Analysis of the Technical Status of High Level Radioactive Waste and Spent Fuel Management Systems

T. English, C. Miller, E. Bullard, R. Campbell, A. Chockie, E. Divita, C. Douthitt (California Institute of Technology), E. Edelson, and L. Lees (California Institute of Technology)

JPL Publication 77-69, December 1, 1977

Analyses were made of the technical status of the "old U.S. mainline program" for high-level radioactive nuclear waste management, and The newly-developing program for disposal of unreprocessed spent fuel. The method of long-term containment for both of these waste forms is considered to be deep geologic isolation in bedded salt. This analysis was designed to assist the members and staff of the California Energy Resources Conservation and Development Commission in carrying out the mandate of California Assembly Bill AB 2822. Each major component of both waste management systems is analyzed in terms of its Scientific Feasibility, Technical Achievability and Engineering Achievability. The resulting matrix leads to a systematic identification of major unresolved technical or scientific questions and/or "gaps" in these programs.

ENGLISH, T. D.

E018 An Analysis of the Back End of the Nuclear Fuel Cycle With Emphasis on High-Level Waste Management

T. D. English

JPL Publication 77-59, Vol. I, August 12, 1977

The programs and plans for the U.S. Government for the "back end of the nuclear fuel cycle" were examined to determine if there were any significant technological or regulatory gaps and inconsistencies. Particular emphasis was placed on analysis of high-level nuclear waste management plans, since the permanent disposal of radioactive waste has emerged as a major factor in the public acceptance of nuclear power. The implications of various light water reactor fuel cycle options were examined including: throwaway, stowaway, uranium recycle, and plutonium plus uranium recycle.

The results of this study indicate that the U.S. program for high-level waste management has significant gaps and inconsistencies. Areas of greatest concern include: the adequacy of the scientific data base for geological disposal; programs for the disposal of spent fuel rods; interagency coordination; and uncertainties in NRC regulatory requirements for disposal of both commercial and military high-level waste.

The appendixes are bound separately as Volume II.

E019 An Analysis of the Back End of the Nuclear Fuel Cycle with Emphasis on High-Level Waste Management

T. D. English

JPL Publication 77-59, Vol. II, August 12, 1977

The programs and plans of the U.S. Government for the "back end of the nuclear fuel cycle" were examined to determine if there were any significant technological or regulatory gaps and inconsistencies. Particular emphasis was placed on analysis of high-level nuclear waste management plans, since the permanent disposal of radioactive waste has emerged as a major factor in the public acceptance of nuclear power. The implications of various light water reactor fuel cycle options were examined including: throwaway, stowaway, uranium recycle, and plutonium plus uranium recycle.

The results of this study indicate that the U.S. program for high-level waste management has significant gaps and inconsistencies. Areas of greatest concern include: the adequacy of the scientific data base for geological disposal; programs for the disposal of spent fuel rods; interagency coordination; and uncertainties in NRC regulatory requirements for disposal of both commercial and military high-level waste.

Volume II contains only appendixes for Volume I.

ESPOSITO, P. B.

E020 The Electron Density profile of the Outer Corona and the Interplanetary Medium From Mariner-6 and Mariner-7 Time-Delay Measurements

D. O. Muhleman (California Institute of Technology), P. B. Esposito, and J. D. Anderson

Astrophys. J., Vol. 211, No. 3, Pt. 1, pp. 943–957, February 1, 1977

For abstract, see Muhleman, D. O.

EVANS, D. D.

E021 Effects of Random Phase Changes on the Formation of Synthetic Aperture Radar Imagery

C. Elachi and D. D. Evans

IEEE Trans. Anten. Prop., Vol. AP-25, No. 1, pp. 149–153, January 1977

For abstract, see Elachi, C.

E022 **Mathematical Models for the Reflection Coefficients of Lossy Dielectric Half-Spaces with Application to Transient Responses of Chirped Pulses**

D. D. Evans

IEEE Trans. Anten. Prop., Vol. AP-25, No. 4, pp. 490–495, July 1977

Reflection coefficients are found at normal incidence for a large class of homogeneous lossy half-spaces with a one-dimensionally inhomogeneous or stratified lossy layer on top. Solutions are in terms of Hankel functions of complex argument to decrease cancellation error at high frequencies. One special case is that of layers on a homogeneous half-space where the dielectric constant in each layer may vary in a quite general manner. A Wronskian is used to insure the critical computations are correct. The reflection of chirped pulses is considered. Solutions are obtained by applying the fast Fourier transform. It is found that for a typical relatively long normalized "long" pulse the power reflected as a function of time is essentially the power reflection coefficient for the frequencies swept out, whereas for a relatively short "long" pulse, with the same relative change in frequency and the time number of oscillations there is only the uniform attenuation by the power reflection coefficient of the center frequency. By a "long" pulse we mean a pulse whose spatial length is long compared to the thickness of the reflecting layer.

EVIATAR, A.

E023 **An Alternative Interpretation of Jupiter's "Plasmapause"**

M. Neugebauer and A. Eviatar (University of California, Los Angeles)

Geophys. Res. Lett., Vol. 3, No. 12, pp. 708–710, December 1976

For abstract, see Neugebauer, M.

FANALE, F. P.

F001 **Io's Surface Composition: Observational Constraints and Theoretical Considerations**

F. P. Fanale, T. V. Johnson, and D. L. Matson

Geophys. Res. Lett., Vol. 4, No. 8, pp. 303–306, August 1977

Observations of line emission from neutral and ionic species in the Io-surrounding cloud, reflectance studies and theoretical considerations suggest Io's surface is unlike that of any other body in the solar system. The cloud has a peculiar composition which we show is probably not due to cloud/surface fractionation. Io's surface may be largely covered with an endogenically produced mixture of S and dehydrated salts, or by accretion-fractionated compounds modified by charged particle bombardment.

F002 **Io's Surface Composition Based on Reflectance Spectra of Sulfur/Salt Mixtures and Proton-Irradiation Experiments**

D. B. Nash and F. P. Fanale

Icarus, Vol. 31, pp. 40–80, 1977

For abstract, see Nash, D. B.

FARMER, C. B.

F003 **The HF:HCl Ratio in the 14–38 km Region of the Stratosphere**

C. B. Farmer and O. F. Raper

Geophys. Res. Lett., Vol. 4, No. 11, pp. 527–527, November 1977

Near infrared absorption spectra covering the 1-0 bands of HF and HCl were recorded with a high resolution Michelson interferometer during a balloon flight near Broken Hill, Australia (30.5°S, 138.5°E) in March 1977. The ratio of the number density of HF to that of HCl as a function of altitude in the stratosphere was deduced from measurements of the R1 features of both gases. The experimental errors vary over the altitude range covered by the measurements, their estimated values being ±25% between 14 and 30 km, increasing to ±50% at the extremes of the range (14 and 38 km). Within these estimated errors the ratio is constant, its mean value being HF:HCl = 0.1.

F004 **The Vertical Distribution of HCl in the Stratosphere**

O. F. Raper, C. B. Farmer, R. A. Toth, and B. D. Robbins

Geophys. Res. Lett., Vol. 4, No. 11, pp. 531–534, November 1977

For abstract, see Raper, O. F.

F005 **Behavior of Volatiles in Mars' Polar Areas: A Model Incorporating New Experimental Data**

D. W. Davies, C. B. Farmer, and D. D. LaPorte (Santa Barbara Research Center)

J. Geophys. Res., Vol. 82, No. 26, pp. 3815–3822, September 10, 1977

For abstract, see Davies, D. W.

F006 **Mars: Northern Summer Ice Cap—Water Vapor Observations from Viking 2**

C. B. Farmer, D. W. Davies, and
D. D. LaPorte (Santa Barbara Research Center)

Science, Vol. 194, pp. 1339–1341, December 17, 1976

Observations of the latitude dependence of water vapor made from the Viking 2 orbiter show peak abundances in the latitude band 70° to 80° north in the northern midsummer season (planetocentric longitude ~108°). Total column abundances in the polar regions require near-surface atmospheric temperatures in excess of 200°K, and are incompatible with the survival of a frozen carbon dioxide cap at martian pressures. The remnant (or residual) north polar cap and the outlying patches of ice at lower latitudes are thus predominantly water ice, whose thickness can be estimated to be between 1 meter and 1 kilometer.

FERRARI, A. J.

F007 **A Lunar Density Model Consistent With Topographic, Gravitational, Librational, and Seismic Data**

B. G. Bills and A. J. Ferrari

J. Geophys. Res., Vol. 82, No. 8, pp. 1306–1314, March 10, 1977

For abstract, see Bills, B. G.

F008 **Lunar Gravity: A Harmonic Analysis**

A. J. Ferrari

J. Geophys. Res., Vol. 82, No. 20, pp. 3065–3084, July 10, 1977

A sixteenth-degree and sixteenth-order spherical harmonic lunar gravity field has been derived from the long-term Keplerian variations in the orbits of the Apollo subsatellites and Lunar Orbiter 5. This model resolves the major mascon gravity anomalies of the lunar nearside and is in very good agreement with line of sight acceleration results. The farside map shows the major ringed basins to be strong localized negative anomalies located in broad regions of positive gravity which correspond closely to the highlands. The rms pressure levels calculated from equivalent surface height variations show that the moon and earth support nearly equal pressures (46 and 57 bars), whereas Mars is appreciably stronger (115 bars). These height variations are equivalent to mean uncompensated loads of 284 kg/cm^2 for the moon, 58 kg/cm^2 for the earth, and 308 kg/cm^2 for Mars. The moon appears to support larger loads than the earth owing to its weaker central gravity field and perhaps a colder upper lithosphere. Significant differences between the low-degree gravity and topography spectra indicate that the longer-wave-length topographic features are isostatically compensated. The effect of compensation reduces the amplitudes of the low-degree gravity harmonics and is responsible for the slower decay in the moon's gravity spectrum. A comparison of the gravity effects of topography for the three planets shows that the moon and Mars support significant topographic features, whereas the earth is nearly in isostatic equilibrium.

F009 **Lunar Gravity: A Long-Term Keplerian Rate Method**

A. J. Ferrari and M. P. Ananda

J. Geophys. Res., Vol. 82, No. 20, pp. 3085–3097, July 10, 1977

Recent reductions of Apollo subsatellite and Lunar Orbiter 5 data have determined the first plausible models for the farside lunar gravity field. This paper presents a selenodesy method which estimates gravity by fitting to the long-term variations of the Kepler element rates. Arguments are presented which conclude that a long-term gravity method of this type is the most plausible technique which can obtain realistic estimates for farside lunar gravity using the currently available data.

FIELDING, J. E.

F010 **State Criminal Justice Telecommunications (STACOM) Final Report: Executive Summary**

J. E. Fielding, H. K. Frewing, J. J. Lee, W. G. Leflang, and N. B. Reilly

JPL Publication 77-53, Vol. I, October 31, 1977

An executive overview is provided in Volume I of the Final Report for the major study components and a summary of a State Criminal Justice Telecommunications (STACOM) project sponsored by the Law Enforcement Assistance Administration (LEAA). The project has developed techniques for identifying user requirements analysis and network designs for criminal justice networks on a state wide basis. Techniques developed for user requirements analysis involve methods for determining data required, data collection (surveys), and data organization procedures, and methods for forecasting network traffic volumes. Developed network design techniques center around a computerized topology program which enables the user to generate least cost network topologies that satisfy network traffic requirements, response time requirements and other specified functional requirements. The developed techniques were applied in the states of Ohio and Texas and results of these studies are presented.

F011 **State Criminal Justice Telecommunications (STACOM) Final Report: Requirements Analysis and Design of Ohio Criminal Justice Telecommunications Network**

J. E. Fielding, H. K. Frewing, J. J. Lee, and N. B. Reilly

JPL Publication 77-53, Vol. II, October 31, 1977

Requirements analysis and design for the Ohio Criminal Justice Telecommunications Network is provided in Volume II of the Final Report of a State Criminal Justice Telecommunications (STACOM) project sponsored by the Law Enforcement Assistance Administration (LEAA). The project has developed techniques for identifying user requirements and network designs for criminal justice networks on a state wide basis. Techniques developed for user requirements analysis involve methods for determining data required, data collection (surveys), and data organization procedures, and methods for forecasting network traffic volumes. Developed network design techniques center around a computerized topology program which enables the user to generate least cost network topologies that satisfy network traffic requirements, response time requirements and other specified functional requirements. The developed techniques were applied in the state of Ohio, and results of these studies are presented.

F012 **State Criminal Justice Telecommunications (STACOM) Final Report: Requirements Analysis and Design of Texas Criminal Justice Telecommunications Network**

J. E. Fielding, H. K. Frewing, J. J. Lee, and N. B. Reilly

JPL Publication 77-53, Vol. III, October 31, 1977

Requirements analysis and design for the Texas Criminal Justice Telecommunications Network is provided in Volume III of the Final Report of a State Criminal Justice Telecommunications (STACOM) project sponsored by the Law Enforcement Assistance Administration (LEAA). The project has developed techniques for identifying user requirements analysis and network designs for criminal justice networks on a state wide basis. Techniques developed for user requirements analysis involve methods for determining data required, data collection (surveys), and data organization procedures, and methods for forecasting network traffic volumes. Developed network design techniques center around a computerized topology program which enables the user to generate least cost network topologies that satisfy network traffic requirements, response time requirements and other specified functional requirements. The developed techniques were applied in the state of Texas, and results of these studies are presented.

FIELDS, N. D.

F013 **Pyrolysis Gas-Liquid Chromatography Studies of the Genus *Bacillus*: Effect of Growth Time on Pyrochromatogram Reproducibility**

G. S. Oxborrow, N. D. Fields, and J. R. Puleo

Anal. Pyrolysis, pp. 69–76, 1977

For abstract, see Oxborrow, G. S.

F014 **Microbiological Profiles of the Viking Spacecraft**

J. R. Puleo, N. D. Fields, S. L. Bergstrom, G. S. Oxborrow, P. D. Stabekis, and R. C. Koukol

Appl. Environ. Microbiol., Vol. 33, No. 2, pp. 379–384, February 1977

For abstract, see Puleo, J. R.

F015 **Pyrolysis Gas-Liquid Chromatography of the Genus *Bacillus*: Effect of Growth Media on Pyrochromatogram Reproducibility**

G. S. Oxborrow, N. D. Fields, and J. R. Puleo

Appl. Environ. Microbiol., Vol. 33, No. 4, pp. 865–870, April 1977

For abstract, see Oxborrow, G. S.

FINNEGAN, E. J.

F016 **Intermodulation Components in the Transmitter RF Output Due to High Voltage Power Supply Ripple**

E. J. Finnegan

The Deep Space Network Progress Report 42-40: May and June 1977, pp. 150–151, August 15, 1977

A study was conducted to determine if it would be economically feasible to eliminate the 400-Hz motor-generator sets used to provide power to the high-voltage power supplies of the 20-kW transmitters and replace them with a 60-Hz high-voltage power supply. The efficiency of a power supply that runs from the 60-Hz line directly would pay for itself in about seven years and could be designed so that the transmitter would meet all the incidental phase and amplitude modulation specifications.

F017 **Measurement of Klystron Phase Modulation Due to AC-Powered Filaments**

E. J. Finnegan

The Deep Space Network Progress Report 42-40: May and June 1977, pp. 152–155, August 15, 1977

This article shows the experiment that was conducted in order to determine the intermodulation components in the RF spectrum of the S-band radar transmitter generated by having the klystron filaments heated by 400-Hz AC power.

FLANAGAN, F. M.

F018 Tracking and Data Systems Support for the Helios Project: DSN Support of Project Helios April 1975 Through May 1976

P. S. Goodwin, M. R. Traxler, W. G. Meeks, and F. M. Flanagan

Technical Memorandum 33-752, Vol. II, January 15, 1977

For abstract, see Goodwin, P. S.

FLAUD, J. M.

F019 Spectrum of $H_2{}^{18}O$ and $H_2{}^{17}O$ in the 5030 to 5640 cm^{-1} Region

R. A. Toth, J. M. Flaud (Campus d'Orsay, France), and C. Camy-Peyret (Campus d'Orsay, France)

J. Mol. Spectros., Vol. 67, Nos. 1–3, pp. 185–205, September 15, 1977

For abstract, see Toth, R. A.

F020 Spectrum of $H_2{}^{18}O$ and $H_2{}^{17}O$ in the 6974 to 7387 cm^{-1} Region

R. A. Toth, J. M. Flaud (Laboratoire de Physique Moleculaire et d' Optique, Orsay), and C. Camy-Peyret (Laboratoire de Physique Moleculaire et d' Optique, Orsay)

J. Mol. Spectros., Vol. 67, Nos. 1–3, pp. 206–218, September 15, 1977

For abstract, see Toth, R. A.

F021 Strengths of H_2O Lines in the 5000–5750 cm^{-1} Region

R. A. Toth, C. Camy-Peyret (Laboratoire de Physique Moleculaire et d'Optique, Orsay), and J. M. Flaud (Laboratoire de Physique Moleculaire et d'Optique, Orsay)

J. Quant. Spectros. Radiat. Transfer, Vol. 18, pp. 515–523, 1977

For abstract, see Toth, R. A.

FLESNER, L. D.

F022 Simple Waveguide Reflection Maser With Broad Tunability

L. D. Flesner (University of California, San Diego), S. Schultz (University of California, San Diego), and R. Clauss

Rev. Sci. Instrum., Vol. 48, No. 8, pp. 1104–1105, August 1977

The design and performance of a simple two-stage reflection maser for use between 9 and 10 GHz are described. The maser is used to improve the sensitivity of a transmission electron spin resonance spectrometer. A ruby-filled waveguide structure permits broad tunability and straightforward construction. All microwave components except the ruby section are at room temperature.

FLOYD, E. L.

F023 Borehole Hydraulic Coal Mining System Analysis

E. L. Floyd

JPL Publication 77-19, April 21, 1977

As a portion of an Advanced Coal Extraction Project at the Jet Propulsion Laboratory, an evaluation method was developed to analyze underground coal extraction systems. The evaluation method was designed to analyze, both technically and economically, underground mining systems to compete with existing coal mining systems. The borehole hydraulic mining system, under development by a Bureau of Mines' Research Center, is considered an advanced extraction system, and may be analyzed by this method. As a result of the coal extraction project work in the evaluation area, JPL was directed to perform an evaluation of the proposed advanced system.

The borehole hydraulic coal mining system assesses the coal seam through a hole drilled in the overburden. The mining device is lowered through the hole into the coal seam where it fragments the coal with high pressure water jets. The fragmented coal is pumped to the surface as a slurry by a jet pump located in the center of the mining device. The coal slurry is then injected into a slurry pipeline for transport to the preparation plant.

The evaluation considered all the aspects of the mining operation for a 20-year mine life, producing 2.64×10^6 tons/yr. The mine was planned from geologic data for the region, and the expected extraction efficiency. Capital equipment to support the operation was determined and costed. Effects on the environment and the cost of

ORIGINAL PAGE IS
OF POOR QUALITY

restoration, as well as the concerns for health and safety, were studied. This report details the assumptions for the design of the mine, the analytical method, and the results of the analysis.

FLURY, W.

F024 Lunar Farside Gravity: An Assessment of Satellite to Satellite Tracking Techniques and Gravity Gradiometry

M. Ananda, J. Lorell, and W. Flury (European Space Operations Center)

Proc. Seventh Lunar Sci. Conf., pp. 2623–2638, 1976

For abstract, see Ananda, M.

FOSTER, C. F.

F025 Automated Fourth-Harmonic Analyzer

C. F. Foster

The Deep Space Network Progress Report 42-37: November and December 1976, pp. 105–111, February 15, 1977

This article describes the final design of a field portable microprocessor-based, microwave measuring and analysis instrument to be used for S-band transmitter fourth-harmonic power analysis and its impact on X-band reception in a dual S-X-band system.

FOWLER, J. W.

F026 Calibration of Viking Imaging System Pointing, Image Extraction, and Optical Navigation Measure

W. G. Breckenridge, J. W. Fowler, and E. M. Morgan (General Electric Co.)

JPL Publication 77-28, September 15, 1977

For abstract, see Breckenridge, W. G.

FRANK, H. A.

F027 Evaluation of Battery Models for Prediction of Electric Vehicle Range

H. A. Frank and A. M. Phillips

JPL Publication 77-29, August 1, 1977

The objective of this investigation was to evaluate three different battery analytical models for predicting electric vehicle battery output and the corresponding electric vehicle range for various driving cycles as described by SAE-J227a. The approach consisted of using the models to predict output and range, then comparing the results with experimentally determined values. The latter were determined by laboratory tests on batteries, using discharge cycles identical to those encountered by an actual electric vehicle while on the SAE cycles. Results indicated that the so-called Modified Hoxie Model gave the best predictions with an accuracy of about 97–98% in most cases and 86% in the worst case. Solution of this model required lengthy iterative calculations that were carried out with a computer. The program that was written to perform these calculations is included in this report. Also described are the program and hardware that were used to automatically discharge the battery in accord with the current profiles corresponding to the SAE driving cycles. Future efforts are recommended using these models to predict the effect of battery type on range of a wide variety of vehicles.

F028 Development of a Multiplexed Bypass Control System for Aerospace Batteries

H. A. Frank

JPL Publication 77-65, November 1, 1977

A breadboard bypass control system was developed to control a battery comprised of 26 JPL-developed Negative Limited Ni-Cd cells. The system was designed to automatically remove cells from the circuit when their voltages exceeded a fixed limit on charge and fell below a fixed limit on discharge. Major components of the system consisted of a cell voltage monitor, a multiplexing circuit, and individual electromechanical relays for each cell. The system was found to function well in controlling the battery during a simulated 10-month MM-71 mission and a 2-month simulated low earth orbit cycling mission. A flight version of the bypass system is estimated to have a total parts count of 150 and total weight of 1.63 kg. When fully developed, the system shows promise for improving life and reliability of spacecraft batteries. The technology developed on this project is recommended for transfer to the on-going Automated Power Systems Management Program.

FRAUENHOLZ, R. B.

F029 Maneuver Sequence Design for the Post-Jupiter Leg of the Pioneer Saturn Mission

R. B. Frauenholz and W. F. Brady

J. Spacecraft Rockets, Vol. 14, No. 7, pp. 395–400, July 1977

A sequence of midcourse maneuvers has been designed for the Pioneer 11 post-Jupiter trajectory to provide Saturn targeting options to aimpoints either inside or outside the visible ring system. An interim aimpoint was selected which retains these options until late 1977 and improves the navigation accuracy to the finally selected

target. An arrival time of September 1, 1979, selected to reduce interference due to solar conjunction, required the use of preprogrammed open-loop maneuvers with a brief communication loss to reach the interim aimpoint. Subsequent targeting will be achieved in continuous communication using simpler and more accurate maneuvers near the Earth-line. This paper develops the maneuver sequence, with emphasis on overall efficiency, flexibility, and navigation system accuracy.

FRAUTNICK, J. C.

F030 **Mission Design for SEASAT-A, An Oceanographic Satellite**

E. Cutting, G. H. Born, J. C. Frautnick, W. I. McLaughlin, R. A. Neilson, and J. A. Thielen (Lockheed Missiles & Space Co.)

Preprint 77-31, AIAA Fifteenth Aerosp. Sci. Meet., Los Angeles, Calif., Jan. 24–26, 1977

For abstract, see Cutting, E.

FRAZER, R. E.

F031 **Feasibility Study on the Design of a Probe for Rectal Cancer Detection**

V. J. Anselmo, R. E. Frazer, D. H. LeCroissette, J. A. Roseboro, and M. I. Smokler

JPL Publication 77-31, April 15, 1977

For abstract, see Anselmo, V. J.

FREDRICKSON, C. D.

F032 **Analysis of Requirements for Accelerating the Development of Geothermal Energy Resources in California**

C. D. Fredrickson

JPL Publication 77-63, November 15, 1977

Various resource data are presented showing that geothermal energy has the potential of satisfying a significant part of California's increasing energy needs. General factors slowing the development of geothermal energy in California are discussed, and required actions to accelerate its progress are presented. Finally, scenarios for developing the most promising prospects in the state directed at timely on-line power are given. Specific actions required to realize each of these individual scenarios are identified.

FREWING, H. K.

F033 **State Criminal Justice Telecommunications (STACOM) Final Report: Executive Summary**

J. E. Fielding, H. K. Frewing, J. J. Lee, W. G. Leflang, and N. B. Reilly

JPL Publication 77-53, Vol. I, October 31, 1977

For abstract, see Fielding, J. E.

F034 **State Criminal Justice Telecommunications (STACOM) Final Report: Requirements Analysis and Design of Ohio Criminal Justice Telecommunications Network**

J. E. Fielding, H. K. Frewing, J. J. Lee, and N. B. Reilly

JPL Publication 77-53, Vol. II, October 31, 1977

For abstract, see Fielding, J. E.

F035 **State Criminal Justice Telecommunications (STACOM) Final Report: Requirements Analysis and Design of Texas Criminal Justice Telecommunications Network**

J. E. Fielding, H. K. Frewing, J. J. Lee, and N. B. Reilly

JPL Publication 77-53, Vol. III, October 31, 1977

For abstract, see Fielding, J. E.

FRICKE, W.

F036 **Expressions for the Precession Quantities Based upon the IAU (1976) System of Astronomical Constants**

J. H. Lieske, T. Lederle (Astronomisches Rechen-Institut, Heidelberg), W. Fricke (Astronomisches Rechen-Institut, Heidelberg), and B. Morando (Bureau des Longitudes, Paris)

Astron. Astrophys., Vol. 58, pp. 1–16, 1977

For abstract, see Lieske, J. H.

FRIEDENBERG, S. E.

F037 **Pioneer Venus 1978 Multiprobe Spacecraft Simulator**

S. E. Friedenberg

The Deep Space Network Progress Report 42-38: January and February 1977, pp. 148–151, April 15, 1977

A test which duplicates the signals of the four probes to be deployed by the PV 78 multiprobe spacecraft has

been developed. It will be used for receiver operator training prior to the mission. This article describes the operation and characteristics of the test set.

FRIEDMAN, L.

F038 Robot Learning and Error Correction

L. Friedman

JPL Publication 77-16, April 15, 1977

A model of robot learning is described that associates previously unknown perceptions with the sensed known consequences of robot actions. For these actions, both the categories of outcomes and the corresponding sensory patterns are incorporated in a knowledge base by the system designer. Thus the robot is able to predict the outcome of an action and compare the expectation with the experience. New knowledge about what to expect in the world may then be incorporated by the robot in a pre-existing structure whether it detects accordance or discrepancy between a predicted consequence and experience Errors committed during plan execution are detected by the same type of comparison process and learning may be applied to avoiding the errors. The model is being implemented as a system called RECOGNIZER, and will be incorporated into the existing JPL robot system so that its performance may be tested in real situations.

FRIEDMAN, L. D.

F039 Orbit Design Concepts for Jupiter Orbiter Missions

C. Uphoff, P. H. Roberts, and L. D. Friedman

J. Spacecraft Rockets, Vol. 13, No. 6, pp. 348–355, June 1976

For abstract, see Uphoff, C.

FUJITA, T.

F040 Projection of Distributed-Collector Solar-Thermal Electric Power Plant Economics to Years 1990–2000

T. Fujita, N. El Gabalawi, G. Herrera, and R. H. Turner

JPL Publication 77-79, December 1977

A preliminary comparative evaluation of distributed-collector solar thermal power plants has been undertaken by projecting power plant economics of selected systems to the 1990–2000 time frame. The selected systems include: (1) fixed orientation (non-tracking) collectors with concentrating reflectors and vacuum tube absorbers, (2) one-axis tracking linear concentrators including parabolic trough and variable slat designs, and (3) two-axis tracking parabolic dish systems including concepts with small heat engine-electric generator assemblies at each focal point as well as approaches having steam generators at the focal point with pipeline collection to a central power conversion unit.

Comparisons are presented primarily in terms of energy cost (mills/kWe hr) and capital cost over a wide range of operating load factors. Sensitivity of energy costs for a range of efficiency and cost of major subsystems/components is presented to delineate critical technological development needs. The baseline central receiver or power tower systems using state-of-the-art 1000°F steam Rankine technology is used as a reference case for making comparisons of the selected distributed collector systems.

FUTRELL, J. H.

F041 Ion Cyclotron Resonance Studies of Some Reactions of N^+ Ions

V. G. Anicich, W. T. Huntress, Jr., and J. H. Futrell (University of Utah)

Chem. Phys. Lett., Vol. 47, No. 3, pp. 488–489, May 1, 1977

For abstract, see Anicich, V. G.

F042 Product Distributions for Some Thermal Energy Charge Transfer Reactions of Rare Gas Ions

V. G. Anicich, J. B. Laudenslager, W. T. Huntress, Jr., and J. H. Futrell (University of Utah)

J. Chem. Phys., Vol. 67, No. 10, pp. 4340–4350, November 15, 1977

For abstract, see Anicich, V. G.

FYMAT, A. L.

F043 A Novel Methodology for Radiative Transfer in a Planetary Atmosphere

A. L. Fymat and R. E. Kalaba (University of Southern California)

Astrophys. Space Sci., Vol. 47, pp. 195–216, 1977

A novel methodology for evaluating the field of anisotropically scattered radiation within a homogeneous slab atmosphere of arbitrary optical thickness is provided. It departs from the traditional radiative transfer approach in first considering that the atmosphere is illuminated by an isotropic light source. From the solution of this problem, it subsequently proceeds to that for the more conventional case of monodirectional illumination.

ORIGINAL PAGE IS OF POOR QUALITY

GALE, G.

G001 64-Meter Antenna Pedestal Tilt at DSS 43, Tidbinbilla, Australia

G. Gale and A. A. Riewe

The Deep Space Network Progress Report 42-40: May and June 1977, pp. 168–173, August 15, 1977

It was discovered in 1973 that the 64-meter antenna pedestal at DSS 43 had settled, causing a level reference plane to be tilted. This article discusses the tilt of the pedestal, its amplitude, rate of change, method of measurement, and the degree of confidence in the measurements. The effect of the tilt and a prognosis for the future effect on tilt are discussed along with recommendations.

G002 Radial Bearing Measurements of the 64-m Antenna, DSS 14

G. Gale

The Deep Space Network Progress Report 42-42: September and October 1977, pp. 207–213, December 15, 1977

This article describes the inspection fixtures and methods used to determine the extent of the azimuth radial bearing deformation at the 64-m DSS 14. An annular separation has developed between the circular steel runner and the grout, suggesting either failure of the grout or, as the case appears to be, stretching of the circular steel runner due to the formation of rust on the runner at the grout interface.

GALINDO-ISRAEL, V.

G003 A New Series Representation for the Radiation Integral with Application to Reflector Antennas

V. Galindo-Israel and R. Mittra

IEEE Trans. Anten. Prop., Vol. AP-25, No. 5, pp. 631–641, September 1977

Given the true or any approximate current on a reflector, the radiated far-field is determined from a rapidly convergent series representation of the radiation integral. The leading term is a well-shaped $J_1(x)/x$ beam pointing in a desired direction. Higher order terms provide perturbations to the leading term. The coefficients of the series are independent of the observation angles. Hence, once they are computed, the field may be determined very rapidly at large numbers of points. Initially, a suitable small angle approximation is made that places the radiation integral in the form of a Fourier transform on a circular disk. The theory is then extended such that the results are valid in both the near and the wide angle regions. Application to a rotationally symmetric paraboloid is presented herein. Other applications include the offset and dual reflectors and near- to far-field integrations. A modified form of the series can also be used for Fresnel zone computations.

GARBA, J. A.

G004 Evaluation of a Cost-Effective Loads Approach

J. A. Garba, B. K. Wada, R. Bamford, and M. R. Trubert

J. Spacecraft Rockets, Vol. 13, No. 11, pp. 675–683, November 1976

A shock spectra/impedance method for loads prediction is used to estimate member loads for the Viking orbiter, a 7800-lb interplanetary spacecraft that has been designed using transient loads analysis techniques. The transient loads analysis approach leads to a lightweight structure but requires complex and costly analyses. To reduce complexity and cost, a shock spectra/impedence method is currently being used to design the Mariner Jupiter Saturn spacecraft. This method has the advantage of using low-cost in-house loads analysis techniques and typically results in more conservative structural loads. The method is evaluated by comparing the increase in Viking member loads to the loads obtained by the transient loads analysis approach. An estimate of the weight penalty incurred by using this method is presented. The paper also compares the calculated flight loads from the transient loads analyses and the shock spectra/impedance method to measured flight data.

GARDNER, R.

G005 X-Band Atmospheric Noise Temperature Statistics at Goldstone DSS 13, 1975–1976

S. Slobin, M. Reid, R. Gardner, and D. Cheng

The Deep Space Network Progress Report 42-38: January and February 1977, pp. 70–76, April 15, 1977

For abstract, see Slobin, S.

GARDNER, R. A.

G006 Precision Insolation Measurement Under Field Conditions

M. S. Reid, R. A. Gardner, and C. M. Berdahl

The Deep Space Network Progress Report 42-37: November and December 1976, pp. 169–175, February 15, 1977

For abstract, see Reid, M. S.

G007 **Precision Insolation Measurement Under Field Conditions**

M. S. Reid, C. M. Berdahl, and R. A. Gardner

Proc. SPIE, Vol. 85, pp. 90–92, 1976

For abstract, see Reid, M. S.

GATEWOOD, J.

G008 **Surface Crystalline Carbon Temperature Sensor**

D. Petrac, J. Gatewood, and P. Mason

Advan. Cryog. Eng., Vol. 21, pp. 242–243, 1976

For abstract, see Petrac, D.

G009 **Sensor for Distinguishing Liquid–Vapor Phases of Superfluid Helium**

D. Petrac, J. Gatewood, and P. Mason

Advan. Cryog. Eng., Vol. 21, pp. 244–246, 1976

For abstract, see Petrac, D.

GATZ, E. C.

G010 **DSN Telemetry System, Mark III-77**

E. C. Gatz

The Deep Space Network Progress Report 42-42: September and October 1977, pp. 4–11, December 15, 1977

This article provides a description of the DSN Telemetry System, Mark III-77, which is now being used to support multiple deep space missions. Telemetry functions performed by the Deep Space Stations, Ground Communications Facility, and the Network Operations Control Center are defined. Recent improvements to the system and planned upgrades are described.

GELLER, M.

G011 **Comment on "New Jacobian Theta Functions and the Evaluation of Lattice Sums" by I. J. Zucker [J. Math. Phys. 16, 2189 (1975)]**

M. Geller

J. Math. Phys., Vol. 18, No. 1, p. 187, January 1977

The "new" Jacobian theta function recently introduced by Zucker has been shown to be related to usual theta functions of $\pi/4$ argument. Several identities are presented for this new theta function, and analytic summation formulas are given for selected arguments.

GILLESPIE, A. R.

G012 **Construction and Interpretation of a Digital Thermal Inertia Image**

A. R. Gillespie and A. B. Kahle

Photogram. Eng. Remote Sensing, Vol. 43, No. 8, pp. 983–1000 August 1977

An image representing the thermal inertia in the vicinity of Pisgah Crater and Lavic Lake in Southern California has been generated from visible, near IR, and thermal images taken from aircraft. Construction of the thermal inertia image required radiometric calibration and geometric rectification of the acquired images as well as registration to a topographic map. The Kahle thermal model used in the construction of the thermal inertia image requires specification of albedo, topographic slope and slope azimuth, diurnal temperature range and local meteorological conditions. Albedo information was derived from the visible image; digital topographic information was computed from digitized stereo aerial photographs; and thermal ranges were calculated by subtracting the predawn from the afternoon thermal image data. Our computed values of thermal inertia were in close agreement with published values for similar surface materials. Thermal inertia provides complementary information to conventional images of reflected solar radiation for use in lithologic mapping.

GOETZ, A. F. H.

G013 **Mapping of Hydrothermal Alteration in the Cuprite Mining District, Nevada, Using Aircraft Scanner Images for the Spectral Region 0.46 to 2.36 μm**

M. J. Abrams, R. P. Ashley (U. S. Geological Survey), L. C. Rowan (U. S. Geological Survey), A. F. H. Goetz, and A. B. Kahle

Geology, Vol. 5, No. 12, pp. 713–718, December 1977

For abstract, see Abrams, M. J.

G014 **Effect of Vegetation on Rock and Soil Type Discrimination**

B. S. Siegal and A. F. H. Goetz

Photogram. Eng. Remote Sensing, Vol. 43, No. 2, pp. 191–196, February 1977

For abstract, see Siegal, B. S.

GOLDSTEIN, B. E.

G015 **Effects of Stream-Associated Fluctuations Upon the Radial Variation of Average Solar Wind Parameters**

B. E. Goldstein and J. R. Jokipii (University of Arizona)

J. Geophys. Res., Space Phys., Vol. 82, No. 7, pp. 1095–1105, March 1, 1977

The effects of nonlinear fluctuations due to solar wind streams upon radial gradients of average solar wind parameters are computed by using a numerical MHD model for both spherically symmetric time-dependent and corotating equatorial flow approximations. We find significant effects of correlations between fluctuations upon the gradients of azimuthal magnetic field, radial velocity, density, and azimuthal velocity. The averages of V_r and r^2n both decrease with increasing radial distance (0–30 km/s, 5–10% by 6 AU) while mass flux is conserved. The cross-variance between V_r and r^2n increases with radial distance from negative values to positive values at distances greater than 3.5 AU. The average azimuthal velocity decreases, and at distances greater than 4 AU it may be opposite to the solar rotation; (V_ϕ of from 0.2 to $\div 1.7$ km/s at 6 AU is predicted. Between 400 and 900 R_S, stream interactions have transferred the major portion of the angular momentum flux to the magnetic field; at even greater distances the plasma again carries the bulk of the angular momentum flux. The average azimuthal component of the magnetic field may decrease as much as 10% faster than the Archimedean spiral out to 6 AU, owing to stream interactions, but this result is dependent upon inner boundary conditions.

G016 Acceleration of Energetic Particles of the Outer Regions of Planetary Magnetospheres: Inferences From Laboratory and Space Experiments

B. T. Tsurutani, B. E. Goldstein, and A. Bratenahl

Planet. Space Sci., Vol. 24, No. 10, pp. 995–999, 1976

For abstract, see Tsurutani, B. T.

G017 Magnetic Evidence Concerning a Lunar Core

B. E. Goldstein, R. J. Phillips, and C. T. Russell (University of California, Los Angeles)

Proc. Seventh Lunar Conf., pp. 3321–3341, 1976

Measurements of the magnetic field induced in the moon while the moon is in the geomagnetic tail lobe field have been interpreted in terms of magnetic permeability due to the lunar free iron content. However, if the moon has a highly conducting core, the core will exclude magnetic fields with an apparent diamagnetic effect. Discussion of lunar chemical and thermal models establishes limits for plausible values of lunar magnetic permeability. These limits and the long period (3 hr to 4 days) magnetic response determine a maximum possible core radius. Measurements by two techniques are reported: (a) comparison of Explorer 35 and Apollo 12 data, and (b) observation of the dipole field configuration by orbiting subsatellites. Results are in moderate disagreement. The subsatellite observations (method b) require the existence of a core, but this measurement conflicts with measurements (method a) that allow, but do not require a small core. Until the discrepancy is resolved the only firm conclusion is that a maximum radius for a lunar core is about 580 km. A scenario for lunar core formation compatible with observations of atmospheric ^{40}Ar and recent cool thermal history models is discussed; the core forms late in lunar history by slow descent of FeS. Remanent magnetism is attributed to subsurface dynamos rather than a lunar core.

GOLDSTEIN, R.

G018 Active Control of Spacecraft Potentials at Geosynchronous Orbit

R. Goldstein and S. E. DeForest (University of Alabama)

Progr. Astronaut. Aeronaut., Vol. 47, pp. 169–181, 1976

The geosynchronous satellites ATS-5 and ATS-6 each carry plasma particle detectors (the University of California at San Diego auroral particle experiment) and two cesium ion thrusters. The detectors have been used to determine spacecraft potential by observing shifts in the particle spectra and appearance of spurious particles at the spacecraft potential. During eclipse, negative potentials as great as 10 keV have been observed. Although the two spacecraft are markedly different in design and were separated by about 10°lon for the tests reported, the potentials of the two, determined by the aforementioned method, agree surprisingly well while both are eclipsed simultaneously. Extensive tests of the effects of ion thruster beam, as well as thruster neutralizer electron source on spacecraft potential, have been performed. Similarly, the magnitude of the potential of the spacecraft, charged negatively during eclipse, was reduced by operation of the ATS-5 thruster thermionic electron emitter. However, it was not always possible to clamp the potential to near zero by this technique.

GOODWIN, P. S.

G019 Tracking and Data Systems Support for the Helios Project: DSN Support of Project Helios April 1975 Through May 1976

P. S. Goodwin, M. R. Traxler, W. G. Meeks, and F. M. Flanagan

Technical Memorandum 33-752, Vol. II, January 15, 1977

This report (Volume II) is in two parts. The first, Part A, summarizes Deep Space Network activities in the development of the Helios-B mission from planning in May 1975 through entry of Helios-2 into first superior conjunction (end of Mission Phase II) in May 1[illegible]. The second, Part B, covers the Deep Space Netwo[illegible]erational support activities for Helios-1 from first [illegible]p[illegible] ior conjunction in April 1975 through entry into thir[illegible] perior conjunction in May 1976.

G020 Helios Mission Support

P. S. Goodwin, E. S. Burke, and T. P. Adamski

The Deep Space Network Progress Report 42-37: November and December 1976, pp. 39–42, February 15, 1977

This article reports on activities of the Network Operations organization in support of the Helios Project during October and November 1976.

G021 Helios Mission Support

P. S. Goodwin, E. S. Burke, and G. M. Rockwell

The Deep Space Network Progress Report 42-38: January and February 1977, pp. 50–54, April 15, 1977

This article reports on activities of the Network Operations organization in support of the Helios Project during December 1976 and January 1977.

G022 Helios Mission Support

P. S. Goodwin, E. S. Burke, and G. M. Rockwell

The Deep Space Network Progress Report 42-39: March and April 1977, pp. 17–22, June 15, 1977

This article reports on activities of the Network Operations organization in support of the Helios Project from 1 February through April 1977.

G023 Helios Mission Support

P. S. Goodwin, E. S. Burke, and G. M. Rockwell

The Deep Space Network Progress Report 42-40: May and June 1977, pp. 52–56, August 15, 1977

This article reports on activities of the Network Operations organization in support of the Helios Project from 15 April through 15 June 1977.

G024 Helios Mission Support

P. S. Goodwin and G. M. Rockwell

The Deep Space Network Progress Report 42-41: July and August 1977, pp. 39–42, October 15, 1977

This article reports on activities of the Network Operations organization in support of the Helios Project from 15 June through 15 August 1977.

G025 Helios Mission Support

P. S. Goodwin and G. M. Rockwell

The Deep Space Network Progress Report 42-42: September and October 1977, pp. 34–41, December 15, 1977

This article reports on activities of the Network Operations organization in support of the Helios Project from 15 August 1977 through 15 October 1977.

GREENHALL, C. A.

G026 Simulation of Time Series by Distorted Gaussian Processes

C. A. Greenhall

The Deep Space Network Progress Report 42-37: November and December 1976, pp. 146–151, February 15, 1977

Distorted stationary gaussian processes can be used to provide computer-generated imitations of experimental time series. A method of analyzing a source time series and synthesizing an imitation is shown, and an example using X-band radiometer data is given.

GROSS, S. H.

G027 Galilean Satellites: Anomalous Temperatures Disputed

D. Morrison (University of Arizona), L. A. Lebofsky, J. A. Cutts (Planetary Science Institute), G. J. Veeder, and S. H. Gross (Polytechnic Institute of New York)

Science, Vol. 195, pp. 90–93, January 7, 1977

For abstract, see Morrison, D.

GUPTA, A.

G028 Electrical, Magnetic, and Optical Properties of the Tetrathiafulvalene (TTF) Pseudohalides, $(TTF)_{12}(SCN)_7$ and $(TTF)_{12}(SeCN)_7$

R. B. Somoano, A. Gupta, V. Hadek, M. Novotny (Stanford University), M. Jones (Tulane University), T. Datta (Tulane University), R. Deck (Tulane University), and A. M. Hermann (Tulane University)

Phys. Rev., Pt. B: Solid State, Vol. 15, No. 2, pp. 595–601, January 15, 1977

For abstract, see Somoano, R. B.

GUPTA, K. K.

G029 On a Finite Dynamic Element Method for Free Vibration Analysis of Structures

K. K. Gupta

Comput. Methods Appl. Mech. Eng., Vol. 9, pp. 105–120, 1976

This paper explores the concept of finite dynamic elements involving higher order dynamic correction terms in the associated stiffness and mass matrices. Such matrices are then developed for a rectangular prestressed membrane element. Next, efficient analysis techniques for the eigenproblem solution of the resulting quadratic matrix equations are described in detail. These are followed by suitable numerical examples which indicate that employment of such dynamic elements in conjunction with an efficient quadratic matrix solution technique will result in a most significant economy in the free vibration analysis of structures.

G030 On a Numerical Solution of the Supersonic Panel Flutter Eigenproblem

K. K. Gupta

Int. J. Numer. Methods Eng., Vol. 10, pp. 637–645, 1976

An automated digital computer procedure is presented in this paper which enables efficient solution of the eigenvalue problem associated with the supersonic panel flutter phenomena. The step-by-step incremental solution procedure is based on an inverse iteration technique which effectively utilizes solution results from the previous step in determining such results during the current solution step. Also, the computations are limited to the determination of a few specific roots only, which are expected to contain the flutter mode, and this is achieved at each step without having to compute any other root.

The structural discretization achieved by the finite element method yields highly banded stiffness, mass, and aerodynamic matrices; the aerodynamic matrix evaluated by the linearized piston theory is real but unsymmetric in nature. The solution algorithm presented fully exploits the banded form of the associated matrices, and the resulting computer program written in FORTRAN V for the JPL UNIVAC 1108 computer proves to be most efficient and economical when compared to existing procedures of such analysis. Numerical results are presented for a two-dimensional panel flutter problem.

G031 Free Vibration Analysis of Spinning Flexible Space Structures

K. K. Gupta

J. Astronaut. Sci., Vol. XXIV, No. 3, pp. 273–280, July–September 1976

Efficient computation of natural frequencies and associated free vibration modes of spinning flexible structures is required to accurately determine the nature of interaction between the flexible structure and the attitude control system, which is vital in relating control torques to attitude angles. While structural discretization is effected by the finite element method, the resulting eigenvalue problem is solved by a combined Sturm sequence and inverse iteration procedure that yields a few specified roots and associated vectors. An eigenvalue procedure, based on a simultaneous iteration technique, provides efficient computation of the first few roots and vectors; a modal synthesis procedure proves to be useful for eigenproblem solutions of unusual structures such as spacecraft.

G032 Numerical Analysis of Free Vibrations of Damped Rotating Structures

K. K. Gupta

Proc. IMechE Conf. Vibrations Rotating Machinery, University of Cambridge, UK, Sept. 15–17, 1976, pp. 27–31

This paper is concerned with the efficient numerical solution of damped and undamped free vibration problems of rotating structures. While structural discretization is achieved by the finite element method, the associated eigenproblem solution is effected by a combined Sturm sequence and inverse iteration technique that enables the computation of a few required roots only without having to compute any other. For structures of complex configurations, a modal synthesis technique is also presented, which is based on appropriate combinations of eigenproblem solution of various structural components. Such numerical procedures are general in nature, which fully exploit matrix sparsity inherent in finite element discretizations, and prove to be most efficient for the vibration analysis of any damped rotating structure, such as rotating machineries, helicopter and turbine blades, spinning space stations, among others.

HADEK, V.

H001 Electrical, Magnetic, and Optical Properties of the Tetrathiafulvalene (TTF) Pseudohalides, $(TTF)_{12}(SCN)_7$ and $(TTF)_{12}(SeCN)_7$

R. B. Somoano, A. Gupta, V. Hadek, M. Novotny (Stanford University), M. Jones (Tulane University), T. Datta (Tulane University), R. Deck (Tulane University), and A. M. Hermann (Tulane University)

Phys. Rev., Pt. B: Solid State, Vol. 15, No. 2, pp. 595–601, January 15, 1977

For abstract, see Somoano, R. B.

HALL, R. I.

H002 Electron Impact Excitation of the Rydberg States in O_2 in the 7–10 eV Energy-Loss Region

S. Trajmar, D. C. Cartwright (Los Alamos Scientific Laboratory), and R. I. Hall (Universite Pierre et Marie Curie, Paris, France)

J. Chem. Phys., Vol. 65, No. 12, pp. 5275–5279, December 15, 1976

For abstract, see Trajmar, S.

HAMILTON, C. L.

H003 Dynamic Modeling and Sensitivity Analysis of Solar Thermal Energy Conversion Systems

C. L. Hamilton

The Deep Space Network Progress Report 42-41: July and August 1977, pp. 226–232, October 15, 1977

Since the energy input to solar thermal conversion systems is both time variant and probabilistic, it is unlikely that simple steady-state methods for estimating lifetime performance will provide satisfactory results. The work described here uses dynamic modeling to begin identifying what must be known about input radiation and system dynamic characteristics to estimate performance reliably. Daily operation of two conceptual solar energy systems was simulated under varying operating strategies with time-dependent radiation intensity ranging from smooth input of several magnitudes to input of constant total energy whose intensity oscillated with periods from 1/4 hour to 6 hours. Integrated daily system output and efficiency were functions of both level and dynamic characteristics of insolation. Sensitivity of output to changes in total input was greater than one. These findings support the feeling that interplay of radiation dynamics and collector response times affects the quality of energy delivered, and therefore system performance.

HAMILTON, G. B.

H004 Implementation of New-Generation Recorders/Reproducers Into the DSN

G. B. Hamilton

The Deep Space Network Progress Report 42-37: November and December 1976, pp. 184–187, February 15, 1977

New-generation recorder/reproducers are being installed in the Pre/Post-Detection Recording Subsystem at DSSs 14 (Goldstone), 43 (Australia), 63 (Spain), and the JPL Compatibility Test Area CTA 21. The performance of these new-generation machines is discussed, and representative corroborating data acquired at CTA 21 are presented.

HANSEN, G. R.

H005 Vehicle Safety Telemetry for Automated Highways

G. R. Hansen

JPL Publication 77-57, November 15, 1977

The concept of automated highways providing the means for motor vehicles to travel between interurban centers without active driver participation has been forwarded by many investigators. Breakdowns of the vehicles using such a highway could be hazardous to life or, at the least, interrupt traffic flow. The proper operation of a vehicle approaching an automated highway would have to be assessed to a high degree of certainty before that vehicle could be allowed entry.

This report summarizes the results of a study of several areas germane to the automated highway and vehicle system. The current state-of-the-art of automatic vehicle testing and diagnosis was investigated and it was determined that the emphasis is primarily centered on the proper operation of the engine. Lateral and longitudinal guidance technologies, including speed control and headway sensing for collision avoidance, were reviewed. The principal guidance technique remains the buried wire. Speed control and headway sensing, even though they show the same basic elements in the braking and fuel systems, are proceeding independently. The applications of on-board electronic and microprocessor techniques were investigated and, again, each application (emission control, spark advance, or anti-slip braking) is being treated as an independent problem. The final portion of the report presents various processor systems leading to a proposed unified bus system of distributed processors for accomplishing the various functions and testing required for vehicles equipped to use automated highways.

HANSEN, O.

H006 Search for Correlation Between Asteroid Families and Classes

O. Hansen

Icarus, Vol. 32, pp. 229–232, 1977

A correlation between membership in a dynamically defined asteroid family and membership in a given asteroid spectral class is sought. Examination of 10 families each with five or more classified members indicates a correlation for the 4 families whose existence is best established, and no correlation for the remaining 6 families. This conclusion supports the break-up hypothesis for the origin of some families, while not contradicting that hypothesis for any family.

H007 On the Prograde Rotation of Asteroids

O. Hansen

Icarus, Vol. 32, pp. 458–460, 1977

Sets of diameter determinations before and after opposition for the asteroids Ceres, Pallas, Vesta, and Fortuna have been studied statistically for indications of spin direction. All four asteroids are tentatively found to have prograde spin. For Ceres, that conclusion is virtually certain.

HANSEN, O. L.

H008 Photometry of the Asteroid 1976 AA at 0.56 and 2.2 μm

G. J. Veeder, D. L. Matson, and O. L. Hansen

Icarus, Vol. 31, pp. 424–426, 1977

For abstract, see Veeder, G. J.

H009 An Explication of the Radiometric Method for Size and Albedo Determination

O. L. Hansen

Icarus, Vol. 31, pp. 456–482, 1977

A new radiometric model for disk-integrated photometry of asteroids is presented. With empirical support from photometry of Mercury and the Moon, the model assumes that observed sunward beaming of the infrared emission is due to craters. In contrast to earlier theoretical studies of the lunar emission, the observable flux ratio between a cratered sphere and a smooth sphere is calculated for large ranges in wavelength, temperature, and phase angle. Revised diameters and albedos based on the crater model are given for 84 asteroids. The revised values are in good agreement with Morrison's (1977) radiometric results. It is shown that the systematic discrepancy between radiometric and polarimetric albedos (Zellner and Gradie, 1976) is probably a double-valued function of albedo. Some typical geometric albedos from this paper, Morrison (1977), and Zellner and Gradie (1976), respectively, are: Ceres (0.050 ± 0.005, 0.053 ± 0.004, 0.068), Vesta (0.235 ± 0.032, 0.235 ± 0.011, 0.271), mean *C* type (0.031 ± 0.009, 0.035 ± 0.009, 0.061 ± 0.005), mean *S* type (0.117 ± 0.030, 0.136 ± 0.032, 0.181 ± 0.23), and mean *M* type (0.105 ± 0.037, 0.115 ± 0.033, 0.157 ± 0.079). Areas of disagreement between radiometry and polarimetry are underscored, and research to resolve them is suggested.

HARSTAD, K. G.

H010 Proposed Computer Model for Electric Discharge Atomic Vapor Lasers

K. G. Harstad

JPL Publication 77-11, March 15, 1977

A detailed computer model for the rate kinetics of an atomic vapor laser excited by electrical discharge is proposed. The model equations are defined, and the computer program structure is discussed.

HARTOP, R.

H011 The High-Power *X*-Band Planetary Radar at Goldstone: Design, Development, and Early Results

R. Hartop and D. A. Bathker

IEEE Trans. Microwave Theor. Tech., Vol. MTT-24, No. 12, pp. 958–963, December 1976

Selected critical microwave components for a 400-kW very-long-pulse (several hours) *X*-band radar system are discussed from theoretical and practical viewpoints. Included are the special-sized waveguide and flanges, hybrid power combiner, couplers, switches, polarizer, rotary joints, feedhorn, and radome. The system is installed on the National Aeronautics and Space Administration/Jet Propulsion Laboratory 64-m-diam reflector antenna at Goldstone, CA.

HARTOP, R. W.

H012 Selectable Polarization at X-Band

R. W. Hartop

The Deep Space Network Progress Report 42-39: March and April 1977, pp. 177–180, June 15, 1977

The X-band feeds in the DSN are being upgraded to include selectable polarization in time for the Voyager missions to the outer planets.

H013 **Dual-Frequency Feed System for 26-Meter Antenna Conversion**

R. W. Hartop

The Deep Space Network Progress Report 42-40: May and June 1977, pp. 146–149, August 15, 1977

New cassegrain feed cone assemblies are being designed as part of the upgrade of three 26-meter diameter antennas to 34-meter diameter with improved performance. The new dual-frequency feed cone (SXD) will provide both S- and X-band feed systems and traveling wave masers, with a reflex reflector system to permit simultaneous operation analogous to the 64-meter antennas.

HEFT, R. C.

H014 **Costs and Energy Efficiency of a Dual-Mode System**

R. C. Heft and C. S. Borden

JPL Publication 77-34, April 30, 1977

This report represents a more detailed examination of two areas of a previous analysis on a Dual-Mode System as documented in "Technical and Cost Considerations for Urban Applications of Dual-Mode Transportation" (JPL, May 1972). The present study is divided into two parts: 1) An Economic Analysis, and 2) An Energy Consumption Analysis. The Economic Analysis examines the present value Life Cycle Costs of the System for both public and semi-private system ownership and presents the costs in terms of levelized required revenue per passenger mile. The Energy Consumption Analysis considers the energy use of the various Dual Mode Vehicle by means of a detailed vehicle simulation program for the control policy and guideway system as described in the previous study. Several different propulsion systems are considered.

HERMANN, A. M.

H015 **Electrical, Magnetic, and Optical Properties of the Tetrathiafulvalene (TTF) Pseudohalides, $(TTF)_{12}(SCN)_7$ and $(TTF)_{12}(SeCN)_7$**

R. B. Somoano, A. Gupta, V. Hadek, M. Novotny (Stanford University), M. Jones (Tulane University), T. Datta (Tulane University), R. Deck (Tulane University), and A. M. Hermann (Tulane University)

Phys. Rev., Pt. B: Solid State, Vol. 15, No. 2, pp. 595–601, January 15, 1977

For abstract, see Somoano, R. B.

HERRERA, G.

H016 **Projection of Distributed-Collector Solar-Thermal Electric Power Plant Economics to Years 1990–2000**

T. Fujita, N. El Gabalawi, G. Herrera, and R. H. Turner

JPL Publication 77-79, December 1977

For abstract, see Fujita, T.

HESS, G. R.

H017 **Computer Image Processing in Marine Resource Exploration**

P. R. Paluzzi, W. R. Normark (U. S. Geological Survey), G. R. Hess (U. S. Geological Survey), H. D. Hess (U. S. Geological Survey), and M. J. Cruickshank (U. S. Geological Survey)

Proc. MTS-IEEE Oceans '76 Conf., Washington, D. C., Sept. 13–15, 1976, pp. 4D-1–4D-10

For abstract, see Paluzzi, P. R.

HESS, H. D.

H018 **Computer Image Processing in Marine Resource Exploration**

P. R. Paluzzi, W. R. Normark (U. S. Geological Survey), G. R. Hess (U. S. Geological Survey), H. D. Hess (U. S. Geological Survey), and M. J. Cruickshank (U. S. Geological Survey)

Proc. MTS-IEEE Oceans '76 Conf., Washington, D. C., Sept. 13–15, 1976, pp. 4D-1–4D-10

For abstract, see Paluzzi, P. R.

HEYSER, R. C.

H019 **Final Report: Medical Ultrasonic Tomographic System**

R. C. Heyser, D. H. Le Croissette, R. Nathan, and R. L. Wilson (Harbor General Hospital, Los Angeles)

JPL Publication 77-72, October 1, 1977

An electro-mechanical scanning assembly has been designed and fabricated for the purpose of generating an ultrasound tomogram. A low cost modality has been demonstrated in which analog instrumentation methods form a tomogram on photographic film. Successful tomogram reconstructions have been obtained on *in vitro* test objects by using the attenuation of the first path ultrasound signal as it passes through the test object.

Thus, the nearly half-century tomographic methods of X-ray analysis have been verified as being useful for ultrasound imaging.

HILBERT, E. E.

H020 **Cluster Compression Algorithm: A Joint Clustering/ Data Compression Concept**

E. E. Hilbert

JPL Publication 77-43, December 1, 1977

This report describes the Cluster Compression Algorithm (CCA), which was developed to reduce costs associated with transmitting, storing, distributing, and interpreting Landsat multispectral image data. The CCA is a preprocessing algorithm that uses feature extraction and data compression to more efficiently represent the information in the image data. The format of the preprocessed data enables simple look-up table decoding and direct use of the extracted features to reduce user computation for either image reconstruction, or computer interpretation of the image data. Basically, the CCA uses spatially local clustering to extract features from the image data to describe spectral characteristics of the data set. In addition, the features may be used to form a sequence of scalar numbers that define each picture element in terms of the cluster features. This sequence, called the feature map, is then efficiently represented by using source encoding concepts. Various forms of the CCA are defined and experimental results are presented to show trade-offs and characteristics of the various implementations. Examples are provided that demonstrate the application of the cluster compression concept to multispectral images from Landsat and other sources.

HINKLEY, E. D.

H021 **Measurement of the Fundamental Vibration–Rotation Spectrum of ClO**

R. T. Menzies, J. S. Margolis, E. D. Hinkley, and R. A. Toth

Appl. Opt., Vol. 16, No. 3, pp. 523–525, March 1977

For abstract, see Menzies, R. T.

HISE, R. E.

H022 **Development and Qualification of the Propellant Management System for Viking 75 Orbiter**

M. W. Dowdy, R. E. Hise (Martin Marietta Corporation), and R. G. Peterson (Martin Marietta Corporation)

J. Spacecraft Rockets, Vol. 14, No. 3, pp. 133–140, March 1977

For abstract, see Dowdy, M. W.

HODGSON, W. D.

H023 **The DSN Programming System**

W. D. Hodgson

The Deep Space Network Progress Report 42-41: July and August 1977, pp. 4–9, October 15, 1977

This article describes the DSN Programming System. The Programming System provides the DSN with implementation tools and practices for producing DSN software. This article provides a general description of the System, as well as its key characteristics, status, plans, and expected benefits.

HOLCOMB, L.

H024 **Effects of Aniline Impurities on Monopropellant Hydrazine Thruster Performance**

L. Holcomb, L. Mattson, and R. Oshiro

J. Spacecraft Rockets, Vol. 14, No. 3, pp. 141–148, March 1977

The phenomenon of monopropellant hydrazine thruster catalyst bed poisoning with various grades of hydrazine was studied. Tests with 0.45-N and 0.9-N thrusters, employing Shell 405 spontaneous catalyst, showed that pulse shape distortion could be encountered very rapidly under certain types of pulse mode operation. It was determined that the pulse distortion, in this particular instance, was largely due to the small amounts of the miscible impurity, aniline, which is normally left in hydrazine during the dehydration process of the manufacturing cycle. It was also found that washout could be accelerated by this impurity. During low-usage duty-cycle operation as encountered in limit cycling, thruster catalyst temperatures are cool enough to permit chemisorption of aniline, resulting in a masking of the active catalyst sites and subsequent loss in the bed activity. Although it was shown that this particular poisoning is generally a reversible condition, it could pose inflight spacecraft control problems if not properly considered beforehand. Removal of the major portions of the aniline from the propellant or artificial heating of the catalyst bed to drive off compounds formed from this impurity was found to be effective in preventing this performance degradation.

HOLLAND, J. C.

H025 **A Method for Reducing Software Life Cycle Costs**

W. O. Paine and J. C. Holland

The Deep Space Network Progress Report 42-39: March and April 1977, pp. 186–191, June 15, 1977

For abstract, see Paine, W. O.

HOWE, T. W.

H026 Viking Mission support

D. W. Johnston, T. W. Howe, and G. M. Rockwell

The Deep Space Network Progress Report 42-37: November and December 1976, pp. 12–25, February 15, 1977

For abstract, see Johnston, D. W.

H027 Viking Extended Mission Support

T. W. Howe and D. J. Mudgway

The Deep Space Network Progress Report 42-40: May and June 1977, pp. 41–51, August 15, 1977

This report covers the period 1 March 1977 through 30 April 1977 and includes DSN Mark III Data System (MDS) testing, status of Viking-related tracking and command support as well as the status of the Viking DSN Discrepancy Reporting System. The DSN Operations support of Viking events and Radio Science activities are also discussed. Current progress on the major new reconfiguration of the Network is presented in the context of support for the Viking Extended Mission.

H028 Viking Extended Mission Support

T. W. Howe

The Deep Space Network Progress Report 42-42: September and October 1977, pp. 28–33, December 15, 1977

This report covers the period from 1 July through 31 August 1977 and includes the remainder of post DSN Mark III Data Subsystem Implementation Project Viking-related testing at DSS 14. It also includes reports on the Viking DSN Discrepancy Reporting System, Viking command support, tracking support, and periodic tests conducted with the Viking spacecraft.

HSU, G.

H029 Modeling of Fluidized Bed Silicon Deposition Process

K. Kim, G. Hsu, R. Lutwack, and A. Praturi

JPL Publication 77-25, June 15, 1977

For abstract, see Kim, K.

H030 Chemical Vapor Deposition of Silicon from Silane Pyrolysis

A. K. Praturi, R. Lutwack, and G. Hsu

JPL Publication 77-38, July 15, 1977

For abstract, see Praturi, A. K.

HUBBARD, W. B.

H031 Pioneer 10 and 11 Radio Occultations by Jupiter

A. J. Kliore, P. M. Woiceshyn, and W. B. Hubbard (University of Arizona)

COSPAR Space Research, Vol. XVII, pp. 703–710, 1977

For abstract, see Kliore, A. J.

H032 Gravitational Fields and Interior Structure of the Giant Planets

J. D. Anderson and W. B. Hubbard (University of Arizona)

Progr. Astronaut. Aeronaut., Vol. 50, pp. 71–83, 1977

For abstract, see Anderson, J. D.

HUNT, G. E.

H033 Interpretation of Spatial and Temporal Variations of Hydrogen Quadrupole Absorptions in the Jovian Atmosphere Observed During the 1972 Apparition

G. E. Hunt (Meteorological Office, Bracknell, Berkshire, England) and J. T. Bergstralh

Icarus, Vol. 30, pp. 511–530, 1977

During the 1972 apparition of Jupiter, a patrol was made of the (3,0) S(1) and (4,0) S(1) quadrupole lines of molecular hydrogen in the equatorial region and in bands bounded by ±15 and ±49° zenographic latitude from the McDonald and Table Mountain Observatories. At the center of the Jovian disk, evidence was found of temporal variability of both lines over the duration of the observing period. A technique was employed that takes into account all radiative transfer processes in an inhomogeneous model of Jupiter's atmosphere, and use it to derive the effective level of formation of the spectral lines and the relative abundance of hydrogen. In this way, measured changes can be correlated in the equivalent widths of the hydrogen lines with variations in cloud structure. The effective pressure level at which the (4,0) S(1) line is formed varies in the range 2 ± 0.5 to 1.3 ± 0.2 atm, while for the (3,0) S(1) line, the pressure varies between 1.6 ± 0.5 and 1 ± 0.4 atm. If these variations are interpreted in terms of changes in elevation of the

top of a dense lower cloud deck, the elevation apparently varied with an amplitude of 25 km during the observational period.

Spatial variations in the strengths of both lines were also found. Both lines are weaker at the east limb than at the center of the disk (15–19%) while the variations toward the west limb are less pronounced (5%). Similar center-to-limb variations were found in the latitude bands bounded by ±15 and ±49°, although the lines were stronger in the northern component at the time of the observations.

HUNT, R. H.

H034 **Line Positions and Strengths of Methane in the 2862 to 3000 cm^{-1} Region**

R. A. Toth, L. R. Brown (Florida State University), and R. H. Hunt (Florida State University)

J. Mol. Spectros., Vol. 67, Nos. 1–3, pp. 1–33, September 15, 1977

For abstract, see Toth, R. A.

HUNTRESS, W. T., JR.

H035 **Laboratory Studies of Bimolecular Reactions of Positive Ions in Interstellar Clouds, in Comets, and in Planetary Atmospheres of Reducing Composition**

W. T. Huntress, Jr.

Astrophys. J. Suppl. Ser., Vol. 33, No. 4, pp. 495–514, April 1977

Laboratory results are presented for over 200 bimolecular ion-molecule reactions of importance in the chemistry of interstellar clouds, comets, and planetary atmospheres with reducing compositions. The product distributions and rate constants measured for these reactions at 300 K using ion cyclotron resonance methods are given in 23 tables covering the reactions of H^+, He^+, Ne^+, Ar^+, C^+, N^+, S^+, H_2^+, CH^+, OH^+, NH^+, HS^+, H_3^+, H_2O^+, NH_2^+, H_2S^+, NH_3^+, CH_2^+, CH_3^+, CH_4^+, $C_2H_2^+$, $C_2H_3^+$, $C_2H_4^+$, $C_2H_5^+$, $C_2H_6^+$, and several other ions with many stable neutral molecules including H_2, O_2, N_2, CO, NO, CO_2, N_2O, HCN, H_2O, NH_3, H_2S, H_2CO, CH_4, C_2H_2, C_2H_4, and C_2H_6. A special compilation is given for the reactions of the above ions with H_2, which also includes the reactions of O^+, HeH^+, CO^+, NO^+, CN^+, HCN^+, HCO^+, H_2CO^+, C_2^+, N_2^+, O_2^+, C_2H^+, O_2H^+, and $C_2H_2^+$ ions with H_2 as well as the exchange reactions of several ions with isotopic hydrogen molecules. In addition to the experimental data, some prescriptions are given for predicting the most probable product channels for reactions for which there are no experimental data yet available. These prescriptions are based on the compilation of observed preferred product channels for reactions involving a particular ion. These laboratory data and prescriptions are used in a few cases to illustrate applications to recent work modeling the chemistry of interstellar clouds, comets, and the atmospheres of the Jovian planets and their satellites. The areas of astrophysical chemistry in which further laboratory work is required are also briefly examined.

H036 **Ion Cyclotron Resonance Studies of Some Reactions of N^+ Ions**

V. G. Anicich, W. T. Huntress, Jr., and J. H. Futrell (University of Utah)

Chem. Phys. Lett., Vol. 47, No. 3, pp. 488–489, May 1, 1977

For abstract, see Anicich, V. G.

H037 **Product Distributions for Some Thermal Energy Charge Transfer Reactions of Rare Gas Ions**

V. G. Anicich, J. B. Laudenslager, W. T. Huntress, Jr., and J. H. Futrell (University of Utah)

J. Chem. Phys., Vol. 67, No. 10, pp. 4340–4350, November 15, 1977

For abstract, see Anicich, V. G.

H038 **Product Distribution and Rate Constants for the Reactions of CH_3^+, CH_4^+, $C_2H_2^+$, $C_2H_3^+$, $C_2H_4^+$, $C_2H_5^+$, and $C_2H_6^+$ Ions with CH_4, C_2H_2, C_2H_4, and C_2H_6**

J. K. Kim, V. G. Anicich, and W. T. Huntress, Jr.

J. Phys. Chem., Vol. 81, No. 19, pp. 1798–1805, 1977

For abstract, see Kim, J. K.

H039 **Calibration of Marginal Oscillator Sensitivity for Use in ICR Spectrometry**

V. G. Anicich and W. T. Huntress, Jr.

Rev. Sci. Instrum., Vol. 48, No. 5, pp. 542–544, May 1977

For abstract, see Anicich, V. G.

HURD, W. J.

H040 **Preliminary Demonstration of Precision DSN Clock Synchronization by Radio Interferometry**

W. J. Hurd

The Deep Space Network Progress Report 42-37: November and December 1976, pp. 57–68, February 15, 1977

Radio interferometry can be used to measure the offsets between the clocks at the various stations of the DSN, and to monitor the rates of the station frequency standards. A wideband digital data acquisition system has been developed to measure the clock offsets to the 10-ns accuracy required to facilitate three-way spacecraft ranging, to monitor the hydrogen maser frequency standard rates to 1 part in 10^{14}, and to potentially reduce operational costs by replacing the current DSN Operational Time Sync System. Three experiments have been conducted with this system, two short-baseline experiments at Goldstone and one long-baseline experiment between Goldstone and Australia. All achieved subnanosecond resolutions. These accuracies were independently confirmed to within about 3 μs, as limited by the accuracy of available independent measurements.

H041 **Concatenated Shift Registers Generating Maximally Spaced Phase Shifts of PN-Sequences**

W. J. Hurd and L. R. Welch (University of Southern California)

The Deep Space Network Progress Report 42-40: May and June 1977, pp. 110–116, August 15, 1977

A large class of linearly concatenated shift registers is shown to generate approximately maximally spaced phase shifts of pn-sequences, for use in pseudorandom number generation. A constructive method is presented for finding members of this class, for almost all degrees for which primitive trinomials exist. The sequences which result are not normally characterized by trinomial recursions, which is desirable since trinomial sequences can have some undesirable randomness properties.

H042 **VLBI Instrumental Effects, Part I**

J. W. Layland and W. J. Hurd

The Deep Space Network Progress Report 42-42: September and October 1977, pp. 54–80, December 15, 1977

For abstract, see Layland, J. W.

HUTCHBY, J. A.

H043 **Comparative Studies of Ion-Implant Josephson-Effect Structures**

R. K. Kirschman, J. A. Hutchby (Langley Research Center), J. W. Burgess (Langley Research Center), R. P. McNamara (California Institute of Technology), and H. A. Notarys (California Institute of Technology)

IEEE Trans. Magnet., Vol. MAG-13, No. 1, pp. 731–734, January 1977

For abstract, see Kirschman, R. K.

IBANEZ, F.

I001 **Calibration of Block 4 Translator Path Delays at DSS 14 and CTA 21**

T. Y. Otoshi, P. D. Batelaan, K. B. Wallace, and F. Ibanez

The Deep Space Network Progress Report 42-37: November and December 1976, pp. 188–197, February 15, 1977

For abstract, see Otoshi, T. Y.

IRVINE, A. P.

I002 **Configuration Control and Audit Assembly**

A. P. Irvine

The Deep Space Network Progress Report 42-41: July and August 1977, pp. 166–171, October 15, 1977

The Configuration Control and Audit Assembly (CCA) Project is responsible for the implementation of a computer-based system for acquiring, managing and distributing a subset of the Deep Space Network (DSN) Data Base of operational and management information. This system is presently scheduled for transfer to Operations July 1, 1981. Early in 1978 a demonstration will be conducted to provide data for a Life Cycle Cost (LCC) Analysis and verify design feasibility.

ISHIMARU, A.

I003 **Structure of Density Fluctuations Near the Sun Deduced From Pioneer-6 Spectral Broadening Measurements**

R. Woo F. C. Yang, and A. Ishimaru (University of Washington)

Astrophys. J., Vol. 210, No. 2, Pt. 1, pp. 593–602, December 1, 1976

For abstract, see Woo, R.

IVIE, C.

I004 An Interstellar Precursor Mission

L. D. Jaffe, C. Ivie, J. C. Lewis, R. Lipes, H. N. Norton, J. W. Stearns, L. D. Stimpson, and P. Weissman

JPL Publication 77-70, October 30, 1977

For abstract, see Jaffe, L. D.

JACKSON, E. B.

J001 DSN Research and Technology Support

E. B. Jackson

The Deep Space Network Progress Report 42-38: January and February 1977, pp. 199–202, April 15, 1977

The activities of the Venus Station (DSS 13) and the Microwave Test Facility (MTF) during the period October 11, 1976, through February 13, 1977, are discussed and progress noted. A significant effort on implementation of equipment for the planned conversion of DSS 13 to unattended operation is discussed. The Receiver and Microwave Subsystems are near completion, and the new feedcone and position encoders have been implemented onto the 26-m antenna. Support of the 400-kW X-band radar, located at DSS 14, is reported, and the activities of the DSN High Power Transmitter Maintenance Facility, located at DSS 13 and MTF, are discussed. The successful completion of the first series of observations planned for VLBI validation is reported, and significant station maintenance activities are briefly covered.

Clock synchronization transmissions to DSS 43 and DSS 63 are reported, and an evaluation of any pointing errors in the new 26-m antenna position transducer are made. Extensive tracking support for various Advanced Systems Development and Ground Based Radio Science activities is reported. In particular, VLBI observations for DSN platform parameters, interplanetary scintillation of signals from the Viking spacecraft at small SEP angles, planetary radio astronomy, radio frequency interference analysis, and geostationary satellite radar cross section experiments were supported and are discussed.

J002 DSN Research and Technology Support

E. B. Jackson

The Deep Space Network Progress Report 42-40: May and June 1977, pp. 200–202, August 15, 1977

The ongoing activities at the Venus Station (DSS 13) and the Microwave Test Facility (MTF) during the period February 14 through June 5, 1977, are discussed and progress noted. Completion of phase one equipment implementation for unattended operation at DSS 13 is noted and operation demonstrated with several "hands off" spacecraft downlink acquisitions, using either locally (DSS 13) directed or remotely (JPL) directed computer control. Salvaging of a 20-kW klystron, at a cost savings of several thousand dollars, was accomplished by the DSN High Power Transmitter Facility, along with its more routine activities of testing and repairing high power transmitter components.

Extensive tracking activities with the 26-m antenna are discussed, including DSN Platform Parameters, Multistation Planetary Radar, Helios II Spectrum Broadening Analysis, VLBI Validation, Planetary Radio Astronomy, and Pulsar Rotation Constancy, for a total time of 219-1/4 observing hours. Clock synchronization transmissions from the DSS 13 master clock to the overseas 64-m antenna complexes are reported and special implementation activities in support of PV-78 are discussed. Implementation of a Hydrogen Maser Frequency Standard and the "pathfinder" installation of a Utility Control System (UCS) are reported, and significant station modification and maintenance activity are noted.

JACOBI, N.

J003 Ground-State Properties of hcp Helium-4 on the Basis of a Cell Model

N. Jacobi and J. S. Zmuidzinas

Phys. Rev., Pt. B: Solid State, Vol. 16, No. 7, pp. 3267–3269, October 1, 1977

A simple cell model is used to compute the ground-state energy and the volume-pressure relation for hcp ^{4}He, in good agreement with experiments and with more sophisticated quantum-mechanical calculations.

JACOBSON, A. S.

J004 Measurement of 0.511-MeV Gamma Rays With a Balloon-Borne Ge(Li) Spectrometer

J. C. Ling, W. A. Mahoney, J. B. Willett, and A. S. Jacobson

J. Geophys. Res., Space Phys., Vol. 82, No. 10, pp. 1463–1473, April 1, 1977

For abstract, see Ling, J. C.

JAFFE, L. D.

J005 An Interstellar Precursor Mission

L. D. Jaffe, C. Ivie, J. C. Lewis, R. Lipes, H. N. Norton, J. W. Stearns, L. D. Stimpson, and P. Weissman

JPL Publication 77-70, October 30, 1977

A mission out of the planetary system, with launch about the year 2000, could provide valuable scientific data as well as test some of the technology for a later mission to another star. A mission to a star is not expected to be practical around 2000 because the flight time with the technology then available is expected to exceed 10,000 yr.

Primary scientific objectives for the precursor mission concern characteristics of the heliopause, the interstellar medium, stellar distances (by parallax measurements), low energy cosmic rays, interplanetary gas distribution, and mass of the solar system. Secondary objectives include investigation of Pluto. Candidate science instruments are suggested.

The mission should extend to 500–1000 AU from the sun. A heliocentric hyperbolic escape velocity of 50–100 km/s or more is needed to attain this distance within a reasonable mission duration. The trajectory should be toward the incoming interstellar wind. For a year 2000 launch, a Pluto encounter can be included. A second mission targeted parallel to the solar axis would also be worthwhile.

The mission duration is 20 years, with an extended mission to a total of 50 years. A system using 1 or 2 stages of nuclear electric propulsion was selected as baseline. The most promising alternatives are ultralight solar sails or laser sailing, with the lasers in Earth orbit, for example. The NEP baseline design allows the option of carrying a Pluto orbiter as a daughter spacecraft.

Individual spacecraft systems for the mission are considered, technology requirements and problem areas noted, and a number of recommendations made for technology study and advanced development. The most critical technology needs include attainment of 50-yr spacecraft lifetime and development of a long-life NEP system.

J006 **Aerospace Technology Can Be Applied to Exploration "Back on Earth"**

L. D. Jaffe

Oil Gas J., pp. 92–97, August 15, 1977

A number of concepts for utilizing aerospace technologies for Earth applications include: seismic reflection concepts, sea-floor imaging and mapping, remote geochemical sensing, identification of geological analogies, drilling concepts, and down-hole acoustic concepts

J007 **Lunar Crater Arcs**

L. D. Jaffe and E. O. Bulkley

The Moon, Vol. 16, pp. 71–114, 1976

An analysis has been made of the tendency of large lunar craters to lie along circles. A catalog of the craters ≥ 50 km in diameter was prepared first, noting position, diameter, rim sharpness and completion, nature of underlying surface, and geological age. The subset of those craters 50–400 km in diameter was then used as input to computer programs which identified each 'family' of four or more craters, of selected geological age, lying on a circular arc. For comparison, families were also identified for randomized crater models in which the crater spatial density was matched to that on the Moon, either overall or separately for mare and highland areas. The observed frequency of lunar arcuate families was statistically highly significantly greater than for the randomized models, for craters classified as either late pre-Imbrian (Nectarian), middle pre-Imbrian, or early pre-Imbrian, as well as for a number of larger age-classes. The lunar families tend to center in specific areas of the Moon: these lie in highlands rather than maria and are different for families of Nectarian craters than for pre-Nectarian. The origin of the arcuate crater groupings is not understood.

JAGGARD, D. L.

J008 **Higher-Order Bragg Coupling in Periodic Media With Gain or Loss**

D. L. Jaggard and C. Elachi

J. Appl. Phys., Vol. 48, No. 4, pp. 1461–1466, April 1977

We consider wave propagation in longitudinally periodic media with gain or loss. An extended coupled-waves (ECW) approach and Floquet approach are used to study index and gain (or loss) coupling in periodic media at the first few Bragg resonances by the use of Brillouin diagrams. Phase speeding or slowing that is dependent upon the type of coupling occurs in periodic media. Even and odd resonances display different dispersion characteristics. Several examples of coupling due to multiharmonic periodicities are also covered. Coupling or feedback strength can be continuously varied by changing the relative phase of multiharmonic periodicities.

JAIN, A.

J009 **Electronic Imaging and Scanning System**

A. Jain

Appl. Opt., Vol. 16, No. 3, pp. 550–553, March 1977

In this article, the results on imaging by frequency scanning to derive the expression for the 2-D image are extended. This is the Fourier transform, with respect to the angle and frequency of illumination, of the electric

ORIGINAL PAGE 16
OF POOR QUALITY

field detected in the far-field region of the object. The case is considered of a rough object to show that, for roughness finer than the resolution of this imaging system, the image has a granular appearance corresponding to the classical speckle effect. Large-scale phase perturbations lead to the elevation displacement effect.

J010 Determination of Ocean Wave Heights for Synthetic Aperture Radar Imagery

A. Jain

Appl. Phys., Vol. 13, pp. 371–382, 1977

A calculation is presented for the cross-correlation of the radar images obtained by processing the same signal data over different portions of the chirp spectrum bandwidth as a function of the center frequency spacings for these portions. This is shown to be proportional to the square of the product of the characteristic function for ocean wave heights and the pupil function describing the chirp spectrum bandwidth used in the processing. Measurements of this function for ocean wave imagery over the coast of Alaska, the North Atlantic, and Monterey Bay, California, and correlation with the significant wave heights reported from ground truth data indicate that the synthetic aperture radar instrument can be used for providing wave height information in addition to the ocean wave imagery.

J011 Radar Speckle Reduction in Synthetic Aperture Radar Processors by a Moving Diffuser

A. Jain

Opt. Commun., Vol. 20, No. 2, pp. 239–242, February 1977

We present some theoretical and experimental results demonstrating the reduction of synthetic aperture radar speckle when a moving diffuser is placed in the processor image plane and is reimaged with a lens whose resolution is not better than the radar resolution. The resolution of the resulting radar image is determined by the resolution of this output lens.

JENNINGS, C.

J012 Evaluation of Coal Feed Systems Being Developed by the Energy Research and Development Administration

R. Phen, C. Jennings, W. Luckow, L. Mattson, D. Otth, and P. Tsou

JPL Publication 77-54, September 1977

For abstract, see Phen, R.

JEPSEN, P. L.

J013 The Software/Hardware Interface for Interactive Image Processing at the Image Processing Laboratory of the Jet Propulsion Laboratory

P. L. Jepsen

Proc. Digital Equip. Computer Users Soc., Las Vegas, Nev., Dec. 1976, pp. 629–654

Image processing is a field where it is frequently necessary to view one's data as it is being processed and then perhaps modify the processing in order to produce satisfactory results. As the need for effective interactive image processing has rapidly blossomed into a requirement, so has there been a continually increasing demand for more display devices and more terminals to support this type of processing. And because of the variety and number of these different devices, it becomes extremely desirable to relieve the central processor of many of the associated data processing functions for these devices. At the Image Processing Laboratory of JPL, a PDP 11/40 has been attached to the host—in this case an IBM 360/65—using a DX11B programmable channel interface. In turn, a number of terminals and gray level/graphics displays have been connected to the UNIBUS on the 11 generally by direct memory access interfaces. The host 360 operating system provides basic time sharing support to the terminal users; to augment this for interactive image processing, a Command Processor program has been developed that gives the image processing analyst access to picture data and the tasks needed to effectively process this data. A set of 360 Fortran callable primitives has been developed to support the various gray level/graphics displays and associated hardware. These are intended as basic building blocks for sophisticated interactive image processing. The software design is flexible so that as new peripherals are added, it will be possible for the programmer/analyst to use existing software for these new peripherals where functions overlap. The Image Processing Laboratory has developed an effective interactive image processing capability that can also be readily expanded as future needs arise.

JET PROPULSION LABORATORY

J014 JPL Basic Research Review

Jet Propulsion Laboratory

JPL Publication 77-5, March 16–17, 1977

Results, current status and projected goals for some fifty Research and Advanced Development programs at the Jet Propulsion Laboratory are reported in abstract form. Some of the papers will be presented orally to the NASA OAST Council while others are provided to delineate additional work in progress at the Laboratory.

J015 Report on Phase I of the Microprocessor Seminar Held at Caltech, October 1976

Jet Propulsion Laboratory

JPL Publication 77-6, April 1, 1977

This report documents a seminar and workshop series on microprocessors and associated large-scale integrated (LSI) circuits attended by NASA center and other government agency representatives. The potential for commonality of device requirements among the agencies was assessed. Candidate processes and mechanisms for qualifying candidate LSI technologies for high reliability applications were reviewed. Specifications for testing and testability were discussed. Various programs and tentative plans of the participating organizations in the development of hi rel LSI are presented.

J016 International Conference on Problems Related to the Stratosphere

Jet Propulsion Laboratory

JPL Publication 77-12, May 15, 1977

On September 15, 16 and 17, 1976, a conference was held in Logan, Utah, U.S.A., on the potential for pollution of the earth's stratosphere by injection of various gases as a result of man's activity on the surface of our planet. The conference was attended by over three hundred participants from countries over the entire globe. Represented were both scientists conducting research into stratospheric problems and policy makers involved in making regulatory decisions on various aspects of the international stratospheric pollution issue.

The conference was focused on four main areas of investigation concerning the potential for reduction of stratospheric ozone: laboratory studies and stratospheric measurements of stratospheric chemistry and constituents, sources for and chemical budget of stratospheric halogen compounds, sources for and chemical budget of stratospheric nitrous oxide, and the dynamics of decision making on regulation of potential pollutants of the stratosphere.

In this volume are included extended abstracts of the scientific sessions of the conference as well as complete transcriptions of the panel discussions on sources for and atmospheric budget of halocarbons and nitrous oxide. It is in these panel discussions that the scientific issues involved are best illustrated.

The political, social and economic issues involving regulation of potential stratospheric pollutants were examined extensively in the final session of the conference by policy makers at the highest levels of U.S. and foreign industry, government and consumer protection agencies. Because of the uniqueness of this type of session in a nominally scientific conference, and because of the importance of the issues involved to the welfare of humanity on this planet, this session is transcribed in its entirety.

The conference as a whole has set the stage for the initial efforts, in the latter part of this decade, to assess the potential damage to the stratospheric ozone layer by man-made pollutants and to examine the necessity for coordination and communication between science and technology, ecological issues, and social-political-economic concerns in order to insure the survivability of our present technological civilization.

J017 Report on Phase II of the Microprocessor Seminar Held at Caltech, April 1977

Jet Propulsion Laboratory

JPL Publication 77-39, August 15, 1977

This report documents Phase II of a Microprocessor Seminar held at the California Institute of Technology. Workshop sessions and papers were devoted to various aspects of microprocessor and large-scale-integrated (LSI) circuit technology. Presentations were made by LSI manufacturers on advanced LSI developments for high-reliability military and NASA applications. Microprocessor testing techniques were discussed, and test data were presented. High-reliability procurement specifications were also discussed.

J018 Compendium of Critiques of JPL Report SP 43-17: Automotive Technology Status and Projections Project

Jet Propulsion Laboratory

JPL Publication 77-40, July 18, 1977

In August 1975, the Jet Propulsion Laboratory completed an assessment of the benefits that could be realized with alternate engines and related vehicle improvements in automobiles of the next decade. The results, documented in JPL Report SP 43-17, *Should We Have a New Engine?*, stirred nationwide interest, and provoked indepth comments and critiques from many interested organizations. This document is a compilation of 49 such critiques and includes JPL responses to almost all of the critiques. Most of the responses are interim in nature and will require considerably more work to properly address the many aspects of each critique.

J019 Report of the Terrestrial Bodies Science Working Group: Executive Summary

Jet Propulsion Laboratory

JPL Publication 77-51, Vol. I, September 15, 1977

In this report the Terrestrial Bodies Science Working Group reviews current knowledge of Mercury, Venus, the Moon, Mars, asteroids, Galilean satellites, and com-

ets, together with related NASA-sponsored programs and available mission concepts and studies. Exploration plans for the period 1980-1990 are presented.

J020 **Report of the Terrestrial Bodies Science Working Group: Mercury**

Jet Propulsion Laboratory

JPL Publication 77-51, Vol. II, September 15, 1977

JPL Publication 77-51, a nine-volume series, documents the work of the NASA-sponsored Terrestrial Bodies Science Working Group in developing plans for the exploration of Mercury, Venus, the Moon, Mars, asteroids, Galilean satellites, and comets during the period 1980–1990. This volume is the report of the Mercury subgroup and includes a summary of knowledge concerning Mercury, principal scientific objectives, mission concepts and science payloads, mission constraints and development requirements, and recommendations.

J021 **Report of the Terrestrial Bodies Science Working Group: Venus**

Jet Propulsion Laboratory

JPL Publication 77-51, Vol. III, September 15, 1977

JPL Publication 77-51, a nine-volume series, documents the work of the NASA-sponsored Terrestrial Bodies Science Working Group in developing plans for the exploration of Mercury, Venus, the Moon, Mars, asteroids, Galilean satellites, and comets during the period 1980–1990. This volume is the report of the Venus subgroup and includes discussions on science objectives, proposed missions, and supporting research.

J022 **Report of the Terrestrial Bodies Science Working Group: The Moon**

Jet Propulsion Laboratory

JPL Publication 77-51, Vol. IV, September 15, 1977

JPL Publication 77-51, a nine-volume series, documents the work of the NASA-sponsored Terrestrial Bodies Science Working Group in developing plans for the exploration of Mercury, Venus, the Moon, Mars, asteroids, Galilean satellites, and comets during the period 1980–1990. This volume is the report of the Moon subgroup and discusses further exploration of the Moon and mission summary for the lunar polar orbiter mission.

J023 **Report of the Terrestrial Bodies Science Working Group: Mars**

Jet Propulsion Laboratory

JPL Publication 77-51, Vol. V, September 15, 1977

JPL Publication 77-51, a nine-volume series, documents the work of the NASA-sponsored Terrestrial Bodies Science Working Group in developing plans for the exploration of Mercury, Venus, the Moon, Mars, asteroids, Galilean satellites, and comets during the period 1980–1990. This volume is the report of the Mars subgroup, including discussions on science and mission objectives, exploration strategy, and supporting research and technology requirements.

J024 **Report of the Terrestrial Bodies Science Working Group: The Asteroids**

Jet Propulsion Laboratory

JPL Publication 77-51, Vol. VI, September 15, 1977

JPL Publication 77-51, a nine-volume series, documents the work of the NASA-sponsored Terrestrial Bodies Science Working Group in developing plans for the exploration of Mercury, Venus, the Moon, Mars, asteroids, Galilean satellites, and comets during the period 1980–1990. This volume is the report of the asteroids subgroup, including results of previous explorations, science objectives, required measurements for potential missions, mission concepts, and recommendations.

J025 **Report of the Terrestrial Bodies Science Working Group: The Galilean Satellites**

Jet Propulsion Laboratory

JPL Publication 77-51, Vol. VII, September 15, 1977

JPL Publication 77-51, a nine-volume series, documents the work of the NASA-sponsored Terrestrial Bodies Science Working Group in developing plans for the exploration of Mercury, Venus, the Moon, Mars, asteroids, Galilean satellites, and comets during the period 1980–1990. This volume is the report of the Galilean satellites subgroup and covers the knowledge of satellites and motivation for future exploration, key scientific questions to be investigated, and key measurements, instruments, and mission considerations.

J026 **Report of the Terrestrial Bodies Science Working Group: The Comets**

Jet Propulsion Laboratory

JPL Publication 77-51, Vol. VIII, September 15, 1977

JPL Publication 77-51, a nine-volume series, documents the work of the NASA-sponsored Terrestrial Bodies Science Working Group in developing plans for the exploration of Mercury, Venus, the Moon, Mars, asteroids, Galilean satellites, and comets during the period 1980–

1990. This volume is the report of the comets subgroup, including discussions on science objectives and rationale, measurements required for principal scientific objectives, mission concepts and science payload, and mission constraints and development requirements.

J027 **Report of the Terrestrial Bodies Science Working Group: Complementary Research and Development**

Jet Propulsion Laboratory

JPL Publication 77-51, Vol. IX, September 15, 1977

JPL Publication 77-51, a nine-volume series, documents the work of the NASA-sponsored Terrestrial Bodies Science Working Group in developing plans for the exploration of Mercury, Venus, the Moon, Mars, asteroids, Galilean satellites, and comets during the period 1980–1990. This volume is the report of the complementary research and development subgroup and covers areas of SRT requiring support, data analysis and synthesis, and earth-based and earth-orbital studies.

J028 **Proceeding of the Conference on Coal Feeding Systems**

Jet Propulsion Laboratory

JPL Publication 77-55, September 15, 1977

The Conference on Coal Feeding Systems was held at the California Institute of Technology, Pasadena, California, on June 21–23, 1977, and was organized and coordinated by the Jet Propulsion Laboratory under U. S. Energy Research and Development Administration contract. The major objective of the conference was to provide a forum to discuss the challenges of coal feeding, to acquaint feeder developers with current operations, and to inform potential users about ongoing operations. The conference attracted approximately 260 representatives from government, industry, and universities, 30 of whom made formal presentations.

JOHNSON, T. V.

J029 **Sodium D-Line Emission From Io: A Second Year of Synoptic Observation From Table Mountain Observatory**

J. T. Bergstralh, J. W. Young, D. L. Matson, and T. V. Johnson

Astrophys. J., Vol. 211, No. 1, Pt. 2, pp. L51–L55, January 1, 1977

For abstract, see Bergstralh, J. T.

J030 **Io's Surface Composition: Observational Constraints and Theoretical Considerations**

F. P. Fanale, T. V. Johnson, and D. L. Matson

Geophys. Res. Lett., Vol. 4, No. 8, pp. 303–306, August 1977

For abstract, see Fanale, F. P.

JOHNSTON, A. R.

J031 **A Scanning Laser Rangefinder for a Robotic Vehicle**

R. A. Lewis and A. R. Johnston

Technical Memorandum 33-809, February 15, 1977

For abstract, see Lewis, R. A.

J032 **Proximity Sensor Technology for Manipulator End Effectors**

A. R. Johnston

Mech. Mach. Theor., Vol. 12, pp. 95–109, 1977

Optical proximity sensing devices suitable for hand mounting on a manipulator are described, which use near IR LED light sources operating at 0.94 μ and silicon detectors, with appropriate signal processing so that the data are unaffected by ambient light. Laboratory tests with simple proximity sensors are described. Extension of the same techniques to yield multipoint or digital sensors is also discussed. A cooperative proximity sensor concept is described, which employs a composite mirror attached to the work piece to generate an unambiguous set of position and orientation signals. A very rudimentary experiment in local control of a manipulator with a pair of hand mounted proximity sensors is also described.

J033 **Control Techniques for an Automated Mixed Traffic Vehicle**

G. W. Meisenholder and A. R. Johnston

Proc. 1977 Joint Automat. Contr. Conf., San Francisco, Calif., June 22–24, 1977, pp. 421–427

For abstract, see Meisenholder, G. W.

JOHNSTON, D. W.

J034 **Viking Mission support**

D. W. Johnston, T. W. Howe, and G. M. Rockwell

The Deep Space Network Progress Report 42-37: November and December 1976, pp. 12–25, February 15, 1977

This report summarizes Deep Space Network support for the four Viking spacecraft during October and November 1976. The period covers the last portion of the prime mission which officially terminated on 15 November 1976 and the start of the Viking Extended Mission

on that date. November also covered the Mars-Sun-Earth superior conjunction period with the rapid degradation of RF link performance resulting in the tapering off and termination of telemetry data coincident with a rapid increase in Radio Science Experiment activity. The various Radio Science Experiments are described in detail and the Computer Aided Countdown Program utilized by the tracking stations during the Viking mission is also described.

JOHNSTON, D. W. H.

J035 Viking Mission Support

D. W. H. Johnston

The Deep Space Network Progress Report 42-38: January and February 1977, pp. 38–42, April 15, 1977

This report covers the relatively quiet Viking On Board Science & Telemetry period from November 15, 1976, through December 31, 1976, when Mars and the Viking spacecraft were in the solar conjunction period. The period therefore presented the Viking Radio Science Team with a unique opportunity to utilize the DSN and Viking spacecraft to exercise their experiments with nonstandard station configurations, without the usual command and telemetry constraints.

J036 Viking Mission Support

D. W. H. Johnston

The Deep Space Network Progress Report 42-39: March and April 1977, pp. 4–8, June 15, 1977

This report covers the period 1 January through 28 February 1977 and includes the initial Viking Extended Mission period of DSN "normal" support, following the nonstandard operations during the Solar Conjunction period. The operational testing subsequent to the MK III Data System installations at DSS 12, 44, and 62 during this period is also discussed.

J037 Viking Extended Mission Support

D. W. H. Johnston

The Deep Space Network Progress Report 42-41: July and August 1977, pp. 16–20, October 15, 1977

This report covers the period from May 1 through June 30, 1977 and includes the initial two weeks of post-MDS Viking related testing at DSS 14. Some of the periodic tests routinely carried out with the Viking Orbiter spacecraft by the spacecraft telecom and DSN teams to ensure optimum performance or detect any degradation in the spacecraft radio or command equipment are also addressed.

JOKIPII, J. R.

J038 Effects of Stream-Associated Fluctuations Upon the Radial Variation of Average Solar Wind Parameters

B. E. Goldstein and J. R. Jokipii (University of Arizona)

J. Geophys. Res., Space Phys., Vol. 82, No. 7, pp. 1095–1105, March 1, 1977

For abstract, see Goldstein, B. E.

JONES, D. E.

J039 August 1972 Solar-Terrestrial Events: Observations of Interplanetary Shocks at 2.2 AU

E. J. Smith, L. Davis, Jr. (California Institute of Technology), P. J. Coleman, Jr. (University of California, Los Angeles), D. S. Colburn (Ames Research Center), P. Dyal (Ames Research Center), and D. E. Jones (Brigham Young University)

J. Geophys. Res., Space Phys., Vol. 82, No. 7, pp. 1077–1086, March 1, 1977

For abstract, see Smith, E. J.

JONES, M.

J040 Electrical, Magnetic, and Optical Properties of the Tetrathiafulvalene (TTF) Pseudohalides, $(TTF)_{12}(SCN)_7$ and $(TTF)_{12}(SeCN)_7$

R. B. Somoano, A. Gupta, V. Hadek, M. Novotny (Stanford University), M. Jones (Tulane University), T. Datta (Tulane University), R. Deck (Tulane University), and A. M. Hermann (Tulane University)

Phys. Rev., Pt. B: Solid State, Vol. 15, No. 2, pp. 595–601, January 15, 1977

For abstract, see Somoano, R. B.

JOSEPHS, R. H.

J041 A Lightweight Solar Array Study

R. H. Josephs

JPL Publication 77-3, February 15, 1977

A sample module was assembled to model a portion of a flexible extendable solar array, a type that promises to become the next generation of solar array design. The resulting study of this module is intended to provide technical support to the array designer for lightweight component selection, specifications, and tests. Selected from available lightweight components were 127-mi-

cron-thick wraparound contacted solar cells, 34-micron-thick sputtered glass covers, and as a substrate a 13-micron-thick polyimide film clad with a copper printed circuit. Each component displayed weaknesses. The thin solar cells had excessive breakage losses. Sputtered glass cover adhesion was poor, and the covered cell was weaker than the cell uncovered. Thermal stresses caused some cell delamination from the model solar array substrate.

JURGENS, R. F.

J042 Radar Detectability of Asteroids: A Survey of Opportunities for 1977 through 1987

R. F. Jurgens and D. F. Bender

Icarus, Vol. 31, pp. 483–497, 1977

The capability of Earth-based radar to study asteroids is assessed with respect to determining the number of detectable objects and the number of detectable events during the next 10 years. Bar graphs have been prepared showing the number of events and objects falling into 5-dB detectability slots based both on estimates of minimum distance and on direct calculations using known orbital elements. These indicate that the Goldstone radar system operating at 3.5-cm wavelength should be able to detect roughly 18 different asteroids at 34 favorable opportunities during the next 10 years. The Arecibo radar system operating at 12.5-cm wavelength may be able to detect 60 asteroids at approximately 97 favorable opportunities in the 10-year period. This sample is sufficiently large that classification of types and correlation with optical data should be possible. The detectability margin for many objects should be large enough to permit more refined analysis of the radar spectrograms. Estimates of the average surface roughness, rotation rate, and direction of the polar axis, as well as estimates of range and Doppler frequency offsets, which can be used to refine the orbital elements, should be obtainable for many objects. Equations are given which indicate the variances expected for measurements of cross section, center frequency, and bandwidth measured either singly or jointly. These are functions of the noise-to-signal ratio and other physical parameters such as the backscattering law. Curves are given based on backscattering functions of the form $\cos^n\theta$.

KAHLE, A. B.

K001 JPL Field Measurements at the Finney County, Kansas, Test Site, October 1976: Meteorological Variables, Surface Reflectivity, Surface and Subsurface Temperatures

A. B. Kahle, J. Schieldge, and H. N. Paley

JPL Publication 77-1, February 1, 1977

Data collected by JPL at the Finney County, Kansas test site as part of the Joint Soil Moisture Experiment (JSME) during October 9–14, 1976 is presented here, prior to analysis, to provide all JSME investigators with an immediate source of primary information. The ground-truth measurements were taken to verify and complement soil moisture data taken by microwave and infrared sensors during aircraft overflights on October 13 and 14. Measurements were made of meteorological variables (air speed, temperature, relative humidity and rainfall), surface reflectivity, and temperatures at and below the surface.

K002 Mapping of Hydrothermal Alteration in the Cuprite Mining District, Nevada, Using Aircraft Scanner Images for the Spectral Region 0.46 to 2.36 μm

M. J. Abrams, R. P. Ashley (U. S. Geological Survey), L. C. Rowan (U. S. Geological Survey), A. F. H. Goetz, and A. B. Kahle

Geology, Vol. 5, No. 12, pp. 713–718, December 1977

For abstract, see Abrams, M. J.

K003 A Simple Thermal Model of the Earth's Surface for Geologic Mapping by Remote Sensing

A. B. Kahle

J. Geophys. Res., Vol. 82, No. 11, pp. 1673–1680, April 10, 1977

Thermal inertia of the earth's surface can be used in geologic mapping as a complement to surface reflectance data as provided by Landsat. Thermal inertia cannot be determined directly but must be inferred from radiation temperature measurements (by thermal IR sensors) made at various times in the diurnal cycle, combined with a model of the surface heating processes. We have developed a model which differs from models created previously for this purpose, because it includes sensible and latent heating. Tests of this model using field data indicate that it accurately determines the surface heating. When the model is used with field measurements of meteorological variables and is combined with remotely sensed temperature data, a thermal inertia image can be produced.

K004 Construction and Interpretation of a Digital Thermal Inertia Image

A. R. Gillespie and A. B. Kahle

Photogram. Eng. Remote Sensing, Vol. 43, No. 8, pp. 983–1000, August 1977

For abstract, see Gillespie, A. R.

KAKAR, R. K.

K005 Unidentified Lines in Molecular Clouds and a Search for ^{14}C in IRC +10216

E. N. R. Kuiper (University of California, Los Angeles), T. B. H. Kuiper, B. Zuckerman (University of Maryland), and R. K. Kakar

Astrophys. J., Vol. 214, No. 2, Pt. 1, pp. 394–398, June 1, 1977

For abstract, see Kuiper, E. N. R.

K006 Mars: Microwave Detection of Carbon Monoxide

R. K. Kakar, J. W. Waters, and W. J. Wilson (Aerospace Corporation)

Science, Vol. 196, pp. 1090–1091, June 3, 1977

The 115-gigahertz microwave line of carbon monoxide has been detected in the spectrum of Mars. The measurement is sensitive to carbon monoxide between the surface and an altitude of approximately 50 kilometers in the martian atmosphere. This extends the altitude region to well above that previously sensed.

KALABA, R. E.

K007 A Novel Methodology for Radiative Transfer in a Planetary Atmosphere

A. L. Fymat and R. E. Kalaba (University of Southern California)

Astrophys. Space Sci., Vol. 47, pp. 195–216, 1977

For abstract, see Fymat, A. L.

KANBER, H.

K008 First-Order Torques and Solid-Body Spinning Velocities in Intense Sound Fields

T. G. Wang H. Kanber, and I. Rudnick (University of California, Los Angeles)

Phys. Rev. Lett., Vol. 38, No. 3, pp. 128–130, January 17, 1977

For abstract, see Wang, T. G.

KATOW, M. S.

K009 Implementation of Wind Performance Studies for Large Antenna Structures

R. Levy and M. S. Katow

Proc. IEEE Mech. Eng. in Radar Symposium, Wash. D. C., Nov. 8–10, 1977, pp. 27–33

For abstract, see Levy, R.

K010 Evaluating Computed Distortions of Parabolic Reflectors

M. S. Katow

Proc. IEEE Mech. Eng. in Radar Symposium, Wash. D. C., Nov. 8–10, 1977, pp. 91–93

Distortion outputs from structural analysis of a 64-m paraboloidal reflector are analyzed by two computer programs for their radio-frequency performance characteristics. The computed and field measured values are compared.

KELLERMANN, K. I.

K011 Very High-Resolution Observations of the Radio Sources NRAO 150, OJ 287, 3C 273, M87, 1633+38, BL Lacertae, and 3C 454.3

K. I. Kellermann, et al.

Astrophys. J., Vol. 211, No. 3, Pt. 1, pp. 658–668, February 1, 1977

Very long baseline interferometer observations made at a wavelength of 2 and 2.8 cm with baselines ranging from 54 to 291 million wavelengths show a number of radio sources with only slightly resolved components, even on the longest baselines; the quasars 1633+38 and 3C 454.3, the objects OJ 287 and BL Lac, and the nucleus of M87 (Virgo A, 3C 274) all contain components $\lesssim$0.4 milli-arcsec. The smallest component we have observed is in the core of 3C 454.3, which contains about 50% of the total flux density and is $\lesssim$0.2 milli-arcsec in diameter. The compact component in the nucleus of M87 is $\lesssim$1.5 light-months across, and contains about one-third of the total flux density of the nucleus at 2.8 cm. NRAO 150 and BL Lac are double; the components of NRAO 150 are separated by 0.6 milli-arcsec, while BL Lac has an elongated structure consisting of a large (1.4 milli-arcsec) component separated by 1.25 milli-arcsec from a smaller (0.5 milli-arcsec) variable one. The present data on 3C 273 are consistent with triple models similar to those we discussed previously, but with a somewhat greater apparent separation of components.

Contributors to this article include:

National Radio Astronomy Observatory: K. I. Kellermann, D. B. Shaffer, and G. H. Purcell

Max-Planck-Institut für Radioastronomie: I. I. K. Pauliny-Toth, E. Preuss, A. Witzel, and D. Graham

Owens Valley Radio Observatory: R. T. Schilizzi, M. H. Cohen, A. T. Moffet, and J. D. Romney

Jet Propulsion Laboratory: A. E. Niell

KEMP, R.

K012 DSN Telemetry System Performance Using a Maximum Likelihood Convolutional Decoder

B. Benjauthrit and R. Kemp

The Deep Space Network Progress Report 42-42: September and October 1977, pp. 149–161, December 15, 1977

For abstract, see Benjauthrit, B.

KEMP, R. P.

K013 Summary Report and Status of the Deep Space Network—Mariner Jupiter/Saturn 1977 Flight Project Telecommunications Compatibility

A. I. Bryan, R. P. Kemp, and B. D. Madsen

The Deep Space Network Progress Report 42-38: January and February 1977, pp. 16–37, April 15, 1977

For abstract, see Bryan, A. I.

K014 Summary Report and Status of the Deep Space Network-Voyager Flight Project Telecommunications Compatibility

A. I. Bryan, R. P. Kemp, and B. D. Madsen

The Deep Space Network Progress Report 42-40: May and June 1977, pp. 21–40, August 15, 1977

For abstract, see Bryan, A. I.

K015 Voyage Flight Project—DSN Telecommunications Compatibility Test Program

A. I. Bryan, R. P. Kemp, and B. D. Madsen

The Deep Space Network Progress Report 42-42: September and October 1977, pp. 13–27, December 15, 1977

For abstract, see Bryan, A. I.

KENDALL, J. M., JR.

K016 Airframe Noise Measurements by Acoustic Imaging

J. M. Kendall, Jr.

Preprint 77-55, AIAA Fifteenth Aerosp. Sci. Meet., Los Angeles, Calif., Jan. 24–26, 1977

Studies of the noise produced by flow past wind tunnel models are presented. The central objective of these is to find the specific locations within a flow which are noisy, and to identify the fluid dynamic processes responsible, with the expectation that noise reduction principles will be discovered. The models tested are mostly simple shapes which result in types of flow that are similar to those occurring on, for example, aircraft landing gear and wheel cavities. A model landing gear and a flap were also tested. Turbulence has been intentionally induced as appropriate in order to simulate full-scale effects more closely. The principal technique involves use of a highly directional microphone system which is scanned about the flow field to be analyzed. The data so acquired are presented as a pictorial image of the noise source distribution. An important finding is that the noise production is highly variable within a flow field and that sources can be attributed to various fluid dynamic features of the flow. Flow separation was not noisy, but separation closure usually was.

KENDALL, W. B.

K017 Measurements of Large-Scale Density Fluctuations in the Solar Wind Using Dual-Frequency Phase Scintillations

R. Woo, F. C. Yang, K. W. Yip, and W. B. Kendall (Mark Resources, Inc.)

Astrophys. J., Vol. 210, No. 2, Pt. 1, pp. 568–574, December 1, 1976

For abstract, see Woo, R.

KENT, S. S.

K018 Baseband Recording and Playback

S. S. Kent and J. I. Molinder

The Deep Space Network Progress Report 42-37: November and December 1976, pp. 136–145, February 15, 1977

Analog recordings of spacecraft telemetry signals are made by Deep Space Network Deep Space Stations to provide backup for both spacecraft and ground station anomalies. In this article the requirements that must be met to insure successful baseband recording and playback are given. Recording and playback procedures are developed to insure that these requirements are met and performance results from tests conducted at the Compatibility Test Area (JPL) are tabulated.

KIEFFER, H. H.

K019 Martian North Pole Summer Temperatures: Dirty Water Ice

H. H. Kieffer (University of California, Los Angeles), S. C. Chase, Jr. (Santa Barbara Research Center), T. Z. Martin (University of California, Los Angeles), E. D. Miner, and F. D. Palluconi

Science, Vol. 194, pp. 1341–1344, December 17, 1976

Broadband thermal and reflectance observations of the Martian north polar region in late summer yield temperatures for the residual polar cap near 205 K with albedos near 43 percent. The residual cap and several outlying smaller deposits are water ice with included dirt; there is no evidence for any permanent carbon dioxide polar cap.

K020 Soil and Surface Temperatures at the Viking Landing Sites

H. H. Kieffer (University of California, Los Angeles)

Science, Vol. 194, pp. 1344–1346, December 17, 1976

The annual temperature range for the Martial surface at the Viking lander sites is computed on the basis of thermal parameters derived from observations made with the infrared thermal mappers. The Viking lander 1 (VL1) site has small annual variations in temperature, whereas the Viking lander 2 (VL2) site has large annual changes. With the Viking lander images used to estimate the rock component of the thermal emission, the daily temperature behavior of the soil alone is computed over the range of depths accessible to the lander; when the VL1 and VL2 sites were sampled, the daily temperature ranges at the top of the soil were 183 to 263 K and 183 to 268 K, respectively. The diurnal variation decreases with depth with an exponential scale of about 5 centimeters. The maximum temperature of the soil sampled from beneath rocks at the VL2 site is calculated to be 230 K. These temperature calculations should provide a reference for study of the active chemistry reported for the Martian soil.

K021 Temperatures of the Martian Surface and Atmosphere: Viking Observation of Diurnal and Geometric Variations

H. H. Kieffer (University of California, Los Angeles), P. R. Christensen (University of California, Los Angeles), T. Z. Martin (University of California, Los Angeles), E. D. Miner, and F. D. Palluconi

Science, Vol. 194, pp. 1346–1351, December 17, 1976

Selected observations made with the Viking infrared thermal mapper after the first landing are reported. Atmospheric temperatures measured at the latitude of the Viking 2 landing site (48°N) over most of a Martian day reveal a diurnal variation of at least 15 K, with peak temperatures occurring near 2.2 hours after noon, implying significant absorption of sunlight in the lower 30 km of the atmosphere by entrained dust. The summit temperature of Arsia Mons varies by a factor of nearly two each day; large diurnal temperature variation is characteristic of the south Tharsis upland and implies the presence of low thermal inertia material. The thermal inertia of material on the floors of several typical large craters is found to be higher than for the surrounding terrain; this suggests that craters are somehow effective in sorting aeolian material. Brightness temperatures of the Viking 1 landing area decrease at large emission angles; the intensity of reflected sunlight shows a more complex dependence on geometry than expected, implying atmospheric as well as surface scattering.

KIM, J. K.

K022 Product Distribution and Rate Constants for the Reactions of CH_3^+, CH_4^+, $C_2H_2^+$, $C_2H_3^+$, $C_2H_4^+$, $C_2H_5^+$, and $C_2H_6^+$ Ions with CH_4, C_2H_2, C_2H_4, and C_2H_6

J. K. Kim, V. G. Anicich, and W. T. Huntress, Jr.

J. Phys. Chem., Vol. 81, No. 19, pp. 1798–1805, 1977

Ion cyclotron resonance methods have been used to measure the product distributions and rate constants for the reactions of various CH_n^+ and $C_2H_n^+$ ions with CH_4, C_2H_2, C_2H_4, and C_2H_6. The product distributions for some of the reactions of $C_2H_2^+$, $C_2H_4^+$, and $C_2H_6^+$ ions are strongly affected by excess ion internal energy. Photoionization mass spectrometer experiments have been conducted in a few cases in order to obtain product distributions for reactions of these ions in the ground vibronic state.

KIM, K.

K023 Modeling of Fluidized Bed Silicon Deposition Process

K. Kim, G. Hsu, R. Lutwack, and A. Praturi

JPL Publication 77-25, June 15, 1977

Modeling of the fluidized bed for silicon deposition is described. The model is intended for use as a means of improving fluidized bed reactor design and for the formulation of the research program in support of the contracts of the Silicon Material Task for the development of the fluidized bed silicon deposition process. A computer program derived from the simple modeling is also described. Results of some sample calculations using the computer program are shown.

K024 **Blast Wave Analysis for Detonation Propulsion**

K. Kim, G. Varsi, and L. H. Back

AIAA J., Vol. 15, No. 10, pp. 1500–1502, October 1977

The details of the blast wave resulting from the detonation-propulsion system are explained by both calculation and experiments. The relative importance of pressure peaks and valleys on the system performance is illustrated; especially, the importance of the under-pressure is emphasized.

KING, D.

K025 **Ocean Wave Patterns Under Hurricane Gloria: Observation with an Airborne Synthetic-Aperture Radar**

C. Elachi, T. W. Thompson, and D. King

Science, Vol. 198, pp. 609–610, November 11, 1977

For abstract, see Elachi, C.

KIRKBRIDE, H. L.

K026 **A Maintenance and Operations Cost Model for the DSN**

R. W. Burt and H. L. Kirkbride

The Deep Space Network Progress Report 42-38: January and February 1977, pp. 109–114, April 15, 1977

For abstract, see Burt, R. W.

KIRSCHMAN, R. K.

K027 **Comparative Studies of Ion-Implant Josephson-Effect Structures**

R. K. Kirschman, J. A. Hutchby (Langley Research Center), J. W. Burgess (Langley Research Center), R. P. McNamara (California Institute of Technology), and H. A. Notarys (California Institute of Technology)

IEEE Trans. Magnet., Vol. MAG-13, No. 1, pp. 731–734, January 1977

The Josephson-effect structures formed by Cu or Fe implant of localized regions in Ta films are compared to those of other types of proximity-effect bridges. Properties investigated include coherence length, penetration depth, critical current versus temperature, critical current versus magnetic field, and rf response. No significant differences are found between the various types of bridges, provided a material-dependent scaling factor is applied to the bridge length.

KLEIN, M. J.

K028 **Calibration Radio Sources for Radio Astronomy: Precision Flux-Density Measurements at 2295 MHz**

M. J. Klein and C. T. Stelzried

Astron. J., Vol. 81, No. 12, pp. 1078–1083, December 1976

The flux densities of 11 small-diameter radio sources, which are commonly used as calibration sources, were measured relative to the flux density of Virgo A at 2295 MHz. The 1-σ precision of the measured ratios is ~1%, the 1-σ accuracy of the flux-density values, including the uncertainty of the flux-density scale as defined by the microwave spectrum of Virgo A, is ~4%. While processing the data we discovered that the intensity of one of the sources, 3C309.1, is decreasing at a rate of 2% ± 0.3%/yr.

K029 **A Search for Radio Emission from Ionized Hydrogen in M15**

M. J. Klein

Astrophys. Lett., Vol. 18, pp. 25–28, 1976

A sensitive search at 3.6 cm for thermal emission from ionized gas in the globular cluster M15 (NGC 7078) reveals no emission greater than the experimental error, which is 0.003 Jy. Based on this flux density limit, the mass of ionized gas within 3 pc of the cluster center is $<26\ M_\odot$. This result suggests that the ionized gas content of M15, which contains an intense X-ray source, is not greatly enhanced compared to similar globular clusters without known X-ray sources. This mass limit is an order of magnitude greater than the amount of gas required to produce the X-ray flux by accretion into massive black holes.

KLEINE, H.

K030 **Software Design and Documentation Language**

H. Kleine

JPL Publication 77-24, July 1, 1977

The objective of the Software Design and Documentation Language (SDDL) is to provide an effective communications medium to support the design and documentation of complex software applications. This objective is met by providing (1) a processor which can convert design specifications into an intelligible, informative machine-reproducible document, (2) a design and documentation language with forms and syntax that are simple,

unrestrictive, and communicative, and (3) methodology for effective use of the language and processor. The SDDL processor is written in the SIMSCRIPT II programming language and has been implemented on the UNIVAC 1108 and the IBM 360/370 machines.

KLIORE, A. J.

K031 Pioneer 10 and 11 Radio Occultations by Jupiter

A. J. Kliore, P. M. Woiceshyn, and W. B. Hubbard (University of Arizona)

COSPAR Space Research, Vol. XVII, pp. 703–710, 1977

Radio occultation data received from Pioneers 10 and 11 during their encounters with Jupiter have been analyzed using an inversion technique which accounts for the oblateness of Jupiter's atmosphere. The center of refraction used for inversion is located by the radius of curvature and the direction of the normal at the closest approach point of the ray. An Abelian integral transform inversion is carried out while holding the center of refraction fixed at some average value for each occultation event. The temperature profiles derived from the different measurements are consistent, showing a temperature inversion between the 10 and 100 millibar levels, with temperatures between 130 and 170 K at the 10 millibar level, and 80–120 K at 100 millibars. The profiles are also in good agreement with models for the temperature structure of the Jovian atmosphere derived from the Pioneer 10 infrared radiometer data as well as those constructed from radiative–convective balance calculations. As with all results derived from radio occultation measurements of oblate planets with dynamically active atmospheres, these results are highly sensitive to the detailed shape of the isodensity contours of the atmosphere, which may deviate significantly from the average figure because of differential rotation, i.e., zonal winds. For the conditions of the Pioneer 10 entry, this effect can produce errors of up to 100 K in the temperature at the deepest penetration level. Known atmospheric currents in Jupiter can change the local vertical angle by at least 10^{-3} radian. However, in order to retain an accuracy in the measured temperature profiles to 1% for an occultation distance of 10 Jupiter radii, the direction of the local vertical must be known with an accuracy to 10^{-5} radian. Since this degree of accuracy in the knowledge of the local vertical is unrealistic, the radio occultation technique could be used for measuring the slope of the isodensity contours in a known planetary atmosphere with an accuracy to about 10^{-5} radian, and therefore this technique may be suited for studies of zonal winds in the atmospheres of the giant planets.

K032 Verification by Viking Landers of Earlier Radio Occultation Measurements of Surface Atmospheric Pressure on Mars

A. J. Kliore

Nature, Vol. 265, No. 5589, pp. 34–35, January 6, 1977

The landing of Viking 1 provided the opportunity to obtain atmospheric pressure measurements on Mars. These were compared to measurements made before landing, obtained by Earth-based planetary radar of 1967, using Mariner IV occultation points. After allowing for seasonal variation, very close agreement was made.

KNOELL, A. C.

K033 A Mathematical Model of an In Vitro Human Mandible

A. C. Knoell

J. Biomech., Vol. 10, pp. 159–166, 1977

This paper presents details concerning the development, analysis and experimental verification of a three-dimensional, finite-element model of a dried human mandible. Basic features of the model are described and highlighted relative to previous modeling work. Analysis results for single tooth loading conditions are presented and compared with test results as well as predictions using other finite-element modeling techniques. Operational computer experience relative to running time (cost) and solution accuracy is described. It is shown that biomechanical response to tooth loading is highly localized in the region of tooth support, thereby requiring careful mathematical simulation of surrounding tooth anatomical structure.

KOMAREK, T. A.

K034 A Solar Plasma Stream Measured by DRVID and Dual-Frequency Range and Doppler Radio Metric Data

F. B. Winn, S. C. Wu, T. A. Komarek, V. W. Lam, H. N. Royden, and K. B. W. Yip

The Deep Space Network Progress Report 42-37: November and December 1976, pp. 43–54, February 15, 1977

For abstract, see Winn, F. B.

KONG, J. A.

K035 Theory for Passive Microwave Remote Sensing of Near-Surface Soil Moisture

ORIGINAL PAGE IS OF POOR QUALITY

E. G. Njoku and J. A. Kong (Massachusetts Institute of Technology)

J. Geophys. Res., Vol. 82, No. 20, pp. 3108–3118, July 10, 1977

For abstract, see Njoku, E. G.

KORBULY, D. K.

K036 Overcoming People Problems in the Switch to Automated Composition

D. K. Korbuly

IEEE Trans. Prof. Commun., Vol. PC-20, No. 2, pp. 58–61, September 1977

When a documentation support function at a company switches to automated composition to lower costs or improve turnaround times, the people problems encountered can be far more difficult to solve than the technical problems of getting the equipment fully operational. To the uninitiated, automation represents a mystery at best and a threat at worst. An acute understanding of this fact by the key technical and management personnel responsible for the automated system is an important element in assuring the success of the transition process. Various types of people problems that can be encountered during a switch to automated composition are examined, and practical ways of alleviating those problems are described.

KOUKOL, R. C.

K037 Microbiological Profiles of the Viking Spacecraft

J. R. Puleo, N. D. Fields, S. L. Bergstrom, G. S. Oxborrow, P. D. Stabekis, and R. C. Koukol

Appl. Environ. Microbiol., Vol. 33, No. 2, pp. 379–384, February 1977

For abstract, see Puleo, J. R.

KREZNAR, J. E.

K038 Image Restoration Consequences of the Lack of a Two Variable Fundamental Theorem of Algebra

J. E. Kreznar

Off. Nav. Res. Meeting Curr. Math. Problems Image Sci., Monterey, Calif., Nov. 10–12, 1976, pp. 153–162

A well-known problem arising in numerous, highly diverse contexts may be stated as follows: Given an array, q, of numbers (output signal) and a linear operator, F (transfer characteristic of a black box), find the array, p (input signal) such that $q = Fp$. A useful approach to this problem is to attempt to find an inverse linear operator, F^{-1}, such that $p = F^{-1}q$. If F has no inverse, it is called a singular operator. This paper highlights some of what is known about this problem and provides a ray of hope that an alternate space of two-dimensional convolution operators may exist for which almost every operator is non-singular and for which every singular operator has a non-singular neighbor.

KROGH, F. T.

K039 Recurrence Relations For Computing With Modified Divided Differences

F. T. Krogh

JPL Publication 77-46, September 15, 1977

Modified divided differences (MDD) provide a good way of representing a polynomial passing through points with unequally spaced abscissas. This report gives recurrence relations for computing coefficients in either the nominal or Chebyshev basis from the MDD coefficients, and for computing the MDD coefficients for either the differentiated or the integrated polynomial. The latter operation is likely to be useful if MDD are used in a method for solving stiff differential equations.

KRONICK, P. L.

K040 Reactions of Human Platelets with Microspheres of Poly(hydroxymethyl Methacrylate) and Polyacrylamide

P. L. Kronick (Franklin Institute Research Laboratories) and A. Rembaum

J. Biomed. Mater. Res. Symp., No. 8, pp. 39–50, 1977

The contact interaction of platelets with hydrogels is studied. In the form of microspheres, 0.6–1.0 μ, poly(glycol methacrylate) (polyHEMA) and poly(methyl methacrylate) beads cause platelets to aggregate at concentrations of about 10^8 beads/ml. Polyacrylamide and (20/80) poly(acrylamide–HEMA) copolymer were ineffective in aggregating platelets. The admixture of 20% methacrylate to polyHEMA rendered the beads inactive. Blood plasma components other than fibrinogen were found essential to the interaction of the beads with platelets. Near-infrared spectra of the hydrogels polyacrylamide and polyHEMA showed the water hydrogen bonds to be the same for both and different from those in pure water. The monomer HEMA is an inhibitor of platelet aggregation and the release reaction at levels of 0.1%. It is concluded that the two hydrogels have different blood compatibilities, which depend more on the network structures than the water structures in the respective gels.

KUEHN, T. J.

K041 **Social and Institutional Constraints of Nuclear Waste Management: An Exploratory Analysis of the Issues**

T. J. Kuehn

JPL Publication 77-45, November 30, 1977

Advances in nuclear energy technology have outpaced the ability of social and political institutions to manage, regulate, and monitor its development and impact. The controversies surrounding reprocessing and nuclear waste disposal include concerns about the proliferation of nuclear weapons, threat of terrorism and sabotage, safety of nuclear reactors, and environmental hazards of radiation. The origins of this controversy are traced to the high degree of public concern about nuclear energy, economic uncertainties, scientific unknowns, and, more recently, the vigorous debates on technological and institutional alternatives that could reduce the risks of proliferation. While disagreements over nuclear waste management increase, private and governmental organizations may be unprepared to solve some of the complex technical and institutional issues involved. This study provides a broad framework for analyzing some of the institutional, social, and regulatory issues and problems of commercial nuclear waste management.

The report begins with an overview of the origins of the present climate in nuclear energy decision-making. The social challenges of nuclear waste management are then explored in the areas of (a) selection and validation of alternative fuel cycles, (b) cost-benefit analysis of reprocessing, and (c) risks and uncertainties of waste disposal. Next, the complex processes of nuclear waste policy, management, and regulation are studied, including the federal decision-making process, policy assessment and decision-making, regulation and siting in the states, and public and private management and regulation. Finally, the complex problems of institutional development are examined by comparing the social, economic, and organizational requirements of the "recycling" and "once-through" alternatives for nuclear waste management. The Summary and Conclusions address the questions of the assessment of goals and alternatives, improvement of management and regulation, and institutional planning and development.

KUIPER, E. N. R.

K042 **High-Velocity Gas in the Orion Infrared Nebula**

B. Zuckerman (University of Maryland)
T. B. H. Kuiper, and E. N. R. Kuiper (University of California, Los Angeles)

Astrophys. J., Vol. 209, No. 3, Pt. 2, pp. L137–L142, November 1, 1976

For abstract, see Zuckerman, B.

K043 **Unidentified Lines in Molecular Clouds and a Search for ^{14}C in IRC +10216**

E. N. R. Kuiper (University of California, Los Angeles), T. B. H. Kuiper,
B. Zuckerman (University of Maryland), and
R. K. Kakar

Astrophys. J., Vol. 214, No. 2, Pt. 1, pp. 394–398, June 1, 1977

We detected two spectral features toward the Kleinmann-Low infrared nebula in Orion that agree in frequency with the 7_{25}–7_{16} and 7_{35}–7_{26} rotational transitions of the ring-structured molecule ethylene oxide $(CH_2)_2O$. A feature agreeing in frequency with the 8_{24}–8_{45} transition probably also was detected; however, seven other transitions in $(CH_2)_2O$ were not. Additional unidentified lines were detected in Ori A and Sgr B2. Searches for $H^{14}CN$ and ^{14}CO in the luminous carbon star IRC +10216 were unsuccessful. However, an unidentified line was found in IRC +10216 that was not detected in the KL nebula.

KUIPER, T. B. H.

K044 **High-Velocity Gas in the Orion Infrared Nebula**

B. Zuckerman (University of Maryland)
T. B. H. Kuiper, and E. N. R. Kuiper (University of California, Los Angeles)

Astrophys. J., Vol. 209, No. 3, Pt. 2, pp. L137–L142, November 1, 1976

For abstract, see Zuckerman, B.

K045 **Unidentified Lines in Molecular Clouds and a Search for ^{14}C in IRC +10216**

E. N. R. Kuiper (University of California, Los Angeles), T. B. H. Kuiper,
B. Zuckerman (University of Maryland), and
R. K. Kakar

Astrophys. J., Vol. 214, No. 2, Pt. 1, pp. 394–398, June 1, 1977

For abstract, see Kuiper, E. N. R.

K046 **Searching for Extraterrestrial Civilizations**

T. B. H. Kuiper and M. Morris

Science, Vol. 196, pp. 616–621, May 6, 1977

The principle followed in this study is that the most meaningful procedure is to make a minimum number of

assumptions consistent with our understanding of natural physical processes and the expectation that behavior of extraterrestrial beings or civilizations may be extrapolated from gross behavioral patterns of terrestrial animals and human beings. The plausibility of interstellar travel is reexamined, as is the transmission of powerful radio beacons across interstellar distances. The likelihood of such civilizations expanding by colonizing their neighboring galactic environments is considered, and the implications for a SETI strategy are discussed. It is concluded that to plan at this time for a large-array SETI appears to be premature since failure to detect a signal implies that (i) the galaxy is devoid of technological civilizations advanced beyond our own, (ii) such civilizations, if they exist, cannot engage in interstellar colonization, or (iii) such civilizations are not attempting contact or their intercommunications are not coded in a simple way.

KWAN, M.

K047 Viking Doppler Noise Used to Determine the Radial Dependence of Electron Density in the Extended Corona

A. L. Berman, J. A. Wackley, S. T. Rockwell, and M. Kwan

The Deep Space Network Progress Report 42-38: January and February 1977, pp. 167–171, April 15, 1977

For abstract, see Berman, A. L.

LAM, V. W.

L001 A Solar Plasma Stream Measured by DRVID and Dual-Frequency Range and Doppler Radio Metric Data

F. B. Winn, S. C. Wu, T. A. Komarek, V. W. Lam, H. N. Royden, and K. B. W. Yip

The Deep Space Network Progress Report 42-37: November and December 1976, pp. 43–54, February 15, 1977

For abstract, see Winn, F. B.

LANDAUER, F. P.

L002 The Viking Orbiter Visual Imaging Subsystem

J. B. Wellman, F. P. Landauer, D. D. Norris, and T. E. Thorpe

J. Spacecraft Rockets, Vol. 13, No. 11, pp. 660–666, November 1976

For abstract, see Wellman, J. B.

LANDEL, R. F.

L003 Nonlinear Viscoelasticity and Relaxation Phenomena of Polymer Solids

S. T. J. Peng, K. C. Valanis (University of Iowa), and R. F. Landel

Acta Mech., Vol. 25, Nos. 3–4, pp. 229–240, 1977

For abstract, see Peng, S. T. J.

LANDON, K. C.

L004 CRISPFLOW, A Structured Program Design Flowcharter

R. C. Tausworthe and K. C. Landon

The Deep Space Network Progress Report 42-41: July and August 1977, pp. 112–126, October 15, 1977

For abstract, see Tausworthe, R. C.

LANSING, F. L.

L005 Computer Modeling of a Regenerative Solar-Assisted Rankine Power Cycle

F. L. Lansing

The Deep Space Network Progress Report 42-37: November and December 1976, pp. 152–168, February 15, 1977

Advanced solar-driven thermodynamic cycles for electric power generation are under study for application of the DSN Energy Conservation Project at Goldstone, California. This article presents a detailed interpretation of the computer program that describes the performance of one of these cycles; namely, a regenerative Rankine power cycle. Water is used as the working medium throughout the cycle. The solar energy collected at relatively low temperature level presents 75 to 80% of the total heat demand and provides mainly the latent heat of vaporization. Another energy source at high temperature level super-heats the steam and supplements the solar energy share. A program summary and a numerical example showing the sequence of computations are included. The outcome from the model comprises line temperatures, pressures, component heat rates, specific steam consumption, percentage of solar energy contribution, and the overall thermal efficiency.

L006 Status of Goldstone Solar Energy System Study of the First Goldstone Energy Project

F. L. Lansing

ORIGINAL PAGE IS OF POOR QUALITY

The Deep Space Network Progress Report 42-38: January and February 1977, pp. 120–140, April 15, 1977

This article summarizes the results reached by the DSN Engineering Section and private consultants in the review of the initial plan of the Goldstone Energy Project. The main objectives were in the areas of energy conservation and the application of solar-driven systems for power and hydrogen generation. This summary will provide background data for management planning decisions both to the DSN Engineering Section and other organizations planning a similar program. The review showed that an add-on solar driven absorption refrigeration unit with its associated changes to the existing system was not cost-effective, having a payback period of 29 years. Similar economically unattractive results were found for both a solar-hydrogen and a wind-hydrogen generation plant. However, cutting the hydrogen generation linkage from this plant improved its economic feasibility.

L007 Piping Design Considerations in a Solar-Rankine Power Plant

F. L. Lansing

The Deep Space Network Progress Report 42-39: March and April 1977, pp. 168–176, June 15, 1977

Two of the main parameters in sizing the piping of a solar power plant are presented. These two parameters are the working pressure of the vapor leaving the solar collectors, and the type of working fluid used. Numerical examples for each case are given using the graphical Moody friction charts and the analytical Darcy-Weisbach equation. Different working pressures of steam vapor in the solar collector-turbine pipe connection indicate their major role in the design. The size variation was found not to be in linear proportion to vapor density variations. On the other hand, high molecular weight organic fluids such as R-11 and R-113, when compared with water, have shown insignificant changes in piping sizes.

L008 Comparative Thermodynamic Performance of Some Rankine/Brayton Cycle Configurations for a Low-Temperature Energy Application

F. L. Lansing

The Deep Space Network Progress Report 42-40: May and June 1977, pp. 156–167, August 15, 1977

Various configurations combining solar-Rankine and fuel-Brayton cycles were analyzed in order to find the arrangement which has the highest thermal efficiency and the smallest fuel share. A numerical example is given to evaluate both the thermodynamic performance and the economic feasibility of each configuration. The solar-assisted regenerative Rankine cycle was found to be leading the candidates from both points of energy utilization and fuel conservation.

L009 A Thermodynamic Analysis of a Solar-Powered Jet Refrigeration System

F. L. Lansing and V. W. Chai

The Deep Space Network Progress Report 42-41: July and August 1977, pp. 209–217, October 15, 1977

The article describes and analyzes a method of using solar energy to drive a jet refrigeration system. A new technique is presented in the form of a performance nomogram combining the energy and momentum equations to determine the performance characteristics. A numerical example, using water as the working fluid, is given to illustrate the nomogram procedure. The resulting coefficient of performance was found comparable with other refrigeration systems such as the solar-absorption system or the solar-Rankine turbocompressor system.

LaPORTE, D. D.

L010 Behavior of Volatiles in Mars' Polar Areas: A Model Incorporating New Experimental Data

D. W. Davies, C. B. Farmer, and D. D. LaPorte (Santa Barbara Research Center)

J. Geophys. Res., Vol. 82, No. 26, pp. 3815–3822, September 10, 1977

For abstract, see Davies, D. W.

L011 Mars: Northern Summer Ice Cap—Water Vapor Observations from Viking 2

C. B. Farmer, D. W. Davies, and D. D. LaPorte (Santa Barbara Research Center)

Science, Vol. 194, pp. 1339–1341, December 17, 1976

For abstract, see Farmer, C. B.

LARSON, V.

L012 Optimal Estimation and Attitude Control of a Solar Electric Propulsion Spacecraft

V. Larson, P. Likins, and E. Marsh

IEEE Trans. Aerosp. Electron. Syst., Vol. AES-13, No. 1, pp.35–47, January 1977

Established procedures of linear, quadratic, Gaussian optimal estimation and control are developed and interpreted for their application to the problem of attitude

control of spacecraft with dynamically significant elastic appendages. Results are presented both in general terms and for specific application to a solar electric spacecraft. Comparisons are made between alternative coordinate systems, and a realistic range of design parameters is considered. For single axis control, system evaluation is accomplished by simulation of a fifteenth-order spacecraft plant with alternative second-order, fourth-order, and sixth-order constant gain estimators. Results point out the importance of modeling errors.

LAU, N. C. S.

L013 GCF Central Performance Monitor—Functional Description

N. C. S. Lau

The Deep Space Network Progress Report 42-41: July and August 1977, pp. 206–208, October 15, 1977

This article describes the Ground Communications Facilities (GCF) Central Performance Monitor (CPM) which gathers information on the operational status of the Central High Speed and Wideband Assemblies. This monitor information is formatted and forwarded to the Central Communication Monitor Processor. The CCM Processor, in turn, provides near real time displays and printouts of the status information and any resulting alarm indications. The ability of the GCF to quickly detect and correct circuit failures will be enhanced by the addition of the CPM.

LAUDENSLAGER, J. B.

L014 A Photoionization Study of the Charge Transfer Reactions: $Xe^+ + O_2 \rightarrow O_2^+ + Xe$ and $O_2^+ + Xe \rightarrow Xe^+ + O_2$

J. M. Ajello and J. B. Laudenslager

Chem. Phys. Lett., Vol. 44, No. 2, pp. 344–347, December 1, 1976

For abstract, see Ajello, J. M.

L015 Product Distributions for Some Thermal Energy Charge Transfer Reactions of Rare Gas Ions

V. G. Anicich, J. B. Laudenslager, W. T. Huntress, Jr., and J. H. Futrell (University of Utah)

J. Chem. Phys., Vol. 67, No. 10, pp. 4340–4350, November 15, 1977

For abstract, see Anicich, V. G.

LAWSON, C. L.

L016 Software for C^1 Surface Interpolation

C. L. Lawson

JPL Publication 77-30, August 15, 1977

This report treats the problem of mathematically defining a smooth surface, $z = f(x,y)$, passing through a finite set of given points $(x_i,y_i,z_i,\ i = 1,\ldots,n)$. In particular, it is not assumed that the given (x_i,y_i) values lie in any special pattern such as at the nodes of a rectangular grid. The literature relating to this problem is briefly reviewed. An algorithm is described that first constructs a triangular grid in the (x,y) domain, next estimates first partial derivatives at the nodal points, and finally does interpolation in the triangular cells using a method that gives C^1 continuity overall. Performance of software implementing this algorithm is discussed. New theoretical results are presented that provide valuable guidance in the development of algorithms for constructing triangular grids.

LAY, R.

L017 Phase and Group Delay of S-Band Megawatt Cassegrain Diplexer and S-Band Megawatt Transmit Filter

R. Lay

The Deep Space Network Progress Report 42-37: November and December 1976, pp. 198–203, February 15, 1977

This article reports the phase characteristic and group delay of the S-band Megawatt Cassegrain Diplexer (MCD) and S-band Megawatt Transmit Filter (MTF). These phase measurements on the MCD and MTF were done in response to the need to obtain the total DSS hardware ground delay required for very long baseline interferometry (VLBI) and ranging radio metric measurements.

LAYLAND, J. W.

L018 VLBI Instrumental Effects, Part I

J. W. Layland and W. J. Hurd

The Deep Space Network Progress Report 42-42: September and October 1977, pp. 54–80, December 15, 1977

Very Long Baseline Interferometry (VLBI) is a method for observation of extragalactic radio sources which appears to have potential for precise long-distance Earth surveying, clock synchronization and spacecraft navigation. For the past several years, many researchers at JPL and elsewhere have been working to establish the accu-

ORIGINAL PAGE IS OF POOR QUALITY

racy of VLBI observations. The intent of the work reported here has been to review the principal components of the VLBI instrument in order to estimate and/or bound the systematic error contributions. In this first of a series of articles, we establish the definitions and tools which we need in order to apply filter transfer-function analysis to the VLBI receiver, and we use it to estimate the sensitivity of the VLBI receiver to plausible filter variations.

L019 VLBI Clock Sync and the Earth's Rotational Instability

J. W. Layland and A. N. Mathews

The Deep Space Network Progress Report 42-42: September and October 1977, pp. 81–84, December 15, 1977

The DSN is currently preparing to monitor the stability of its clocks and frequency standards in the 64-meter net by means of VLBI. Since variations in the Earth's rotation rate represent an error source to VLBI clock synchronization, we calculated the Allan Variance of the Earth rotation to find that, in a long-term sense at least, these variations do not noticeably increase the differential instability of two clocks as measured by Intercontinental VLBI.

LE CROISSETTE, D. H.

L020 Final Report: Medical Ultrasonic Tomographic System

R. C. Heyser, D. H. Le Croissette, R. Nathan, and R. L. Wilson (Harbor General Hospital, Los Angeles)

JPL Publication 77-72, October 1, 1977

For abstract, see Heyser, R. C.

LEBOFSKY, L. A.

L021 Galilean Satellites: Anomalous Temperatures Disputed

D. Morrison (University of Arizona), L. A. Lebofsky, J. A. Cutts (Planetary Science Institute), G. J. Veeder, and S. H. Gross (Polytechnic Institute of New York)

Science, Vol. 195, pp. 90–93, January 7, 1977

For abstract, see Morrison, D.

LeCROISSETTE, D. H.

L022 Feasibility Study on the Design of a Probe for Rectal Cancer Detection

V. J. Anselmo, R. E. Frazer, D. H. LeCroissette, J. A. Roseboro, and M. I. Smokler

JPL Publication 77-31, April 15, 1977

For abstract, see Anselmo, V. J.

LEDERLE, T.

L023 Expressions for the Precession Quantities Based upon the IAU (1976) System of Astronomical Constants

J. H. Lieske, T. Lederle (Astronomisches Rechen-Institut, Heidelberg), W. Fricke (Astronomisches Rechen-Institut, Heidelberg), and B. Morando (Bureau des Longitudes, Paris)

Astron. Astrophys., Vol. 58, pp. 1–16, 1977

For abstract, see Lieske, J. H.

LEE, B. G.

L024 Design and Implementation of Viking Mission

B. G. Lee and J. D. Porter (Martin Marietta Aerospace)

Preprint 77-270, AIAA Thirteenth Annu. Meet. Tech. Display Incorporating Forum on Future of Air Transp., Wash., D.C., Jan. 10–13, 1977

The Viking missions that were actually implemented were substantially different from those that were planned prior to arrival at the planet. These differences were not, however, unexpected because the fundamental tenet of the Viking mission operations strategy was adaptability. In this paper, this unique "design for change" strategy is explained in detail with particular emphasis on the way that the strategy allowed the missions to respond to both scientific and engineering surprises. The total result of using such an adaptive strategy is shown in a comparison of the expected mission profiles before Mars encounter and the mission profiles that were actually flown.

LEE, J. J.

L025 State Criminal Justice Telecommunications (STACOM) Final Report: Executive Summary

J. E. Fielding, H. K. Frewing, J. J. Lee, W. G. Leflang, and N. B. Reilly

JPL Publication 77-53, Vol. I, October 31, 1977

For abstract, see Fielding, J. E.

L026 **State Criminal Justice Telecommunications (STACOM) Final Report: Requirements Analysis and Design of Ohio Criminal Justice Telecommunications Network**

J. E. Fielding, H. K. Frewing, J. J. Lee, and N. B. Reilly

JPL Publication 77-53, Vol. II, October 31, 1977

For abstract, see Fielding, J. E.

L027 **State Criminal Justice Telecommunications (STACOM) Final Report: Requirements Analysis and Design of Texas Criminal Justice Telecommunications Network**

J. E. Fielding, H. K. Frewing, J. J. Lee, and N. B. Reilly

JPL Publication 77-53, Vol. III, October 31, 1977

For abstract, see Fielding, J. E.

L028 **State Criminal Justice Telecommunications (STACOM) Final Report: Network Design Software User's Guide**

J. J. Lee

JPL Publication 77-53, Vol. IV, October 31, 1977

A user's guide is provided in this volume for the network design software developed during the State Criminal Justice Telecommunications (STACOM) project sponsored by the Law Enforcement Assistance Administration (LEAA). The network design program is written in FORTRAN V and implemented on a UNIVAC 1108 computer under the EXEC-8 operating system which enables the user to construct least-cost network topologies for criminal justice digital telecommunications networks. A complete description of program features, inputs, processing logic, and outputs is presented. Also included is a sample run and a program listing.

LEE, S. H.

L029 **Comparison of Model Test Results: Multipoint Sine Versus Single-Point Random**

E. L. Leppert, S. H. Lee, F. D. Day, P. C. Chapman, and B. K. Wada

Preprint 760879, SAE Aerosp. Eng. Manuf. Meeting, San Diego, CA, Nov. 29–Dec. 2, 1976

For abstract, see Leppert, E. L.

LEES, L.

L030 **An Analysis of the Technical Status of High Level Radioactive Waste and Spent Fuel Management Systems**

T. English, C. Miller, E. Bullard, R. Campbell, A. Chockie, E. Divita, C. Douthitt (California Institute of Technology), E. Edelson, and L. Lees (California Institute of Technology)

JPL Publication 77-69, December 1, 1977

For abstract, see English, T.

LEFLANG, W. G.

L031 **State Criminal Justice Telecommunications (STACOM) Final Report: Executive Summary**

J. E. Fielding, H. K. Frewing, J. J. Lee, W. G. Leflang, and N. B. Reilly

JPL Publication 77-53, Vol. I, October 31, 1977

For abstract, see Fielding, J. E.

LEPPERT, E. L.

L032 **Comparison of Model Test Results: Multipoint Sine Versus Single-Point Random**

E. L. Leppert, S. H. Lee, F. D. Day, P. C. Chapman, and B. K. Wada

Preprint 760879, SAE Aerosp. Eng. Manuf. Meeting, San Diego, CA, Nov. 29–Dec. 2, 1976

Several software packages have been developed for use with minicomputers to decrease the test schedule and cost of modal surveys. The newer development, referred to as "single-point random," appears to have potential cost and schedule advantages, but evaluations of the adequacy of test results and test experience on complex structures are almost nonexistent. The tests, performed on the Mariner Jupiter/Saturn spacecraft, provide an additional comparison of the more traditional multipoint sine dwell and the single-point random modal test methods.

LESH, J. R.

L033 **Radio Frequency Interference from Near-Earth Satellites**

B. K. Levitt and J. R. Lesh

The Deep Space Network Progress Report 42-37: November and December 1976, pp. 69–77, February 15, 1977

For abstract, see Levitt, B. K.

L034 **Maintenance and Operations Cost Model for DSN Subsystems**

R. W. Burt and J. R. Lesh

The Deep Space Network Progress Report 42-40: May and June 1977, pp. 91 - 96, August 15, 1977

For abstract, see Burt, R. W.

L035 **The Effects of Bandpass Limiters on n-Phase Tracking Systems**

S. A. Butman and J. R. Lesh

IEEE Trans. Commun., Vol. COM-25, No. 6, pp. 569–576, June 1977

For abstract, see Butman, S. A.

LEU, M. T.

L036 **Rate Constant for the Reaction of Atomic Bromine With Ozone**

M. T. Leu and W. B. DeMore

Chem. Phys. Lett., Vol. 48, No. 2, pp. 317–320, June 1, 1977

The rate constant for the reaction Br + O_3 → BrO + O_2 has been measured over the temperature range 224 to 422 K in a discharge flow system using a mass spectrometer as a detector. Results, expressed in the form $k_1 = (3.34 \pm 0.40) \times 10^{-11} \times \exp[-(978 \pm 36)/T]$ cm^3 s^{-1}, are compared with previous measurements.

L037 **Rate Constant for Formation of Chlorine Nitrate by the Reaction ClO + NO_2 + M**

M. T. Leu, C. L. Lin, and W. B. DeMore

J. Phys. Chem., Vol. 81, No. 3, pp. 190–195, 1977

A discharge flow/mass spectrometer apparatus has been used to measure rate constants for the reaction ClO + NO_2 + M. The results are: (cm^6 molecule^{-1} s^{-1}) k(M = He) = $(2.66 \pm 0.35) \times 10^{-33} \exp[(1140 \pm 40)/T]$ (248–417 K, 1–9 torr); k(M = N_2) = $(3.69 \pm 0.24) \times 10^{-33} \exp[(1150 \pm 20)/T]$ (298–417 K, 1–6 torr); k(M = Ar) = $(1.15 \pm 0.10) \times 10^{-31}$ (298 K, 1–4 torr). The results are compared with other current measurements of this reaction rate.

LEVITT, B. K.

L038 **Radio Frequency Interference from Near-Earth Satellites**

B. K. Levitt and J. R. Lesh

The Deep Space Network Progress Report 42-37: November and December 1976, pp. 69–77, February 15, 1977

In the near future, radio frequency interference (RFI) from a growing number of Earth-orbiting satellites may seriously degrade deep space telemetry reception. This article develops a pessimistic statistical model for predicting the extent of this interference. Based on the assumptions underlying the model, DSN S-band operations can expect one RFI interruption every 4.1 days, with the average incident lasting 24 s. This implies that 52 or more such satellites, with uncorrelated orbital trajectories, will cause in excess of 5 min of RFI per day at a DSN station (the maximum level recommended by the Consultative Committee for International Radio).

L039 **Analysis of a Discrete Spectrum Analyzer for the Detection of Radio Frequency Interference**

B. K. Levitt

The Deep Space Network Progress Report 42-38: January and February 1977, pp. 83–98, April 15, 1977

As the radio frequency spectrum becomes increasingly overcrowded, interference with mission-critical DSN operations is rising at an alarming rate. To alleviate this problem the DSN is developing a wideband surveillance system for on-site detection and identification of potential sources of radio frequency interference (RFI), which will complement the existing frequency coordination activities. The RFI monitoring system is based on a wideband, multi-look discrete spectrum analyzer operating on fast Fourier transform principles. This article presents an extensive general statistical analysis of such spectrum analyzers and derives threshold detection performance formulas for signals of interest. These results are then applied to the design of the RFI spectrum analyzer under development.

L040 **An Improved Digital Algorithm for Fast Amplitude Approximations of Quadrature Pairs**

B. K. Levitt and G. A. Morris

The Deep Space Network Progress Report 42-40: May and June 1977, pp. 97–101, August 15, 1977

The authors have discovered a computationally fast algorithm for approximating the amplitude $A = (I^2 + Q^2)^{1/2}$ of a quadrature pair (I,Q); specifically, the piecewise linear formula

$$\hat{A} = \begin{cases} X + (1/8)Y; & X \geq 3Y \\ (7/8)X + (1/2)Y; & X \leq 3Y \end{cases}$$

where $X \equiv \max(|I|,|Q|)$, $Y \equiv \min(|I|,|Q|)$. Assuming a uniformly distributed quadrature pair phase angle, the maximum approximation error is 0.028A, the mean error is 0.000066A, and the standard deviation about A is 0.00828A. This algorithm is far more accurate than modified versions of Robertson's approximation ($\hat{A} = X + bY$, $b = 1/2$ or $3/8$ or $1/4$) currently being used for most digital signal processing applications. An immediate application is the wideband digital spectrum analyzer under development for monitoring radio frequency interference (RFI) at DSN stations. The algorithm could also be used in digital radar processors.

L041 Results of Pioneer-Venus 1978 Sequential Decoding Tests Over a Simulated Lognormal Fading Channel

B. K. Levitt

The Deep Space Network Progress Report 42-41: July and August 1977, pp. 21–32, October 15, 1977

Tests were performed in 1976 at the Jet Propulsion Laboratory's Compatibility Test Area (CTA 21) to investigate the effects of lognormal fading on Pioneer-Venus 1978 (PV78) sequential decoding performance. The results of these simulations were used to refine a previously developed empirical model for predicting PV78 telemetry link performance.

L042 Doppler Profiles of Radio Frequency Interference

B. K. Levitt

The Deep Space Network Progress Report 42-41: July and August 1977, pp. 82–85, October 15, 1977

The DSN is currently developing a wideband, digital system for monitoring the RF environment at each receive complex. One of the characteristics that will be used to identify observed RFI (radio frequency interference) sources is the time variations of their received spectra. As a preliminary aid to this effort, doppler profiles were computed for Earth satellites and planes with typical flight parameters. The analysis shows that doppler rates will be high enough to cause spectral smearing and degrade the surveillance station detection capability under certain conditions.

LEVY, G. S.

L043 Mariner Venus Mercury 1973 S/X-Band Experiment

G. S. Levy

JPL Publication 77-17, July 1, 1977

The S/X-band experiment on the Mariner Venus/Mercury 1973 spacecraft constituted a unique opportunity to demonstrate the capability of an X-band downlink coherent with the normal S-band downlink. This was both a technological and scientific experiment, and the results indicated that it was successful in both cases. Analysis of the tracking data shows that the new S/X data type was capable of reducing the miss distance at the planet Mercury by 80% (post-processed data). The use of S/X electron content was demonstrated by comparison with Faraday rotation data. An X-band turnaround telemetry experiment showed the feasibility of a planetary X-band link.

In the science area, the model atmospheric environment of Venus was refined. The ionosphere of the planet was measured to a higher accuracy than before, and the value of the dual-frequency link for measuring the scale size of turbulence was demonstrated. The estimate of the scale size was increased from 100 m to above 5 km.

At the planet Mercury, the S/X data helped establish a minimum atmospheric density. The superior conjunction data refined our knowledge of solar corona density and scintillation characteristics. The overall block diagram of the link as well as the implementation of the spacecraft and ground station were validated. Even those areas that were troublesome in the mission were of great value in establishing an experience base for future use of X-band for a telecommunication link.

LEVY, R.

L044 Digital Generation of Alongwind Velocity Field

M. Shinozuka (Columbia University) and R. Levy

J. Eng. Mech. Div., ASCE, Vol. 103, No. EM4, pp. 689–700, August 1977

For abstract, see Shinozuka, M.

L045 Implementation of Wind Performance Studies for Large Antenna Structures

R. Levy and M. S. Katow

Proc. IEEE Mech. Eng. in Radar Symposium, Wash. D. C., Nov. 8–10, 1977, pp. 27–33

Structural design procedures are described for a large antenna system to meet performance requirements under gravity and wind loading. A computational method is shown for the evaluation of performance in response to wind loading. Cumulative probability distribution curves for wind loading gain reductions for 100-m-diameter antennas are developed to compare a relatively heavy baseline reflector backup structure with two lighter-weight structures; all have equivalent, acceptable performance for gravity loading.

L046 Antenna Bias Rigging for Performance Objective

R. Levy

Proc. IEEE Mech. Eng. in Radar Symposium, Wash. D. C., Nov. 8–10, 1977, pp. 94–97

An optimum bias rigging for a paraboloidal antenna can be used to minimize the expected average mean-square half-pathlength surface deviations. Statistics of deep space planetary missions are employed to develop weighting factors for antenna elevation angles during these missions. A procedure is shown to compute the optimum rigging angle from these weights.

LEWIS, J. C.

L047 An Interstellar Precursor Mission

L. D. Jaffe, C. Ivie, J. C. Lewis, R. Lipes, H. N. Norton, J. W. Stearns, L. D. Stimpson, and P. Weissman

JPL Publication 77-70, October 30, 1977

For abstract, see Jaffe, L. D.

LEWIS, R. A.

L048 A Scanning Laser Rangefinder for a Robotic Vehicle

R. A. Lewis and A. R. Johnston

Technical Memorandum 33-809, February 15, 1977

A scanning Laser Rangefinder (LRF) which operates in conjunction with a minicomputer as part of a robotic vehicle is described. The description, in sufficient detail for replication, modification, and maintenance, includes both hardware and software. Also included is a discussion of our functional requirements relative to the state-of-the-art; a detailing of the instrument and its performance; a summary of the robot system in which the LRF functions; the software organization, interfaces, and description; and the applications to which the LRF has been put.

LI, S. P.

L049 The Effect of Oxidation-Expanded Defects Upon MOS Parameters

S. Prussin, S. P. Li, and R. H. Cockrum

J. Appl. Phys., Vol. 48, No. 11, pp. 4613–4617, November 1977

For abstract, see Prussin, S.

LIESKE, J. H.

L050 Theory of Motion of Jupiter's Galilean Satellites

J. H. Lieske

Astron. Astrophys., Vol. 56, pp. 333–352, 1977

The final results for the theory enabling one to calculate the positions of the Galilean satellites and their partial derivatives are presented, following the techniques outlined in earlier papers. Extensive use of algebraic manipulation software on a digital computer is employed to generate the final expressions. The new theory is, in effect, a revitalization of Sampson's theory in which we (a) remove algebraic and mathematical errors existing in Sampson's work, (b) introduce some neglected effects due to solar interactions and the 3–7 commensurability, (c) allow for non-zero amplitude and phase of the free libration, (d) express the final results as analytic functions of variations in 49 arbitrary constants of integration and physical parameters, (e) construct the theory in a manner which readily allows for future revision, and (f) provide analytic expressions for the partial derivatives with respect to the 49 parameters.

L051 Expressions for the Precession Quantities Based upon the IAU (1976) System of Astronomical Constants

J. H. Lieske, T. Lederle (Astronomisches Rechen-Institut, Heidelberg), W. Fricke (Astronomisches Rechen-Institut, Heidelberg), and B. Morando (Bureau des Longitudes, Paris)

Astron. Astrophys., Vol. 58, pp. 1–16, 1977

Expressions for the precession quantities enabling one to precess to and from an arbitrary epoch are developed as a function of the fundamental astronomical constants. The expressions with numerical values of the coefficients are given relative to epoch J2000.0 in Table 5 for the IAU (1976) System of Astronomical Constants adopted at the XVI General Assembly of the IAU in Grenoble. They must be used with the introduction of the new constants into the ephemerides and in constructing the new fundamental reference system, the FK5. Finally, the developments presented here are applicable for revising revelant precession quantities whenever the system of astronomical constants is changed.

LIKINS, P.

L052 Optimal Estimation and Attitude Control of a Solar Electric Propulsion Spacecraft

V. Larson, P. Likins, and E. Marsh

IEEE Trans. Aerosp. Electron. Syst., Vol. AES-13, No. 1, pp.35–47, January 1977

For abstract, see Larson, V.

ORIGINAL PAGE IS OF POOR QUALITY

LIN, C. L.

L053 Rate Constant for Formation of Chlorine Nitrate by the Reaction ClO + NO_2 + M

M. T. Leu, C. L. Lin, and W. B. DeMore

J. Phys. Chem., Vol. 81, No. 3, pp. 190–195, 1977

For abstract, see Leu, M. T.

LING, J. C.

L054 Measurement of 0.511-MeV Gamma Rays With a Balloon-Borne Ge(Li) Spectrometer

J. C. Ling, W. A. Mahoney, J. B. Willett, and A. S. Jacobson

J. Geophys. Res., Space Phys., Vol. 82, No. 10, pp. 1463–1473, April 1, 1977

Measurements are reported of the terrestrial and extraterrestrial 0.511-MeV gamma rays with a collimated high-resolution gamma ray spectrometer which was flown on a balloon over Palestine, Texas, on June 10, 1974. The instrument consists of four 40-cm^3 Ge(Li) crystals surrounded by a CsI(Na) shield. The angular resolution of the instrument is 30° full width at half maximum, and the energy resolution is 2.3 keV at 0.511 MeV. Our measurements of the atmospheric fluxes are consistent with reported fluxes measured with omnidirectional scintillation detectors and with angular distributions and depth variations of the intensities derived from a semiempirical model after allowance is made for a component of the background rate due to β^+ decays produced by neutron- and proton-initiated interactions with materials near the detectors. Our 2σ upper-limit measurement of the cosmic diffuse flux from the galactic anticenter direction is 9.2×10^{-3} photon/(cm^2 s sr), and the 2σ upper-limit flux from the Crab Nebula and the quiet sun at the top of the atmosphere is 4.6×10^{-3} photon/(cm^2 s).

LIPES, R.

L055 An Interstellar Precursor Mission

L. D. Jaffe, C. Ivie, J. C. Lewis, R. Lipes, H. N. Norton, J. W. Stearns, L. D. Stimpson, and P. Weissman

JPL Publication 77-70, October 30, 1977

For abstract, see Jaffe, L. D.

LIU, K. Y.

L056 A New Fast Algorithm for Computing a Complex Number–Theoretic Transforms

I. S. Reed (University of Southern California), K. Y. Liu (University of Southern California), and T. K. Truong

The Deep Space Network Progress Report 42-39: March and April 1977, pp. 71–75, June 15, 1977

For abstract, see Reed, I. S.

LOBB, V. B.

L057 26-Meter S-X Conversion Project

V. B. Lobb

The Deep Space Network Progress Report 42-39: March and April 1977, pp. 157–167, June 15, 1977

The 26-meter S-X Conversion Project provides for the conversion of an existing 26-meter S-band subnet to a 34-meter S- and X-band subnet. The subnet chosen for conversion consists of the following stations: DSS 12 near Barstow, DSS 44 in Australia, and DSS 62 in Spain. The Conversion Project has evolved from its formative stages, where many options were considered and alternates chosen, to its present status. The main subsystems effected by this project are the Antenna Mechanical, Antenna Microwave, and Receiver-Exciter. In addition to these, there are many project-related electronic equipments that have been added to the existing station equipment. Functional Requirements and Design Response Reviews were held. The major subsystems are essentially through the design stage with the Antenna Mechanical Subsystem completed through detail design with procurement in process.

LOHMAN, G. M.

L058 Optimal Policy for Batch Operations: Backup, Checkpointing, Reorganization, and Updating

G. M. Lohman and J. A. Muckstadt (Cornell University)

ACM Trans. Database Syst., Vol. 2, No. 3, pp. 209–222, September 1977

Many database maintenance operations are performed periodically in batches, even in real-time systems. The purpose of this paper is to present a general model for determining the optimal frequency of these batch operations. Specifically, optimal backup, checkpointing, batch updating, and reorganization policies are derived. The approach used exploits inventory parallels by seeking the optimal number of items—rather than a time interval—to trigger a batch. The Renewal Reward Theorem is used to find the average long run costs for backup, recovery, and item storage, per unit time, which is then minimized to find the optimal backup policy. This approach permits

far less restrictive assumptions about the update arrival process than did previous models, as well as inclusion of storage costs for the updates. The optimal checkpointing, batch updating, and reorganization policies are shown to be special cases of this optimal backup policy. The derivation of previous results as special cases of this model, and an example, demonstrate the generality of the methodology developed.

LORDEN, G.

L059 Life-Cycle Costing: Practical Considerations

I. Eisenberger and G. Lorden

The Deep Space Network Progress Report 42-40: May and June 1977, pp. 102–109, August 15, 1977

For abstract, see Eisenberger, I.

L060 Dynamic Spares Provisioning for the DSN

I. Eisenberger and G. Lorden

The Deep Space Network Progress Report 42-42: September and October 1977, pp. 119–124, December 15, 1977

For abstract, see Eisenberger, I.

LORELL, J.

L061 Lunar Farside Gravity: An Assessment of Satellite to Satellite Tracking Techniques and Gravity Gradiometry

M. Ananda, J. Lorell, and W. Flury (European Space Operations Center)

Proc. Seventh Lunar Sci. Conf., pp. 2623–2638, 1976

For abstract, see Ananda, M.

LORRE, J.

L062 Image Processing of Galaxy Photographs

H. Arp (Hale Observatories) and J. Lorre

Astrophys. J., Vol. 210, No. 1, Pt. 1, pp. 58–64, November 15, 1976

For abstract, see Arp, H.

LOW, P. W.

L063 Radio Frequency Interference Effects of Continuous Sinewave Signals on Telemetry Data

P. W. Low

The Deep Space Network Progress Report 42-40: May and June 1977, pp. 174–193, August 15, 1977

This report presents the results of an investigation of continuous sinewave interference effects on telemetry data based on testing at the Goldstone Deep Space Station (DSS 11) in 1976. To analyze the effects, the continuous sinewave interference is treated as an extraneous noise. Empirical telemetry data degradation and drop-lock models are then developed based on test data and certain physical characteristics of the telemetry data processing system. These models will be used as a portion of the radio frequency interference detection tools in the first version of the Deep Space Interference Prediction Software.

LUCKOW, W.

L064 Evaluation of Coal Feed Systems Being Developed by the Energy Research and Development Administration

R. Phen, C. Jennings, W. Luckow, L. Mattson, D. Otth, and P. Tsou

JPL Publication 77-54, September 1977

For abstract, see Phen, R.

LUTWACK, R.

L065 Modeling of Fluidized Bed Silicon Deposition Process

K. Kim, G. Hsu, R. Lutwack, and A. Praturi

JPL Publication 77-25, June 15, 1977

For abstract, see Kim, K.

L066 Chemical Vapor Deposition of Silicon from Silane Pyrolysis

A. K. Praturi, R. Lutwack, and G. Hsu

JPL Publication 77-38, July 15, 1977

For abstract, see Praturi, A. K.

LYNN, D. J.

L067 Digital Processing of the Mariner 10 Images of Venus and Mercury

J. M. Soha, D. J. Lynn, J. A. Mosher, and D. A. Elliott

J. Appl. Photogr. Eng., Vol. 3, No. 2, pp. 82–92, 1977

For abstract, see Soha, J. M.

LYON, R. B.

L068 Dual Coupler Configuration at DSS 14 for the Voyager Era

T. Y. Otoshi, K. B. Wallace, and R. B. Lyon

The Deep Space Network Progress Report 42-42: September and October 1977, pp. 184–192, December 15, 1977

For abstract, see Otoshi, T. Y.

LYTTLETON, R. A.

L069 Effects of Solar Radiation on the Orbits of Small Particles

R. A. Lyttleton

Astrophys. Space Sci., Vol. 44, pp.119–140, 1976

Revised equations of motion are formulated on more general assumptions than hitherto making allowance for some reflection of sunlight by a dust-particle, and from these the secular rates of change of the orbital elements of the particle are obtained. The equation for the eccentricity yields numerical results for the time taken for given changes in this element to occur. Other elements turn out to be expressible in terms of the eccentricity and thence are effectively also known in terms of the time. More general forms of earlier results are found, and some new mathematical results in the theory of the process are derived. The time of infall to the Sun associated with almost circular initial motion of a particle is calculated, and also the time from an orbit of initially high eccentricity. In this latter case, infall takes place much more rapidly than from a circular orbit of radius comparable with the average distance in the eccentric orbit. The effect on a particle of a long-period comet during a single return is negligible compared with the change in its binding-energy to the Sun that will in general result from planetary action. The possible history of a dust-particle from original capture by the Sun to final infall to the solar surface is briefly considered.

MACK, L. M.

M001 Transition and Laminar Instability

L. M. Mack

JPL Publication 77-15, May 15, 1977

A review is given of the application of linear stability theory to the problem of boundary-layer transition in incompressible flow. The theory is put into a form suitable for three-dimensional boundary layers; both the temporal and spatial theories are examined; and a generalized Gaster relation for three-dimensional boundary layers is derived. Numerical examples include the stability characteristics of Falkner-Skan boundary layers, the accuracy of the two-dimensional Gaster relation for these boundary layers, and the magnitude and direction of the group velocity for oblique waves in the Blasius boundary layer. A review is given of the available experiments which bear on the validity of stability theory and its relation to transition. The final section is devoted to the application of stability theory to transition prediction. Liepmann's method, the e^n method, and the modified e^n method, where n is related to the external disturbance level, are all discussed. A different type of method, called the amplitude method, is described in which the wide-band disturbance amplitude in the boundary layer is estimated from stability theory and an interaction relation for the initial amplitude density of the most unstable frequency. This method is applied to the effect of free-stream turbulence on the transition of Falkner-Skan boundary layers.

MADRID, G. A.

M002 Range Validation Using Kalman Filter Techniques

G. A. Madrid

The Deep Space Network Progress Report 42-39: March and April 1977, pp. 109–118, June 15, 1977

A method is presented whereby range pseudo-residuals may be improved to the level required for the purposes of data validation. Basically, the method proposed is a measurement updating process which utilizes Bierman's adaptation of the Kalman filter measurement updating algorithms together with process noise compensation to account for model errors. This algorithm involves combining the currently available range predictions and measurements to produce an updated range residual measurement whose accuracy is constrained by the range data quality and by the estimated error in the prediction. The algorithm is compact and fast, and is thus suitable for on-line applications in network control or at the station.

MADSEN, B. D.

M003 Summary Report and Status of the Deep Space Network—Mariner Jupiter/Saturn 1977 Flight Project Telecommunications Compatibility

A. I. Bryan, R. P. Kemp, and B. D. Madsen

ORIGINAL PAGE IS OF POOR QUALITY

The Deep Space Network Progress Report 42-38: January and February 1977, pp. 16–37, April 15, 1977

For abstract, see Bryan, A. I.

M004 Summary Report and Status of the Deep Space Network-Voyager Flight Project Telecommunications Compatibility

A. I. Bryan, R. P. Kemp, and B. D. Madsen

The Deep Space Network Progress Report 42-40: May and June 1977, pp. 21–40, August 15, 1977

For abstract, see Bryan, A. I.

M005 Voyage Flight Project—DSN Telecommunications Compatibility Test Program

A. I. Bryan, R. P. Kemp, and B. D. Madsen

The Deep Space Network Progress Report 42-42: September and October 1977, pp. 13–27, December 15, 1977

For abstract, see Bryan, A. I.

MAHONEY, W. A.

M006 Measurement of 0.511-MeV Gamma Rays With a Balloon-Borne Ge(Li) Spectrometer

J. C. Ling, W. A. Mahoney, J. B. Willett, and A. S. Jacobson

J. Geophys. Res., Space Phys., Vol. 82, No. 10, pp. 1463–1473, April 1, 1977

For abstract, see Ling, J. C.

MALIN, M. C.

M007 Comparison of Volcanic Features of Elysium (Mars) and Tibesti (Earth)

M. C. Malin

Geol. Soc. Amer. Bull., Vol. 88, pp. 908–919, July 1977

The Elysium volcanic province on Mars and the Tibesti volcanic province in Chad, Africa, were studied using Mariner 9, Landsat and Apollo photography. Elysium Mons on Mars and Emi Koussi on Earth show remarkable similarities in summit caldera and flank morphologies. Each has a large central caldera ~12 km in diameter and from 500 to 1000 m deep; both calderas contain numerous craters and large, irregular pits. Channel-like features which head at the calderas and taper downslope show evidence of collapse and possible lava erosion. Elysium Mons rises some 14 ± 1.5 km above its base, and the summit is about 20 km above the 6.1-mbar mean martian pressure surface. Crater size/frequency analysis indicates most of the craters are of endogenic origin. The subdued, hummocky terrain on the flanks are distinctly different from the slopes of the younger Tharsis Ridge volcanoes, showing little if any sign of recent material flow.

The lack of aqueous erosional forms on Elysium Mons argues strongly against recent (~10^5 to 10^6 yr) pluvial episodes. The forms and associations of features throughout the Elysium region suggest that central volcanism started earlier in Elysium than in Tharsis and that the source of the Elysium volcanics has been chemically evolved, with evidence of silicic magma. Finally, the data are consistent with the view that the martian crust has been stable and essentially motionless for an extended period of martian geologic time.

M008 Geologic Interpretation of New Observations of the Surface of Venus

R. S. Saunders and M. C. Malin

Geophys. Res. Lett., Vol. 4, No. 11, pp. 547–550, November 1977

For abstract, see Saunders, R. S.

M009 Landform Degradation on Mercury, the Moon, and Mars: Evidence From Crater Depth/Diameter Relationships

M. C. Malin and D. Dzurisin (California Institute of Technology)

J. Geophys. Res., Vol. 82, No. 2, pp. 376–388, January 10, 1977

Morphologic classification of craters and quantitative measurements of crater depth as a function of diameter are used to investigate the relative degradational histories of Mercury, the moon, and Mars. Martian craters exhibit considerable depth variation and are generally shallower than their lunar or mercurian counterparts. On Mercury and the moon, visually fresh and degraded craters on smooth plains show no significant depth degradation except that attributed to lava flooding or local inundation by ejecta from large impacts. More heavily cratered regions on both planets display a large range of both visual and depth degradation, suggesting that most landform modification occurred before the final phase of formation of the oldest smooth plains on both planets. Depth/diameter data presented are discussed as they relate to two early history scenarios. One scenario based on cratering and the ballistic transport of material has been suggested for Mercury, the moon, and Mars by several authors. Owing to discrepancies between this ballistic scenario and observations of crater densities and morphologies, we suggest that landforms on all these

bodies also record nonballistic degradation associated with the formation of intercrater plains. Whichever scenario is applied, early, intense, bombardment-associated degradation appears to be a common element in the histories of the terrestrial planets.

M010 **Comparison of Large Crater and Multiringed Basin Populations on Mars, Mercury, and the Moon**

M. C. Malin (California Institute of Technology)

Proc. Seventh Lunar Sci. Conf., pp. 3589–3602, 1976

The maximum regional areal densities of large impact craters on Mars, Mercury, and the Moon appear to be inversely proportional to the surface areas of the planets. This would not be expected if the objects impacting the planetary surfaces came from common sources and were moving with high velocities relative to the planets; rather, a uniform areal density would be anticipated. Another way of stating the observation is that each planet was bombarded by the same number of objects. Two speculative explanations for the observation are that (1) all planets underwent a uniform bombardment but were resurfaced by processes proportional to planetary surface area, or (2) equally populated families of objects, moving about the sun in orbits similar to those of the planets, were independently depopulated by the respective planets.

M011 **Surface of Venus: Evidence of Diverse Landforms from Radar Observations**

M. C. Malin and R. S. Saunders

Science, Vol. 196, pp. 987–990, May 27, 1977

Recent radar images of the surface of Venus reveal a complex and varied terrain. By applying a set of simplifying assumptions about the nature of the surfaces returning the radar signal, it is possible to make a number of plausible interpretations. In one region on Venus, several circular features have the gross morphology of degraded impact craters. If they are indeed of impact origin, these features suggest that there exist on Venus areas which are ancient and where erosion or resurfacing has not been as intense or as pervasive as on the earth. In other regions there are intriguing features that may evidence active internal processes. One is a large trough-like depression (0°,76°W; measuring 1400 by 150 by 2 kilometers) planimetrically suggestive of both the Valles Marineris on Mars and the East African Rift on the earth. Another feature, about 250 kilometers in diameter and of positive relief, includes an 80-kilometer-diameter circular depression at its summit, suggestive of a large volcanic construct. A third region, near 0°,10°E, contains roughly parallel ranges of mountains separated by valley-like features, with relief varying from small isolated hills several hundred meters high to low ranges on the order of 1000 meters to large mountains approaching 2 kilometers in height. If Venus has a mobile crust similar to the earth's, these mountains may have been produced by compressional tectonics. These interpretations of the radar data indicate that Venus has been a geologically active planet which has developed diverse landforms and therefore is an exciting candidate for future exploration.

MANATT, S. L.

M012 **Fluorine-19 NMR Studies of Fluoroaromatic Systems with Complete Proton Decoupling: The Signs and Magnitudes of Certain F...F and $^{13}C...F$ Spin–Spin Couplings**

S. L. Manatt and M. A. Cooper (ICI, Ltd., Grangemouth, Scotland)

J. Amer. Chem. Soc., Vol. 99, No. 14, pp. 4561–4567, July 6, 1977

Using complete proton decoupling, the fluorine-19 NMR spectra of the ^{13}C satellites of a particular isotopomer of each of the difluorobenzenes and 1,8-difluoronaphtalene and two isotopomers of 2-fluorotrifluoromethylbenzene have been studied in $^{19}F[^{19}F]$ and $^{19}F[^{13}C]$ experiments. Based on the sign of the ^{13}C–F spin–spin coupling as negative, the signs and magnitudes of various F...F and $^{13}C...F$ couplings have been determined. These results are compared with other available pertinent spin–spin coupling information. Also, it was noted that the directly bonded ^{13}C-fluorine isotope chemical shift in the trifluoromethyl group is larger (11.1 Hz upfield) than observed in the case of fluorine bonded to sp^2 carbon (all about 8 Hz upfield). A significant result emerges relative to the sign of ^{13}C–C–C–F coupling, at least for molecular fragments involving sp^2 carbon. The stereochemical disposition of the spin coupled nuclei appears to matter very little and the observed sign must depend in a complicated manner on substituent effects. The conclusion stands in contrast to all previous observations on other types of vicinal couplings where stereochemical orientation has been demonstrated to be much more important than electronic substituent effects and can be determined from the coupling magnitude with some reliability.

MARGOLIS, J. S.

M013 **Measurement of the Fundamental Vibration–Rotation Spectrum of ClO**

R. T. Menzies, J. S. Margolis, E. D. Hinkley, and R. A. Toth

Appl. Opt., Vol. 16, No. 3, pp. 523–525, March 1977

For abstract, see Menzies, R. T.

M014 **Observations of NH_3 in the Atmosphere of Jupiter During 1973, 1974**

K. A. Young and J. S. Margolis

Icarus, Vol. 30, pp. 129–137, 1977

For abstract, see Young, K. A.

M015 **Absorption Strength Measurement of the ν_1 Band of Methyl Chloride**

J. S. Margolis and R. A. Toth

J. Mol. Spectros., Vol. 66, pp. 30–34, 1977

The absorption strengths of the *Q*-branch manifolds of the ν_1 band of methyl chloride have been measured. The results have been used to deduce the band strength which is 32.1 ± 2.9 cm^{-2} atm^{-1} at 297 K. The *P*-branch absorptions have been investigated to determine the possibility of determining a vibration-rotation factor for the band. This factor is $1 + (2\alpha\beta + \gamma) \sim 1.026$.

MARKIEWICZ, B. R.

M016 **Sampled Data Analysis of a Computer-Controlled Manipulator**

B. R. Markiewicz

JPL Publication 77-66, October 15, 1977

A comprehensive sampled data analysis of a computer-controlled manipulator is presented in terms of root loci for gain selection and transient responses to step input functions. All parameter values and their derivations where applicable are tabulated. The analysis, while quite specific, uses normalized gain parameters, which allows the results to be applied to any similar system regardless of individual hardware parameter values.

MARSH, E.

M017 **Optimal Estimation and Attitude Control of a Solar Electric Propulsion Spacecraft**

V. Larson, P. Likins, and E. Marsh

IEEE Trans. Aerosp. Electron. Syst., Vol. AES-13, No. 1, pp.35–47, January 1977

For abstract, see Larson, V.

MARTIN, K. E.

M018 **Voyager Electronic Parts Radiation Program: Final Report**

A. G. Stanley, K. E. Martin, and W. E. Price

JPL Publication 77-41, Vol. I, September 15, 1977

For abstract, see Stanley, A. G.

MARTIN, T. Z.

M019 **Martian North Pole Summer Temperatures: Dirty Water Ice**

H. H. Kieffer (University of California, Los Angeles), S. C. Chase, Jr. (Santa Barbara Research Center), T. Z. Martin (University of California, Los Angeles), E. D. Miner, and F. D. Palluconi

Science, Vol. 194, pp. 1341–1344, December 17, 1976

For abstract, see Kieffer, H. H.

M020 **Temperatures of the Martian Surface and Atmosphere: Viking Observation of Diurnal and Geometric Variations**

H. H. Kieffer (University of California, Los Angeles), P. R. Christensen (University of California, Los Angeles), T. Z. Martin (University of California, Los Angeles), E. D. Miner, and F. D. Palluconi

Science, Vol. 194, pp. 1346–1351, December 17, 1976

For abstract, see Kieffer, H. H.

MARTIN, W. L.

M021 **Mu-II Ranging**

W. L. Martin and A. I. Zygielbaum

Technical Memorandum 33-768, May 15, 1977

This report describes the Mu-II Dual-Channel Sequential Ranging System designed as a model for future Deep Space Network ranging equipment. A list of design objectives is followed by a theoretical explanation of the digital demodulation techniques first employed in this machine. Thereafter, both hardware and software implementation are discussed, together with the details relating to the construction of the device. The report concludes with a section describing the system's performance in both the field and laboratory, with the authors' recommendations for future ranging equipment. Finally, in the interest of completeness, two appendixes are included relating to the programming and operation of this equipment to yield the maximum scientific data.

MASON, P.

M022 Surface Crystalline Carbon Temperature Sensor

D. Petrac, J. Gatewood, and P. Mason

Advan. Cryog. Eng., Vol. 21, pp. 242–243, 1976

For abstract, see Petrac, D.

M023 Sensor for Distinguishing Liquid–Vapor Phases of Superfluid Helium

D. Petrac, J. Gatewood, and P. Mason

Advan. Cryog. Eng., Vol. 21, pp. 244–246, 1976

For abstract, see Petrac, D.

M024 Experiments on the Properties of Superfluid Helium in Zero Gravity

P. Mason, D. Collins, D. Petrac, L. Yang, F. Edeskuty, and K. Williamson

Proc. Sixth Int. Cryog. Eng. Conf., Grenoble, France, May 11–14,1976, pp. 272–277

A description is given of experiments to study the behavior of superfluid liquid helium in low and zero gravity to determine its use as a stored cryogen for cooling scientific instruments aboard spacecraft for periods up to several months.

MASSIER, P. F.

M025 Investigation of Pressure Oscillations in Axi-Symmetric Cavity Flows

V. Sarohia and P. F. Massier

JPL Publication 77-68, September 1977

For abstract, see Sarohia, V.

M026 Experimental Results of Large Scale Structures in Jet Flows and Their Relation to Jet Noise Production

V. Sarohia and P. F. Massier

Preprint 77-1350, AIAA Fourth Aeroacoustics Conf., Atlanta, Ga., Oct. 3–5, 1977

For abstract, see Sarohia, V.

M027 Effects of External Boundary-Layer Flow on Jet Noise in Flight

V. Sarohia and P. F. Massier

AIAA J., Vol. 15, No. 5, pp. 659–[illegible], May 1977

For abstract, see Sarohia, V.

M028 Mach Wave Emission from Supersonic Jets

S. P. Parthasarathy and P. F. Massier

AIAA J., Vol. 15, No. 10, pp. 1462–1468, October 1977

For abstract, see Parthasarathy, S. P.

M029 Control of Cavity Noise

V. Sarohia and P. F. Massier

Preprint 76-528, AIAA Third Aero-Acoust. Conf., Palo Alto, Calif., July 20–23, 1976

For abstract, see Sarohia, V.

M030 Control of Cavity Noise

V. Sarohia and P. F. Massier

J. Aircraft, Vol. 14, No. 9, pp. 833–837, September 1977

For abstract, see Sarohia, V.

MATHEWS, A. N.

M031 VLBI Clock Sync and the Earth's Rotational Instability

J. W. Layland and A. N. Mathews

The Deep Space Network Progress Report 42-42: September and October 1977, pp. 81–84, December 15, 1977

For abstract, see Layland, J. W.

MATSON, D. L.

M032 Sodium D-Line Emission From Io: A Second Year of Synoptic Observation From Table Mountain Observatory

J. T. Bergstralh, J. W. Young, D. L. Matson, and T. V. Johnson

Astrophys. J., Vol. 211, No. 1, Pt. 2, pp. L51–L55, January 1, 1977

For abstract, see Bergstralh, J. T.

M033 Io's Surface Composition: Observational Constraints and Theoretical Considerations

F. P. Fanale, T. V. Johnson, and D. L. Matson

Geophys. Res. Lett., Vol. 4, No. 8, pp. 303–306, August 1977

For abstract, see Fanale, F. P.

M034 **Photometry of the Asteroid 1976 AA at 0.56 and 2.2 μm**

G. J. Veeder, D. L. Matson, and O. L. Hansen

Icarus, Vol. 31, pp. 424–426, 1977

For abstract, see Veeder, G. J.

MATTSON, L.

M035 **Evaluation of Coal Feed Systems Being Developed by the Energy Research and Development Administration**

R. Phen, C. Jennings, W. Luckow, L. Mattson, D. Otth, and P. Tsou

JPL Publication 77-54, September 1977

For abstract, see Phen, R.

M036 **Effects of Aniline Impurities on Monopropellant Hydrazine Thruster Performance**

L. Holcomb, L. Mattson, and R. Oshiro

J. Spacecraft Rockets, Vol. 14, No. 3, pp. 141–148, March 1977

For abstract, see Holcomb, L.

McELIECE, R. J.

M037 **On the Inherent Intractability of Finding Good Codes**

R. J. McEliece and H. C. A. van Tilborg

The Deep Space Network Progress Report 42-37: November and December 1976, pp. 83–87, February 15, 1977

In this article we will show that the problem of computing the minimum distance of an arbitrary binary linear code is *NP* complete. This strongly suggests, but does not imply, that it is impossible to design a computer algorithm for computing the minimum distance of an arbitrary code whose running time is bounded by a polynomial in the number of inputs.

M038 **Synchronization Strategies for RFI Channels**

R. J. McEliece, H. van Tilborg (California Institute of Technology), and S. Tung (Cornell University)

The Deep Space Network Progress Report 42-38: January and February 1977, pp. 103–108, April 15, 1977

In this article we define an RFI channel to be a multiple-access channel in which no sender can know when any other starts, and study the problem of determining the relative phases of the senders at the receiver. Along the way we prove a new result about binary deBruijn sequences.

M039 **An Asymptotic Analysis of a General Class of Signal Detection Algorithms**

R. J. McEliece and E. R. Rodemich

The Deep Space Network Progress Report 42-39: March and April 1977, pp. 30–35, June 15, 1977

For applications to the problem of radio frequency interference identification, or in the search for extraterrestrial intelligence, it is important to have a basic understanding of signal detection algorithms. In this article we give a general technique for assessing the asymptotic sensitivity of a broad class of signal detection algorithms. In these algorithms, the decision is based on the value of $X_1 + X_2 + \ldots + X_n$, where the X_i's are obtained by sampling and preliminary processing of a physical process.

M040 **New Upper Bounds on the Rate of a Code via the Delsarte–MacWilliams Inequalities**

R. J. McEliece, E. R. Rodemich, H. Rumsey, Jr., and L. R. Welch (University of Southern California)

IEEE Trans. Inform. Theor., Vol. IT-23, No. 2, pp. 157–166, March 1977

With the Delsarte–MacWilliams inequalities as a starting point, an upper bound is obtained on the rate of binary code as a function of its minimum distance. This upper bound is asymptotically less than Levenshtein's bound, and so also Elias's.

M041 **An Improved Upper Bound on the Block Coding Error Exponent for Binary-Input Discrete Memoryless Channels**

R. J. McEliece and J. K. Omura (University of California, Los Angeles)

IEEE Trans. Inform. Theor., Vol. IT-23, No. 5, pp. 611–613, September 1977

The recent upper bounds on the minimum distance of binary codes given by McEliece, Rodemich, Rumsey, and Welch are shown to result in improved upper bounds on the block coding error exponent for binary-input memoryless channels.

M042 **There is No MacWilliams Identity for Convolutional Codes**

J. B. Shearer and R. J. McEliece

IEEE Trans. Inform. Theor., Vol. IT-23, No. 6, pp. 775–776, November 1977

For abstract, see Shearer, J. B.

McGINNESS, H.

M043 Estimated Displacements for the VLBI Reference Point of the DSS 14 Antenna

H. McGinness

The Deep Space Network Progress Report 42-41: July and August 1977, pp. 218–225, October 15, 1977

The maximum displacement of the defined VLBI reference point is shown to be primarily a function of the ambient air temperature.

McKENZIE, M.

M044 Cost Reduction Potential of the DSN Data Base

M. McKenzie

The Deep Space Network Progress Report 42-38: January and February 1977, pp. 203–220, April 15, 1977

The cost of the DSN data base can be reduced by computerizing and unifying the current multiplicity of separate manual, computer, and hybrid data bases. Savings would accrue from eliminating all manual system costs, increasing efficiency in data base implementation and maintenance-and-operation, and increasing data accuracy. By applying a simple mathematical savings model to current data base costs, this study estimates the probable range of net ten-year savings. The minimum net savings, under the assumptions of the study, is calculated as $7.5 million.

M045 Cost Evaluation of a DSN High Level Real-Time Language

M. McKenzie

The Deep Space Network Progress Report 42-42: September and October 1977, pp. 214–225, December 15, 1977

The hypothesis that the implementation of a DSN High Level Real-Time Language will reduce real-time software expenditures is explored. The High Level Real-Time Language is found to be both affordable and cost-effective.

McLAUGHLIN, W. I.

M046 Mission Design for SEASAT-A, An Oceanographic Satellite

E. Cutting, G. H. Born, J. C. Frautnick, W. I. McLaughlin, R. A. Neilson, and J. A. Thielen (Lockheed Missiles & Space Co.)

Preprint 77-31, AIAA Fifteenth Aerosp. Sci. Meet., Los Angeles, Calif., Jan. 24–26, 1977

For abstract, see Cutting, E.

M047 On the Timing of an Interstellar Communication

W. I. McLaughlin

Icarus, Vol. 32, pp. 464–470, 1977

By considering prominent events that are observable from both Earth and nearby stellar systems, it is possible to establish common clocks that may be useful in estimating arrival times for signals of intelligent extraterrestrial origin. The geometry and statistics of a timing strategy are developed together with quantitative estimates of its effectiveness and limits on its application. Effectiveness is measured by comparing the timing strategy with one randomized in time. Limitations arise from inaccuracies inherent in the determination of stellar parallaxes and result in standard deviations of the order of weeks to months for time estimates. The problem can be alleviated by choosing clocks close to Sender in angular distance. Signal opportunities for several nearby Sun-like stars are calculated using the bright Nova Cygni 1975 as a clock.

M048 On the Mass of Saturn's Rings

W. I. McLaughlin and T. D. Talbot

Mon. Not. R. Astr. Soc., Vol. 179, pp. 619–634, 1977

A gravitational model of the Saturnian system which included rings, satellites and the oblate planet was fit to the observed secular apsidal and nodal rates of the inner satellites. The solution

Mass of the rings $= (6.2 \pm 2.4) \times 10^{-6}$ masses of Saturn

Mass of Rhea $= (4.8 \pm 0.8) \times 10^{-6}$ masses of Saturn

$J_2 = (1.664 \pm 0.001) \times 10^{-2}$

$J_4 = -(8.7 \pm 0.1) \times 10^{-4}$

was obtained using a functional relationship between the zonal harmonics J_2 and J_4 derived from the planetary interior modelling of Hubbard, Slattery & DeVito. The planetary model due to Podolak & Cameron was shown to be inconsistent with the observed secular apsidal and nodal rates of the natural satellites. A solution for the planetary figure by Garcia was found to suffer from

defective data for Titan. The apsidal commensurability of particles in the rings with Titan was shown to produce no significant effect on the structure of the rings and, in particular, is not the cause of Guerin's division.

McLEMORE, B. D.

M049 Computability of Five-Color Maps

B. D. McLemore (Informatics, Inc.) and A. L. Zobrist

Image Sci. Math., pp. 256–260, Western Periodicals Co., North Hollywood, Calif., 1977

Aside from the mathematical question as to whether any planar map can be colored with four or five colors so that no adjacent regions are assigned the same color, there is a computational problem of finding a coloration for a given map. This report presents an algorithm for the five-color problem which has an asymptotic computing time which is proportional to the square of the number of regions, at worst. The algorithm can be modified to produce six-color maps in linear time. The algorithm has been implemented for practical use in an image processing system and can be used in practical cases to produce four-color maps.

McLYMAN, C. W. T.

M050 Transformer Design Tradeoffs

C. W. T. McLyman

Technical Memorandum 33-767, Rev. 1, March 15, 1977

In space, power system transformer components are frequently the heaviest and bulkiest items in the power conversion circuit. They also have a significant effect upon the overall performance and efficiency of the system. Accordingly, the design of such transformers has an important effect on overall system weight, power-inversion efficiency, and cost. The author has developed relationships between the parameters used by transformer designers that can be used as new tools to standardize and simplify transformer design. They can be used to optimize the design either for small size and weight or efficiency. The metric system of units, rather than the familiar English units, is used; however, material is presented to assist the reader in the transition from one system to the other.

M051 Spacecraft Transformer and Inductor Design

C. W. T. McLyman

JPL Publication 77-35, August 15, 1977

The conversion process in spacecraft power electronics requires the use of magnetic components which frequently are the heaviest and bulkiest items in the conversion circuit. They also have a significant effect upon the performance, weight, cost, and efficiency of the power system. This handbook contains eight chapters, which pertain to magnetic material selection, transformer and inductor design tradeoffs, transformer design, iron core dc inductor design, toroidal powder core inductor design, window utilization factors, regulations, and temperature rise. Relationships are given which simplify and standardize the design of transformers and the analysis of the circuits in which they are used. The interactions of the various design parameters are also presented in simplified form so that tradeoffs and optimizations may easily be made.

McNAMARA, R. P.

M052 Comparative Studies of Ion-Implant Josephson-Effect Structures

R. K. Kirschman, J. A. Hutchby (Langley Research Center), J. W. Burgess (Langley Research Center), R. P. McNamara (California Institute of Technology), and H. A. Notarys (California Institute of Technology)

IEEE Trans. Magnet., Vol. MAG-13, No. 1, pp. 731–734, January 1977

For abstract, see Kirschman, R. K.

MEEKS, W. G.

M053 Tracking and Data Systems Support for the Helios Project: DSN Support of Project Helios April 1975 Through May 1976

P. S. Goodwin, M. R. Traxler, W. G. Meeks, and F. M. Flanagan

Technical Memorandum 33-752, Vol. II, January 15, 1977

For abstract, see Goodwin, P. S.

MEISENHOLDER, G. W.

M054 Control Techniques for an Automated Mixed Traffic Vehicle

G. W. Meisenholder and A. R. Johnston

Proc. 1977 Joint Automat. Contr. Conf., San Francisco, Calif., June 22–24, 1977, pp. 421–427

An initial experiment has been conducted to investigate the feasibility of operating a driverless low-speed tram in

ORIGINAL PAGE IS
OF POOR QUALITY

mixed pedestrian and vehicular traffic. Since neither driver nor expensive guideway is needed, this concept has the potential of making very low cost service possible in some applications.

A six-passenger electric tram has been equipped with sensing and control which permit it to function on existing streets in an automatic mode. The vehicle design involved development of simple, active, near-IR headway sensors, and used established wire-following techniques for steering. A 7-mph cruise speed is reduced to 2 mph or a complete stop in response to sensor or passenger inputs.

In this paper, the Automated Mixed Traffic Vehicle (AMTV) concept and applications are discussed, and the vehicle design is described. Analytical results describing the vehicle control system and predicting on a statistical basis the effect of interacting pedestrian traffic are also presented.

MENZIES, R. T.

M055 Ozone Spectroscopy With a CO_2 Waveguide Laser

R. T. Menzies

Appl. Opt., Vol. 15, No. 11, pp. 2597–2599, November 1976

The frequencies of several ozone lines in the ν_3 band near CO_2 laser line frequencies in the 9.5-μm wavelength region have been determined. The absolute measurement accuracy is estimated to be ±6 MHz ($\pm 2 \times 10^{-4}$ cm^{-1}). The measurements indicate that ozone line frequencies listed in currently available spectral compilations are 0.003 to 0.006 cm^{-1} too high.

M056 Measurement of the Fundamental Vibration–Rotation Spectrum of ClO

R. T. Menzies, J. S. Margolis, E. D. Hinkley, and R. A. Toth

Appl. Opt., Vol. 16, No. 3, pp. 523–525, March 1977

The spectrum of the ClO fundamental absorption band near 850 cm^{-1} has been observed using a tunable PbSnTe diode laser as a source of monochromatic radiation. Several line frequencies were measured by using nearby ammonia lines as frequent standards. Intensities were also deduced by measuring peak absorption in the Doppler limit. The resulting band strength is 30 ± 10 cm^{-1} atm^{-1} at 298 K.

MEYER, R. F.

M057 Hydrogen Maser Frequency Standards for the Deep Space Network

P. R. Dachel, S. M. Petty, R. F. Meyer, and R. L. Sydnor

The Deep Space Network Progress Report 42-40: May and June 1977, pp. 76–83, August 15, 1977

For abstract, see Dachel, P. R.

MILLER, C.

M058 An Analysis of the Technical Status of High Level Radioactive Waste and Spent Fuel Management Systems

T. English C. Miller, E. Bullard, R. Campbell, A. Chockie, E. Divita, C. Douthitt (California Institute of Technology), E. Edelson, and L. Lees (California Institute of Technology)

JPL Publication 77-69, December 1, 1977

For abstract, see English, T.

MILLER, J. K.

M059 The Application of Differential VLBI to Planetary Approach Orbit Determination

J. K. Miller and K. H. Rourke

The Deep Space Network Progress Report 42-40: May and June 1977, pp. 84–90, August 15, 1977

The development of multistation tracking techniques has resulted in improved orbit determination accuracies. Differential Very Long Baseline Interferometry (VLBI), which involves performing measurements of a spacecraft and nearby extra galactic radio source and differencing, potentially offers at least an order of magnitude improvement over data types currently implemented. In this article, the application of differential VLBI to planetary approach orbit determination is described.

MILLER, R. B.

M060 Pioneer Venus 1978 Mission Support

R. B. Miller

The Deep Space Network Progress Report 42-38: January and February 1977, pp. 43–49, April 15, 1977

The Ground Data System configuration for support of the Pioneer Venus 1978 Mission is described. Current status of the DSN portion of the Ground Data System is described.

M061 Pioneer Venus 1978 Mission Support

R. B. Miller

The Deep Space Network Progress Report 42-40: May and June 1977, pp. 14–20, August 15, 1977

The DSN Master Schedule for preparations for the Pioneer Venus 1978 Mission is updated and the current support status for the mission described.

MINER, E. D.

M062 Martian North Pole Summer Temperatures: Dirty Water Ice

H. H. Kieffer (University of California, Los Angeles), S. C. Chase, Jr. (Santa Barbara Research Center), T. Z. Martin (University of California, Los Angeles), E. D. Miner, and F. D. Palluconi

Science, Vol. 194, pp. 1341–1344, December 17, 1976

For abstract, see Kieffer, H. H.

M063 Temperatures of the Martian Surface and Atmosphere: Viking Observation of Diurnal and Geometric Variations

H. H. Kieffer (University of California, Los Angeles), P. R. Christensen (University of California, Los Angeles), T. Z. Martin (University of California, Los Angeles), E. D. Miner, and F. D. Palluconi

Science, Vol. 194, pp. 1346–1351, December 17, 1976

For abstract, see Kieffer, H. H.

MITTRA, R.

M064 A New Series Representation for the Radiation Integral with Application to Reflector Antennas

V. Galindo-Israel and R. Mittra

IEEE Trans. Anten. Prop., Vol. AP-25, No. 5, pp. 631–641, September 1977

For abstract, see Galindo-Israel, V.

MIYAHARA, T. F.

M065 Electrical Characteristics of 2-Ω-cm 0.046-cm-Thick Silicon Solar Cells as a Function of Intensity and Temperature

P. A. Berman, T. F. Miyahara, and B. E. Anspaugh

JPL Publication 77-27, July 1, 1977

For abstract, see Berman, P. A.

M066 Electrical Characteristics of 2-Ω-cm 0.046-cm-Thick Silicon Solar Cells as a Function of Intensity and Temperature

P. A. Berman, T. F. Miyahara, and B. E. Anspaugh

JPL Publication 77-27, Rev. 1, August 15, 1977

For abstract, see Berman, P. A.

MOLINDER, J. I.

M067 Baseband Recording and Playback

S. S. Kent and J. I. Molinder

The Deep Space Network Progress Report 42-37: November and December 1976, pp. 136–145, February 15, 1977

For abstract, see Kent, S. S.

M068 The CTA 21 Radio Science Subsystem—Non-Real-Time Bandwidth Reduction of Wideband Radio Science Data

A. L. Berman and J. I. Molinder

The Deep Space Network Progress Report 42-41: July and August 1977, pp. 127–134, October 15, 1977

For abstract, see Berman, A. L.

MORANDO, B.

M069 Expressions for the Precession Quantities Based upon the IAU (1976) System of Astronomical Constants

J. H. Lieske, T. Lederle (Astronomisches Rechen-Institut, Heidelberg), W. Fricke (Astronomisches Rechen-Institut, Heidelberg), and B. Morando (Bureau des Longitudes, Paris)

Astron. Astrophys., Vol. 58, pp. 1–16, 1977

For abstract, see Lieske, J. H.

MORGAN, E. M.

M070 Calibration of Viking Imaging System Pointing, Image Extraction, and Optical Navigation Measure

W. G. Breckenridge, J. W. Fowler, and E. M. Morgan (General Electric Co.)

JPL Publication 77-28, September 15, 1977

For abstract, see Breckenridge, W. G.

MORRILL, M. E.

M071 Viking Lander Camera Radiometry Calibration Report

M. R. Wolf, D. L. Atwood, and M. E. Morrill

JPL Publication 77-62, Vols. I and II, November 1, 1977

For abstract, see Wolf, M. R.

MORRIS, G. A.

M072 An Improved Digital Algorithm for Fast Amplitude Approximations of Quadrature Pairs

B. K. Levitt and G. A. Morris

The Deep Space Network Progress Report 42-40: May and June 1977, pp. 97–101, August 15, 1977

For abstract, see Levitt, B. K.

MORRIS, J. F.

M073 Thermionic Energy Conversion Technology—Present and Future

K. Shimada and J. F. Morris (Lewis Research Center)

Preprint 77-500, AIAA Conf. Future Aerosp. Power Sys., St. Louis, Mo., Mar. 1–3, 1977

For abstract, see Shimada, K.

MORRIS, M.

M074 Searching for Extraterrestrial Civilizations

T. B. H. Kuiper and M. Morris

Science, Vol. 196, pp. 616–621, May 6, 1977

For abstract, see Kuiper, T. B. H.

MORRISON, D.

M075 Galilean Satellites: Anomalous Temperatures Disputed

D. Morrison (University of Arizona). L. A. Lebofsky, J. A. Cutts (Planetary Science Institute), G. J. Veeder, and S. H. Gross (Polytechnic Institute of New York)

Science, Vol. 195, pp. 90–93, January 7, 1977

A refutation by Morrison, Lebofsky, Cutts, and Veeder of the equilibrium temperature equations computed by Gross is given, followed by Gross's rebuttal.

MOSHER, J. A.

M076 Digital Processing of the Mariner 10 Images of Venus and Mercury

J. M. Soha, D. J. Lynn, J. A. Mosher, and D. A. Elliott

J. Appl. Photogr. Eng., Vol. 3, No. 2, pp. 82–92, 1977

For abstract, see Soha, J. M.

MOYD, K. I.

M077 Modcomp Version of Tutorial Input

K. I. Moyd

The Deep Space Network Progress Report 42-39: March and April 1977, pp. 38–48, June 15, 1977

The version of Tutorial Input implemented on the Modcomp used for antenna control at DSS 13 is described. Emphasis is on the use of the Tutorial Input; program operation is described to the extent that it makes the use more understandable. Flow charts are provided.

MUCKSTADT, J. A.

M078 Optimal Policy for Batch Operations: Backup, Checkpointing, Reorganization, and Updating

G. M. Lohman and J. A. Muckstadt (Cornell University)

ACM Trans. Database Syst., Vol. 2, No. 3, pp. 209–222, September 1977

For abstract, see Lohman, G. M.

MUDGWAY, D. J.

M079 Tracking and Data System Support for the Viking 1975 Mission to Mars: Prelaunch Planning, Implementation, and Testing

D. J. Mudgway and M. R. Traxler

Technical Memorandum 33-783, Vol. I, January 15, 1977

This report describes the Tracking and Data Acquisition support for the 1975 Viking Missions to Mars. In this volume the history of the effort from its inception in late 1968 through the launches of Vikings 1 and 2 from Cape Kennedy in August and September 1975 is given. The Viking mission requirements for tracking and data acquisition support in both the near Earth and deep space phases involved multiple radar tracking and telemetry stations and communications networks of the Air Force Eastern Test Range and the Goddard Spaceflight and

Tracking Acquisition Network, together with the global network of tracking stations, communications, and control center of NASA's Deep Space Network and NASA Communications Network. The planning, implementation, testing and management of this vast complex of people and facilities to meet the demands of the 1975 Viking Mars launch opportunity is the subject of this particular volume.

M080 **Tracking and Data System Support for the Viking 1975 Mission to Mars: Launch Through Landing of Viking I**

D. J. Mudgway and M. R. Traxler

Technical Memorandum 33-783, Vol. II, March 15, 1977

The Viking 1975 mission to Mars depended on NASA's Deep Space Network and Spaceflight Tracking and Data Network, together with the NASA Communications Network and support from stations of the Air Force Eastern Test Range, to provide its tracking and data acquisition support. This document describes the Tracking and Data System support for the Viking Mars mission from launch in August and September 1975 through the cruise phase to the landing of the first Lander on the surface of Mars in July 1975.

Beginning with tracking coverage of the launch phase, the report describes the deep space operations during the long cruise phase that occupied approximately 11 months, the implementation of a vast worldwide network of tracking stations and global communications systems, and the performance of the personnel, hardware, and software involved in this vast undertaking.

Some of the unique problems inherent in the deployment and management of a worldwide tracking and data acquisition network to support the two Viking Orbiters and two Viking Landers simultaneously over 320 million kilometers (200 million miles) of deep space are highlighted.

M081 **Tracking and Data System Support for the Viking 1975 Mission to Mars: Planetary Operations**

D. J. Mudgway

Technical Memorandum 33-783, Vol. III, September 1, 1977

This document describes and evaluates the support provided by the Deep Space Network to the 1975 Viking Mission from the first landing on Mars in July 1976 to the end of the Prime Mission on November 15, 1976. Tracking and data acquisition support required the continuous operation of a worldwide network of tracking stations with 64-meter and 26-meter diameter antennas, together with a global communications system for the transfer of commands, telemetry, and radio metric data between the stations and the Network Operations Control Center in Pasadena, California. Performance of the deep-space communications links between Earth and Mars, and innovative new management techniques for operations and data handling are included.

M082 **Viking Extended Mission Support**

T. W. Howe and D. J. Mudgway

The Deep Space Network Progress Report 42-40: May and June 1977, pp. 41–51, August 15, 1977

For abstract, see Howe, T. W.

MUHLEMAN, D. O.

M083 **The Electron Density profile of the Outer Corona and the Interplanetary Medium From Mariner-6 and Mariner-7 Time-Delay Measurements**

D. O. Muhleman (California Institute of Technology), P. B. Esposito, and J. D. Anderson

Astrophys. J., Vol. 211, No. 3, Pt. 1, pp. 943–957, February 1, 1977

The round-trip propagation time delays to the Mariner-6 and Mariner-7 spacecraft were measured over a 6 month period, including the occultations by the solar corona during April and May of 1970. The interplanetary medium was sampled over a range of ray impact parameters from about 5 to 100 solar radii. Electron density models fitted to the observations show that the density profile falls off nearly exactly as the inverse square of the distance from about 10 solar radii out to the Earth's orbit. The estimated values of the slopes are −2.05 and −2.08 for Mariner-6 and Mariner-7, respectively. The formal standard deviation on each estimate is ±0.24. In general, the densities are about a factor of 2 smaller than those determined by eclipse photometric measurements. The latter result agrees with recent radio ray-bending and pulsar time-delay measurements. The fluctuations in the measured time delays show that the true standard deviation of the electron density at a given point is about 100% of the local mean density. The evaluations of the estimated electron density profiles at 1 AU yield 9 ± 3 electrons cm^{-3} for both spacecraft experiments, which were analyzed independently. Our results are strictly correct only if the general-relativistic effects are those predicted by Einsteins's general theory.

MULHALL, B. D. L.

M084 **Review of Finite Fields: Applications to Discrete Fourier Transforms and Reed-Solomon Coding**

J. S. L. Wong, T. K. Truong, B. Benjauthrit, B. D. L. Mulhall, and I. S. Reed

ORIGINAL PAGE IS
OF POOR QUALITY

JPL Publication 77-23, July 15, 1977

For abstract, see Wong, J. S. L.

M085 X-Band Antenna Gain and System Noise Temperature of 64-Meter Deep Space Stations

B. Benjauthrit and B. D. L. Mulhall

The Deep Space Network Progress Report 42-39: March and April 1977, pp. 76–99, June 15, 1977

For abstract, see Benjauthrit, B.

M086 DSN Radio Science System Description and Requirements

B. D. L. Mulhall

The Deep Space Network Progress Report 42-39: March and April 1977, pp. 119–129, June 15, 1977

A new DSN data system has been created to collect the functions performed by the DSN in support of spacecraft radio science experiments. The system is described and some of its major functions are delineated.

NASH, D. B.

N001 Io's Surface Composition Based on Reflectance Spectra of Sulfur/Salt Mixtures and Proton-Irradiation Experiments

D. B. Nash and F. P. Fanale

Icarus, Vol. 31, pp. 40–80, 1977

The available full-disk reflectance spectra of Io in the range of 0.3 to 2.5 μm have been interpreted by comparison with new laboratory spectra of a wide variety of natural and synthetic mineral phases in order to determine a surface compositional model for Io that is consistent with Io's other known chemical and physical properties. Our results indicate that the dominant mineral phases are sulfates and free sulfur derived from them, which points toward a low temperature and initially water-rich surface assemblage. Our current preferred mineral phase mixture that best matches the Io data and is simultaneously most consistent with other constraints consists of a fine-grained particulate mixture of free sulfur (55 vol%), dehydrated bloedite (30 vol%), ferric sulfate (15 vol%), and trace amounts of hematite. Other salts may be present, such as halite and sodium nitrate, as well as clay minerals. Such a model is consistent with a probable pre- and post-accretion thermal history of Io-forming material and Io's observed Na emission and other properties. These results further support the evaporite surface hypothesis of Fanale *et al.*, while not precluding the presence of certain silicate phases such as montmorillonite.

The average surface of Io's leading hemisphere appears to contain less free sulfur and more salts and to be finer grained than that of the trailing hemisphere. Since Io is immersed in Jupiter's magnetosphere, irradiation damage effects from low-energy proton bombardment were studied. Irradiation damage of lattices is estimated to be a relatively minor but operative process on the surface of Io; irradiation darkening by sulfate reduction to free sulfur and by F-center production in salts may be partly responsible for the differences in albedo of leading and trailing hemispheres and equatorial and polar regions of Io, but slight regional differences in relative intrinsic phase concentration on the surface may likewise account for these global variations in albedo.

Possible unusual surface properties predicted by this model include: posteclipse darkening in certain wavelengths, limb brightening in certain wavelengths, and unusual surface electrical properties. Further refinement of Io's surface composition model and better understanding of surface irradiation effects will be possible when observational data in the range 0.20 to 0.30 μm are obtained and when improved spectra in the range of 0.30 to 5.0 μm are obtained having increased spectral, spatial, and temporal resolution.

NATHAN, R.

N002 Final Report: Medical Ultrasonic Tomographic System

R. C. Heyser, D. H. Le Croissette, R. Nathan, and R. L. Wilson (Harbor General Hospital, Los Angeles)

JPL Publication 77-72, October 1, 1977

For abstract, see Heyser, R. C.

N003 Computer Synthesis of High Resolution Electron Micrographs

R. Nathan

Digital Processing of Biomedical Images, Plenum Pub. Corp., New York, pp. 75–88, 1976

Two independent methods for obtaining ultra-high resolution for biological specimens in the electron microscope are described. The first method accepts the physical limits of the electron objective lens and uses a series of dark field images of biological crystals to obtain direct information concerning the phases of the Fourier diffraction maxima. This information is then used in the computer to synthesize a large aperture lens to obtain 1-angstrom resolution. The second method assumes that there is sufficient amplitude scatter from images recorded in focus which can be used with a sensitive densitometer and computer contrast stretching to give rise to fine

structure image details which have been previously ignored.

NEAD, M. W.

N004 A Parameter Estimation Subroutine Package

G. J. Bierman and M. W. Nead

JPL Publication 77-26, July 1, 1977

For abstract, see Bierman, G. J.

NEILSON, R. A.

N005 Mission Design for SEASAT-A, An Oceanographic Satellite

E. Cutting, G. H. Born, J. C. Frautnick, W. I. McLaughlin, R. A. Neilson, and J. A. Thielen (Lockheed Missiles & Space Co.)

Preprint 77-31, AIAA Fifteenth Aerosp. Sci. Meet., Los Angeles, Calif., Jan. 24–26, 1977

For abstract, see Cutting, E.

NERHEIM, N. M.

N006 Addition of HCl to the Double-Pulse Copper Chloride Laser

A. A. Vetter and N. M. Nerheim

Appl. Phys. Lett., Vol. 30, No. 8, pp. 405–407, April 15, 1977

For abstract, see Vetter, A. A.

N007 A Parametric Study of the Copper Chloride Laser

N. M. Nerheim

J. Appl. Phys., Vol. 48, No. 3, pp. 1186–1190, March 1977

A parametric study of the double-pulsed copper chloride laser is reported. The effects of a wide range of variables on the laser energy density and on three characteristic time intervals (the minimum, maximum, and optimum delay time) between the two electrical discharge pulses were studied. The geometric variables investigated included the tube diameter from 2.3 to 40 mm and the tube length from 3 to 60 cm. Three buffer gases, helium, neon, and argon, were studied over the pressure range 0.5–50 torr and the tube temperature was varied from 270 to 500°C. The energy density and voltage of both the dissociation and pumping pulse were varied independently from less than 1 mJ/cm^3 at 8.5 kV to over 500 mJ/cm^3 at 20 kV. The optimum conditions for maximum laser energy density were found to be with 20 torr neon in a 10-mm by 30-cm tube at 400°C. The maximum energy density obtained was 22 μJ/cm^3.

N008 Measurements of Copper Ground-State and Metastable Level Population Densities in a Copper-Chloride Laser

N. M. Nerheim

J. Appl. Phys., Vol. 48, No. 8, pp. 3244–3250, August 1977

The population densities of both the ground and $^2D_{5/2}$ metastable states of copper atoms in a double-pulsed copper-chloride laser are correlated with the laser energy as a function of time after the dissociation current pulse. Time-resolved density variations of the ground and excited copper atoms were derived from measurements of the optical absorption at 324.7 and 510.6 nm, respectively, over a wide range of operating conditions in laser tubes with diameters from 4 to 40 mm. The minimum delay between the two current pulses at which lasing was observed is shown to be a function of the initial density and subsequent decay of the metastable state. Similarly, the maximum delay is shown to be a function of the initial density and decay of the ground state.

NEUGEBAUER, M.

N009 An Alternative Interpretation of Jupiter's "Plasmapause"

M. Neugebauer and A. Eviatar (University of California, Los Angeles)

Geophys. Res. Lett., Vol. 3, No. 12, pp. 708–710, December 1976

It has recently been suggested that Io is an important source of ions for the plasma detected by Pioneer 10 in the inner magnetosphere of Jupiter. Assuming this to be true, we show that near the orbit of Io the central collector of the Pioneer-10 plasma instrument could detect only inwardly diffusing ions created at a radial distance greater than that of the spacecraft. The rapid decrease in ion density observed beyond Io's orbit is attributed, at least partially, to this effect and thus may not represent a real plasma boundary such as a "plasmapause." Instead, the drop in observed ion density could correspond to a decrease in the density of Io-associated neutral particles orbiting Jupiter.

NG, E. W.

N010 Computations and Applications of Linear Hypergeometric Transformations

E. W. Ng

Comput. Math. Appl., Vol. 3, No. 1, pp. 65–70, 1977

Linear transformations are well-known in the theory of hypergeometric functions. In this note, it is indicated, both by analyses and by supporting numerical experiments, how these transformations can be applied to the computation of Legendre's functions, the incomplete Beta function, and the variance-ratio probability distribution function. It is shown that a simple transformation can in many cases cause dramatic improvement in computation.

NISHIMURA, H.

N011 Pioneer Venus Wind Experiment Receiver

H. Nishimura

The Deep Space Network Progress Report 42-38: January and February 1977, pp. 141–147, April 15, 1977

The final design of the Pioneer Venus Wind Experiment Receiver and Phase Calibrator is discussed from the block diagram viewpoint. Measured phase data are shown to derive the predicted performance. The STDN receiver implementation is also discussed.

NIXON, D. L.

N012 S-/X-Band Microwave Optics Design and Analysis for DSN 34-Meter-Diameter Antenna

D. L. Nixon and D. A. Bathker

The Deep Space Network Progress Report 42-41: July and August 1977, pp. 146–165, October 15, 1977

This article discusses the feed system configuration, RF optics design and predicted gain and noise temperature performance of the DSN 26-meter antenna S-/X-Band upgrade project. A previously developed and demonstrated dual band feed system employing separately located feeds, combined in a reflex-dichroic reflector arrangement, has been adapted to a particularly compact overall design. Special design techniques to minimize aperture blockage and then evaluate resultant performance are discussed in detail. Final predicted antenna gain and noise temperature performance values are given.

NJOKU, E. G.

N013 JPL Field Measurements at the Finney County, Kansas, Test Site, October 1976: Ground-Based Microwave Radiometric Measurements

E. G. Njoku and N. I. Yamane

JPL Publication 77-13, April 1, 1977

Microwave brightness temperature measurements were made at the Finney County, Kansas, test site as part of the Joint Soil Moisture Experiment (JSME) during October 9–14, 1976. These measurements are reported, with a description of the JPL microwave radiometry van facility. The data will be used with ground truth data from the test site and microwave data from aircraft overflights to investigate the potential of microwave radiometry for soil moisture remote sensing under field conditions.

N014 Theory for Passive Microwave Remote Sensing of Near-Surface Soil Moisture

E. G. Njoku and J. A. Kong (Massachusetts Institute of Technology)

J. Geophys. Res., Vol. 82, No. 20, pp. 3108–3118, July 10, 1977

The theory of microwave thermal emission from a nonscattering half-space medium is developed for application to regions with nonuniform subsurface soil moisture and temperature variations. A coherent stratified model is presented which is valid for nonuniform temperature profiles and rapidly varying moisture profiles, under which conditions the commonly used emissivity and radiative transfer approaches become inaccurate. For naturally occurring profiles the stratified model gives more accurate results than the other approaches at frequencies below about 4 GHz. Experimental results from ground-based radiometric observations of a controlled target area compare systematically with brightness temperatures predicted from the theoretical model to within approximately 10°K. Results of dielectric constant measurements of the sand are given at seven frequencies in the microwave range and for moisture contents in the range 0–30% by volume. By using this model the thermal microwave emission spectrum is computed for a number of representative moisture and temperature profiles in the frequency range 0.25–25 GHz. A regression technique is used to show that multifrequency data can be used to obtain moisture and temperature gradients in the soil when an estimate of the surface temperature is available.

NORMARK, W. R.

N015 Computer Image Processing in Marine Resource Exploration

P. R. Paluzzi, W. R. Normark (U. S. Geological Survey), G. R. Hess (U. S. Geological Survey), H. D. Hess (U. S. Geological Survey), and M. J. Cruickshank (U. S. Geological Survey)

Proc. MTS-IEEE Oceans '76 Conf., Washington, D. C., Sept. 13–15, 1976, pp. 4D-1–4D-10

For abstract, see Paluzzi, P. R.

NORRIS, D.

N016 **Imaging Air Pollutants in the Near Ultraviolet**

D. Norris, J. Conley, and S. Seng

Proc. SPIE, Vol. 91, pp. 116–122, 1976

This paper discusses a program for remote sensing of air pollutants called "Multispectral Observation of Pollutants System (MOPS)." The broad objective of the program is to photograph "invisible" gaseous pollutants by combining ultraviolet imaging in several spectral bands with portable data processing equipment. Electronic cameras using solid state imaging arrays of large dynamic range will permit very low contrast images to be electronically ratioed and contrast enhanced, thus bringing out pollutant images which are below the contrast threshold of film. Such photographs will allow synoptic coverage of geographic areas providing source, sink, and flow data on pollutants, and will provide reconnaissance and pointing information for other remote sensors. The principal gases to be mapped by MOPS will be ozone, sulfur dioxide, and nitrogen dioxide.

NORRIS, D. D.

N017 **The Viking Orbiter Visual Imaging Subsystem**

J. B. Wellman, F. P. Landauer, D. D. Norris, and T. E. Thorpe

J. Spacecraft Rockets, Vol. 13, No. 11, pp. 660–666, November 1976

For abstract, see Wellman, J. B.

NORTON, H. N.

N018 **An Interstellar Precursor Mission**

L. D. Jaffe, C. Ivie, J. C. Lewis, R. Lipes, H. N. Norton, J. W. Stearns, L. D. Stimpson, and P. Weissman

JPL Publication 77-70, October 30, 1977

For abstract, see Jaffe, L. D.

NOTARYS, H. A.

N019 **Comparative Studies of Ion-Implant Josephson-Effect Structures**

R. K. Kirschman, J. A. Hutchby (Langley Research Center), J. W. Burgess (Langley Research Center), R. P. McNamara (California Institute of Technology), and H. A. Notarys (California Institute of Technology)

IEEE Trans. Magnet., Vol. MAG-13, No. 1, pp. 731–734, January 1977

For abstract, see Kirschman, R. K.

NOVOTNY, M.

N020 **Electrical, Magnetic, and Optical Properties of the Tetrathiafulvalene (TTF) Pseudohalides, $(TTF)_{12}(SCN)_7$ and $(TTF)_{12}(SeCN)_7$**

R. B. Somoano, A. Gupta, V. Hadek, M. Novotny (Stanford University), M. Jones (Tulane University), T. Datta (Tulane University), R. Deck (Tulane University), and A. M. Hermann (Tulane University)

Phys. Rev., Pt. B: Solid State, Vol. 15, No. 2, pp. 595–601, January 15, 1977

For abstract, see Somoano, R. B.

NULL, G. W.

N021 **Gravity Field of Jupiter and Its Satellites From Pioneer 10 and Pioneer 11 Tracking Data**

G. W. Null

Astron. J., Vol. 81, No. 12, pp. 1153–1161, December 1976

Accurate two-way Doppler tracking data were obtained from the Pioneer 10 and Pioneer 11 spacecraft during their Jupiter encounters. A comprehensive combined analysis of these data has yielded significantly improved values of the masses of the Galilean satellites and the harmonic coefficients of Jupiter, and a mass of Jupiter of comparable accuracy to the best previous determinations using asteroid motions. The ratios of the masses of the four Galilean satellites to the mass of Jupiter are $(4.684 \pm 0.022) \times 10^{-5}$ for Io, $(2.523 \pm 0.025) \times 10^{-5}$ for Europa, $(7.803 \pm 0.030) \times 10^{-5}$ for Ganymede, and $(5.661 \pm 0.19) \times 10^{-5}$ for Callisto. (All error estimates presented in this paper are standard errors, those for Pioneer 10 and Pioneer 11 are an evaluation of real errors as distinguished from formal errors.) The ratio of the mass of the Sun to the mass of the Jupiter system is 1047.346 ± 0.004. The second, third, fourth, and sixth zonal harmonic coefficients of Jupiter are $J_2 = (14733 \pm 4) \times 10^{-6}$, $J_3 = (0.4 \pm 9) \times 10^{-6}$, $J_4 = (-587 \pm 7) \times 10^{-6}$, and $J_6 = (34 \pm 50) \times 10^{-6}$ at an equatorial radius of 71,398 km. The sectorial harmonics C_{22} and S_{22} and the ratio of a hypothetical mass concentration

at the Red Spot to the mass of Jupiter are approximately (0 ± 0.5) × 10^{-6}. The instantaneous 3 December 1974 right ascension and declination of the pole of Jupiter relative to the mean Earth equator and equinox of 1950.0 are 267°.998 ± 0.016 and 64°.504 ± 0.004, respectively. The harmonic results, which will have an important application as boundary conditions for theoretical models of Jupiter's interior, are consistent with a planet in hydrostatic equilibrium at all levels.

OMURA, J. K.

0001 An Improved Upper Bound on the Block Coding Error Exponent for Binary-Input Discrete Memoryless Channels

R. J. McEliece and J. K. Omura (University of California, Los Angeles)

IEEE Trans. Inform. Theor., Vol. IT-23, No. 5, pp. 611–613, September 1977

For abstract, see McEliece, R. J.

ONDRASIK, V. J.

0002 Improvements in Navigation Resulting from the Use of Dual Spacecraft Radiometric Data

C. C. Chao, H. L. Siegel, and V. J. Ondrasik

The Deep Space Network Progress Report 42-38: January and February 1977, pp. 55–65, April 15, 1977

For abstract, see Chao, C. C.

ORTON, G. S.

0003 The Abundance of Acetylene in the Atmosphere of Jupiter

G. S. Orton and H. H. Aumann

Icarus, Vol. 32, pp. 431–436, 1977

The Q and R branches of the C_2H_2 ν_5 fundamental, observed in emission in an aircraft spectrum of Jupiter near 750 cm^{-1}, have been analyzed with the help of an improved line listing for this band. The line parameters have been certified in the laboratory with the same interferometer used in the Jovian observations. The maximum mixing ratio of C_2H_2 is found to be between 5×10^{-8} and 6×10^{-9}, depending on the form of its vertical distribution and the temperature structure assumed for the lower stratosphere. Most consistent with observations of both Q and R branches are: (1) distributions of C_2H_2 with a constant mixing ratio in the stratosphere and a cutoff at a total pressure of 100 mbar or less, and (2) the assumption of a temperature at 10^{-2} bar which is near 155 K.

OSHIRO, R.

0004 Effects of Aniline Impurities on Monopropellant Hydrazine Thruster Performance

L. Holcomb, L. Mattson, and R. Oshiro

J. Spacecraft Rockets, Vol. 14, No. 3, pp. 141–148, March 1977

For abstract, see Holcomb, L.

OTOSHI, T. Y.

0005 Calibration of Block 4 Translator Path Delays at DSS 14 and CTA 21

T. Y. Otoshi, P. D. Batelaan, K. B. Wallace, and F. Ibanez

The Deep Space Network Progress Report 42-37: November and December 1976, pp. 188–197, February 15, 1977

Ground station range delays are currently being performed at 64-m stations in the DSN by use of the "Translator Method." This method requires the absolute calibrations of the delays of the Block 4 Doppler Translator Assembly as well as the cables connecting it to the high-power coupler uplink sampling point and the downlink injection points into S- and X-band masers. In this article the techniques for calibrating the translator path by means of a portable zero delay device are described. In addition, some translator path data taken at DSS 14, Goldstone, over a period of about one year is presented.

0006 Dual Coupler Configuration at DSS 14 for the Voyager Era

T. Y. Otoshi, K. B. Wallace, and R. B. Lyon

The Deep Space Network Progress Report 42-42: September and October 1977, pp. 184–192, December 15, 1977

This article describes the dual coupler configuration which was recently installed at DSS 14 for station delay calibrations during the Voyager era. The Z-correction values determined for this new and previous configurations are presented.

0007 A High-Power Dual-Directional Coupler

K. B. Wallace and T. Y. Otoshi

The Deep Space Network Progress Report 42-42: September and October 1977, pp. 193–206, December 15, 1977

For abstract, see Wallace, K. B.

0008 Development and Evaluation of a Set of Group Delay Standards

T. Y. Otoshi and R. W. Beatty (National Bureau of Standards)

IEEE Trans. Instrum. Meas., Vol. IM-25, No. 4, pp. 335–342, December 1976

Group delay standards of 15, 30 and 60 ns have been developed at JPL. Calibration data provided by NBS and others are presented and compared. Calibrations were performed at microwave frequencies of 2113, 2295, and 8415 MHz as well as at a baseband modulation frequency of 500 kHz. The uncertainties of the measurement and effects of dispersion and cable reflections are discussed.

OTTH, D.

0009 Evaluation of Coal Feed Systems Being Developed by the Energy Research and Development Administration

R. Phen, C. Jennings, W. Luckow, L. Mattson, D. Otth, and P. Tsou

JPL Publication 77-54, September 1977

For abstract, see Phen, R.

OXBORROW, G. S.

0010 Pyrolysis Gas-Liquid Chromatography Studies of the Genus *Bacillus*: Effect of Growth Time on Pyrochromatogram Reproducibility

G. S. Oxborrow, N. D. Fields, and J. R. Puleo

Anal. Pyrolysis, pp. 69–76, 1977

Pyrolysis gas-liquid chromatography was performed on six species of the genus *Bacillus*, which are deemed to be important in space research. The purpose was to evaluate the effects of culture age. Cultures grown on membrane filters were harvested and samples of approximately 150 μg were pyrolyzed at 800°C for 10 s. Resultant products were separated on a 10% Carbowax-packed column. For each of the *Bacillus spp.* studied the more pronounced changes occurred at the high boiling end of the chromatogram (retention time 26–45 min). When samples of *Bacillus subtilis* var. *niger*(*B. globigii*), *B. coagulans*, and *B. firmus* were pyrolyzed, a marked peak for the physiological process of sporulation consistently appeared on the chromatogram at a retention time of 12 min. Initially, this peak was small, but with the approach of sporulation, the peak emerged as the largest of the profile. Chromatographic criteria for identification proved to be constant when cultures were incubated for a specific time span. On the other hand, cultures sampled at different incubation times had different chromatograms and could be compared only to chromatograms of cultures of equal age. Pyrolysis gas-liquid chromatography has been demonstrated to be a useful tool for physiological studies and identification or characterization of the genus *Bacillus*.

0011 Microbiological Profiles of the Viking Spacecraft

J. R. Puleo, N. D. Fields, S. L. Bergstrom, G. S. Oxborrow, P. D. Stabekis, and R. C. Koukol

Appl. Environ. Microbiol., Vol. 33, No. 2, pp. 379–384, February 1977

For abstract, see Puleo, J. R.

0012 Pyrolysis Gas-Liquid Chromatography of the Genus *Bacillus*: Effect of Growth Media on Pyrochromatogram Reproducibility

G. S. Oxborrow, N. D. Fields, and J. R. Puleo

Appl. Environ. Microbiol., Vol. 33, No. 4, pp. 865–870, April 1977

Pyrolysis gas-liquid chromatography was performed on dried *Bacillus* microorganisms to evaluate the effects of growth media. Six cultures of *Bacillus* and six lot numbers of Trypticase soy agar (BBL) were used to test the hypothesis that a microorganism grown on various lot numbers of the same media would have the same chromatogram. Also tested was the effect of three different media on chromatogram reproduction using the same six cultures. Results show little or no differences observed between the chromatograms of the individual *Bacillus* spp. grown on the six lot numbers of Trypticase soy agar. When chromatograms of the three different media were compared, several differences were observed, particularly in the areas most characteristic of individual species.

PAINE, G.

P001 The Automation of Remote Vehicle Control

G. Paine

Proc. 1977 Joint Automat. Contr. Conf., San Francisco, Calif., June 22–24, 1977, pp. 216–224

The automation of remote vehicles is becoming necessary to overcome the requirement of having man present as a controller. By removing man, remote vehicles can be operated in areas where the environment is too hostile for man, his reaction times are too slow, time delays are too long, and where his presence is too costly, or where

system performance can be improved. This paper addresses the development of automated remote vehicle control for non-space and space tasks from warehouse vehicles to proposed Mars rovers. The state-of-the-art and the availability of new technology for implementing automated control are reviewed and the major problem areas are outlined. The control strategies are divided into those where the path is planned in advance or constrained, or where the system is a teleoperator, or where automation or robotics have been introduced.

PAINE, W. O.

P002 A Method for Reducing Software Life Cycle Costs

W. O. Paine and J. C. Holland

The Deep Space Network Progress Report 42-39: March and April 1977, pp. 186–191, June 15, 1977

The advent of new hardware and software tools permits a new approach to preparing, presenting, and maintaining software specifications and corresponding source programs. The method described could significantly reduce many of the associated costs compared with techniques now in general use in industry.

PALEY, H. N.

P003 JPL Field Measurements at the Finney County, Kansas, Test Site, October 1976: Meteorological Variables, Surface Reflectivity, Surface and Subsurface Temperatures

A. B. Kahle, J. Schieldge, and H. N. Paley

JPL Publication 77-1, February 1, 1977

For abstract, see Kahle, A. B.

PALLUCONI, F. D.

P004 Martian North Pole Summer Temperatures: Dirty Water Ice

H. H. Kieffer (University of California, Los Angeles), S. C. Chase, Jr. (Santa Barbara Research Center), T. Z. Martin (University of California, Los Angeles), E. D. Miner, and F. D. Palluconi

Science, Vol. 194, pp. 1341–1344, December 17, 1976

For abstract, see Kieffer, H. H.

P005 Temperatures of the Martian Surface and Atmosphere: Viking Observation of Diurnal and Geometric Variations

H. H. Kieffer (University of California, Los Angeles), P. R. Christensen (University of California, Los Angeles), T. Z. Martin (University of California, Los Angeles), E. D. Miner, and F. D. Palluconi

Science, Vol. 194, pp. 1346–1351, December 17, 1976

For abstract, see Kieffer, H. H.

PALUZZI, P. R.

P006 Computer Image Processing in Marine Resource Exploration

P. R. Paluzzi, W. R. Normark (U. S. Geological Survey), G. R. Hess (U. S. Geological Survey), H. D. Hess (U. S. Geological Survey), and M. J. Cruickshank (U. S. Geological Survey)

Proc. MTS-IEEE Oceans '76 Conf., Washington, D. C., Sept. 13–15, 1976, pp. 4D-1–4D-10

Pictographic data or imagery is commonly used in marine exploration. Preexisting image processing techniques (software) similar to those used on imagery obtained from unmanned planetary exploration were used to improve marine photography and side-scan sonar imagery. Features and details not visible by conventional photo processing methods were enhanced by filtering and noise removal on selected deep-sea photographs. Information gained near the periphery of photographs allows improved interpretation and facilitates construction of bottom mosaics where overlapping frames are available. Similar processing techniques were applied to side-scan sonar imagery, including corrections for slant range distortion, and along-track scale changes. The use of digital data processing and storage techniques greatly extends the quantity of information that can be handled, stored, and processed.

PANG, K.

P007 Complex Refractive Index of Martian Dust: Wavelength Dependence and Composition

K. Pang and J. M. Ajello

Icarus, Vol. 30, pp. 63–74, 1977

Mariner 9 ultraviolet spectra of the 1971 dust clouds were analyzed to obtain the phase function times single scattering albedo of the dust particles. The phase functions were matched with Mie scattering calculations for size distributions of spheres of homogeneous and isotropic material. The absorption index of the dust particles was found to increase with decreasing wavelength from 350 nm down to about 210 nm, and drop off shortward of this wavelength. A structural shoulder oc-

C-2

curs in the absorption spectrum between 240 and 250 nm. Titanium dioxide (anatase) has the correct transitions at 210 and 250 nm to match the absorption curve of Martian dust, and is proposed as a candidate constituent in Martian surface material. The spectral neutrality of TiO_2 between 0.5 and 4 μm is consistent with visible and infrared observations of Mars. The high refractive index of TiO_2 can explain the large refringence of Martian dust. The titanium dioxide content of the dust particles is estimated to be a few percent or less. Uncertainties in the results due to limitations in the model and data are discussed.

PARHAM, O. B.

P008 Microcomputer Central Processing Unit Module

O. B. Parham

The Deep Space Network Progress Report 42-41: July and August 1977, pp. 172–175, October 15, 1977

A new multipurpose microcomputer central processing unit (CPU) module is described and illustrated in this article. The module is designed to stand alone and also be upward expandable.

PARTHASARATHY, S. P.

P009 Mach Wave Emission from Supersonic Jets

S. P. Parthasarathy and P. F. Massier

AIAA J., Vol. 15, No. 10, pp. 1462–1468, October 1977

An experimental investigation has been conducted on supersonic jets at a Mach number of 1.43 over a temperature range from about 420 K to 1370 K (300°F to 2000°F) in which it was found that the noise in the far field was dominated by eddy Mach waves. It is shown both from experimental and theoretical considerations that the strength of the Mach waves is determined by the product of the mean shear and the density fluctuations of the jet. Thus, the source of sound arises from the mixing of hot and cold streams as well as from those compressions and expansions that are intuitively associated with sound generation. For the temperature range investigated, the Mach waves were emitted at angles between 37 and 59 deg with respect to the jet axis with the smaller angle occurring at the lower temperature, which is also at the lower jet velocity. These values represent those in the region of the jet where the Mach angle was constant, that is, beginning at the nozzle exit and extending downstream to a distance ranging from 5 to 12 jet diameters, depending on temperature.

PASSAMANECK, R. S.

P010 Monopropellant Thruster Exhaust Plume Contamination Measurements

R. K. Baerwald and R. S. Passamaneck

JPL Publication 77-61, September 15, 1977

For abstract, see Baerwald, R. K.

P011 Small Monopropellant Thruster Contamination Measurement in a High-Vacuum Low-Temperature Facility

R. S. Passamaneck and J. E. Chirivella

J. Spacecraft Rockets, Vol. 14, No. 7, pp. 419–426, July 1977

The contamination that results from the exhaust plume of small thrusters used for attitude control maneuvers can pose severe problems for long-lift satellite systems. In order to assess this type of contamination problem, analytical and experimental techniques must be developed. Mass deposition rate measurements of a representative 0.44-N thrust hydrazine thruster were made in the Jet Propulsion Laboratory (JPL) Molsink space simulation chamber using five appropriately placed variable-temperature quartz crystal microbalances. The mass deposition rates within the thruster plume were measured while operating the thruster over a wide range of operating parameters, including duty cycles, catalyst bed start temperatures, propellant water variation, as well as thruster aging effects. The contamination measurements were made over a temperature range of 144 to 256 K for all duty cycles. In addition, the nominal duty cycle of 100 msec on and 10 sec off was run at a temperature of 106 K. These data will make possible better prediction of deposition rates of contaminants from thrusters used in satellite systems.

PAWLIK, E. V.

P012 A Nuclear Electric Propulsion Vehicle for Planetary Exploration

E. V. Pawlik and W. M. Phillips

J. Spacecraft Rockets, Vol. 14, No. 9, pp. 518–525, September 1977

A design study currently is underway for a nuclear electric propulsion vehicle capable of performing detailed exploration of the outer planets. Evaluation of the design indicates that it also is applicable to orbit raising. Primary emphasis is on the power subsystem. Work on the design of the power system, along with both the mission rationale and preliminary spacecraft design, is summarized. A propulsion system at a 400-kWe power level with a specific weight goal of $\leq$25 kg/kW was selected

for this study. Study results indicate that this goal can be realized, together with compatibility with the shuttle launch vehicle constraints.

PENG, S. T. J.

P013 Nonlinear Viscoelasticity and Relaxation Phenomena of Polymer Solids

S. T. J. Peng, K. C. Valanis (University of Iowa), and R. F. Landel

Acta Mech., Vol. 25, Nos. 3–4, pp. 229–240, 1977

The specific Helmholtz free energy of nonlinear viscoelastic isotropic polymer solids is assumed to be a separable, symmetric function along three orthogonal principal strain directions, i.e. $\Psi = \psi(\lambda_1, q_n^{(1)}) + \psi(\lambda_2, q_n^{(2)}) + \psi(\lambda_3, q_n^{(3)})$, where the λ_r $(r = 1, 2, 3)$ are three principal stretch ratios and the $q_n^{(r)}$ are a set of internal state variables. It is shown that, by using this postulated form of the free energy function, one can readily characterize the mechanical response of viscoelastic polymer solids.

PETERSON, R. G.

P014 Development and Qualification of the Propellant Management System for Viking 75 Orbiter

M. W. Dowdy, R. E. Hise (Martin Marietta Corporation), and R. G. Peterson (Martin Marietta Corporation)

J. Spacecraft Rockets, Vol. 14, No. 3, pp. 133–140, March 1977

For abstract, see Dowdy, M. W.

PETRAC, D.

P015 Surface Crystalline Carbon Temperature Sensor

D. Petrac, J. Gatewood, and P. Mason

Advan. Cryog. Eng., Vol. 21, pp. 242–243, 1976

A surface sensor for measuring small temperature changes is described. As a static sensor it exhibits an accuracy and reproducibility better than 10 mK; as a transient detector, it detects changes of 1 mK with a rise time of 10 ms.

P016 Sensor for Distinguishing Liquid–Vapor Phases of Superfluid Helium

D. Petrac, J. Gatewood, and P. Mason

Advan. Cryog. Eng., Vol. 21, pp. 244–246, 1976

A new sensor, based on the resistance change of the normal-superconductive transition, has been developed. The sensor can be adapted for use in either normal or superfluid helium by proper choice of material for the superconductive coating.

P017 Experiments on the Properties of Superfluid Helium in Zero Gravity

P. Mason, D. Collins, D. Petrac, L. Yang, F. Edeskuty, and K. Williamson

Proc. Sixth Int. Cryog. Eng. Conf., Grenoble, France, May 11–14,1976, pp. 272–277

For abstract, see Mason, P.

PETTY, S. M.

P018 Hydrogen Maser Frequency Standards for the Deep Space Network

P. R. Dachel, S. M. Petty, R. F. Meyer, and R. L. Sydnor

The Deep Space Network Progress Report 42-40: May and June 1977, pp. 76–83, August 15, 1977

For abstract, see Dachel, P. R.

PHEN, R.

P019 Evaluation of Coal Feed Systems Being Developed by the Energy Research and Development Administration

R. Phen, C. Jennings, W. Luckow, L. Mattson, D. Otth, and P. Tsou

JPL Publication 77-54, September 1977

This report documents an evaluation by the Jet Propulsion Laboratory of the ERDA-sponsored coal feed systems development program. The evaluation includes development and performance criteria and recommendations for selections with supporting data.

PHILLIPS, A. M.

P020 Evaluation of Battery Models for Prediction of Electric Vehicle Range

H. A. Frank and A. M. Phillips

JPL Publication 77-29, August 1, 1977

For abstract, see Frank, H. A.

PHILLIPS, R. J.

P021 Electrical Structure in a Region of the Transverse Ranges, Southern California

I. K. Reddy, R. J. Phillips, J. H. Whitcomb (California Institute of Technology), and D. Rankin (University of Alberta)

Earth Planet. Sci. Lett., Vol. 34, pp. 313–320, 1977

For abstract, see Reddy, I. K.

P022 **Three-Dimensional Modelling in Magnetotelluric and Magnetic Variational Sounding**

I. K. Reddy, D. Rankin (University of Alberta), and R. J. Phillips

Geophys. J. Roy. Astron. Soc., Vol. 51, pp. 313–326, 1977

For abstract, see Reddy, I. K.

P023 **The Nature of the Gravity Anomalies Associated With Large Young Lunar Craters**

J. Dvorak (California Institute of Technology) and R. J. Phillips

Geophys. Res. Lett., Vol. 4, No. 9, pp. 380–382, September 1977

For abstract, see Dvorak, J.

P024 **Magnetic Evidence Concerning a Lunar Core**

B. E. Goldstein, R. J. Phillips, and C. T. Russell (University of California, Los Angeles)

Proc. Seventh Lunar Conf., pp. 3321–3341, 1976

For abstract, see Goldstein, B. E.

PHILLIPS, W. M.

P025 **A Nuclear Electric Propulsion Vehicle for Planetary Exploration**

E. V. Pawlik and W. M. Phillips

J. Spacecraft Rockets, Vol. 14, No. 9, pp. 518–525, September 1977

For abstract, see Pawlik, E. V.

POON, P. T. Y.

P026 **Curvature Effects on Stagnation Radiative Transfer for Shocks Around Blunt Axisymmetric Bodies**

P. T. Y. Poon

Progr. Astronaut. Aeronaut., Vol. 56, pp. 423–431, 1977

During hypersonic entry of a probe into the atmospheres of outer planets, the radiative energy transport in the shock-heated layer is of great significance in computing the heating to the heat shield. The so-called tangential slab approximation is employed frequently to evaluate the radiative flux to the surface of entry probes. A simple assessment of the accuracy of the tengential slab approximation at the stagnation point is given here for blunt axisymmetric bodies of various shock shapes, which include spheres, paraboloids, hyperboloids, and ellipsoids of different shock parameters.

PORTER, J. D.

P027 **Design and Implementation of Viking Mission**

B. G. Lee and J. D. Porter (Martin Marietta Aerospace)

Preprint 77-270, AIAA Thirteenth Annu. Meet. Tech. Display Incorporating Forum on Future of Air Transp., Wash., D.C., Jan. 10–13, 1977

For abstract, see Lee, B. G.

POSNER, E. C.

P028 **Behaviour of Queues at Signalized Intersections in Heavy traffic**

E. C. Posner and E. R. Rodemich

Utilitas Math., Vol. 10, pp. 3–50, November 1976

This paper derives the asymptotic behaviour of traffic queues at signalized intersections when the excess of departure capacity over arrivals approaches zero from above. The most interesting result is that the distribution of queue length approaches a negative exponential, with fewer restrictive assumptions than hitherto known. The main improvement results from more precise use of a combinatorial lemma of Spitzer, giving the maximum of the partial sums of a sequence of independent identically distributed random variables, plus some specific constructive probability calculations, many of them involving the Fourier transform. New results are presented on the probability that the queue be below a fixed bound and/or on the probability that the queue be empty. Applications to on-line estimators for real-time traffic control are suggested.

PRASAD, S. S.

P029 **The Photochemistry of Ammonia in the Jovian Atmosphere**

S. S. Prasad and L. A. Capone (Ames Research Center)

J. Geophys. Res., Space Phys., Vol. 81, No. 31, pp. 5596–5600, November 1, 1976

To resolve the discrepancy between the Jovian albedo in the IR and UV, a model of ammonia photochemistry was recently proposed by Strobel (1973) which led to a severe depletion of the ammonia concentration with altitude. Some features of this photochemistry, for example, the use of a pressure-independent rate coefficient NH_2 recombination and the formation of hydrogen and nitrogen molecules in photodissociation of N_2H_4, were inconsistent with several laboratory and theoretical results. The treatment of the reaction between H and N_2H_3 was also controversial. When these shortcomings are removed and the basic photochemistry proposed by Strobel is made relatively more consistent with the available theoretical and laboratory data, as far as possible within the limits set by the present paucity of data, then only a moderate ammonia depletion is obtained. The discrepancy between the Jovian albedo in the IR and UV therefore may still be an open question. However, if condensation nuclei were present to such an extent that N_2H_4 condensed before it reacted or photodissociated, then a new solution of the discrepancy could be possible. Alternatively, existence of a stratospheric "cold trap" may also explain the decreased ammonia abundance. We have also identified and stressed the specific needs for laboratory measurement.

P030 **Some Aspects of the Stratospheric Cl–ClO–Cl Cycle: Possible Roles of ClO*, $ClNO_3$ and HOCl**

S. S. Prasad

Planet. Space Sci., Vol. 24, pp. 1187–1193, 1976

Depending on such factors as (a) the probabilities of exciting the various vibrational states in ClO formed in the reaction of Cl with O_3, (b) the radiative lifetime of ClO*, (c) $\Delta H_f(ClO_3)$, and (d) the rate coefficient of the relevant three-body reaction, the production of ClO_3 via the reaction $ClO^* + O_2 + M \rightarrow ClO_3 + M$ may be quite substantial in the stratosphere. The significance of this result lies in the subsequent elimination (from the stratosphere) of ClO_3 and its associated chlorine atom as $HClO_4$, in the manner recently suggested by Samonaitis and Heicklen. In the stratosphere, ClO_3 most probably photodissociates primarily into OClO and O. Upon photodissociation, OClO may also yield atomic oxygen. Thus the formation of ClO_3 from ClO* and O_2, and the above-mentioned photodissociation steps constitute an interesting, indirect mechanism of O_2 dissociation into two odd oxygen species. Other aspects of ClO* chemistry, applicable in stratospheric conditions, also deserve attention in view of Nicholl's recent interpretation of the Umkehr measurements by Brewer *et al.* The reactions of ClO with HO_2, and NO_2, possess the potential of significantly obstructing the completion of the Cl–ClO–Cl cycle, at least in the region below 35 km.

PRATURI, A.

P031 **Modeling of Fluidized Bed Silicon Deposition Process**

K. Kim, G. Hsu, R. Lutwack, and A. Praturi

JPL Publication 77-25, June 15, 1977

For abstract, see Kim, K.

PRATURI, A. K.

P032 **Chemical Vapor Deposition of Silicon from Silane Pyrolysis**

A. K. Praturi, R. Lutwack, and G. Hsu

JPL Publication 77-38, July 15, 1977

The four basic elements in the chemical vapor deposition (CVD) of silicon from silane are mass transport of silane, pyrolysis of silane, nucleation of silicon and silicon crystal growth. These four elements are analytically treated from a kinetic standpoint. Rate expressions that describe the various conceivable steps involved in the chemical vapor deposition of silicon are derived from elementary principles. Applications of the rate expressions for (1) modeling and the simulation of the silicon CVD process and (2) the analysis of experimental data on silicon CVD are discussed. The lack of an experimentally established mechanism of the silicon CVD process and established values for various constants involved in the rate expressions is the major impediment to the modeling of the CVD process. Experimental data are needed to determine the equilibrium absorption coefficients for silane, hydrogen and silicon vapor and the activation energies and frequency factors for the various rate processes involved in the silicon CVD.

PRICE, W. E.

P033 **Voyager Electronic Parts Radiation Program: Final Report**

A. G. Stanley, K. E. Martin, and W. E. Price

JPL Publication 77-41, Vol. I, September 15, 1977

For abstract, see Stanley, A. G.

PRUSSIN, S.

P034 **The Effect of Oxidation-Expanded Defects Upon MOS Parameters**

S. Prussin, S. P. Li, and R. H. Cockrum

J. Appl. Phys., Vol. 48, No. 11, pp. 4613–4617, November 1977

Implantation of Ne ions was chosen as a means of introducing a uniformly distributed quantitatively controllable and reproducible amount of microdefects at the silicon surface. Each wafer was ion implanted on one-half of its surface, the other half remaining as a control. Seven implant fluences from 1×10^{12} to 5×10^{14} Ne cm^{-2} were used. The fluences, as well as the concentrations of defects expanded by the subsequent gate oxidation, were correlated with seven different MOS parameters. For implant fluences of 1×10^{14} cm^{-2} and above, increasing stacking-fault densities were found. The oxide defect density associated with time-dependent breakdown increased significantly with Ne dose. The presence of oxidation-expanded defects drastically increases the surface-generation velocity and decreases the bulk lifetime. Slight increases in flatband voltage and surface-state density occurred only for the wafers having the greatest defect concentrations. Oxidation of a P-containing damaged silicon surface results in a greater pileup of P at the surface than occurs for the oxidation of a similar but undamaged surface. It appears that the expanding defects restrain the diffusion of P inward from the surface.

PULEO, J. R.

P035 Pyrolysis Gas-Liquid Chromatography Studies of the Genus *Bacillus*: Effect of Growth Time on Pyrochromatogram Reproducibility

G. S. Oxborrow, N. D. Fields, and J. R. Puleo

Anal. Pyrolysis, pp. 69–76, 1977

For abstract, see Oxborrow, G. S.

P036 Microbiological Profiles of the Viking Spacecraft

J. R. Puleo, N. D. Fields, S. L. Bergstrom, G. S. Oxborrow, P. D. Stabekis, and R. C. Koukol

Appl. Environ. Microbiol., Vol. 33, No. 2, pp. 379–384, February 1977

Planetary quarantine requirements associated with the launch of two Viking spacecraft necessitated microbiological assessment during assembly and testing at Cape Canaveral and the Kennedy Space Center. Samples were collected from selected surfaces of the Viking Lander Capsules (VLC), Orbiters (VO), and Shrouds at predetermined intervals during assembly and testing. Approximately 7,000 samples were assayed. Levels of bacterial spores per square meter on the VLC-1 and VLC-2 were 1.6×10^2 and 9.7×10^1, respectively, prior to dry-heat sterilization. The ranges of aerobic mesophilic microorganisms detected on the VO-1 and VO-2 at various sampling events were 4.2×10^2 to 4.3×10^3 and 2.3×10^2 to $8.9 \times 10^3/m^2$, respectively. Approximately 1,300 colonies were picked from culture plates, identified, lyophilized, and stored for future reference. About 75% of all isolates were microorganisms considered indigenous to humans; the remaining isolates were associated with soil and dust in the environment. The percentage of microorganisms of human origin was consistent with results obtained with previous automated spacecraft but slightly lower than those observed for manned (Apollo) spacecraft.

P037 Pyrolysis Gas-Liquid Chromatography of the Genus *Bacillus*: Effect of Growth Media on Pyrochromatogram Reproducibility

G. S. Oxborrow, N. D. Fields, and J. R. Puleo

Appl. Environ. Microbiol., Vol. 33, No. 4, pp. 865–870, April 1977

For abstract, see Oxborrow, G. S.

QUINN, R.

Q001 Low-Noise Receivers: Microwave Maser Development

R. Quinn and E. Wiebe

The Deep Space Network Progress Report 42-37: November and December 1976, pp. 78–82, February 15, 1977

An S-Band traveling-wave maser with a 2260- to 2400-MHz tuning capability has been built and installed on the 26-m antenna at the Venus Station of the Goldstone Deep Space Communications Complex. The Traveling-Wave Maser/Closed Cycle Refrigerator package was assembled within a limited time schedule and at low cost to meet the requirements of the Very Long Baseline Interferometry Validation Task. The maser uses a superconducting magnet with a field staggering coil for gain/bandwidth adjustment. The maser pump source is a Gunn effect oscillator with the capability of continuous tuning throughout the entire maser tuning range. The package was assembled from surplus components that have been used previously in the Deep Space Network in a variety of applications since 1967.

RADBILL, J. R.

R001 Analysis of Pulsatile, Viscous Blood Flow Through Diseased Coronary Arteries of Man

L. D. Back, J. R. Radbill, and D. W. Crawford (University of Southern California)

J. Biomech., Vol. 10, pp. 339–353, 1977

For abstract, see Back, L. D.

RAJARAMAN, R.

R002 **Interaction of Living Cells with Polyionenes and Polyionene-Coated Surfaces**

A. Rembaum, A. E. Senyei, and R. Rajaraman (University of Halifax)

J. Biomed. Mater. Res. Symp., No. 8, pp. 101–110, 1977

For abstract, see Rembaum, A.

RAMOHALLI, K.

R003 **Composite Propellant Combustion Modeling Studies**

K. Ramohalli

Twelfth Int. Symp. Space Technol. Sci., Tokyo, Japan, May 1977, 12 pp.

Theoretical and experimental techniques aimed at obtaining a better understanding of the fundamentals of composite propellant combustion, and applications to current problems of technological interest, are summarized. Based on estimates of typical time-scales, the condensed phase is hypothesized to be the site of overall rate-controlling reactions in composite propellant combustion. Pressure-dependent degradation of ammonium perchlorate in a thin melt layer on the AP crystals determines the burning rate; the vapor phase details need be studied only to supply the proper boundary conditions at the surface. Where applicable, a melt layer on the propellant surface supplements these subsurface reactions. The extent of degradation before vaporization is specified through the vapor pressure equilibrium criterion. The pressure exponent in propellant burning(n) emerges as a combination of these two separate pressure dependences and allows for mean pressure dependence of normalized response function during oscillatory combustion and also for instability of zero-n propellants. The minute vapor phase combustion details are studied in a scale-expanded porous plate apparatus which has demonstrated the importance of diffusion/mixing. Instability is studied in L-star and T-burners and also with a microwave apparatus which measures dynamic burning rates directly. Problems with minor compositional changes and low smoke Space Shuttle separation motors are mentioned as typical applications.

RAMOHALLI, K. N.

R004 **Role of Condensed Phase Details in the Oscillatory Combustion of Composite Propellants**

K. N. Ramohalli and F. E. C. Culick (California Institute of Technology)

Combust. Sci. Technol., Vol. 15, pp. 179–199, 1977

The response functions of composite propellants are theoretically derived, including explicitly the pressure-dependent degradation term in the condensed phase, hypothesizing that the overall rate-limiting reactions are in the relatively low temperature condensed phase. The method of "inner" and "outer" expansions with the reduced activation energy as the singular perturbation parameter has been employed. The results cover subsurface reactions with and without surface reactions, adiabatic and uniform-combustion models for the quasi-steady gas phase processes. The response functions display several experimentally observed features like dependence on mean pressure and the instability behavior of some "zero-*n*" propellants.

RAMOHALLI, K. N. R.

R005 **Theoretical Combustion Modeling Study of Nitramine Propellants**

K. N. R. Ramohalli (California Institute of Technology) and L. D. Strand

J. Spacecraft Rockets, Vol. 14, No. 7, pp. 427–433, July 1977

A theoretical investigation of the current problems with nitramine (composite) propellant combustion is summarized. This study has, as its distinctive feature, a detailed examination of the condensed-phase processes in the combustion of nitramine propellants. As a consequence of a recently developed model for the combustion of ammonium perchlorate (AP)/composite propellants, it is hypothesized that the condensed-phase degradation of the nitramine oxidizer particles to a vaporizable state is the overall rate-limiting step. It also is assumed that the gas-phase details are secondary in importance and need to be studied only to the extent of supplying the correct boundary condition on the condensed-phase/vapor-phase heat transfer. Because of our imprecise understanding of the vapor-phase processes in presence of combustion, two limiting models are considered for the vapor phase. It is found that both of the vapor-phase models lead to predictions sufficiently close to experimental trends for us to conclude that the precise details of the vapor-phase processes are not of critical importance in determining propellant combustion behavior. More to the point, we are led to believe that a thorough examination of the condensed-phase details may be sufficient in itself not only to interpret most of the available data on experimental regression rate vs pressure of nitramine propellants but also to aid in the formulation of propellants to suit our needs.

RANKIN, D.

R006 **Electrical Structure in a Region of the Transverse Ranges, Southern California**

I. K. Reddy, R. J. Phillips, J. H. Whitcomb (California Institute of Technology), and D. Rankin (University of Alberta)

Earth Planet. Sci. Lett., Vol. 34, pp. 313–320, 1977

For abstract, see Reddy, I. K.

R007 **Three-Dimensional Modelling in Magnetotelluric and Magnetic Variational Sounding**

I. K. Reddy, D. Rankin (University of Alberta), and R. J. Phillips

Geophys. J. Roy. Astron. Soc., Vol. 51, pp. 313–326, 1977

For abstract, see Reddy, I. K.

RAPER, O. F.

R008 **The HF:HCl Ratio in the 14–38 km Region of the Stratosphere**

C. B. Farmer and O. F. Raper

Geophys. Res. Lett., Vol. 4, No. 11, pp. 527–527, November 1977

For abstract, see Farmer, C. B.

R009 **The Vertical Distribution of HCl in the Stratosphere**

O. F. Raper, C. B. Farmer, R. A. Toth, and B. D. Robbins

Geophys. Res. Lett., Vol. 4, No. 11, pp. 531–534, November 1977

The vertical distribution of HCl in the stratosphere has been measured from infrared solar absorption spectra recorded with a balloon-borne interferometer. The flights were made in September, 1975, and May, 1976 at float altitudes of 40 km and 37 km, respectively, near Palestine, Texas. Concentration profiles derived from the data show an increase from 0.6 ppbv at 20 km to 1.7 ± 0.5 ppbv in the region of 37 km. Above 37 km, the data permit only the total abundance to be determined; this value is found to be equivalent to 1.6 ± 0.6 ppbv if the gas were uniformly mixed. The results from the two flights are closely similar, and no significant seasonal variation in the HCl concentrations can be discerned. The balloon data are consistent with the profile in the 14–21 km altitude region of the stratosphere reported earlier from U-2 observations.

RAYERMANN, P.

R010 **A Photoionization Study of the Formation of NO_2^+ by Reaction of Excited O_2^+ Ions With NO**

J. M. Ajello and P. Rayermann

J. Chem. Phys., Vol. 66, No. 3, pp. 1372–1374, February 1, 1977

For abstract, see Ajello, J. M.

REDDY, I. K.

R011 **Electrical Structure in a Region of the Transverse Ranges, Southern California**

I. K. Reddy, R. J. Phillips, J. H. Whitcomb (California Institute of Technology), and D. Rankin (University of Alberta)

Earth Planet. Sci. Lett., Vol. 34, pp. 313–320, 1977

Magnetotelluric sounding at a site in the Transverse Ranges province in southern California indicates a low-resistivity region in the lower crust and possibly also the upper mantle. A two-dimensional model fit to the data indicates that the resistivity of this region is between 1 and 10 Ωm. The depth to the top surface of this zone is between 15 and 20 km. The lateral extent of this feature, which strikes N65°W, appears to be confined to the Transverse Ranges province. The petrological characteristics of this region cannot be deduced unambiguously from the magnetotelluric sounding alone.

R012 **Three-Dimensional Modelling in Magnetotelluric and Magnetic Variational Sounding**

I. K. Reddy, D. Rankin (University of Alberta), and R. J. Phillips

Geophys. J. Roy. Astron. Soc., Vol. 51, pp. 313–326, 1977

The Galerkin finite element method is used to obtain approximate solutions for the three-dimensional induction problem. A rectangular conductive prism is considered as an example, and solutions are obtained for linear and circularly polarized incident plane wave fields. Magnetotelluric tensor impedances and magnetic transfer functions are computed. Polar diagrams of the tensor impedances and magnetic transfer functions along with their amplitude contour maps are presented. The dimensionality parameter, skew, is contoured at the surface of the Earth. It is shown that the relative amplitudes and shapes of the additional and principal impedance polar diagrams can be used to determine the dimensionality of the geoelectrical structures. Stations with the skew values greater than 0.2 are significantly influenced by the three-dimensionality of the geoelectric structure. The

amplitudes of the magnetic transfer function and the orientations of its polar diagrams exhibit large anomalies in the vicinity of the intersection of the lateral contacts.

REED, I. S.

R013 Review of Finite Fields: Applications to Discrete Fourier Transforms and Reed-Solomon Coding

J. S. L. Wong, T. K. Truong, B. Benjauthrit, B. D. L. Mulhall, and I. S. Reed

JPL Publication 77-23, July 15, 1977

For abstract, see Wong, J. S. L.

R014 A New Fast Algorithm for Computing a Complex Number—Theoretic Transforms

I. S. Reed (University of Southern California), K. Y. Liu (University of Southern California), and T. K. Truong

The Deep Space Network Progress Report 42-39: March and April 1977, pp. 71–75, June 15, 1977

A high-radix FFT algorithm for computing transforms over $GF(q^2)$, where q is a Mersenne prime, is developed to implement fast circular convolutions. This new algorithm requires substantially fewer multiplications than the conventional FFT.

R015 On the Fundamental Structure of Galois Switching Functions

B. Benjauthrit and I. S. Reed (University of Southern California)

The Deep Space Network Progress Report 42-40: May and June 1977, pp. 117–13, August 15, 1977

For abstract, see Benjauthrit, B.

R016 Fast Algorithms for Computing Mersenne-Prime Number-Theoretic Transforms

I. S. Reed (University of Southern California) and T. K. Truong

The Deep Space Network Progress Report 42-41: July and August 1977, pp. 176–205, October 15, 1977

It is shown that Winograd's algorithm can be used to compute an integer transform over $GF(q)$, where q is a Mersenne prime. This new algorithm requires fewer multiplications than the conventional fast Fourier transform (FFT). This transform over $GF(q)$ can be implemented readily on a digital computer. This fact makes it possible to more easily encode and decode BCH and RS codes.

REID, M.

R017 A K-Band Radiometer for the Microwave Weather Project

K. Wallace, M. Reid, and H. Reilly

The Deep Space Network Progress Report 42-38: January and February 1977, pp. 66–69, April 15, 1977

For abstract, see Wallace, K.

R018 X-Band Atmospheric Noise Temperature Statistics at Goldstone DSS 13, 1975—1976

S. Slobin, M. Reid, R. Gardner, and D. Cheng

The Deep Space Network Progress Report 42-38: January and February 1977, pp. 70–76, April 15, 1977

For abstract, see Slobin, S.

REID, M. S.

R019 Precision Insolation Measurement Under Field Conditions

M. S. Reid, R. A. Gardner, and C. M. Berdahl

The Deep Space Network Progress Report 42-37: November and December 1976, pp. 169–175, February 15, 1977

A solar energy instrumentation project was started at Goldstone to support the DSN energy conservation project. The objective is to help provide an adequate technological foundation for supporting a solar energy based facilities design at Goldstone. The lack of historical records of insolation for the Goldstone area required that a program of instrumentation development and solar data recording be started as quickly as possible. Prior NASA-supported work at the Jet Propulsion Laboratory had resulted in the development of a primary absolute cavity radiometer (PACRAD), which was recently accepted as an international standard of irradiance. This report discusses the development of an all-weather, fieldworthy solar radiometer based on the PACRAD, and describes its calibration stability over a two-year period in the field.

R020 Precision Insolation Measurement Under Field Conditions

M. S. Reid, C. M. Berdahl, and R. A. Gardner

Proc. SPIE, Vol. 85, pp. 90–92, 1976

A primary absolute cavity radiometer, developed by the Jet Propulsion Laboratory, has been accepted as an International Standard. With this instrument accurate mea-

surements of absolute solar irradiance can be made. The design minimizes all unwanted heat transfers.

REILLY, H.

R021 A K-Band Radiometer for the Microwave Weather Project

K. Wallace, M. Reid, and H. Reilly

The Deep Space Network Progress Report 42-38: January and February 1977, pp. 66–69, April 15, 1977

For abstract, see Wallace, K.

REILLY, N. B.

R022 State Criminal Justice Telecommunications (STACOM) Final Report: Executive Summary

J. E. Fielding, H. K. Frewing, J. J. Lee, W. G. Leflang, and N. B. Reilly

JPL Publication 77-53, Vol. I, October 31, 1977

For abstract, see Fielding, J. E.

R023 State Criminal Justice Telecommunications (STACOM) Final Report: Requirements Analysis and Design of Ohio Criminal Justice Telecommunications Network

J. E. Fielding, H. K. Frewing, J. J. Lee, and N. B. Reilly

JPL Publication 77-53, Vol. II, October 31, 1977

For abstract, see Fielding, J. E.

R024 State Criminal Justice Telecommunications (STACOM) Final Report: Requirements Analysis and Design of Texas Criminal Justice Telecommunications Network

J. E. Fielding, H. K. Frewing, J. J. Lee, and N. B. Reilly

JPL Publication 77-53, Vol. III, October 31, 1977

For abstract, see Fielding, J. E.

REINHART, E. E.

R025 Sharing the 620–790 MHz Band Allocated to Terrestrial Television With an Audio-Bandwidth Social Service Satellite System

E. K. Smith and E. E. Reinhart

JPL Publication 77-71, October 31, 1977

For abstract, see Smith, E. K.

REMBAUM, A.

R026 Reactions of Human Platelets with Microspheres of Poly(hydroxymethyl Methacrylate) and Polyacrylamide

P. L. Kronick (Franklin Institute Research Laboratories) and A. Rembaum

J. Biomed. Mater. Res. Symp., No. 8, pp. 39–50, 1977

For abstract, see Kronick, P. L.

R027 Interaction of Living Cells with Polyionenes and Polyionene-Coated Surfaces

A. Rembaum, A. E. Senyei, and R. Rajaraman (University of Halifax)

J. Biomed. Mater. Res. Symp., No. 8, pp. 101–110, 1977

Polyionenes have been shown recently (A. Rembaum, *Appl. Polym. Symp. No. 22*, 299, 1973) to produce the following biological effects: 1) bactericidal action, 2) formation of insoluble complexes with DNA and heparin, 3) neuromuscular blocking action, 4) cell aggregation and lysis, and (5) cell adhesion.

In the present study, polyionenes of various structures (mainly $I_{3,3}$, $I_{6,10}$) were used as molecular probes to gain an understanding of the cell surface phenomena of adhesion on glass- and polyionenes-treated surfaces. Since tumor cells show different surface cell properties, including an increase in the anodic mobility, they bind preferentially to polyionene-treated surfaces. Normal human diploid WI-38 cells were found to adhere at a lower rate than SV-transformed WI-38 cells. However, cell spreading was accelerated in both cases.

A study of the interaction of polyionenes in solution *in vitro* and *in vivo* and polyionenes covalently bound to polymeric microspheres with leukemic murine EL 4 cells and normal thymocytes showed specific cytotoxity towards the leukemic cells

REMER, D. S.

R028 A Life Cycle Cost Economics Model for Projects With Uniformly Varying Operating Costs

D. S. Remer

The Deep Space Network Progress Report 42-39: March and April 1977, pp. 60–70, June 15, 1977

A mathematical model is developed for calculating the life cycle costs for a project where the operating costs increase or decrease in a linear manner with time. The life cycle cost is shown to be a function of the (1) investment costs, (2) initial operating costs, (3) operating

cost gradient, (4) project life time, (5) interest rate for capital, and (6) salvage value. The results show that the life cycle cost for a project can be grossly underestimated (or overestimated) if the operating costs increase (or decrease) uniformly over time rather than being constant as is often assumed in project economic evaluations. The following range of variables is examined: (1) project life from 2 to 30 years, (2) interest rate from 0 to 15 percent per year, and (3) operating cost gradient from 5 to 90 percent of the initial operating cost. A numerical example plus tables and graphs is given to help the reader calculate project life cycle costs over a wide range of variables.

RENNELS, D. A.

R029 An Application of Microprocessors to a Mars Roving Vehicle

B. M. Dobrotin and D. A. Rennels

Proc. 1977 Joint Automat. Contr. Conf., San Francisco, Calif., June 22–24, 1977, pp. 185–196

For abstract, see Dobrotin, B. M.

RENZETTI, N. A.

R030 Network Functions and Facilities

N. A. Renzetti

The Deep Space Network Progress Report 42-37: November and December 1976, pp. 1–3, February 15, 1977

The objectives, functions, and organization of the Deep Space Network are summarized; deep space station, ground communication, and network operations control capabilities are described.

R031 Network Functions and Facilities

N. A. Renzetti

The Deep Space Network Progress Report 42-38: January and February 1977, pp. 1–3, April 15, 1977

The objectives, functions, and organization of the Deep Space Network are summarized; deep space station, ground communication, and network operations control capabilities are described.

R032 Network Functions and Facilities

N. A. Renzetti

The Deep Space Network Progress Report 42-39: March and April 1977, pp. 1–3, June 15, 1977

The objectives, functions, and organization of the Deep Space Network are summarized; deep space station, ground communication, and network operations control capabilities are described.

R033 Network Functions and Facilities

N. A. Renzetti

The Deep Space Network Progress Report 42-40: May and June 1977, pp. 1–3, August 15, 1977

The objectives, functions, and organization of the Deep Space Network are summarized; deep space station, ground communication, and network operations control capabilities are described.

R034 Network Functions and Facilities

N. A. Renzetti

The Deep Space Network Progress Report 42-41: July and August 1977, pp. 1–3, October 15, 1977

The objectives, functions, and organization of the Deep Space Network are summarized; deep space station, ground communication, and network operations control capabilities are described.

R035 Network Functions and Facilities

N. A. Renzetti

The Deep Space Network Progress Report 42-42: September and October 1977, pp. 1–3, December 15, 1977

The objectives, functions, and organization of the Deep Space Network are summarized; deep space station, ground communication, and network operations control capabilities are described.

RHIM, W. K.

R036 ADRF Experiments Using Near $n\pi$ Pulse Strings

W. K. Rhim, D. P. Burum, and D. D. Elleman

Phys. Lett., Vol. 62A, No. 7, pp. 507–508, October 3, 1977

An ADRF and inverse repolarization phenomenon was observed in dipolar solids by applying a string of rf pulses in which the pulse angle was gradually varied past $n\pi$. This phenomenon, which is characteristic of discrete excitation schemes, is explained qualitatively.

R037 Multiple-Pulse Spin Locking in Dipolar Solids

W. K. Rhim, D. P. Burum, and D. D. Elleman

ORIGINAL PAGE IS OF POOR QUALITY

Phys. Rev. Lett., Vol. 37, No. 26, pp. 1764–1766, December 27, 1976

We report our preliminary results on a multiple-pulse spin-locking effect in dipolar solids. This effect has significant experimental advantages over prior techniques because of its high duty cycle for data collection. We show that the spin temperature assumption can be applied to explain the rather long-term behavior of the spin system. We also demonstrate how this method can be applied to obtain magnetization curves almost instantly for $T_{1\rho}$ decay and adiabatic demagnetization.

RHODES, E. J., JR.

R038 Further Evidence of a Latitude Gradient in the Solar Wind Velocity

E. J. Rhodes, Jr., and E. J. Smith

J. Geophys. Res., Space Phys., Vol. 81, No. 34, pp. 5833–5840, December 1, 1976

The large-scale gradient in the bulk velocity of the solar wind, previously inferred from a study of large numbers of solar wind measurements made at two widely separated locations by Mariner 5 and the near-earth Explorers 33, 34, and 35 during mid-1967, is interpreted to be a heliographic latitude gradient. Nearly 2000 differences in hourly averages of the solar wind velocity observed at the two locations, after being corrected for differences in solar longitude, are analyzed by using a technique previously applied to the propagation of sector boundaries between Mariner 5 and earth. The higher velocities at the higher-latitude Explorers, as compared with those observed at the lower-latitude Mariner 5, imply a latitude gradient of roughly 15 km/s/deg. This value for the gradient is in excellent agreement with that obtained previously from the study of sector boundaries. A simple model of the velocity-latitude dependence is developed to illustrate that the observed relationship between the velocities at Mariner and the Explorers, $(V_M - 275) = 11 + 0.76(V_E - 275)$, is consistent with this gradient and with the latitude separation of the spacecraft. Further evidence of a latitude gradient is obtained by analyzing separately the velocities at the Explorers and at Mariner 5 as functions of latitude. This technique yields essentially the same relation between velocity and latitude as the multispacecraft analysis. The Vela 2, 3, and 4 solar rotation velocity averages observed near earth from 1964 through 1967 (interpreted by Hundhausen et al. (1971) as being due to a latitude gradient) are combined with solar rotation averages of the Mariner and Explorer data and then analyzed as a function of latitude to obtain a long-term value for the gradient. These single-location analyses consistently yield latitude gradients in the northern hemisphere below 7-1/4° that range between 10 and 15 km/s/deg. Interplanetary scintillation estimates of the solar wind velocity, obtained in 1972 and 1973, are also analyzed and yield a somewhat smaller latitude gradient of 4–6 km/s/deg. The latter values provide evidence of the existence of the gradient at higher heliographic latitudes.

RIEWE, A. A.

R039 64-Meter Antenna Pedestal Tilt at DSS 43, Tidbinbilla, Australia

G. Gale and A. A. Riewe

The Deep Space Network Progress Report 42-40: May and June 1977, pp. 168–173, August 15, 1977

For abstract, see Gale, G.

ROBBINS, B. D.

R040 The Vertical Distribution of HCl in the Stratosphere

O. F. Raper, C. B. Farmer, R. A. Toth, and B. D. Robbins

Geophys. Res. Lett., Vol. 4, No. 11, pp. 531–534, November 1977

For abstract, see Raper, O. F.

ROBERTS, P. H.

R041 Orbit Design Concepts for Jupiter Orbiter Missions

C. Uphoff, P. H. Roberts, and L. D. Friedman

J. Spacecraft Rockets, Vol. 13, No. 6, pp. 348–355, June 1976

For abstract, see Uphoff, C.

ROCKWELL, G. M.

R042 Viking Mission support

D. W. Johnston, T. W. Howe, and G. M. Rockwell

The Deep Space Network Progress Report 42-37: November and December 1976, pp. 12–25, February 15, 1977

For abstract, see Johnston, D. W.

R043 Helios Mission Support

P. S. Goodwin, E. S. Burke, and G. M. Rockwell

The Deep Space Network Progress Report 42-38: January and February 1977, pp. 50–54, April 15, 1977

For abstract, see Goodwin, P. S.

R044 **Helios Mission Support**

P. S. Goodwin, E. S. Burke, and G. M. Rockwell

The Deep Space Network Progress Report 42-39: March and April 1977, pp. 17–22, June 15, 1977

For abstract, see Goodwin, P. S.

R045 **Helios Mission Support**

P. S. Goodwin, E. S. Burke, and G. M. Rockwell

The Deep Space Network Progress Report 42-40: May and June 1977, pp. 52–56, August 15, 1977

For abstract, see Goodwin, P. S.

R046 **Helios Mission Support**

P. S. Goodwin and G. M. Rockwell

The Deep Space Network Progress Report 42-41: July and August 1977, pp. 39–42, October 15, 1977

For abstract, see Goodwin, P. S.

R047 **Helios Mission Support**

P. S. Goodwin and G. M. Rockwell

The Deep Space Network Progress Report 42-42: September and October 1977, pp. 34–41, December 15, 1977

For abstract, see Goodwin, P. S.

ROCKWELL, S. T.

R048 **Viking Doppler Noise Used to Determine the Radial Dependence of Electron Density in the Extended Corona**

A. L. Berman, J. A. Wackley, S. T. Rockwell, and M. Kwan

The Deep Space Network Progress Report 42-38: January and February 1977, pp. 167–171, April 15, 1977

For abstract, see Berman, A. L.

R049 **A Model of SNR Degradation During Solar Conjunction**

S. T. Rockwell

The Deep Space Network Progress Report 42-38: January and February 1977, pp. 187–198, April 15, 1977

The downlink signal from spacecraft in solar conjunction phases suffers a drastic reduction in signal-to-noise ratio (SNR). Responsible in large part for this effect is the increase in system noise temperature (SNT) in the ground antenna-receiver system. This article presents an empirical model of SNR degradation due to increasing SNT during solar conjunction phases.

RODEMICH, E. R.

R050 **An Asymptotic Analysis of a General Class of Signal Detection Algorithms**

R. J. McEliece and E. R. Rodemich

The Deep Space Network Progress Report 42-39: March and April 1977, pp. 30–35, June 15, 1977

For abstract, see McEliece, R. J.

R051 **New Upper Bounds on the Rate of a Code via the Delsarte–MacWilliams Inequalities**

R. J. McEliece, E. R. Rodemich, H. Rumsey, Jr., and L. R. Welch (University of Southern California)

IEEE Trans. Inform. Theor., Vol. IT-23, No. 2, pp. 157–166, March 1977

For abstract, see McEliece, R. J.

R052 **Behaviour of Queues at Signalized Intersections in Heavy traffic**

E. C. Posner and E. R. Rodemich

Utilitas Math., Vol. 10, pp. 3–50, November 1976

For abstract, see Posner, E. C.

ROSEBORO, J. A.

R053 **Feasibility Study on the Design of a Probe for Rectal Cancer Detection**

V. J. Anselmo, R. E. Frazer, D. H. LeCroissette, J. A. Roseboro, and M. I. Smokler

JPL Publication 77-31, April 15, 1977

For abstract, see Anselmo, V. J.

R054 **Ultrastructure of Hela Cells and Thoracic Duct Lymphocytes: Pre- and Post-Ultrasonic Irradiation**

J. A. Roseboro (University of North Carolina)

Ultrasound Med., Vol. 3B, pp. 2063–2074, 1977

This paper presents extended results of previous work. Human lymphocytes and cervical cancer cells (Hela cells), ultrasound irradiated and unradiated, were examined by scanning and transmission electron microscopy.

ROSS, W. J.

R055 VLBI Validation Project

W. J. Ross

The Deep Space Network Progress Report 42-39: March and April 1977, pp. 181–185, June 15, 1977

This article summarizes the DSN operations support of the first session of a series of yearly sessions being conducted by the VLBI Validation Project. It covers the period November 1976 through January 1977 wherein two training and three operational experiments were conducted at the Deep Space Communications Complex (DSCC) at Goldstone, California.

ROURKE, K. H.

R056 The Application of Differential VLBI to Planetary Approach Orbit Determination

J. K. Miller and K. H. Rourke

The Deep Space Network Progress Report 42-40: May and June 1977, pp. 84–90, August 15, 1977

For abstract, see Miller, J. K.

ROWAN, L. C.

R057 Mapping of Hydrothermal Alteration in the Cuprite Mining District, Nevada, Using Aircraft Scanner Images for the Spectral Region 0.46 to 2.36 μm

M. J. Abrams, R. P. Ashley (U. S. Geological Survey), L. C. Rowan (U. S. Geological Survey), A. F. H. Goetz, and A. B. Kahle

Geology, Vol. 5, No. 12, pp. 713–718, December 1977

For abstract, see Abrams, M. J.

ROYDEN, H. N.

R058 A Solar Plasma Stream Measured by DRVID and Dual-Frequency Range and Doppler Radio Metric Data

F. B. Winn, S. C. Wu, T. A. Komarek, V. W. Lam, H. N. Royden, and K. B. W. Yip

The Deep Space Network Progress Report 42-37: November and December 1976, pp. 43–54, February 15, 1977

For abstract, see Winn, F. B.

RUDNICK, I.

R059 First-Order Torques and Solid-Body Spinning Velocities in Intense Sound Fields

T. G. Wang H. Kanber, and I. Rudnick (University of California, Los Angeles)

Phys. Rev. Lett., Vol. 38, No. 3, pp. 128–130, January 17, 1977

For abstract, see Wang, T. G.

RUMSEY, H., JR.

R060 New Upper Bounds on the Rate of a Code via the Delsarte–MacWilliams Inequalities

R. J. McEliece, E. R. Rodemich, H. Rumsey, Jr., and L. R. Welch (University of Southern California)

IEEE Trans. Inform. Theor., Vol. IT-23, No. 2, pp. 157–166, March 1977

For abstract, see McEliece, R. J.

RUSSELL, C. T.

R061 Magnetic Evidence Concerning a Lunar Core

B. E. Goldstein, R. J. Phillips, and C. T. Russell (University of California, Los Angeles)

Proc. Seventh Lunar Conf., pp. 3321–3341, 1976

For abstract, see Goldstein, B. E.

RYASON, P. R.

R062 Extended Soot Limits for Rich *n*-Heptane/Air Flames

P. R. Ryason

Combust. Flame, Vol. 29, pp. 329–331, 1977

This work was undertaken to find a means of burning rich flames soot-free as a possible route to constructing a thermal hydrogen generation device. The results, though incomplete, had a notable degree of success.

R063 Hydrogen Quantum Yields in the 360 nm Photolysis of Eu^{2+} Solutions and Their Relationship to Photochemical Fuel Formation

P. R. Ryason

Solar Energy, Vol. 19, No. 5, pp. 445–448, 1977

Water decomposition by a cyclic photoredox process is discussed in general terms. Thermodynamics determines the wavelength of the charge transfer band correspond-

ing to electron transfer to or from water of hydration of a cation. These relationships indicate that it is unlikely that a photoreduction reaction resulting in water decomposition will occur in the sea level solar range of wavelengths. Such is not the case for photo-oxidation, and an example is known: the photolysis of Eu^{2+} in aqueous solution. Hydrogen quantum yields have been determined for this reaction. They are sufficiently high (~0.3) as to offer encouragement for the further exploration of photoredox reactions as a means of solar energy conversion.

SACKMANN, I.-J.

S001 What Quenches the Helium Shell Flashes?

I.-J. Sackmann

Astrophys. J., Vol. 212, No. 1, Pt. 1, pp. 159–170, February 15, 1977

A typical helium shell flash cycle has been studied in detail, and criteria for the turning points in the flash cycle have been developed. The flash is quenched by the interaction of three terms: (i) a decreasing nuclear physics term, (ii) an increasing radiation pressure term, and (iii) an increasing geometrical term. The most important are the first and the third terms, with the radiation pressure term the least important of the three, for the stars followed here with core masses $M_c = 0.6$ to 10 $M_\odot$. It is shown that stars of high core masses have weaker flashes. Peak flash conditions can be approximately predicted by conditions at the beginning of the flash. Peak nuclear energy generation and peak temperature can never coincide in the flash cycle, the former always occurring before the latter. It is similar for the corresponding minima. Conditions are shown under which secondary components may occur, but these subpulses are always of considerably weaker intensity than the main flash.

SAROHIA, V.

S002 Investigation of Pressure Oscillations in Axi-Symmetric Cavity Flows

V. Sarohia and P. F. Massier

JPL Publication 77-68, September 1977

An experimental investigation was conducted of subsonic turbulent flows over shallow, axi-symmetric cavities located downstream of the leading edge of a flat-nosed fuse contour and on an ellipsoidal nose contour. The objective was to evaluate cavity performance in terms of pressure oscillations inside the cavity for various cavity configurations and other pertinent parameters for various modes of cavity operation. Free-stream velocities over the contours ranged up to 650 ft/sec, and Reynolds numbers based on maximum diameter of the contour ranged between 10^4 and about 10^6.

It was found that pressure signals at the base of the cavity for an oscillating cavity flow as high as 150 dB, referred to 20 $\mu N/m^2$, could be obtained and that a total acoustic power as high as 20 W was estimated. Furthermore, pressure oscillations existed for cavity depths as small as 0.050 in. It may be that this is not the minimum depth for which oscillations are generated, since the next smaller depth tested was 0.020 in. For the smallest depth (0.020 in.), pressure oscillations in the cavity did not occur.

Cavity oscillations were more pronounced when the cavity was located in the favorable (negative) pressure gradient region of the axi-symmetric body. Instant spark shadowgraphs taken for both laminar and for turbulent boundary layer flow separation at the upstream cavity corner showed the presence of large, organized vortex structures in the oscillating shear layer. Mean velocity measurements of an oscillating cavity shear layer indicated an entrainment rate as large as 0.046 as compared to a non-oscillating cavity shear layer entrainment of approximately 0.021. The above large entrainment rates for a turbulent separated cavity flow appeared to have been caused by the presence of these organized large-scale vortex structures imposed on the flow by the oscillating cavity flow system.

S003 Effect of Flight on Jet Noise from Supersonic Underexpanded Flows

V. Sarohia

Preprint 77-1328, AIAA Fourth Aeroacoustics Conf., Atlanta, Ga., Oct. 3–5, 1977

Experiments on underexpanded cold jet flows from a convergent nozzle under simulated flight conditions have shown that a large periodic spinning motion of the jet can occur with greatly enhanced broadband noise production. Shadowgraph pictures indicate that this oscillatory jet motion accompanies the generation of random weak shock waves at the source. These waves appear to be generated at the point downstream of the nozzle exit where the shock cells in the jet begin to disappear. The weak shock waves propagate upstream and have been identified to be the cause of enhanced broadband jet noise production in flight. In addition, the results show that the boundary layer flow conditions over the outside of the primary nozzle (simulating engine cowl flow in flight) have a key role in the production of these random weak shock waves.

S004 Experimental Results of Large Scale Structures in Jet Flows and Their Relation to Jet Noise Production

V. Sarohia and P. F. Massier

Preprint 77-1350, AIAA Fourth Aeroacoustics Conf., Atlanta, Ga., Oct. 3–5, 1977

Experiments have been performed to determine the role of large-scale turbulent structures in the production of jet noise. Axisymmetric turbulent jet flows at ambient stagnation temperature have been observed with the aid of flow visualization techniques. Jet Mach numbers at the nozzle exit ranged between 0.1 and 0.9, and the Reynolds number, based on nozzle exit diameter, was approximately 10^6. Large organized turbulent structures existed as far downstream of the nozzle exit as 7 diameters. High-speed Schlieren motion pictures synchronized with near-field pressure measurements of an excited jet indicated that strong instantaneous peaks in the pressure signal occurred whenever a merging process between two large-scale organized structures occurred. This pressure pulse propagated at a speed which was somewhat larger than the velocity of the jet at the nozzle exit.

S005 Effects of External Boundary-Layer Flow on Jet Noise in Flight

V. Sarohia and P. F. Massier

AIAA J., Vol. 15, No. 5, pp. 659–664, May 1977

The effects on jet flow of the external boundary-layer flow emanating from the trailing edge of an engine cowl in flight has been shown to be the main reason for the disparity between predicted and experimental results obtained from flight measurements. Flight simulation experiments indicate that the external boundary-layer flow tends to shield the jet flow in flight. This in turn modifies the jet noise source in flight and consequently the radiated noise from aircraft in flight. Close to $\theta_I = 90°$ and in the forward quadrant, this study indicates that the far-field jet noise and its spectrum scales approximately with the absolute jet velocity instead of the relative velocity as has been assumed in the existing prediction models.

S006 Experimental Investigation of Oscillations in Flows Over Shallow Cavities

V. Sarohia

AIAA J., Vol. 15, No. 7, pp. 984–991, July 1977

Laminar axisymmetric flows over shallow cavities at low subsonic speeds were experimentally investigated. The results indicate that the cavity depth has little effect on oscillations in shallow cavities, except when the depth is of the order of the thickness of the cavity shear flow. For such cavity configurations, measurements indicate a strong stabilizing effect of depth on laminar cavity shear layer. Results of motion picture and hot-wire surveys of the cavity shear layer show that, close to the downstream cavity corner, large lateral motion of the shear layer occurs, which results in a periodic shedding of vortices at a frequency of cavity oscillation. Mean velocity measurements show growth rates as high as $d\theta/dx \cong 0.022$, where θ is the shear layer momentum thickness and x is the streamwise coordinate. These are attributed to strong imposed velocity fluctuations on the flow, by the oscillating cavity system. Phase measurements indicate that the disturbances propagate at a constant phase speed through the cavity shear layer. The wavelength of the propagating disturbance bears an approximate integral relation to cavity width, in each mode of cavity oscillation given by $b \cong \lambda(n + 1/2)$, where b is the cavity width, λ the wavelength of the propagating disturbance, and n is an integer, which takes values 0, 1, 2, ...etc., depending upon the mode of oscillation.

S007 Control of Cavity Noise

V. Sarohia and P. F. Massier

Preprint 76-528, AIAA Third Aero-Acoust. Conf., Palo Alto, Calif., July 20–23, 1976

Experiments have been conducted on axisymmetric shallow cavity flows with the aim of investigating methods to modify cavity shear flows such that cavity noise may be reduced. The experiments indicate the presence of large gross lateral motion of the shear layer close to the downstream cavity corner which, on interaction with it, results in production of cavity flow noise. Results also show that the continuous injection of a fluid mass at the base of the cavity has a stabilizing effect on cavity shear flows. This stability is believed to have been achieved by supplying the mass required for cavity shear layer entrainment externally. This was also accompanied by a delay in large periodic lateral motion of the cavity shear layer close to the downstream cavity corner as observed without the mass injection. Thus the addition of a continuous fluid mass appears to be an effective means of suppressing cavity flow noise.

S008 Control of Cavity Noise

V. Sarohia and P. F. Massier

J. Aircraft, Vol. 14, No. 9, pp. 833–837, September 1977

Experiments have been conducted on axisymmetric shallow cavity flows with the aim of investigating methods to modify cavity shear flows such that cavity noise may be reduced. The experiments indicate the presence of large gross lateral motion of the shear layer close to the downstream cavity corner which, on interaction with it, results in production of cavity flow noise. Results also show that the continuous injection of a fluid mass at the base of the cavity has a stabilizing effect on cavity shear flows. This stability is believed to have been achieved by supplying the mass required for cavity shear-layer entrainment externally. This also was accompanied by a delay in large periodic lateral motion of the cavity shear layer close to the downstream cavity corner as observed

without the mass injection. Thus, the addition of a continuous fluid mass appears to be an effective means of suppressing cavity flow noise.

SATO, T.

S009 Feasibility Study of Far-Field Methods for Calibrating Ground Station Delays

T. Sato

The Deep Space Network Progress Report 42-37: November and December 1976, pp. 55–56, February 15, 1977

The first phase of a study to survey various methods of directly implementing a far field means of calibrating ranging systems is described. Consideration is given to means of determining test range distances independent of microwave techniques.

S010 Feasibility Study of Far-Field Methods for Calibrating Ground Station Delays:.An Interim Report

T. Sato

The Deep Space Network Progress Report 42-41: July and August 1977, pp. 51–56, October 15, 1977

This interim report presents the results of a study to survey and arrive at cost/performance estimates of various methods of implementing far-field calibrations of ground station delays. Both direct and indirect methods for far-field calibrations are discussed.

SAUNDERS, R. S.

S011 Geologic Interpretation of New Observations of the Surface of Venus

R. S. Saunders and M. C. Malin

Geophys. Res. Lett., Vol. 4, No. 11, pp. 547–550, November 1977

New radar observations of the surface of Venus provide further evidence of a diverse and complex geologic evolution. The radar bright feature "Beta" (24°N, 85°W) is seen to be a 700 km diameter region elevated a maximum of approximately 10 km relative to its surroundings with a 60 × 90 km wide depression at its summit. "Beta" is interpreted to be a large volcanic construct, analogous to terrestrial and martian shield volcanoes. Two large, quasi-circular areas of low reflectivity, examples of a class of features interpreted to be impact basins by previous investigators who were without the benefit of actual topographic information, are shown in altimetry maps to be depressions. Thus the term "basin" can be applied, although we urge a nongenetic usage until more complete understanding of their origin is achieved through analysis of future observations.

S012 Surface of Venus: Evidence of Diverse Landforms from Radar Observations

M. C. Malin and R. S. Saunders

Science, Vol. 196, pp. 987–990, May 27, 1977

For abstract, see Malin, M. C.

SCHIELDGE, J.

S013 JPL Field Measurements at the Finney County, Kansas, Test Site, October 1976: Meteorological Variables, Surface Reflectivity, Surface and Subsurface Temperatures

A. B. Kahle, J. Schieldge, and H. N. Paley

JPL Publication 77-1, February 1, 1977

For abstract, see Kahle, A. B.

SCHULTZ, S.

S014 Simple Waveguide Reflection Maser With Broad Tunability

L. D. Flesner (University of California, San Diego), S. Schultz (University of California, San Diego), and R. Clauss

Rev. Sci. Instrum., Vol. 48, No. 8, pp. 1104–1105, August 1977

For abstract, see Flesner, L. D.

SCHWARTZ, A. A.

S015 Transformations From an Oblate Spheroid to a Plane and Vice Versa—The Equations Used in the Cartographic Projection Program MAP2

D. A. Elliott and A. A. Schwartz

JPL Publication 77-7, February 15, 1977

For abstract, see Elliott, D. A.

S016 Variable Threshold Zonal Filtering

A. A. Schwartz and J. M. Soha

Appl. Opt., Vol. 16, No. 7, pp. 1779–1781, July 1977

Variable threshold zonal filtering is an active, nonlinear image enhancement process designed to avoid ringing artifacts introduced by filtering near sharp brightness transitions. Large-scale shading which obscures local de-

ORIGINAL PAGE IS
OF POOR QUALITY

tail can be removed with low-frequency notch filtering in cases where the shading is slowly varying. The filtering procedure can be implemented in the Fourier domain by subtractive box filtering. A new nonlinear filtering algorithm has been devised which is helpful in relieving ringing by allowing contrast to be increased so that detail becomes readily apparent. The new filtering procedure is implemented as a variation of the box filter.

SCHWARTZ, R. L.

S017 Parallel Compilation: A Design and Its Application to SIMULA 67

R. L. Schwartz

JPL Publication 77-4, February 1, 1977

This paper presents a design for a parallel compilation facility for the SIMULA 67 programming language. The proposed facility allows top-down, bottom-up, or parallel development and integration of program modules. An evaluation of the proposal and a discussion of its applicability to other languages are then given.

S018 An MBASIC™ User Profile

R. L. Schwartz

The Deep Space Network Progress Report 42-41: July and August 1977, pp. 103–111, October 15, 1977

An important aspect of any programming language development is an awareness of how the language is actually being used. This article presents the preliminary results of an empirical study of MBASIC user programs. The study, part of an ongoing effort, seeks to discover the features and capabilities of the MBASIC processor which are being utilized. This will aid in future decisions to be made concerning language extensions and the development of a batch compiler.

SEIDELMANN, P. K.

S019 Evaluation of Jupiter Longitudes in System III(1965)

P. K. Seidelmann (U. S. Naval Observatory) and N. Divine

Geophys. Res. Lett., Vol. 4, No. 2, pp. 65–68, February 1977

Commission 40 of the International Astronomical Union has adopted a new longitude system for Jupiter, labelled System III(1965), to replace the provisional System III(1957.0). The specification of the prime meridian and epoch for the new system differs slightly from that recently published. Its rotation rate implies a period of 9 h 55 min 29.711 s ±0.04 s, consistent with recent determinations from decimetric and decametric data. For both the new and older systems, equations are provided which are useful in the evaluation of longitudes for the analysis of Jupiter radio, particle and field data from Earth and spacecraft observations.

SEIDMAN, J. B.

S020 VICAR Image Processing System

J. B. Seidman

JPL Publication 77-37, May 1, 1977

This document describes the functional characteristics and operating requirements of the VICAR (Video Image Communication and Retrieval) system. The information contained herein is applicable to the version of the VICAR system operating in conjunction with the IBM OS and VS operating systems.

Section 1 contains an introduction to the system describing the functional characteristics and the basic theory of operation. A brief description of the data flow as well as tape and disk formats is also presented.

Section 2 is a formal presentation of the control statement formats. This section is intended to serve as a reference guide for the programmer.

Section 3 is organized as a guide to the usage of the system. It provides a step-by-step reference to the creation of a VICAR control card deck. Simple examples are employed to illustrate the various options and the system response thereto.

SELCUK, M. K.

S021 A Fixed Tilt Solar Collector Employing Reversible Vee-Trough Reflectors and Vacuum Tube Receivers for Solar Heating and Cooling Systems: Final Report

M. K. Selcuk

JPL Publication 77-78, December 1977

The objective of the Vee-Trough/Vacuum Tube Collector (VTVTC) Project undertaken for the DOE Solar Heating and Cooling Branch was to prove the usefulness of vee-trough concentrators in improving the efficiency and reducing the cost of collectors assembled from evacuated tube receivers.

The VTVTC was analyzed rigorously and various mathematical models were developed to calculate the optical performance of the vee-trough concentrator and the thermal performance of the evacuated tube receiver. A test bed was constructed to verify the mathematical analysis and compare reflectors made out of glass, Alzak and aluminized FEP Teflon. Tests were run at tempera-

tures ranging from 95 to 180°C during the months of April, May, June, July and August 1977. Vee-trough collector efficiencies of 35 to 40% were observed at an operating temperature of about 175°C. Test results compared well with the calculated values. Test data covering a complete day are presented for selected dates throughout the season.

Predicted daily useful heat collection and efficiency values are presented for a year's duration at operation temperatures ranging from 65 to 230°C. Estimated collector costs and resulting thermal energy costs are presented. Analytical and experimental results are discussed along with a complete economic evaluation. Recommendations for the continuation of the project are presented.

SENG, S.

S022 Imaging Air Pollutants in the Near Ultraviolet

D. Norris, J. Conley, and S. Seng

Proc. SPIE, Vol. 91, pp. 116–122, 1976

For abstract, see Norris, D.

SENYEI, A. E.

S023 Interaction of Living Cells with Polyionenes and Polyionene-Coated Surfaces

A. Rembaum, A. E. Senyei, and R. Rajaraman (University of Halifax)

J. Biomed. Mater. Res. Symp., No. 8, pp. 101–110, 1977

For abstract, see Rembaum, A.

SHEARER, J. B.

S024 There is No MacWilliams Identity for Convolutional Codes

J. B. Shearer and R. J. McEliece

IEEE Trans. Inform. Theor., Vol. IT-23, No. 6, pp. 775–776, November 1977

An example is provided of two convolutional codes that have the same transmission gain but whose dual codes do not. This shows that no analog of the MacWilliams identity for block codes can exist relating the transmission gains of a convolutional code and its dual.

SHEMDIN, O. H.

S025 Momemtum Transfer at the Air–Water Interface

O. H. Shemdin

Transport Processes in Lakes and Oceans, pp. 263–284, Plenum Publishing Corp., New York, N. Y., 1977

Wind action over water generates waves and surface drift. The logarithmic velocity profile in air can be used to determine the surface stress with a suitable choice of roughness height. A corresponding logarithmic profile is found below the interface and yields a surface stress equivalent to that found from the air profile. The wind induced set-up depends on water depth, surface and bottom boundary stresses, and atmospheric pressure gradient. Modelling relationships to simulate set-up under laboratory conditions are discussed. The momentum transfer from wind to waves is found to be approximately 10–20 percent of the total wind induced stress. The net energy transfer to any wave spectral component depends on nonlinear wave–wave transfers in addition to that received directly from wind less that dissipated by viscosity or turbulence.

SHIMADA, K.

S026 Thermionic Energy Conversion Technology—Present and Future

K. Shimada and J. F. Morris (Lewis Research Center)

Preprint 77-500, AIAA Conf. Future Aerosp. Power Sys., St. Louis, Mo., Mar. 1–3, 1977

Thermionic energy conversion has been and is being considered for potential applications in space nuclear power systems. More recently, terrestrial power systems utilizing thermionic energy conversion are being investigated for their potential system performance and technological requirements. Salient features of thermionic converters, which are the key elements in the system, are: (1) a static device, (2) relatively high conversion efficiency, and (3) high operating temperatures. The static operation is probably one of the most important factors in space application. On the other hand, high temperature operations make topping applications attractive for terrestrial use. For space applications, conversion efficiencies in the order of 20% appear adequate for space missions being considered, whereas considerably higher efficiencies and lower cost have to be realized for terrestrial applications.

SHINOZUKA, M.

S027 Digital Generation of Alongwind Velocity Field

M. Shinozuka (Columbia University) and R. Levy

J. Eng. Mech. Div., ASCE, Vol. 103, No. EM4, pp. 689–700, August 1977

The loss of surface efficiency performance of a paraboloidal reflector antenna results from various sources. In

particular, the surface deformation from its ideal paraboloidal shape due to random wind and temperature as well as deterministic gravity loading is an important factor to be considered. The loss of efficiency associated with the surface deformation is usually measured in terms of the rms of the "half-path length difference" of the microwave (RF) energy beam. When the reflector surface is subjected to such random loading as environmental wind pressures, the rms value is also a random quantity and its statistical variation is of obvious engineering significance. The present paper proposes use of a Monte Carlo method of estimating such statistical variation of the rms value and describes in detail how digital generation of the two-dimensional wind velocity field, which plays a vital role in the current Monte Carlo approach, can be carried out.

SIEGAL, B. S.

S028 Detection of Alteration Associated With a Porphyry Copper Deposit in Southern Arizona

M. J. Abrams and B. S. Siegal

Technical Memorandum 33-810, February 1, 1977

For abstract, see Abrams, M. J.

S029 Effect of Vegetation on Rock and Soil Type Discrimination

B. S. Siegal and A. F. H. Goetz

Photogram. Eng. Remote Sensing, Vol. 43, No. 2, pp. 191–196, February 1977

The effect of naturally occurring vegetation on the spectral reflectance of earth materials in the wavelength region of 0.45 to 2.4 μm has been determined by computer averaging of in situ acquired spectral data. Natural vegetation can significantly mask and alter the spectral response of the ground as measured by aircraft and satellite multispectral scanners. The significance of the vegetative cover depends on the amount and type of vegetation and the spectral reflectance of the ground. Low albedo materials are the most significantly affected and may be altered beyond recognition with only ten percent green vegetation cover. Dead or dry vegetation does not greatly alter the shape of the spectral reference curve and only changes the albedo with minimum wavelength dependency. With increasing amounts of vegetation the LANDSAT MSS band ratios 4/6, 4/7, 5/6, and 5/7 are significantly decreased whereas MSS ratios 4/5 and 6/7 remain relatively constant.

SIEGEL, H. L.

S030 Improvements in Navigation Resulting from the Use of Dual Spacecraft Radiometric Data

C. C. Chao, H. L. Siegel, and V. J. Ondrasik

The Deep Space Network Progress Report 42-38: January and February 1977, pp. 55–65, April 15, 1977

For abstract, see Chao, C. C.

SIEVERS, M. W.

S031 A High-Speed Computer Link for Moderate Distances and Noisy Environments

M. W. Sievers

The Deep Space Network Progress Report 42-42: September and October 1977, pp. 95–99, December 15, 1977

To satisfy the need for a fully duplex high-speed computer data link for the antenna automation project at DSS 13, a very simple and inexpensive scheme was employed. The link requires two coaxial cables over which is sent a unipolar "digital frequency modulated" signal in which a logical 1 has twice the frequency of a logical 0. Optical isolators and filters reduce ground loop effects and increase noise immunity. Tests conducted in various environments and over different cable lengths at JPL, DSS 14, and DSS 13 have indicated that the link is highly effective.

S032 DSS 13 Automated Antenna Pointing Subsystem Phase 1 Hardware

M. W. Sievers

The Deep Space Network Progress Report 42-42: September and October 1977, pp. 100–109, December 15, 1977

An automated antenna pointing subsystem (APS) is being installed at DSS 13 as part of the unattended station project. The function of the APS is to track an instructed position with the 26-meter antenna and to monitor the antenna servo system and meteorological conditions to ensure a proper operational environment. This article discusses the now-completed first phase of the digital hardware portion of the APS development.

SIMON, M. K.

S033 Noncoherent Pseudonoise Code Tracking Performance of Spread Spectrum Receivers

M. K. Simon

IEEE Trans. Commun., Vol. COM-25, No. 3, pp. 327–345, March 1977

The optimum design and performance of two noncoherent PN tracking loop configurations, namely the delay-

locked loop and tau-dither loop, are described. In particular, the bandlimiting effects of the bandpass arm filters are considered by demonstrating that for a fixed data rate and data signal-to-noise ratio, there exists an optimum filter bandwidth in the sense of minimizing the loop's tracking jitter. Both the linear and nonlinear loop analyses are presented and the region of validity of the former relative to the latter is indicated. In addition, numerical results are given for several filter types. For example, assuming ideal bandpass arm filters, it is shown that the tau-dither loop requires approximately 1 dB more signal-to-noise ratio than the delay-locked loop for equal rms tracking jitters.

SINES, G.

S034 Spalling and Cracking in Alumina by Compression

M. Adams and G. Sines

J. Amer. Ceram. Soc., Vol. 60, Nos. 5–6, pp. 221–226, May–June 1977

For abstract, see Adams, M.

SJOGREN, W. L.

S035 Quantitative Mass Distribution Models for Mare Orientale

W. L. Sjogren and J. C. Smith (Pennsylvania State University)

Proc. Seventh Lunar Sci. Conf., pp. 2639–2648, 1976

Six theoretical models for the mass distribution of Mare Orientale were tested using five gravity profiles extracted from radio-tracking data of orbiting spacecraft. The models with surface mass and moho relief produced the best results. Although there is a mascon-type anomaly in the central maria region, Mare Orientale is a large negative gravity anomaly. This is produced primarily by the empty ring basin. Had the basin filled with maria material, it seems likely that it would have produced a mascon such as those presently existing in flooded frontside circular basins.

SLAUGHTER, D. W.

S036 Standard High-Reliability Integrated Circuit Logic Packaging

D. W. Slaughter

The Deep Space Network Progress Report 42-39: March and April 1977, pp. 130–156, June 15, 1977

A family of standard, high-reliability hardware used for packaging digital integrated circuits is described. The design transition from early prototypes to production hardware is covered and future plans are discussed. This article includes detail descriptions of the interconnection techniques, connectors and related hardware available, both at the microcircuit packaging and main-frame level; general applications information is also provided.

SLOBIN, S.

S037 X-Band Atmospheric Noise Temperature Statistics at Goldstone DSS 13, 1975–1976

S. Slobin, M. Reid, R. Gardner, and D. Cheng

The Deep Space Network Progress Report 42-38: January and February 1977, pp. 70–76, April 15, 1977

X-band noise temperature data have been taken at Goldstone DSS 13 for the period August 1975 through January 1977. A description of the experiment is given along with probability density functions for zenith noise temperature increase during all year quarters and day quarters. Elevation angle modeling of the data is described along with a discussion of the problems associated with relating wide beamwidth statistics (this report) to narrow beamwidth antennas.

SLOBIN, S. D.

S038 DSN Water Vapor Radiometer Development—A Summary of Recent Work, 1976–1977

S. D. Slobin and P. D. Batelaan

The Deep Space Network Progress Report 42-40: May and June 1977, pp. 71–75, August 15, 1977

A water vapor radiometer (WVR) has been developed which measures the atmospheric noise temperature at two different frequencies. These noise temperatures are used in empirical-theoretical equations which yield tropospheric range delay, in centimeters, through the atmosphere along the beam of the WVR. This range correction is then applied, as needed, to measurements concerning spacecraft range and to VLBI baseline determinations. The results of the March 1976 Pt. Mugu tests are given and equipment modifications and JPL tests since that time are discussed.

SMITH, E. J.

S039 Further Evidence of a Latitude Gradient in the Solar Wind Velocity

E. J. Rhodes, Jr., and E. J. Smith

J. Geophys. Res., Space Phys., Vol. 81, No. 34, pp. 5833–5840, December 1, 1976

For abstract, see Rhodes, E. J., Jr.

S040 August 1972 Solar-Terrestrial Events: Observations of Interplanetary Shocks at 2.2 AU

E. J. Smith, L. Davis, Jr. (California Institute of Technology), P. J. Coleman, Jr. (University of California, Los Angeles), D. S. Colburn (Ames Research Center), P. Dyal (Ames Research Center), and D. E. Jones (Brigham Young University)

J. Geophys. Res., Space Phys., Vol. 82, No. 7, pp. 1077–1086, March 1, 1977

Pioneer 10 magnetic field measurements, supplemented by previously published plasma data, have been used to identify shocks at 2.2 AU associated with the large solar flares of early August 1972. The first three flares, which gave rise to three forward shocks at Pioneer 9 and at earth, led to only a single forward shock at Pioneer 10. The plasma driver accompanying the shock has been tentatively identified. A local shock velocity at Pioneer 10 of 717 km/s has been estimated by assuming that the shock was propagating radially across the interplanetary magnetic field. This velocity and the rise time of $\cong 2$ s simply a shock thickness of $\sim$1400 km, which appears to be large in comparison with the characteristic plasma lengths customarily used to account for the thickness of the earth's bow shock. This Pioneer 10 shock is identified with the second forward shock observed at Pioneer 9, which was then at 0.8 AU and radially aligned with Pioneer 10, since it was apparently the only Pioneer 9 shock that was also driven.

The general finding that the local velocities of both shocks are approximately equal at 0.8 and 2.2 AU but significantly slower than the average speeds nearer the sun is interpreted as evidence of a major deceleration of the shocks as they propagate outward from the sun that is essentially completed when the shocks reach 0.8 AU, there being little, if any, subsequent deceleration. This conclusion is qualitatively inconsistent with previous inferences of a deceleration of the shocks as they propagate from 0.8 to 2.2 AU. A third, reverse shock is also identified in the Pioneer 10 data which was not seen either at Pioneer 9 or at earth. The estimated speed of this shock is 530 km/s, and its estimated thickness is $<$500 km, which compares well with an anticipated proton inertial length of 500 km.

S041 Two Types of Magnetospheric ELF Chorus and Their Substorm Dependences

B. T. Tsurutani and E. J. Smith

J. Geophys. Res., Space Phys., Vol. 82, No. 32, pp. 5112–5128, November 1, 1977

For abstract, see Tsurutani, B. T.

S042 The August 1972 Solar-Terrestrial Events: Interplanetary Magnetic Field Observations

E. J. Smith

Space Sci. Rev., Vol. 19, pp. 661–686, 1976

A review is presented of the interplanetary magnetic field observations acquired in early August 1972 when four solar flares erupted in McMath Plage region 11976. Measurements of the interplanetary field were obtained by Earth satellites, HEOS-2 and Explorer 41, and by Pioneers 9 and 10 which, by good fortune, were radially aligned and only 45° east of the Earth–Sun direction. In response to the four flares, four interplanetary shocks were seen at Earth and at Pioneer 9, which was then at a heliocentric distance of 0.78 AU. However, at Pioneer 10, which was 2.2 AU from the Sun, only two forward shocks and one reverse shock were seen. The available magnetic field data acquired in the vicinity of the shocks are presented. Efforts to identify corresponding shocks at the several locations and to deduce their velocities of propagation between 0.8 and 2.2 AU are reviewed. The early studies were based on average velocities between the Sun and Pioneer 9, the Sun and Earth and the Sun and Pioneer 10. A large deceleration of the shocks between the Sun and 0.8 AU as well as between 0.8 and 2.2 AU was inferred. More recently the local velocities of the shocks at Pioneers 9 and 10 have become available. A comparison of these velocities shows little, if any, deceleration between 0.8 and 2.2 AU and implies that most or all of the deceleration actually occurred nearer the Sun. Evidence is also presented that shows a significant departure of the flare-generated shock fronts from spherical symmetry.

SMITH, E. K.

S043 Sharing the 620–790 MHz Band Allocated to Terrestrial Television With an Audio-Bandwidth Social Service Satellite System

E. K. Smith and E. E. Reinhart

JPL Publication 77-71, October 31, 1977

A social service satellite system (S^4) is proposed for 620 to 800 MHz (UHF TV channels 39 through 68) to satisfy a need for thin-route, interactive, audio-bandwidth communication circuits between one or more sophisticated base stations and a large number of smaller fixed stations.

Each S^4 provides 126 simplex audio-bandwidth channels. Five S^4 systems fill the available channels in a given geographic area. However, only three S^4 systems can be accommodated in a single satellite owing to the need to provide adequate separation between uplink and downlink channels.

Basically, the S^4 proposes to use the 2 MHz wide, 40 dB deep (relative to the luminance carrier) trough, which exists 1–3 MHz above the luminance carrier in the NTSC (National Television Systems Committee) color television system. Each 2 MHz segment is divided into 42 audio-bandwidth channels, each 47.2 kHz wide, operating with frequency modulation in a single channel per carrier mode. Six of these 2 MHz segments (3 downlink, 3 uplink) constitute one S^4.

Interference calculations indicate that the S^4 can be accommodated in the UHF television band if restricted to power flux density values currently given in the International Telecommunications Union Radio Regulations under Footnote 332A, and to protection ratios specified by the CCIR (International Radio Consultative Committee) for non-synchronized CW interference. It is proposed to synchronize the S^4 to the line-scan frequency of the television transmissions, but the S^4 is engineered so that this synchronization is not required.

SMITH, J. C.

S044 Quantitative Mass Distribution Models for Mare Orientale

W. L. Sjogren and J. C. Smith (Pennsylvania State University)

Proc. Seventh Lunar Sci. Conf., pp. 2639–2648, 1976

For abstract, see Sjogren, W. L.

SMITH, J. G.

S045 A Bandwidth-Compressive Modulation System

J. G. Smith

Progr. Astronaut. Aeronaut., Vol. 54, pp. 513–539, 1977

As a result of a 4-yr NASA-sponsored research program in efficient spectrum utilization, the technical feasibility of very high-rate, bandwidth-compressive, digital modulation techniques has been established. Its space qualification and utility are to be demonstrated on an early Shuttle Spacelab. The term "bandwidth-compressive" means that less signal bandwidth is required than data bandwidth or, more precisely, that the signal transmitted switches at a slower rate than the data rate. The phrase "bandwidth-compressive modulation" means that the compression is achieved not by removing redundancy from the data (data compression), but rather by modulating the carrier phase and amplitude with blocks of data bits. The modulation described here is quadrature amplitude shift keying (QASK), a logical extension of quadrature phase shift keying (QPSK, or quadriphase). QASK is a cost-effective form of combined phase-and-amplitude modulation. That is, n-bit QASK, like most phase-amplitude forms of modulation, requires considerably less transmitter power than comparably performing n-PSK, whereas among the class of all n-bit phase-modulation types, n-bit QASK performs nearly optimally but requires the least circuit complexity. A simple, unique microwave transmitter is described which provides high-rate QASK modulation with 4:1 bandwidth compression. A suppressed carrier multiple loop QASK receiver provides the necessary phase tracking, automatic gain control (AGC), and symbol timing.

SMOKLER, M. I.

S046 Feasibility Study on the Design of a Probe for Rectal Cancer Detection

V. J. Anselmo, R. E. Frazer, D. H. LeCroissette, J. A. Roseboro, and M. I. Smokler

JPL Publication 77-31, April 15, 1977

For abstract, see Anselmo, V. J.

SOHA, J. M.

S047 Variable Threshold Zonal Filtering

A. A. Schwartz and J. M. Soha

Appl. Opt., Vol. 16, No. 7, pp. 1779–1781, July 1977

For abstract, see Schwartz, A. A.

S048 Digital Processing of the Mariner 10 Images of Venus and Mercury

J. M. Soha, D. J. Lynn, J. A. Mosher, and D. A. Elliott

J. Appl. Photogr. Eng., Vol. 3, No. 2, pp. 82–92, 1977

An extensive effort was devoted to the digital processing of the Mariner 10 images of Venus and Mercury at the Image Processing Laboratory of the Jet Propulsion Laboratory. This effort was designed to optimize the display of the considerable quantity of information contained in the images. Several image restoration, enhancement, and transformation procedures were applied; examples of these techniques are included. A particular task was the construction of large mosaics which characterize the

surface of Mercury and the atmospheric structure of Venus.

SOMOANO, R. B.

S049 Electrical, Magnetic, and Optical Properties of the Tetrathiafulvalene (TTF) Pseudohalides, $(TTF)_{12}(SCN)_7$ and $(TTF)_{12}(SeCN)_7$

R. B. Somoano, A. Gupta, V. Hadek, M. Novotny (Stanford University), M. Jones (Tulane University), T. Datta (Tulane University), R. Deck (Tulane University), and A. M. Hermann (Tulane University)

Phys. Rev., Pt. B: Solid State, Vol. 15, No. 2, pp. 595–601, January 15, 1977

The electrical, magnetic, and optical properties of charge-transfer salts containing tetrathiafulvalene (TTF) and the pseudohalides, thiocyanate (SCN) and selenocyanate (SeCN) have been investigated. These salts are quasi-one-dimensional compounds containing cation radicals only, in contrast to a cation-radical-anion-radical system, such as tetrathiafulvalene tetracyanoquinodimethane (TTF) (TCNQ). Measurements of electrical conductivity, thermoelectric power, and optical reflectivity of single crystals of the nonstoichiometric salts $(TTF)_{12}(SCN)_7$ and $(TTF)_{12}(SeCN)_7$ show metal-like characteristics above 200°K (high-temperature region). The conductivities at room temperature are ~750 $\Omega^{-1}cm^{-1}$, comparable to those found in (TTF)(TCNQ), and increase with decreasing temperature down to ~200°K. The thermoelectric power at room temperature is small and positive (~9 $\mu V/°K$), and decreases linearly with decreasing temperature in this region (as expected for metal-like hole conduction along the TTF chains). The ESR intensity, however, decreases with decreasing temperature above 200°K. At 170°K a metal-nonmetal transition occurs, and the transport and magnetic properties below this temperature are characteristic of a semiconducting state.

SRIVASTAVA, S. K.

S050 Quantum Mechanical and Crossed Beam Study of Vibrational Excitation of N_2 by Electron Impact at 30–75 eV

D. G. Truhlar (University of Minnesota), M. A. Brandt (University of Minnesota), S. K. Srivastava, S. Trajmar, and A. Chutjian

J. Chem. Phys., Vol. 66, No. 2, pp. 655–663, January 15, 1977

For abstract, see Truhlar, D. G.

STABEKIS, P. D.

S051 Microbiological Profiles of the Viking Spacecraft

J. R. Puleo, N. D. Fields, S. L. Bergstrom, G. S. Oxborrow, P. D. Stabekis, and R. C. Koukol

Appl. Environ. Microbiol., Vol. 33, No. 2, pp. 379–384, February 1977

For abstract, see Puleo, J. R.

STALLKAMP, J. A.

S052 Parametric Studies of North East Corridor Rail Passenger Service Between New York City and Washington, D. C.

J. A. Stallkamp

JPL Publication 77-75, October 3, 1977

A parametric study of high speed rail passenger service between New York City and Washington, D.C. is carried out. From published data a series of speed profiles is developed that progressively have fewer speed restrictions and increasing maximum speeds. The significant equipment characteristics include the portion of the total weight on driven axles, i.e., Multiple Unit (MU) cars versus locomotive hauled trains, and the short term tractive effort rating of the motors. The ratio of acceleration plus braking time to total time is provided for validation of the use of the short term propulsion equipment ratings. Absolute trip times are shown to be determined primarily by the allowed speed profile. Locomotive hauled train weights and lengths and the locomotive capabilities and characteristics that are required to make the performance of this type of train comparable to that of MU trains are given.

STANLEY, A. G.

S053 Voyager Electronic Parts Radiation Program: Final Report

A. G. Stanley, K. E. Martin, and W. E. Price

JPL Publication 77-41, Vol. I, September 15, 1977

In the final report for the Voyager parts radiation program, the program philosophy, radiation, environment, device hardening efforts, and radiation test methods are discussed in detail. In addition, the results of characterization testing and sample screening of over 200 device types, in a radiation environment, are summarized.

STANTON, P. H.

S054 Effects of an Ion-Thruster Exhaust Plume on S-Band Carrier Transmission

W. E. Ackerknecht and P. H. Stanton

J. Spacecraft Rockets, Vol. 14. No. 7, pp. 445–446, July 1977

For abstract, see Ackerknecht, W. E.

STEARNS, J. W.

S055 An Interstellar Precursor Mission

L. D. Jaffe, C. Ivie, J. C. Lewis, R. Lipes, H. N. Norton, J. W. Stearns, L. D. Stimpson, and P. Weissman

JPL Publication 77-70, October 30, 1977

For abstract, see Jaffe, L. D.

STELZRIED, C.

S056 Computation of Spacecraft Signal Raypath Trajectories Relative to the Sun

R. Cannon and C. Stelzried

The Deep Space Network Progress Report 42-38: January and February 1977, pp. 77–82, April 15, 1977

For abstract, see Cannon, R.

STELZRIED, C. T.

S057 Calibration Radio Sources for Radio Astronomy: Precision Flux-Density Measurements at 2295 MHz

M. J. Klein and C. T. Stelzried

Astron. J., Vol. 81, No. 12, pp. 1078–1083, December 1976

For abstract, see Klein, M. J.

STEVENS, G. L.

S058 Complex Mixer System Modifications

G. L. Stevens

The Deep Space Network Progress Report 42-42: September and October 1977, pp. 88–91, December 15, 1977

Modifications of the complex mixer system to increase bandwidth and number of channels have been made. Three modified complex mixers have been installed at DSS 14 and were used to process planetary radar signals in March and April of 1977.

STIMPSON, L. D.

S059 An Interstellar Precursor Mission

L. D. Jaffe, C. Ivie, J. C. Lewis, R. Lipes, H. N. Norton, J. W. Stearns, L. D. Stimpson, and P. Weissman

JPL Publication 77-70, October 30, 1977

For abstract, see Jaffe, L. D.

STINNETT, W. G.

S060 Mark III-77 DSN Command System

W. G. Stinnett

The Deep Space Network Progress Report 42-37: November and December 1976, pp. 4–11, February 15, 1977

A description of the Mark III-77 DSN Command System configuration is discussed. A comparison is made with the Mark III-75 System Configuration to explain the implementation required to establish the Mark III-77 System Configuration.

S061 DSN Monitor and Control System, Mark III-77

W. G. Stinnett

The Deep Space Network Progress Report 42-41: July and August 1977, pp. 10–15, October 15, 1977

A description of the DSN Monitor and Control System, Mark III-77 configuration is discussed. The implementation is noted that explains the evolution from the Mark III-75 to the Mark III-77 configuration.

STIRN, R. J.

S062 High Efficiency Thin-Film GaAs Solar Cells

R. J. Stirn

JPL Publication 77-60, September 1977

A solar-cell research task was begun in January 1976 with the following objectives: (1) to investigate the feasibility of growing large-grain polycrystalline GaAs by chemical vapor deposition on recrystallized Ge films, (2) to fabricate AMOS (Antireflection-Coated Metal-Oxide-Semiconductor) solar cells on the films, and (3) to investigate the physics and chemistry of AMOS solar cells on single crystal GaAs. This report discusses the several oxidation techniques investigated that have been found to increase the open circuit of metal-GaAs Schottky barrier solar cells, the oxide chemistry, the attempts to measure surface state parameters, the evolving characteristics of the solar cell as background contamination was decreased (but not eliminated), the results of focused Nd/YAG laser beam recrystallization of Ge films evaporated onto tungsten, and the studies of AMOS solar cells

fabricated on sliced polycrystalline GaAs wafers. Also discussed are projected materials availability and costs for GaAs thin-film solar cells.

S063 Technology of GaAs Metal–Oxide–Semiconductor Solar Cells

R. J. Stirn and Y. C. M. Yeh

IEEE Trans. Electron Devices, Vol. ED-24, No. 4, pp. 476–483, April 1977

The growth of an oxide interfacial layer was recently found to increase the open-circuit voltage (V_{oc}) and efficiency by up to 60 percent in GaAs metal-semiconductor solar cells. Several oxidation techniques have been developed which will provide the necessary oxide thickness and chemical structure. Details of these techniques using ozone, water-vapor-saturated oxygen, or oxygen gas discharges are described, as well as apparent crystallographic orientation effects. Preliminary results of the oxide chemistry obtained from X-ray, photoelectron spectroscopy are given. Ratios of arsenic oxide to gallium oxide of unity or less seem to be preferable. Samples with the highest V_{oc} predominantly have As^{+3} in the arsenic oxide rather than As^{+5}. A major difficulty at this time is a reduction in open-circuit voltage by 100–200 mV when the antireflection coating is vacuum-deposited. Without this effect, values of about 750 mV for V_{oc} and 15-percent efficiency with air mass of 1 sun can be obtained with single-crystal GaAs. All techniques are compatible with polycrystalline GaAs thin films.

STRAND, L. D.

S064 Theoretical Combustion Modeling Study of Nitramine Propellants

K. N. R. Ramohalli (California Institute of Technology) and L. D. Strand

J. Spacecraft Rockets, Vol. 14, No. 7, pp. 427–433, July 1977

For abstract, see Ramohalli, K. N. R.

STULTZ, J. W.

S065 Viking Mars Orbiter 1975 Solar Energy Controller

J. W. Stultz

J. Spacecraft Rockets, Vol. 14, No. 5, pp. 294–299, May 1977

The Viking Orbiter system is part of the overall Viking Project managed by the Viking Project Office at NASA Langley Research Center. Two spacecraft were launched on Titan IIIE/Centaur launch vehicles in August and September 1975. Solar energy for temperature-control purposes is introduced into the propulsion module of the Orbiter. The energy enters by way of four individually commandable solar energy controllers (SEC's). This paper summarizes the SEC thermal development, design, test, and flight results.

SWINDLEHURST, J. A.

S066 Intermediate Data Record Support for the Viking Prime Mission

J. A. Swindlehurst

The Deep Space Network Progress Report 42-37: November and December 1976, pp. 26–34, February 15, 1977

In producing Intermediate Data Records (IDRs) to satisfy the demanding requirements of the Viking Prime Mission, the DSN was called upon to make many procedural, hardware, and software workarounds to compensate for the deficiencies that inevitably come to light when a complex new capability such as the Network Data Processing Area is exposed to a high-demand operational environment for the first time. In due course, most of the problems were identified and corrected, or modifications were made to the IDR system design. Despite these difficulties, IDR production for the Viking Prime Mission achieved an astonishing level of performance both in quantity of data delivered and timeliness of delivery. This article discusses the more significant problems encountered in IDR production during the mission and gives a definitive statement of the production levels accomplished.

SYDNOR, R. L.

S067 Hydrogen Maser Frequency Standards for the Deep Space Network

P. R. Dachel, S. M. Petty, R. F. Meyer, and R. L. Sydnor

The Deep Space Network Progress Report 42-40: May and June 1977, pp. 76–83, August 15, 1977

For abstract, see Dachel, P. R.

TADA, H. Y.

T001 Solar Cell Radiation Handbook

H. Y. Tada (TRW Systems Group) and J. R. Carter, Jr.

JPL Publication 77-56, November 1, 1977

This handbook is intended to furnish the reader with the necessary tools to permit him to predict the degradation of solar cell electrical performance in any given space

radiation environment. It begins with an introduction to solar cell theory, describing how cells are manufactured and how they are modeled mathematically. The interaction of energetic charged particle radiation with solar cells is discussed in detail and the concept of 1 MeV equivalent electron fluence is introduced. The space radiation environment is described and methods of calculating equivalent fluences for the space environment are developed. A computer program was written to perform the equivalent fluence calculations and a Fortran listing of the program is included. Finally, an extensive body of data detailing the degradation of solar cell electrical parameters as a function of 1 MeV electron fluence is presented.

TALBOT, T. D.

T002 On the Mass of Saturn's Rings

W. I. McLaughlin and T. D. Talbot

Mon. Not. R. Astr. Soc., Vol. 179, pp. 619–634, 1977

For abstract, see McLaughlin, W. I.

TAUKE, G. J.

T003 Dual-Spin Attitude Control for Outer Planet Missions

R. S. Ward and G. J. Tauke

JPL Publication 77-74, December 15, 1977

For abstract, see Ward, R. S.

TAUSWORTHE, R. C.

T004 Stochastic Models for Software Project Management

R. C. Tausworthe

The Deep Space Network Progress Report 42-37: November and December 1976, pp. 118–126, February 15, 1977

This article presents a method for determining the number and characteristics of milestones to be achieved during a development project in order that effective monitors of progress can be provided. Projections of progress data lead to estimates of the completion with determinable accuracy, but accuracy imposes a requirement that the number of milestones be inversely proportional to the estimate-error variance, and that the milestones themselves be defined in such a way that each represents approximately the same level of effort to complete.

T005 Discovery and Repair of Software Anomalies

R. C. Tausworthe

The Deep Space Network Progress Report 42-39: March and April 1977, pp. 49–59, June 15, 1977

This article presents a simple model which explains anomaly discovery and repair phenomena when applied to variations in work load and multiple-stage testing. The theory shows that estimates of anomaly levels and team capability can be predicted after a significant fraction of the anomalies has been found, and indicates procedures for applying these figures to schedule estimation and work-load assignment. Of particular interest is the demonstration that end-to-end testing of programs in other than the operational environment is not generally cost effective.

T006 CRISPFLOW, A Structured Program Design Flowcharter

R. C. Tausworthe and K. C. Landon

The Deep Space Network Progress Report 42-41: July and August 1977, pp. 112–126, October 15, 1977

This article describes the design, prototype implementation, and use of an automated tool, called CRISPFLOW, for generating design flowcharts of structured programs. The user of this tool provides a file of English-like textual statements which directs the drawing of the flowcharts. Layout, symbol sizing, location of text, scaling, and other routine tasks are performed automatically.

TAYLOR, F. H. J.

T007 Deep Space Network to Viking Orbiter Telecommunication Link Effects During 1976 Superior Conjunction

F. H. J. Taylor

The Deep Space Network Progress Report 42-40: May and June 1977, pp. 57–70, August 15, 1977

Viking superior conjunction occurred November 25, 1976 with an angular separation between the sun and Mars of one-quarter degree. For three years prior to this date, the Viking Project and the Deep Space Network had planned the spacecraft and ground station activities and configuration during the three-month superior conjunction period. This article describes, in a narrative and qualitative manner, the planning for and the observations made during Viking superior conjunction. These results are built upon observations made during previous Mariner missions and will, in turn, be useful for the next Viking conjunction and for future Mariner-class superior conjunction planning.

TAYLOR, F. W.

T008 Remote Sounding of Cloudy Atmospheres. III. Experimental Verifications

M. T. Chahine, H. H. Aumann, and F. W. Taylor

J. Atmos. Sci., Vol. 34, No. 5, pp. 758–765, May 1977

For abstract, see Chahine, M. T.

TAYLOR, H.

T009 On the Existence of Binary Simplex Codes

H. Taylor

The Deep Space Network Progress Report 42-39: March and April 1977, pp. 36–37, June 15, 1977

Using a very simple combinatorial construction, we prove the existence of a binary simplex code with m codewords for all $m \geq 1$. The problem of the shortest possible length is left open.

THIELEN, J. A.

T010 Mission Design for SEASAT-A, An Oceanographic Satellite

E. Cutting, G. H. Born, J. C. Frautnick, W. I. McLaughlin, R. A. Neilson, and J. A. Thielen (Lockheed Missiles & Space Co.)

Preprint 77-31, AIAA Fifteenth Aerosp. Sci. Meet., Los Angeles, Calif., Jan. 24–26, 1977

For abstract, see Cutting, E.

THOMPSON, A. M.

T011 The Navigation System of the JPL Robot

A. M. Thompson

JPL Publication 77-20, July 15, 1977

The control structure of the JPL research robot and the operations of the navigation subsystem are discussed. The robot functions as a network of interacting concurrent processes distributed among several computers and coordinated by a central executive. The results of scene analysis are used to create a segmented terrain model in which surface regions are classified by traversibility. The model is used by a path-planning algorithm, PATH*, which uses tree search methods to find the optimal path to a goal. In PATH*, the search space is defined dynamically as a consequence of node testing. Maze-solving and the use of an associative data base for context-dependent node generation are also discussed. Execution of a planned path is accomplished by a feedback guidance process with automatic error recovery.

THOMPSON, T. W.

T012 Ocean Wave Patterns Under Hurricane Gloria: Observation with an Airborne Synthetic-Aperture Radar

C. Elachi, T. W. Thompson, and D. King

Science, Vol. 198, pp. 609–610, November 11, 1977

For abstract, see Elachi, C.

THORMAN, H. C.

T013 Evaluation of DSN Data Processing With 7200-b/s GCF High-Speed Data Interfaces

H. C. Thorman

The Deep Space Network Progress Report 42-37: November and December 1976, pp. 132–135, February 15, 1977

Test results confirm that the Deep Space Station (DSS) and Network Operations Control Center (NOCC) processing of telemetry, command, radio metric, and monitor data with the existing DSN Mark III-75 configuration will be unaffected by the recent change of the Ground Communications Facility (GCF) High-Speed Data Subsystem to a clock rate of 7200 bits per second.

T014 DSN Test and Training System, Mark III-77

H. C. Thorman

The Deep Space Network Progress Report 42-38: January and February 1977, pp. 4–15, April 15, 1977

Implementation of the DSN Test and Training System, Mark III-77, is currently in progress. The Mark III-77 system is configured to support DSN testing and training in preparation for the Mariner-Jupiter-Saturn 1977 and Pioneer-Venus 1978 missions, in addition to the on-going in-flight missions. DSN Test and Training System capabilities include functions performed in the Deep Space Stations, Ground Communications Facility, and Network Operations Control Center.

THORNTON, C. L.

T015 Givens Transformation Techniques for Kalman Filtering

C. L. Thornton and G. J. Bierman

ORIGINAL PAGE IS
OF POOR QUALITY

Acta Astronautica, Vol. 4, pp. 847–863, 1977

This paper examines the numerical stability and accuracy of a new Kalman filtering technique. The filter algorithm is based upon square-root-free Givens transformation methods and involves an upper triangular covariance factorization $P = UDU^T$. Stability of the U–D algorithm is studied by applying this method and several other Kalman filter algorithms to a realistic orbit determination problem. This study demonstrates how the U–D filter can produce results which are orders of magnitude more accurate than those obtained with the conventional and stabilized Kalman algorithms. Computational efficiency of our algorithms is demonstrated by showing that CPU timing requirements for our U–D formulation differ negligibly from the conventional Kalman requirements.

T016 **Gram–Schmidt Algorithms for Covariance Propagation**

C. L. Thornton and G. J. Bierman

Int. J. Control, Vol. 25, No. 2, pp. 243–260, 1977

This paper addresses the time propagation of triangular covariance factors. Attention is focused on the square-root free factorization, $P = UDU^T$, where U is unit upper triangular and D is diagonal. An efficient and reliable algorithm for U–D propagation is derived which employs Gram–Schmidt orthogonalization. Partitioning the state vector to distinguish bias and coloured process noise parameters increases mapping efficiency. Cost comparisons of the U–D, Schmidt square-root covariance and conventional covariance propagation methods are made using weighted arithmetic operation counts. The U–D time update is shown to be less costly than the Schmidt method; and, except in unusual circumstances, it is within 20% of the cost of conventional propagation.

T017 **Numerical Comparison of Discrete Kalman Filter Algorithms: Orbit Determination Case Study**

G. J. Bierman and C. L. Thornton

Proc. IEEE Conf. Decision and Control, Clearwater, Fla., Dec. 1–3, 1976, pp. 859–872

For abstract, see Bierman, G. J.

THORPE, T. E.

T018 **The Viking Orbiter Visual Imaging Subsystem**

J. B. Wellman, F. P. Landauer, D. D. Norris, and T. E. Thorpe

J. Spacecraft Rockets, Vol. 13, No. 11, pp. 660–666, November 1976

For abstract, see Wellman, J. B.

TOMOVIC, R.

T019 **Pattern Recognition and Control in Manipulation**

A. K. Bejczy and R. Tomovic (University of California, Los Angeles)

Proc. IEEE Conf. Decision and Control, Clearwater Beach, Fla., Dec. 1–3, 1976, pp. 374–381

For abstract, see Bejczy, A. K.

TOTH, R. A.

T020 **Measurement of the Fundamental Vibration–Rotation Spectrum of ClO**

R. T. Menzies, J. S. Margolis, E. D. Hinkley, and R. A. Toth

Appl. Opt., Vol. 16, No. 3, pp. 523–525, March 1977

For abstract, see Menzies, R. T.

T021 **Temperature Sounding From the Absorption Spectrum of CO_2 at 4.3 μm**

R. A. Toth

Appl. Opt., Vol. 16, No. 10, pp. 2661–2668, October 1977

A new method is described for obtaining the temperature profile in the stratosphere and lower mesosphere from observations of the absorption spectrum of the high J lines of carbon dioxide at 4.3 μm. This concept is based upon the measurement of the integrated absorption of individual CO_2 lines whose strengths depend strongly on temperature and that the absorption of these lines are obtained from measurements of the solar or stellar spectrum through an atmospheric path. The technique involves a rapidly converging iterative process in which the equivalent widths of the individual vibration–rotation lines of CO_2 are used. Theoretical calculations are presented for balloon and satellite observations using a model atmosphere. Experimental results are given from spectra obtained with a balloon-borne Fourier interferometer spectrometer in which the sun was observed at low zenith angles. The experimental results are compared to rocketsonde data.

T022 **The Vertical Distribution of HCl in the Stratosphere**

O. F. Raper, C. B. Farmer, R. A. Toth, and B. D. Robbins

Geophys. Res. Lett., Vol. 4, No. 11, pp. 531–534, November 1977

For abstract, see Raper, O. F.

T023 Absorption Strength Measurement of the ν_1 Band of Methyl Chloride

J. S. Margolis and R. A. Toth

J. Mol. Spectros., Vol. 66, pp. 30–34, 1977

For abstract, see Margolis, J. S.

T024 Line Positions and Strengths of Methane in the 2862 to 3000 cm^{-1} Region

R. A. Toth, L. R. Brown (Florida State University), and R. H. Hunt (Florida State University)

J. Mol. Spectros., Vol. 67, Nos. 1–3, pp. 1–33, September 15, 1977

Measurements of line center positions and strengths of 1591 absorptions of CH_4 in the 2862 to 3000 cm^{-1} region have been made at high resolution. New assignments have been determined for several components in the P14 and P15 manifolds of the ν_3 band of $^{12}CH_4$. The strength data of the allowed transitions in the ν_3 band have been analyzed to determine the band strength and the coefficients of the F factor. The strength data given by Pine (1976) were also included in the analysis. For the ν_3 band, a strength of 259.5 cm^{-2} atm^{-1} at 296 K was obtained. Many forbidden lines in the ν_3 band were also observed in the spectra. Line strengths in the ν_3 band of $^{13}CH_4$ were determined from the spectra. The quantum assignments for the majority of the observed absorption were not determined. These absorptions arise primarily from the bands $2\nu_2$, $\nu_2 + \nu_4$, $\nu_2 + \nu_3 - \nu_2$ and $\nu_3 + \nu_4 - \nu_4$ for which there is presently little or no information.

T025 Spectrum of $H_2{}^{18}O$ and $H_2{}^{17}O$ in the 5030 to 5640 cm^{-1} Region

R. A. Toth, J. M. Flaud (Campus d'Orsay, France), and C. Camy-Peyret (Campus d'Orsay, France)

J. Mol. Spectros., Vol. 67, Nos. 1–3, pp. 185–205, September 15, 1977

Measurements of the center positions of $H_2{}^{18}O$ and $H_2{}^{17}O$ in the 5030 to 5640 cm^{-1} region have been made at high resolution. This region contains absorptions of the (011) and (110) bands of $H_2{}^{18}O$ and $H_2{}^{17}O$. Values of the ground state levels of $H_2{}^{18}O$ and $H_2{}^{17}O$ as well as those for the states of (011) and (110) of $H_2{}^{18}O$ and $H_2{}^{17}O$ were determined from the data. Strength measurements of 23 strong absorbing lines of $H_2{}^{18}O$ were also included and compared to values obtained for $H_2{}^{16}O$ multiplied by the O^{18}/O^{16} isotopic abundance ratio. These results indicate that $H_2{}^{18}O$ line strengths can be calculated, to good approximation, from the $H_2{}^{16}O$ values for the (011) and (110) bands.

T026 Spectrum of $H_2{}^{18}O$ and $H_2{}^{17}O$ in the 6974 to 7387 cm^{-1} Region

R. A. Toth, J. M. Flaud (Laboratoire de Physique Moleculaire et d' Optique, Orsay), and C. Camy-Peyret (Laboratoire de Physique Moleculaire et d' Optique, Orsay)

J. Mol. Spectros., Vol. 67, Nos. 1–3, pp. 206–218, September 15, 1977

Measurements of the line center positions of $H_2{}^{18}O$ and $H_2{}^{17}O$ in the 6974 to 7387 cm^{-1} region have been made at a spectral resolution of ~0.07 cm^{-1}. The region contains absorptions of the (101) and (200) bands of $H_2{}^{18}O$ and $H_2{}^{17}O$. R-branch transitions of the (021) band of $H_2{}^{18}O$ were also observed. Values of the energy levels in the (101) and (200) states of $H_2{}^{18}O$ were determined from the data and the ground state levels derived by Toth, Flaud, and Camy-Peyret [*J. Mol. Spectrosc.*67, 185–205 (1977)]. Seven levels in the (101) state of $H_2{}^{17}O$ were also obtained.

T027 Strengths of H_2O Lines in the 5000–5750 cm^{-1} Region

R. A. Toth, C. Camy-Peyret (Laboratoire de Physique Moleculaire et d'Optique, Orsay), and J. M. Flaud (Laboratoire de Physique Moleculaire et d'Optique, Orsay)

J. Quant. Spectros. Radiat. Transfer, Vol. 18, pp. 515–523, 1977

Measurements of the strengths of 311 lines of water vapor have been made with high resolution in the region 5000–5750 cm^{-1}. The strength data of lines in the (011) and (110) bands are analyzed to determine the band strengths and the coefficients of the F factors. The band strengths of the (011) and (110) bands were found to be 20.65 ± 0.21 and 0.384 ± 0.015 cm^{-2} atm^{-1} at 296 K, respectively. Many of the measured strengths in the (011) and (110) bands differ from the calculated values because of strong Coriolis interactions. Also included in the present work are measurements of strengths of four lines in the (030) band and 36 lines in the "hot" band (021)–(010).

TRAJMAR, S.

T028 Electron Impact Excitation of the Rydberg States in O_2 in the 7–10 eV Energy-Loss Region

S. Trajmar, D. C. Cartwright (Los Alamos Scientific Laboratory), and R. I. Hall (Universite Pierre et Marie Curie, Paris, France)

ORIGINAL PAGE IS
OF POOR QUALITY

J. Chem. Phys., Vol. 65, No. 12, pp. 5275–5279, December 15, 1976

Electron impact energy-loss spectra of O_2 in the 7–10 eV region has been investigated at low impact energies and high scattering angles. Under these conditions a number of new transitions have been found which do not appear in optical spectra. Bands at 8.595, 8.826, 9.045, and 9.27 eV have been assigned to the $3s\sigma_g {}^1\Pi(v' = 0, 1, 2, \text{and } 3)$ excitations, respectively, and the identification of the corresponding $^3\Pi_g$ bands have been reconfirmed. New transitions appearing at 9.13, 9.32, 9.51, 9.58, and 9.78 eV cannot be unambiguously assigned on the basis of the presently available information.

T029 Quantum Mechanical and Crossed Beam Study of Vibrational Excitation of N_2 by Electron Impact at 30–75 eV

D. G. Truhlar (University of Minnesota), M. A. Brandt (University of Minnesota), S. K. Srivastava, S. Trajmar, and A. Chutjian

J. Chem. Phys., Vol. 66, No. 2, pp. 655–663, January 15, 1977

For abstract, see Truhlar, D. G.

T030 Electron Impact Excitation of Potassium at 6.7, 16 and 60 eV

W. Williams and S. Trajmar

J. Phys. B: At. Mol. Phys., Vol. 10, No. 10, pp. 1955–1966, 1977

For abstract, see Williams, W.

T031 Electron Impact Excitation of SF_6

S. Trajmar and A. Chutjian

J. Phys. B: At. Mol. Phys., Vol. 10, No. 14, pp. 2943–2949, 1977

A study of the electron impact energy-loss spectrum of SF_6 under both optical (low scattering angle, high impact energy) and nonoptical conditions (high scattering angle, low impact energy) has revealed a number of electronic excitation processes. With the help of theoretical calculations, several of these transitions have been assigned and approximate cross sections associated with four features have been determined. In addition, a strong resonance at 12 eV has been observed in both elastic and vibrationally inelastic ($\Delta E = 0.092$ eV) channels.

T032 Electron-Metal Atom Collision

S. Trajmar and W. Williams

Proc. Int. Summer School on Phys. of Ionized Gases, Dubrovnik, Yugoslavia, Aug. 27–Sept. 3, 1976, pp. 199–215

Electron-metal atom collision measurements were carried out in the laboratory on Li, K, Mg, Ba, Mn, Cu, Zn, Pb, and Bi. Comparisons with other measurements and theoretical calculations are made where such data are available, and sufficient theory to enable the interpretation of the experimental results is discussed. The discussion is divided into two parts: (1) elastic scattering, momentum transfer, and single electron excitations of the outer valence shell and (2) the inner shell and multielectron excitations.

TRAXLER, M. R.

T033 Tracking and Data Systems Support for the Helios Project: DSN Support of Project Helios April 1975 Through May 1976

P. S. Goodwin, M. R. Traxler, W. G. Meeks, and F. M. Flanagan

Technical Memorandum 33-752, Vol. II, January 15, 1977

For abstract, see Goodwin, P. S.

T034 Tracking and Data System Support for the Viking 1975 Mission to Mars: Prelaunch Planning, Implementation, and Testing

D. J. Mudgway and M. R. Traxler

Technical Memorandum 33-783, Vol. I, January 15, 1977

For abstract, see Mudgway, D. J.

T035 Tracking and Data System Support for the Viking 1975 Mission to Mars: Launch Through Landing of Viking I

D. J. Mudgway and M. R. Traxler

Technical Memorandum 33-783, Vol. II, March 15, 1977

For abstract, see Mudgway, D. J.

T036 Tracking and Data System Support for the Mariner Venus/Mercury 1973 Project

E. K. Davis and M. R. Traxler

Technical Memorandum 33-797, May 1, 1977

For abstract, see Davis, E. K.

TREDER, A. J.

T037 In-Flight Gyro Drift Rate Calibration on the Viking Orbiters

W. G. Breckenridge and A. J. Treder

AAS/AIAA Astrodyn. Conf., Jackson Hole, Wyoming, September 8, 1977, 33 pp.

For abstract, see Breckenridge, W. G.

T038 A Hybrid Technique for Spacecraft Attitude Interpolation With Arbitrary Attitude Data Gaps

A. J. Treder

Modeling Sim. Conf., University of Pittsburgh, Pa., April 21, 1977, 9 pp.

Incomplete time records of attitude data for an orbiting spacecraft are filled out with sufficiently accurate estimates in the normal mode of data processing. Available information is used to maximum advantage without requiring extensive spacecraft modeling for good results. Uncertainty of interpolated estimates is derived as a function of data outage time. This method will be used for the upcoming SEASAT-A mission.

TRUBERT, M. R.

T039 Evaluation of a Cost-Effective Loads Approach

J. A. Garba, B. K. Wada, R. Bamford, and M. R. Trubert

J. Spacecraft Rockets, Vol. 13, No. 11, pp. 675–683, November 1976

For abstract, see Garba, J. A.

TRUHLAR, D. G.

T040 Quantum Mechanical and Crossed Beam Study of Vibrational Excitation of N_2 by Electron Impact at 30–75 eV

D. G. Truhlar (University of Minnesota), M. A. Brandt (University of Minnesota), S. K. Srivastava, S. Trajmar, and A. Chutjian

J. Chem. Phys., Vol. 66, No. 2, pp. 655–663, January 15, 1977

The ratios of differential cross sections for excitation of the first excited vibrational state and for elastic scattering for electron impact on N_2 have been measured at scattering angles ranging from 20° to 135° at 30, 35, 40, 45, and 75 eV impact energies and from 25° to 90° scattering angle at 20 eV impact energy. The results at 20 eV are in good agreement with two previous sets of measurements. Using previously measured and normalized elastic differential cross sections for N_2, the ratios have been converted to inelastic cross sections. Calculations using a four-state vibrational-rotational basis set and an effective interaction potential developed previously are reported at the five energies in the 30–75 eV region. It is shown that the potential scattering model can account for the magnitude and the qualitative behavior of the cross sections at 35–75 eV but there are some significant quantitative differences between theory and experiment. The most striking of these is the way the theoretical model overestimates the scattering at scattering angles less than about 50°. Core-excited resonances apparently make an appreciable contribution to the vibrationally inelastic scattering at 30 eV.

TRUONG, T. K.

T041 Review of Finite Fields: Applications to Discrete Fourier Transforms and Reed-Solomon Coding

J. S. L. Wong, T. K. Truong, B. Benjauthrit, B. D. L. Mulhall, and I. S. Reed

JPL Publication 77-23, July 15, 1977

For abstract, see Wong, J. S. L.

T042 Encoding and Decoding a Telecommunication Standard Command Code

B. Benjauthrit and T. K. Truong

The Deep Space Network Progress Report 42-38: January and February 1977, pp. 115–119, April 15, 1977

For abstract, see Benjauthrit, B.

T043 A New Fast Algorithm for Computing a Complex Number—Theoretic Transforms

I. S. Reed (University of Southern California), K. Y. Liu (University of Southern California), and T. K. Truong

The Deep Space Network Progress Report 42-39: March and April 1977, pp. 71–75, June 15, 1977

For abstract, see Reed, I. S.

T044 Fast Algorithms for Computing Mersenne-Prime Number-Theoretic Transforms

I. S. Reed (University of Southern California) and T. K. Truong

The Deep Space Network Progress Report 42-41: July and August 1977, pp. 176–205, October 15, 1977

For abstract, see Reed, I. S.

TSOU, P.

T045 Evaluation of Coal Feed Systems Being Developed by the Energy Research and Development Administration

R. Phen, C. Jennings, W. Luckow, L. Mattson, D. Otth, and P. Tsou

JPL Publication 77-54, September 1977

For abstract, see Phen, R.

TSURUTANI, B. T.

T046 Two Types of Magnetospheric ELF Chorus and Their Substorm Dependences

B. T. Tsurutani and E. J. Smith

J. Geophys. Res., Space Phys., Vol. 82, No. 32, pp. 5112–5128, November 1, 1977

Extremely low frequency (10–1500 Hz) magnetospheric chorus has been analyzed to investigate a possible dependence on substorms. Care was taken to separate spatial effects from temporal effects by analyzing an entire year of data acquired by the Ogo 5 search coil magnetometer. A major finding of the study of spatial dependences is that chorus occurs principally in two magnetic latitude regions. Equatorial chorus is detected near the equator, and high-latitude chorus is found at magnetic latitudes above 15°. When chorus in these two regions is analyzed separately, substorm dependences become apparent. Comparisons with AE indicate that equatorial chorus occurs primarily during substorms. High-latitude chorus is not strongly dependent on AE and often occurs during intervals of prolonged quiet with $AE < 100\ \gamma$ for the previous 12 hours or more. The dependence of equatorial chorus on local time, magnetic latitude, and L is consistent with generation by a cyclotron resonance between the whistler mode chorus and 10- to 100-keV trapped substorm electrons. Equatorial chorus has an abrupt onset in the postmidnight sector and a second enhancement from dawn to noon, a pattern which is similar to that of energetic electron precipitation. The occurrence frequency of equatorial chorus peaks at the equator, |magnetic latitude| $< 5°$, a region where cyclotron resonance is most efficient. The L value of maximum chorus occurrence increases from 5–8 postmidnight to 7–11 postdawn, a dependence which is consistent with generation by electrons which have undergone drift shell splitting. Delay times between substorms and the onset of equatorial chorus are consistent with a gradient drift of ~25-keV electrons. Equatorial postmidnight chorus and postdawn chorus have similar occurrence rates and wave intensities. The maximum chorus occurrence rates are 54% postmidnight and 56% postdawn. Time-averaged equatorial chorus intensities $\geq 10^{-3}\ \gamma^2$ are detected up to 17% of the time for $6 \leq L \leq 7$ postmidnight and up to 14% of the time for $7 \leq L \leq 10$ from dawn to noon. Such wave intensities are sufficient to cause near-strong pitch angle diffusion of electrons for $L > 6$ and strong diffusion for $L > 8$. Instantaneous diffusion rates may be considerably higher owing to the discrete burstlike nature of the chorus. The spatial and temporal dependences of high-latitude chorus are considerably different from those of equatorial chorus. High-latitude chorus occurs in local day and evening and at large L. The emission is detected primarily on the dayside, at $0800 \leq$ LT ≤ 1600, and often within 1–2 R_E of the magnetopause. The occurrence of high-latitude chorus during quiet intervals is consistent with local generation within 'minimum B pockets.'

T047 Acceleration of Energetic Particles of the Outer Regions of Planetary Magnetospheres: Inferences From Laboratory and Space Experiments

B. T. Tsurutani, B. E. Goldstein, and A. Bratenahl

Planet. Space Sci., Vol. 24, No. 10, pp. 995–999, 1976

High energy particles, with energies above those attainable by adiabatic or steady-state electric field acceleration, have been observed in and around the outer regions of planetary magnetospheres. Acceleration by large amplitude sporadic cross-tail electric fields over an order of magnitude greater than steady-state convection fields is proposed as a source of these particles. It is suggested that such explosive electric fields will occur intermittently in the vicinity of the tail neutral line in the expansive phases of substorms. We use laboratory Double Inverse Pinch Device (DIPD) and satellite evidence to estimate this electric potential for substorms at Earth; values of 500 kV to 2 MV are calculated, in agreement with particle observations. It is further suggested that these particles, which have been accelerated in the nightside magnetosphere, drift to the dayside on closed field lines, and under certain interplanetary conditions can escape to regions upstream of the bow shock.

TUNG, S.

T048 Synchronization Strategies for RFI Channels

R. J. McEliece, H. van Tilborg (California Institute of Technology), and S. Tung (Cornell University)

The Deep Space Network Progress Report 42-38: January and February 1977, pp. 103–108, April 15, 1977

For abstract, see McEliece, R. J.

TURNER, R. H.

T049 Projection of Distributed-Collector Solar-Thermal Electric Power Plant Economics to Years 1990–2000

T. Fujita, N. El Gabalawi, G. Herrera, and R. H. Turner

JPL Publication 77-79, December 1977

For abstract, see Fujita, T.

UDLOCK, D. E.

U001 Heat Sterilizable Propellants for Planetary Missions

D. E. Udlock

J. Spacecraft Rockets, Vol. 14, No. 4, pp. 197–201, April 1977

Dry-heat sterilization, a requirement of all planetary lander missions, places severe requirements on solid rocket propellants that will be used on them. In an ongoing program, which has a goal of producing heat sterilizable motors with 130 kg of propellant, numerous insights into the problems associated with developing dry-heat sterilizable propellants have been gained. The one most significant means of increasing propellant stability at sterilization temperature (125°C) is to decrease the ammonium perchlorate (AP) particle size. One possible explanation is that some of the AP crystals larger than 250 μ in diameter are unstable at sterilization temperature. Another important finding is the effect grain diameter has on survivability at sterilization temperature. As the grain diameter increases, the time to failure decreases. This is probably due to the increased stress that results from the thermal gradients, which occur during grain heat up or cool down. In this work, 7-cm-diam grains have been made that survived 70 sterilization cycles (the requirement is eight); however, 71-cm-diam grains from the same propellant batch have survived only seven cycles.

UPHOFF, C.

U002 Orbit Design Concepts for Jupiter Orbiter Missions

C. Uphoff, P. H. Roberts, and L. D. Friedman

J. Spacecraft Rockets, Vol. 13, No. 6, pp. 348–355, June 1976

Advanced mission and orbit planning efforts are in progress for a Jupiter orbiter mission in the early 1980's. Baseline spacecraft and orbit design criteria are the goals of a NASA effort to define such a mission. Orbit design concepts that have been discovered during the early stages of mission planning are both challenging and exciting. This paper is a description of several such concepts that may greatly increase the flexibility and scientific return of orbiters designed for close study of the Galilean satellites and exploration of the Jovian system. Some new jargon is introduced in discussions to describe the exploitation of gravity-assist trajectories using the giant satellites for orbit control. Orbit pumping and cranking and resonance hopping are defined and shown to be dynamically feasible means of controlling the orbit and, thus, the scientific return. A candidate encounter sequence is presented for an equatorial tour of the Galilean moons. The analytic development of the orbit design concept is performed by zero-sphere of influence patched conics. The navigation feasibility and the accuracy of this work are discussed and shown to yield high confidence in the applicability of the concepts to the ultimate mission design.

VALANIS, K. C.

V001 Nonlinear Viscoelasticity and Relaxation Phenomena of Polymer Solids

S. T. J. Peng, K. C. Valanis (University of Iowa), and R. F. Landel

Acta Mech., Vol. 25, Nos. 3–4, pp. 229–240, 1977

For abstract, see Peng, S. T. J.

VAN TILBORG, H.

V002 Synchronization Strategies for RFI Channels

R. J. McEliece, H. van Tilborg (California Institute of Technology), and S. Tung (Cornell University)

The Deep Space Network Progress Report 42-38: January and February 1977, pp. 103–108, April 15, 1977

For abstract, see McEliece, R. J.

VAN TILBORG, H. C. A.

V003 On the Inherent Intractability of Finding Good Codes

R. J. McEliece and H. C. A. van Tilborg

The Deep Space Network Progress Report 42-37: November and December 1976, pp. 83–87, February 15, 1977

For abstract, see McEliece, R. J.

VARSI, G.

V004 Blast Wave Analysis for Detonation Propulsion

K. Kim, G. Varsi, and L. H. Back

AIAA J., Vol. 15, No. 10, pp. 1500–1502, October 1977

For abstract, see Kim, K.

VEEDER, G. J.

V005 Photometry of the Asteroid 1976 AA at 0.56 and 2.2 μm

G. J. Veeder, D. L. Matson, and O. L. Hansen

Icarus, Vol. 31, pp. 424–426, 1977

We report observations at 0.56 and 2.2 μm of the Apollo asteroid 1976 AA made during its discovery apparition. We derive a 2.2-μm relative spectral reflectance (scaled to unity at 0.56 μm) of $R(2.2\ \mu m) = 1.5 \pm 0.3$. This 2.2-μm reflectance is not compatible with a carbonaceous surface composition. However, it is compatible with a wide variety of meteoritic types including ordinary chondrites, stony irons, and mesosiderites. Thus, 1976 AA may have a silicate surface similar to other Apollo–Amor objects.

V006 Galilean Satellites: Anomalous Temperatures Disputed

D. Morrison (University of Arizona), L. A. Lebofsky, J. A. Cutts (Planetary Science Institute), G. J. Veeder, and S. H. Gross (Polytechnic Institute of New York)

Science, Vol. 195, pp. 90–93, January 7, 1977

For abstract, see Morrison, D.

VETTER, A. A.

V007 Addition of HCl to the Double-Pulse Copper Chloride Laser

A. A. Vetter and N. M. Nerheim

Appl. Phys. Lett., Vol. 30, No. 8, pp. 405–407, April 15, 1977

Addition of small amounts of hydrogen chloride to the buffer gas of a double-pulse CuCl laser causes an increase in the production of copper atoms in the ground state. A maximum laser energy increase of 15% was observed and the span of delay times for which laser action occurred increased.

V008 Quantitative Effect of Initial Current Rise on Pumping the Double-Pulsed Copper Chloride Laser

A. A. Vetter

IEEE J. Quantum Electron., Vol. QE-13, No. 11, November 1977

The laser energy output of a double-pulsed copper chloride laser has been found to be a logarithmic function of the circuit inductance over the range of 1 to 12 μH. The initial current rise was inversely proportional to the circuit inductance so that the laser energy was also a logarithmic function of the initial current rise.

WACKLEY, J. A.

W001 Viking S-Band Doppler RMS Phase Fluctuations Used to Calibrate the Mean 1976 Equatorial Corona

A. L. Berman and J. A. Wackley

The Deep Space Network Progress Report 42-38: January and February 1977, pp. 152–166, April 15, 1977

For abstract, see Berman, A. L.

W002 Viking Doppler Noise Used to Determine the Radial Dependence of Electron Density in the Extended Corona

A. L. Berman, J. A. Wackley, S. T. Rockwell, and M. Kwan

The Deep Space Network Progress Report 42-38: January and February 1977, pp. 167–171, April 15, 1977

For abstract, see Berman, A. L.

WADA, B. K.

W003 Matrix Perturbation for Structural Dynamic Analysis

J. C. Chen and B. K. Wada

AIAA J., Vol. 15, No. 8, pp. 1095–1100, August 1977

For abstract, see Chen, J. C.

W004 Evaluation of a Cost-Effective Loads Approach

J. A. Garba, B. K. Wada, R. Bamford, and M. R. Trubert

J. Spacecraft Rockets, Vol. 13, No. 11, pp. 675–683, November 1976

For abstract, see Garba, J. A.

W005 Comparison of Model Test Results: Multipoint Sine Versus Single-Point Random

E. L. Leppert, S. H. Lee, F. D. Day, P. C. Chapman, and B. K. Wada

Preprint 760879, SAE Aerosp. Eng. Manuf. Meeting, San Diego, CA, Nov. 29–Dec. 2, 1976

For abstract, see Leppert, E. L.

WALLACE, K.

W006 A K-Band Radiometer for the Microwave Weather Project

K. Wallace, M. Reid, and H. Reilly

The Deep Space Network Progress Report 42-38: January and February 1977, pp. 66–69, April 15, 1977

The design of a K-band radiometer for use in the microwave weather project is discussed. The major components of the system, such as feedhorn, waveguide switch, and receiver assembly, are described. The system will be installed at DSS 13 at Goldstone, California, when completed.

WALLACE, K. B.

W007 Calibration of Block 4 Translator Path Delays at DSS 14 and CTA 21

T. Y. Otoshi, P. D. Batelaan, K. B. Wallace, and F. Ibanez

The Deep Space Network Progress Report 42-37: November and December 1976, pp. 188–197, February 15, 1977

For abstract, see Otoshi, T. Y.

W008 Dual Coupler Configuration at DSS 14 for the Voyager Era

T. Y. Otoshi, K. B. Wallace, and R. B. Lyon

The Deep Space Network Progress Report 42-42: September and October 1977, pp. 184–192, December 15, 1977

For abstract, see Otoshi, T. Y.

W009 A High-Power Dual-Directional Coupler

K. B. Wallace and T. Y. Otoshi

The Deep Space Network Progress Report 42-42: September and October 1977, pp. 193–206, December 15, 1977

A dual-directional loop coupler in WR 430 waveguide has been installed at DSS 14 as part of the system to measure station range delay. This installation was necessary to provide special test translator signal injection ports for the Voyager near-earth calibration sequence, which required that the SPD maser be bypassed to prevent saturation of the receivers. The design of the dual coupler and testing of this device at high power is discussed.

WANG, T. G.

W010 First-Order Torques and Solid-Body Spinning Velocities in Intense Sound Fields

T. G. Wang H. Kanber, and I. Rudnick (University of California, Los Angeles)

Phys. Rev. Lett., Vol. 38, No. 3, pp. 128–130, January 17, 1977

The first observation is given of first-order nonzero time-averaged torques and solid-body spinning velocities in intense acoustic fields, which occur when the acoustic displacement amplitude exceeds the viscous penetration depth.

WARD, R. S.

W011 Dual-Spin Attitude Control for Outer Planet Missions

R. S. Ward and G. J. Tauke

JPL Publication 77-74, December 15, 1977

The applicability of dual-spin technology to a Jupiter Orbiter with Probe mission has been investigated. Basic mission and system level attitude control requirements were established and preliminary mechanization and control concepts developed. A comprehensive 18-degree-of-freedom digital simulation was utilized extensively to establish control laws, study dynamic interactions, and determine key sensitivities. Fundamental system/subsystem constraints have been identified, and the applicability of dual-spin technology to a Jupiter Orbiter with Probe mission has been validated.

WATERS, J. W.

W012 Mars: Microwave Detection of Carbon Monoxide

R. K. Kakar, J. W. Waters, and W. J. Wilson (Aerospace Corporation)

Science, Vol. 196, pp. 1090–1091, June 3, 1977

For abstract, see Kakar, R. K.

WATSON, R. T.

W013 Kinetic Studies of Diatomic Free Radicals Using Mass Spectrometry: Part 4. The Br + OClO and BrO + ClO Reactions

M. A. A. Clyne (Queen Mary College, London) and R. T. Watson

J. Chem. Soc., Faraday Trans. I, Vol. 73, pp. 1169–1187, 1977

For abstract, see Clyne, M. A. A.

W014 Rate Constants for Reactions of ClO_x of Atmospheric Interest

R. T. Watson

J. Phys. Chem. Ref. Data, Vol. 6, No. 3, pp. 871–917, 1977

Chemical kinetics measurements on 82 gas phase reactions of chlorine containing species are reviewed. Recommended rate constants are given. The principal species of interest are Cl, Cl_2, ClO, Cl_2O, ClOO, OClO, ClNO, HCl and halo derivatives of methane and ethane. Absorption spectra are given for 21 species. In addition the chemical kinetics methods used to obtain these data are discussed with regard to their applicability and reliability.

WEINER, J. M.

W015 Robotics Control Using Isolated Word Recognition of Voice Input

J. M. Weiner

JPL Publication 77-73, December 15, 1977

A speech input/output system is presented that can be used to communicate with a task oriented system. Human speech commands and synthesized voice output extend conventional information exchange capabilities between man and machine by utilizing audio input and output channels.

The speech input facility described consists of a hardware feature extractor and a microprocessor implemented isolated word or phrase recognition system. The recognizer offers a medium sized (100 commands), syntactically constrained vocabulary and exhibits close to real-time performance. The major portion of the recognition processing required is accomplished through software, minimizing the complexity of the hardware feature extractor.

The speech output facility incorporates a commercially available voice synthesizer based upon phonetic representations of words. The same DEC PDP-11/03 microcomputer used in the voice input system controls the speech output operation.

WEISSMAN, P.

W016 An Interstellar Precursor Mission

L. D. Jaffe, C. Ivie, J. C. Lewis, R. Lipes, H. N. Norton, J. W. Stearns, L. D. Stimpson, and P. Weissman

JPL Publication 77-70, October 30, 1977

For abstract, see Jaffe, L. D.

WELCH, L. R.

W017 Walsh Transforms and Signal Detection

L. R. Welch (University of Southern California)

The Deep Space Network Progress Report 42-37: November and December 1976, pp. 127–131, February 15, 1977

This paper analyzes the detection of signals using Walsh power spectral estimates. In addition, a generalization of this method of estimation is analyzed. The conclusion is that Walsh transforms are not suitable tools for the detection of weak signals in noise.

W018 Concatenated Shift Registers Generating Maximally Spaced Phase Shifts of PN-Sequences

W. J. Hurd and L. R. Welch (University of Southern California)

The Deep Space Network Progress Report 42-40: May and June 1977, pp. 110–116, August 15, 1977

For abstract, see Hurd, W. J.

W019 Minimum-Weight Codewords in the (128,64) BCH Code

L. D. Baumert and L. R. Welch (University of Southern California)

The Deep Space Network Progress Report 42-42: September and October 1977, pp. 92–94, December 15, 1977

For abstract, see Baumert, L. D.

W020 New Upper Bounds on the Rate of a Code via the Delsarte–MacWilliams Inequalities

R. J. McEliece, E. R. Rodemich, H. Rumsey, Jr., and L. R. Welch (University of Southern California)

IEEE Trans. Inform. Theor., Vol. IT-23, No. 2, pp. 157–166, March 1977

For abstract, see McEliece, R. J.

WELLER, R. E.

W021 S-X Conversion for the Block III Receiver-Exciter

R. E. Weller

The Deep Space Network Progress Report 42-42: September and October 1977, pp. 141–148, December 15, 1977

An S-X conversion modification has been designed for the Block III receiver-exciter to be used in the 26-meter S-X Conversion Project. The description, design, specifications and data are presented.

WELLMAN, J. B.

W022 The Viking Orbiter Visual Imaging Subsystem

J. B. Wellman, F. P. Landauer, D. D. Norris, and T. E. Thorpe

J. Spacecraft Rockets, Vol. 13, No. 11, pp. 660–666, November 1976

A Visual Imaging Subsystem consisting of two slow-scan television cameras forms part of the scientific payload of each of two Viking Orbiter Spacecraft presently photographing the surface of Mars. These cameras are used to evaluate the potential landing sites on Mars, and to conduct other scientific investigations of the planet. The camera system described in this paper was subjected to an extensive test and calibration program prior to launch. Based on this calibration and subsequent analyses, surface resolution exceeding 100 m will be achieved from the periapsis portion of the Viking orbits. The inherent geometric accuracies of the Orbiter cameras surpass those of cameras used in previous planetary missions. The analyses of images acquired during the cruise phase of the mission confirm that the cameras have survived the rigors of launch and are performing in a manner consistent with the prelaunch calibrations.

WHITCOMB, J. H.

W023 Electrical Structure in a Region of the Transverse Ranges, Southern California

I. K. Reddy, R. J. Phillips, J. H. Whitcomb (California Institute of Technology), and D. Rankin (University of Alberta)

Earth Planet. Sci. Lett., Vol. 34, pp. 313–320, 1977

For abstract, see Reddy, I. K.

WIEBE, E.

W024 Low-Noise Receivers: Microwave Maser Development

R. Quinn and E. Wiebe

The Deep Space Network Progress Report 42-37: November and December 1976, pp. 78–82, February 15, 1977

For abstract, see Quinn, R.

WILLETT, J. B.

W025 Measurement of 0.511-MeV Gamma Rays With a Balloon-Borne Ge(Li) Spectrometer

J. C. Ling, W. A. Mahoney, J. B. Willett, and A. S. Jacobson

J. Geophys. Res., Space Phys., Vol. 82, No. 10, pp. 1463–1473, April 1, 1977

For abstract, see Ling, J. C.

WILLIAMS, W.

W026 Electron Impact Excitation of Potassium at 6.7, 16 and 60 eV

W. Williams and S. Trajmar

J. Phys. B: At. Mol. Phys., Vol. 10, No. 10, pp. 1955–1966, 1977

Normalized momentum-transfer cross sections and differential and integral cross sections for elastic scattering and for the excitation of the 4p $^2P_{3/2,1/2}$ and the (5s $^2S_{1/2}$ + 3d $^2D_{5/2,3/2}$) levels in potassium are reported at 6.7, 16 and 60 eV impact energies. There is considerable disagreement between the present experimental results and previous optical excitation measurements and theoretical results. Autoionization features associated with the 3p inner-shell excitations, some of which have been observed previously in optical absorption and ejected-electron spectra, have been detected in the electron impact energy-loss spectrum.

W027 Electron-Metal Atom Collision

S. Trajmar and W. Williams

Proc. Int. Summer School on Phys. of Ionized Gases, Dubrovnik, Yugoslavia, Aug. 27–Sept. 3, 1976, pp. 199–215

For abstract, see Trajmar, S.

WILLIAMSON, K.

W028 Experiments on the Properties of Superfluid Helium in Zero Gravity

P. Mason, D. Collins, D. Petrac, L. Yang, F. Edeskuty, and K. Williamson

Proc. Sixth Int. Cryog. Eng. Conf., Grenoble, France, May 11–14,1976, pp. 272–277

For abstract, see Mason, P.

WILLSON, R. C.

W029 Instrumentation for Measurements of Solar Irradiance and Atmospheric Optical Properties

R. C. Willson

Proc. SPIE, Vol. 68, pp. 31–40, 1975

The Active Cavity Radiometer (ACR), an accurate absolute pyrheliometer, has been developed at the Jet Propulsion Laboratory for measurements of total solar irradiance. They have been used to discover a −2.2% error in the International Pyrheliometric Scale and to make measurements in balloon flight experiments yielding a solar constant value of 136.6 (±0.7) mW/cm^2. New ACR's are being developed to monitor the total output of solar optical radiation in balloon, satellite and space shuttle experiments with longterm absolute uncertainty of ±0.1% or less. In a separate program, instrumentation for the measurement of the scattering and extinction of solar radiation by the atmosphere is being constructed to provide data for modeling atmospheric aerosol content. The aerosol models will facilitate computation of radiative transfer effects yielding quantitative net fluxes useful in evaluating the climatological impact of aerosols.

WILSON, R. L.

W030 Final Report: Medical Ultrasonic Tomographic System

R. C. Heyser, D. H. Le Croissette, R. Nathan, and R. L. Wilson (Harbor General Hospital, Los Angeles)

JPL Publication 77-72, October 1, 1977

For abstract, see Heyser, R. C.

WILSON, W. J.

W031 Mars: Microwave Detection of Carbon Monoxide

R. K. Kakar, J. W. Waters, and W. J. Wilson (Aerospace Corporation)

Science, Vol. 196, pp. 1090–1091, June 3, 1977

For abstract, see Kakar, R. K.

WINKELSTEIN, R. A.

W032 Control and Computation Module Development

R. A. Winkelstein

The Deep Space Network Progress Report 42-37: November and December 1976, pp. 112–117, February 15, 1977

The control and computation module (CCM) project has selected on the basis of developed criteria the 8080A microprocessor as its first candidate CCM. Software development methods have been investigated and two test bed projects have been chosen to evaluate application techniques of the 8080A and support microcircuits which will satisfy DSN requirements. Final recommendations will reflect successful JPL applications experience.

W033 Sampled-Data System Analysis of Antenna Conical-Scan Tracking

R. A. Winkelstein

The Deep Space Network Progress Report 42-41: July and August 1977, pp. 86–100, October 15, 1977

The conical-scan tracking system described by Ohlson and Reid in JPL Technical Report 32-1605 is analyzed as a sampled-data feedback control system. Tracking mode equations for both spacecraft signals and radio source signals are developed. In the case of spacecraft tracking, a rationale is presented for selection of parameters which minimizes the sum of the required scan radius and three times the RMS error jitter. With this criterion, reasonable system performance can be obtained with signals down to receiver threshold. For radio source tracking, the RMS error jitter is negligible, and a set of system parameters is recommended which allows conservative operation of the sytems.

WINN, F. B.

W034 A Solar Plasma Stream Measured by DRVID and Dual-Frequency Range and Doppler Radio Metric Data

F. B. Winn, S. C. Wu, T. A. Komarek, V. W. Lam, H. N. Royden, and K. B. W. Yip

The Deep Space Network Progress Report 42-37: November and December 1976, pp. 43–54, February 15, 1977

S- and X-Band DRVID, S- and X-band dual-frequency range, and doppler measured a 15-fold increase in the line-of-sight electron content of the solar plasma above the normal plasma background. A general increase in the plasma electron content continued for nearly 50 hours: it started about 12:00 (GMT) on 12 March 1976 and continued to grow until 17:00 (GMT) on 14 March. For the next 55 hours, between 17:00 (GMT) on 14 March to 00:54 (GMT) on 17 March, the plasma level diminished as the background level was again approached. Not only were the temporal changes and absolute level of the

plasma content measured but the measurements were also used to ascertain the mean-plasma-concentration location: it was estimated to be 4.1 light minutes from Earth. It is demonstrated that if round-trip S-band range is to be calibrated for plasma influence to the meter level, then some knowledge of the plasma distribution must exist.

W035 Solar Plasma: Viking 1975 Interplanetary Spacecraft Dual-Frequency Doppler Data

S. C. Wu, F. B. Winn, and K. B. W. Yip

The Deep Space Network Progress Report 42-37: November and December 1976, pp. 204–223, February 15, 1977

For abstract, see Wu, S. C.

W036 A Technique to Determine Uplink Range Calibration Due to Charged Particles

S. C. Wu and F. B. Winn

The Deep Space Network Progress Report 42-41: July and August 1977, pp. 57–81, October 15, 1977

For abstract, see Wu, S. C.

WOICESHYN, P. M.

W037 Pioneer 10 and 11 Radio Occultations by Jupiter

A. J. Kliore, P. M. Woiceshyn, and W. B. Hubbard (University of Arizona)

COSPAR Space Research, Vol. XVII, pp. 703–710, 1977

For abstract, see Kliore, A. J.

WOLF, M. R.

W038 Viking Lander Camera Radiometry Calibration Report

M. R. Wolf, D. L. Atwood, and M. E. Morrill

JPL Publication 77-62, Vols. I and II, November 1, 1977

This report describes the test methods and data reduction techniques used to determine and remove instrumental signatures from Viking Lander Camera Radiometry Data. Included are detailed descriptions of all tests and reduced data. Tables of gain, offset, and calibration constants included in the figures allow the reader to remove the instrumental signature from Viking Lander Flight Radiometry Data.

Volume II contains voluminous plots and tables of responsivity for diodes of all cameras and is published separately as a microfiche package.

WONG, J. S. L.

W039 Review of Finite Fields: Applications to Discrete Fourier Transforms and Reed-Solomon Coding

J. S. L. Wong, T. K. Truong, B. Benjauthrit, B. D. L. Mulhall, and I. S. Reed

JPL Publication 77-23, July 15, 1977

This report attempts to provide a step-by-step approach to the subject of finite fields. Rigorous proofs and highly theoretical materials are avoided. The simple concepts of groups, rings, and fields are discussed and developed more or less heuristically. Examples are used liberally to illustrate the meaning of definitions and theories. Applications include discrete Fourier transforms and Reed-Solomon coding.

WOO, R.

W040 Measurements of Large-Scale Density Fluctuations in the Solar Wind Using Dual-Frequency Phase Scintillations

R. Woo, F. C. Yang, K. W. Yip, and W. B. Kendall (Mark Resources, Inc.)

Astrophys. J., Vol. 210, No. 2, Pt. 1, pp. 568–574, December 1, 1976

In this paper we demonstrate that the phase-difference scintillations measured with a coherent dual-frequency radio system such as that on Mariner 10 can be used to study the structure of density fluctuations in the solar wind covering a wider range of scale sizes than has ever been possible before. The Mariner 10 observations at solar elongations of 11.5 and 12.6 deg show that the density spectrum in the frequency range of $10^{-4} \lesssim f \lesssim 5 \times 10^{-1}$ Hz, which corresponds to the spatial wavenumber range $2 \times 10^{-6} \lesssim \kappa \lesssim 10^{-3}$ km^{-1} if the solar wind velocity is assumed to be 350 km s^{-1}, is approximately power-law and close to Kolmogorov (spectral index $p = 11/3$). The results are consistent with direct spacecraft observations near Earth and provide strong evidence that the density fluctuations are produced by turbulence. The potential and benefits of future extensive measurements are also discussed.

W041 Structure of Density Fluctuations Near the Sun Deduced From Pioneer-6 Spectral Broadening Measurements

R. Woo F. C. Yang, and A. Ishimaru (University of Washington)

Astrophys. J., Vol. 210, No. 2, Pt. 1, pp. 593–602, December 1, 1976

In this paper we present an analysis of the spectral broadening of monochromatic radio waves by density fluctuations near the Sun using the parabolic equation method. Application of the analysis to the 1968 Pioneer-6 spectral broadening observations yields indirect measurements of the density spectrum within 14 $R_\odot$ of the Sun. For spatial wavenumbers $\kappa \gtrsim 8.4 \times 10^{-3}$ km^{-1}, the three-dimensional density spectrum is found to be close to the Kolmogorov spectrum (power law with spectral index $p = 11/3$) and is consistent with the IPS (interplanetary scintillations) and in situ spacecraft measurements farther from the Sun. The magnitude of the density spectrum increases but the shape of the density spectrum remains the same during the "solar events" marked by increases in the bandwidth.

W042 Measuring Solar Wind Velocity With Spacecraft Phase Scintillations

R. Woo

Nature, Vol. 266, No. 5602, p. 514, April 7, 1977

The measurement of spacecraft phase scintillations with a coherent dual-frequency radio system paves the way for making solar wind velocity measurements with multiple-station phase scintillations. Phase scintillations do not saturate when they are strong, and observations can be carried out closer to the Sun than with amplitude scintillations. Spectral broadening has this same property, and measurements of 2.3 GHz as close as 1.7 $R_\odot$ have been made with the Helios spacecraft.

WU, S. C.

W043 A Solar Plasma Stream Measured by DRVID and Dual-Frequency Range and Doppler Radio Metric Data

F. B. Winn, S. C. Wu, T. A. Komarek, V. W. Lam, H. N. Royden, and K. B. W. Yip

The Deep Space Network Progress Report 42-37: November and December 1976, pp. 43–54, February 15, 1977

For abstract, see Winn, F. B.

W044 Solar Plasma: Viking 1975 Interplanetary Spacecraft Dual-Frequency Doppler Data

S. C. Wu, F. B. Winn, and K. B. W. Yip

The Deep Space Network Progress Report 42-37: November and December 1976, pp. 204–223, February 15, 1977

Viking 1975 interplanetary S- and X-band doppler data are surveyed. These data show consistency with differenced range versus integrated doppler (DRVID) data when there is solar plasma and with Faraday rotation data otherwise. An increase of solar plasma effects with decreasing Sun-Earth-probe (SEP) angle (approaching Mars orbit insertion) is demonstrated. The 2-way/3-way data indicate a homogeneous solar plasma structure over a 8000-km spread. Occasional cycle slips in the data are pinpointed and tabulated.

W045 A Technique to Determine Uplink Range Calibration Due to Charged Particles

S. C. Wu and F. B. Winn

The Deep Space Network Progress Report 42-41: July and August 1977, pp. 57–81, October 15, 1977

A technique is presented to determine uplink range change due to line-of-sight charged particles using downlink S/X range and doppler and 2-way DRVID data. The line-of-sight relative charged-particle distribution is first estimated from these data by a point-matching method. The uplink range change is then synthesized by the weighted sum of the delayed downlink range changes. Simulation analysis shows 2 to 6 cm agreement between the "true" and the synthesized uplink range changes. Demonstration using Viking 1975 radio metric data shows 4 to 22 cm consistency between the uplink range calibration solutions synthesized from S-DRVID and X-DRVID. The consistency is an order of magnitude superior to that equating uplink and downlink effects.

YAMANE, N. I.

Y001 JPL Field Measurements at the Finney County, Kansas, Test Site, October 1976: Ground-Based Microwave Radiometric Measurements

E. G. Njoku and N. I. Yamane

JPL Publication 77-13, April 1, 1977

For abstract, see Njoku, E. G.

YANG, F. C.

Y002 Measurements of Large-Scale Density Fluctuations in the Solar Wind Using Dual-Frequency Phase Scintillations

R. Woo, F. C. Yang, K. W. Yip, and W. B. Kendall (Mark Resources, Inc.)

Astrophys. J., Vol. 210, No. 2, Pt. 1, pp. 568–574, December 1, 1976

For abstract, see Woo, R.

Y003 **Structure of Density Fluctuations Near the Sun Deduced From Pioneer-6 Spectral Broadening Measurements**

R. Woo F. C. Yang, and A. Ishimaru (University of Washington)

Astrophys. J., Vol. 210, No. 2, Pt. 1, pp. 593–602, December 1, 1976

For abstract, see Woo, R.

YANG, L.

Y004 **Experiments on the Properties of Superfluid Helium in Zero Gravity**

P. Mason, D. Collins, D. Petrac, L. Yang, F. Edeskuty, and K. Williamson

Proc. Sixth Int. Cryog. Eng. Conf., Grenoble, France, May 11–14,1976, pp. 272–277

For abstract, see Mason, P.

YANOW, G.

Y005 **Options for Demonstrating the Use of Solar Energy in California Buildings**

E. S. Davis and G. Yanow

JPL Publication 77-33, September 1976

For abstract, see Davis, E. S.

YASUI, R. K.

Y006 **Performance Data for a Terrestrial Solar Photovoltaic/Water Electrolysis Experiment**

E. N. Costogue and R. K. Yasui

Solar Energy, Vol. 19, pp. 205–210, 1977

For abstract, see Costogue, E. N.

YEE, S. H.

Y007 **Modification of Simulation Conversion Assembly for Support of Voyager Project and Pioneer-Venus 1978 Project**

S. H. Yee

The Deep Space Network Progress Report 42-39: March and April 1977, pp. 100–108, June 15, 1977

The Simulation Conversion Assembly (SCA) has been upgraded to provide the additional capabilities of simulating Voyager and Pioneer-Venus 1978 telemetry data streams for verifying the integrity of the Deep Space Stations while continuing to fulfill the DSN test and training support requirements. A summary of the requirements and the implementations are presented in this article.

YEH, Y. C. M.

Y008 **Technology of GaAs Metal–Oxide–Semiconductor Solar Cells**

R. J. Stirn and Y. C. M. Yeh

IEEE Trans. Electron Devices, Vol. ED-24, No. 4, pp. 476–483, April 1977

For abstract, see Stirn, R. J.

YEOMANS, D. K.

Y009 **Comet Halley—The Orbital Motion**

D. K. Yeomans

Astron. J., Vol. 82, No. 6, pp. 435–440, June 1977

The orbital motion of Comet Halley is investigated over the interval 837–2061 A.D. Using the observations from 1607 through 1911, least-squares differential orbit corrections were successfully computed using the existing model for the nongravitational forces. The nongravitational force model was found to be consistent with the outgassing rocket effect of a water-ice cometary nucleus and, prior to the 1910 return, these forces are time independent for nearly a millennium. For the 1986 return, viewing conditions are outlined for the comet and the related Orionid and η Aquarid meteor showers.

Y010 **The Origin of North American Astronomy—Seventeenth Century**

D. K. Yeomans

Isis, Vol. 68, No. 243, pp. 414–425, September 1977

A foundation of German scientific methods enabled the rapid growth of North American astronomy in the nineteenth century. However, during the seventeenth century and most of the eighteenth, the colonial men of science looked only to the English mother country for scientific patronage and guidance. The science of astronomy was successfully transplanted from England to North Amer-

ORIGINAL PAGE IS
OF POOR QUALITY

ica during the seventeenth century. The ingenuity of men like Winthrop, Danforth, Mather, Foster, and Brattle, whose achievements in astronomy during the seventeenth century, provided the impetus for subsequent astronomical research in North America.

YIP, K. B. W.

Y011 A Solar Plasma Stream Measured by DRVID and Dual-Frequency Range and Doppler Radio Metric Data

F. B. Winn, S. C. Wu, T. A. Komarek, V. W. Lam, H. N. Royden, and K. B. W. Yip

The Deep Space Network Progress Report 42-37: November and December 1976, pp. 43–54, February 15, 1977

For abstract, see Winn, F. B.

Y012 Solar Plasma: Viking 1975 Interplanetary Spacecraft Dual-Frequency Doppler Data

S. C. Wu, F. B. Winn, and K. B. W. Yip

The Deep Space Network Progress Report 42-37: November and December 1976, pp. 204–223, February 15, 1977

For abstract, see Wu, S. C.

YIP, K. W.

Y013 Measurements of Large-Scale Density Fluctuations in the Solar Wind Using Dual-Frequency Phase Scintillations

R. Woo, F. C. Yang, K. W. Yip, and W. B. Kendall (Mark Resources, Inc.)

Astrophys. J., Vol. 210, No. 2, Pt. 1, pp. 568–574, December 1, 1976

For abstract, see Woo, R.

YOUNG, J. W.

Y014 Sodium D-Line Emission From Io: A Second Year of Synoptic Observation From Table Mountain Observatory

J. T. Bergstralh, J. W. Young, D. L. Matson, and T. V. Johnson

Astrophys. J., Vol. 211, No. 1, Pt. 2, pp. L51–L55, January 1, 1977

For abstract, see Bergstralh, J. T.

YOUNG, K. A.

Y015 Observations of NH_3 in the Atmosphere of Jupiter During 1973, 1974

K. A. Young and J. S. Margolis

Icarus, Vol. 30, pp. 129–137, 1977

The 6450 Å ammonia absorption band in the atmosphere of Jupiter was observed during the summers of 1973 and 1974. High-dispersion spectra of this band were obtained and analyzed on a line-by-line basis to derive ammonia abundances in the Jovian atmosphere. The abundances determined this way show strikingly large fluctuations.

ZAWACKI, B. E.

Z001 Multispectral Photographic Analysis: A New Quantitative Tool to Assist in the Early Diagnosis of Thermal Burn Depth

V. J. Anselmo and B. E. Zawacki (Los Angeles County/USC Medical Center)

Ann. Biomed. Eng., Vol. 5, pp. 179–193, 1977

For abstract, see Anselmo, V. J.

Z002 Effect of Evaporative Surface Cooling on Thermographic Assessment of Burn Depth

V. J. Anselmo and B. E. Zawacki (University of Southern California)

Radiology, Vol. 123, No. 2, pp. 331–332, May 1977

For abstract, see Anselmo, V. J.

ZMUIDZINAS, J. S.

Z003 Ground-State Properties of hcp Helium-4 on the Basis of a Cell Model

N. Jacobi and J. S. Zmuidzinas

Phys. Rev., Pt. B: Solid State, Vol. 16, No. 7, pp. 3267–3269, October 1, 1977

For abstract, see Jacobi, N.

ZOBRIST, A. L.

Z004 Detection of Combined Occurrences

A. L. Zobrist and F. R. Carlson, Jr. (University of Southern California)

Commun. ACM, Vol. 20, No. 1, pp. 31–35, January 1977

In this paper it is supposed that the variables $x_1, \ldots, x_n$ each have finite range with the variable x_i taking on p_i possible values and that the values of the variables are changing with time. It is supposed further that it is desired to detect occurrences in which some subset of the variables achieve particular values. Finally, it is supposed that the problem involves the detection of a large number of combined occurrences for a large number of changes of values of variables. Two efficient solutions for this problem are described. Both methods have the unusual property of being faster for systems where the sum $p_1 + \ldots + p_n$ is larger. The first solution is error-free and suitable for most cases. The second solution is slightly more elegant and allows negation as well as conjunction, but is subject to the possibility of errors. An error analysis is given for the second method and an empirical study is reported.

Z005 IBIS: A Geographic Information System Based on Digital Image Processing and Image Raster Data Type

N. A. Bryant and A. L. Zobrist

IEEE Trans. Geosci. Electron., Vol. GE-15, No. 3, pp. 152–159, July 1977

For abstract, see Bryant, N. A.

Z006 Computability of Five-Color Maps

B. D. McLemore (Informatics, Inc.) and A. L. Zobrist

Image Sci. Math., pp. 256–260, Western Periodicals Co., North Hollywood, Calif., 1977

For abstract, see McLemore, B. D.

ZUCKERMAN, B.

Z007 High-Velocity Gas in the Orion Infrared Nebula

B. Zuckerman (University of Maryland) T. B. H. Kuiper, and E. N. R. Kuiper (University of California, Los Angeles)

Astrophys. J., Vol. 209, No. 3, Pt. 2, pp. L137–L142, November 1, 1976

Sensitive observations of carbon monoxide toward the Kleinmann-Low (KL) infrared nebula in Orion have revealed the presence of low-level emission extending over a radial velocity range of at least 150 km s^{-1}. The high-velocity emission appears to be localized to a region $\lesssim 1'$ in diameter centered on KL. The high-velocity gas is probably associated with pre- rather than post-main-sequence object(s). However, the intensity of line radiation at these high velocities is not easily explained with simple models of mass-outflow, gravitational collapse, or rotation.

Z008 Unidentified Lines in Molecular Clouds and a Search for ^{14}C in IRC +10216

E. N. R. Kuiper (University of California, Los Angeles), T. B. H. Kuiper, B. Zuckerman (University of Maryland), and R. K. Kakar

Astrophys. J., Vol. 214, No. 2, Pt. 1, pp. 394–398, June 1, 1977

For abstract, see Kuiper, E. N. R.

ZYGIELBAUM, A. I.

Z009 Mu-II Ranging

W. L. Martin and A. I. Zygielbaum

Technical Memorandum 33-768, May 15, 1977

For abstract, see Martin, W. L.

Z010 Near Sun Ranging

A. I. Zygielbaum

The Deep Space Network Progress Report 42-41: July and August 1977, pp. 43–50, October 15, 1977

Near superior solar conjunction, radiowaves traveling between Earth and a spacecraft graze the sun. Ranging, or determining the round-trip radio signal propagation time, provides measurements of signal delay induced by the solar corona and gravity field. This article describes techniques which enhance range data quality during the harsh signal conditions existing at solar conjunction.

Subject Index

Subject Categories

Subjects

ORIGINAL PAGE IS OF POOR QUALITY

ORIGINAL PAGE IS
OF POOR QUALITY

ORIGINAL PAGE IS
OF POOR QUALITY

ORIGINAL PAGE IS OF POOR QUALITY

ORIGINAL PAGE IS
OF POOR QUALITY

Publication Index

JPL Publications

ORIGINAL PAGE IS
OF POOR QUALITY

JPL Publications (contd)

Number	Entry
42-40 (contd)	B031
	B032
	B057
	B060
	B073
	C016
	D001
	E003
	F016
	F017
	G001
	H013
	H027
	H041
	J002
	L008
	L040
	L063
	M059
	M061
	R033
	S038
	T007
42-41	A008
	B033
	B034
	E016
	G024
	H003
	H023
	I002
	J037
	L009
	L013
	L041
	L042
	M043
	N012
	P008
	R016
	R034
	S010
	S018
	S061
	T006
	W033
	W045
	Z010
42-42	B011
	B020
	B035
	B036
42-42 (contd)	B037
	B058
	C002
	C031
	D011
	D019
	E004
	G002
	G010
	G025
	H028
	L018
	L019
	M045
	O006
	R035
	S031
	S032
	S058
	W009
	W021
77-1	K001
77-3	J041
77-4	S017
77-5	J014
77-6	J015
77-7	E013
77-9	B048
77-11	H010
77-12	J016
77-13	N013
77-15	M001
77-16	F038
77-17	L043
77-19	F023
77-20	T011
77-21	B008
77-23	W039
77-24	K030
77-25	K023

JPL Publications (contd)

Number	Entry
77-26	B040
77-27	B038
77-27, Rev. 1	B039
77-28	B052
77-29	F027
77-30	L016
77-31	A025
77-33	D008
77-34	H014
77-35	M051
77-36	E015
77-37	S020
77-38	P032
77-39	J017
77-40	J018
77-41, Vol. I	S053
77-43	H020
77-44	C009
77-45	K041
77-46	K039
77-51, Vol. I	J019
77-51, Vol. II	J020
77-51, Vol. III	J021
77-51, Vol. IV	J022
77-51, Vol. V	J023
77-51, Vol. VI	J024
77-51, Vol. VII	J025
77-51, Vol. III	J026
77-51, Vol. IX	J027
77-53, Vol. I	F010
77-53, Vol. II	F011
77-53, Vol. III	F012
77-53, Vol. IV	L028
77-54	P019
77-55	J028
77-56	T001
77-57	H005
77-59, Vol. I	E018
77-59, Vol. II	E019
77-60	S062
77-61	B004
77-62, Vols. I and II	W038
77-63	F032
77-65	F028
77-66	M016
77-68	S002
77-69	E017
77-70	J005
77-71	S043
77-72	H019
77-73	W015
77-74	W011
77-75	S052
77-78	S021
77-79	F040

Open Literature Reporting (contd)

Open Literature Reporting (contd)

NASA—JPL—Coml., L.A., Calif.